The Physiological Role of Kidney Anion Exchanger 1 Protein Interaction with Adaptor Protein 1 A and B

by

Ensaf Yousef Almomani

A thesis submitted in partial fulfillment of the requirements for the degree of

Doctor of Philosophy

Department of Physiology
University of Alberta

© Ensaf Yousef Almomani, 2015

ABSTRACT

Distal Renal Tubular Acidosis (dRTA) is a disease characterized by metabolic acidosis, an inability to acidify urine, development of kidney stones and renal failure if untreated. dRTA patients can carry a mutation in the SLC4A1 gene encoding the kidney anion exchanger 1 (kAE1), a Cl^-/HCO_3^- exchanger basolaterally expressed in kidney acid-secreting alpha intercalated cells. Three reported SLC4A1 mutations that cause dRTA, including the kAE1 R901X mutation, affect the interaction site of kAE1 with adaptor protein 1 (AP-1). AP-1 is a cytosolic tetrameric protein complex, which has two forms, A and B. It is involved in protein trafficking in polarized cells from the trans Golgi network or recycling endosomes to the plasma membrane.

The general hypothesis of my thesis was AP-1A and/or B interaction with kAE1 is crucial for kAE1 residency at the basolateral membrane in polarized epithelial cell. I proposed that lack of proper interaction between kAE1 and AP-1A and/or B affects kAE1 trafficking and surface expression and may cause dRTA disease.

Data presented here confirmed the interaction between kAE1 and the AP-1A and B protein complexes *in vitro* by reciprocal coimmunoprecipitation or the protein is heterologously expressed in epithelial cells and *in vivo* by coimmunoprecipitation from mouse kidney extract. When endogenous μ1A and μ1B subunits from AP-1A and B, respectively, were knocked down using short interfering RNA, kAE1 protein was unable to traffic to the plasma membrane and was rapidly degraded via a lysosomal pathway. Expression of siRNA-resistant μ1A or μ1B rescued kAE1 trafficking to the cell surface and increased its stability. Furthermore, I found that newly synthesized kAE1 does not traffic through recycling endosomes to the plasma membrane, suggesting that AP-1B,

located in these endosomes, is not primarily involved in trafficking of newly synthesized kAE1 when AP-1A is present in the cells.

The physiological role of AP-1B was investigated in LLC-PK1 cells, a renal epithelial cell line that lacks the endogenous AP-1B. Surprisingly, μ1B expression in these cells reduced the amount of cell surface kAE1-WT at steady state. This decrease was due to μ1B expression increasing the endocytosis rate and decreasing the recycling rate of kAE1-WT. Although kAE1-R901X mutant, which lacks a canonical AP-1 binding site, was endocytosed slightly faster than kAE1-WT, its recycling rate was significantly decreased compared to that of kAE1-WT. Unlike kAE1-WT, kAE1-R901X recycling was independent from μ1B expression. Importantly, kAE1 endocytosis was dynamin and clathrin dependent.

Finally, this thesis showed that heterologous expression of μ1A or μ1B displaces the physical interaction of endogenous glyceraldehyde-3-phosphate dehydrogenase with kAE1-WT, supporting that AP-1A or B and glyceraldehyde-3-phosphate dehydrogenase bind to an overlapping site on kAE1. This work also revealed that phosphorylation of tyrosine 904 within the canonical AP interaction motif does not alter the interaction between kAE1 and AP-1A/B. My results suggest that AP-1A regulates the processing of the newly synthesized kAE1 to the basolateral surface while AP-1B plays a role in kAE1 trafficking in absence of AP-1A. Further, kAE1 recycling and endocytosis are dependent on AP-1B expression. In conclusion, both AP-1A and B adaptors are required for normal kAE1 trafficking, and we propose that the apically mis-targeted kAE1- R901X dRTA mutant may fail to recycle back to the basolateral membrane due to its inability to properly interact with AP-1B.

PREFACE

Contributions of authors

Chapter 2

All experiments were performed by Ensaf Almomani. This study was coordinated and supervised by Dr. Emmanuelle Cordat.

Chapter 3

Almomani E. A., King J. C., Netsawang J., Yenchitsomanus P., Malasit P., Limjindaporn T, Todd Alexander R., and Cordat E., "Adaptor protein 1 complexes regulate intracellular trafficking of the kidney anion exchanger 1 in epithelial cells", *Am J Physiol Cell Physiol 303: C554–C566, 2012*.

Ensaf Almomani performed the majority of the experiments in this paper including: immunoprecipitation of kAE1 protein with AP-1A and B complexes (Fig 3.1 A & B), determination of the effect of knocking-down endogenous AP-1A and B on kAE1 trafficking (Fig 3.2 B), rescue of kAE1 trafficking after expression of siRNA resistant AP-1A and B complexes (Fig 3.4), and real time PCR experiments, optimization of kAE1-HaloTag protein expression in non polarized and polarized renal kidney cells (Fig 3.5 A), examining the role of AP-1A and B in kAE1 trafficking to the cell surface (Fig 3.6). Ensaf Almomani also participated in manuscript preparation and editing. Jenny King performed the rest of the experiments (Fig 3.1C, D; Fig 3.2 A; Fig 3.3 and Fig 3.5 B), participated in the manuscript preparation and edition. Drs. Yenchitsomanus, Malasit and Limjindaporn co-supervised the thesis work of a visiting Thai graduate student, Miss Janjuree Netsawang, who initiated the study. Dr. Todd Alexander participated in

conception and design of the experiments as well as editing of the manuscript. Dr. Emmanuelle Cordat coordinated and supervised the study and prepared the manuscript.

Chapter 4

Almomani E. A., Jung M., Zimmermann R., Todd Alexander R., and Cordat E., "Adaptor protein 1 B regulates recycling of the kidney anion exchanger 1 in renal epithelial cells", *submitted to Traffic, January 2015*.

Ensaf Almomani performed all experiments in this manuscript and prepared the manuscript. In addition to editing the manuscript, Drs. Jung and Zimmermann provided the cellulose membrane used for the peptide spot assay. Dr. Todd Alexander participated in conception and design of the experiments as well as editing of the manuscript. Dr. Emmanuelle Cordat coordinated and supervised the study, and edited the manuscript.

DEDICATIONS

For the two great hearts that gave me love, care, and support throughout my life. Without their continuous support and encouragement, I would not be who I am now. I dedicate my PhD thesis to my parents with love.

To my husband Abbas and my kids, Kareem and Nadeen: literally, my success and achievements are meaningless without you. You have shared with me the stressful and the joyful moments during my PhD trip. I love you.

To my brother Anas, and my sisters Yamamh, Ekhlas, Wafa, and Huda: I'm so lucky to have you around. Thank you for your continuous support and encouragement.

To my friends: moments talking and hanging out with you were the resting stations that renewed my energy during my PhD. I spent unforgettable moments with you. Thank you for adding wonderful memories to my life, and for being around when I needed you.

ACKNOWLEDGMENTS

Many endless thanks and gratefulness are for my supervisor Dr. Emmanuelle Cordat. Thank you for giving me this opportunity to finish my PhD degree. For helping me to plan, design, and perform my project experiments. For your continuous support and encouragement despite the depressing and disappointing moments in my thesis project.

My sincere thanks are to my committee members, Dr. James Young, Dr. Joseph Casey, and Dr. Todd Alexander for their valuable feedback during my committee meetings. A special thank is for Dr. Alexander for his fruitful ideas and suggestions regarding my project.

During my PhD program, I met many people who either worked with me in the same laboratory or at the department of Physiology; I would like to thank them all for their support and advices.

Finally, I would like to acknowledge the funding agencies that supported my project: the Kidney Foundation of Canada, the Women and Children Health Research Institute (WCHRI), and the 75th Anniversary Graduate Student Award from the School of Medicine and Dentistry.

TABLE OF CONTENTS

1. Chapter one: General Introduction……..1

1.1 Thesis overview……..2

1.2 Bicarbonate transporters role in acid-base homeostasis……....3

1.2.1 Sodium- independent Cl^-/HCO_3^- exchange ……...4

1.2.1.1 AE1……..4

1.2.1.2 kAE1……8

1.2.1.3 AE2 and AE3……10

1.2.2 Electrogenic Na^+-HCO_3^- cotransporters……..11

1.2.3 Electroneutral Na^+- HCO_3^- cotransporter…….....12

1.2.4 SLC26 family…….....12

1.3 Blood pH regulation……..13

1.4 Renal response to acid-base imbalance and bicarbonate reabsorption……14

1.4.1 Bicarbonate reabsorption in the PT…….……15

1.4.2 Bicarbonate reabsorption in TAL……....18

1.4.3 Bicarbonate reabsorption in the DT and CCD……..…18

1.5 Diseases associated with acid-base imbalance……...…..20

1.5.1 Proximal renal tubular acidosis (pRTA)……..20

1.5.2 Pendred Syndrome……...…23

1.5.3 Distal renal tubular acidosis (Type 1 RTA)……...…..25

1.5.3.1 Mutations in the SLC4A1 gene……..…26

1.5.3.2 Mutations in the vacular H^+-ATPase gene…….....28

1.5.3.3 Mutations in the SLC26A7 gene ……...……28

1.5.3.4 Mutations in the CAII gene ……...29

1.6 Membrane protein trafficking and endocytosis……....29

1.6.1 Membrane proteins sorting signals in epithelial cells……..……....30

1.6.2 Membrane proteins processing and trafficking in epithelial cell….....30

1.6.3 Membrane protein endocytosis……...…31

1.7 Adaptor proteins and their role in proteins trafficking……..…..33

1.7.1 Adaptor protein 1A/B……..…35

1.7.1.1 Adaptor protein 1 A/B subunits……..…35

1.7.1.2 Adaptor protein 1 A/B function……...…35

1.7.1.3 Adaptor protein 1 A/B diversity……...…36

1.7.1.4 Adaptor protein 1 A/B knockout mice models …….....37

1.7.2 Adaptor protein 2……..…38

1.7.3 Adaptor protein 3 A/B……...…..38

1.7.4 Adaptor protein 4 ……...….39

1.7.5 Adaptor protein 5 ……....39

1.8 The role of adaptor proteins in regulating kAE1 trafficking

……39

1.9 Thesis hypothesis……..42

1.10 Thesis objectives……...42

2. Chapter two: kAE1 HaloTag as a tool to study kAE1 trafficking in MDCK cells……...43

2.1 Introduction……...44

2.2 Materials and methods…….....45

2.2.1 kAE1 HaloTag construct…….45

2.2.2 kAE1 deglycosylation…….45

2.2.3 Immunofluorescence …….…48

2.2.4 Pulse chase experiment……...49

2.2.5 SITS Affi-gel binding assay……..…..50

2.2.6 kAE1-HT mutants' preparation …….….50

2.2.7 Imaging of kAE1-HT expressing cells …….....50

2.3 Results……...51

2.3.1 kAE1-HT protein is expressed as a 129 kDa protein in SDS-PAGE and carries complex oligosaccharides ……...…51

2.3.2 kAE1-HT protein is properly folded in MDCK cells ……..…...51

2.3.3 HT ligands bind specifically to kAE1 HT protein ……..…53

2.3.4 kAE1-HT is expressed at the plasma membrane of non-polarized MDCK cells and at the basolateral membrane of polarized MDCK cells …….…53

2.3.5 A new pool of kAE1–HT protein is synthesized 60 min after blocking……...….57

2.3.6 Newly synthesized kAE1 – HT protein colocalizes with giantin one hour after synthesis and reaches plasma membrane after three hours ……60

2.3.6.1 Pulse chase experiment ……60

2.3.6.2 Live cell imaging……..60

2.3.7 kAE1 – HT mutants reach the cell surface of non-polarized MDCK cells ……63

2.4 Discussion ……....63

3. Chapter three: Adaptor protein 1A complex regulates intracellular trafficking of the kidney Anion Exchanger 1 in Epithelial cells ……...69

3.1 Introduction ……..70

3.2 Materials and Methods ……72

3.2.1 Recombinant plasmid constructs and antibodies……72

3.2.2 Cell culture ……..74

3.2.3 Immunoprecipitation ……...……75

3.2.4 Immunocytochemistry……..…….. 76

3.2.5 Knockdown of Canine μ1A adaptin with siRNA duplexes …….....77

3.2.6 Expression of siRNA resistant μ1A in μ1A/B siRNA transfected cells……..78

3.2.7 Recycling endosomes inactivation and immunolocalization ……..78

3.2.8 Pulse chase like experiment ……80

3.2.9 Statistical analysis ……...81

3.3 Results ……..81

3.3.1 μ 1A and B subunits bind to kAE1 in epithelial cells….…….....81

3.3.2 kAE1 protein co-immunoprecipitates with AP-3 but not with AP-4 adaptor protein complex …….82

3.3.3 KAE1 protein colocalizes with AP-1A and /or B in mouse kidney sections and coimmunoprecipitates with μ1A from mouse kidney homogenates ……...85

3.3.4 KAE1 is degraded in μ1A/B knocked- down MDCK cells ……86

3.3.5 Expression of human μ1A-HA and μ1B-HA rescues kAE1 stability in μ1A/B siRNA transfected cells ……..……91

3.3.6 In presence of AP-1A, newly synthesized kAE1 does not traffic through recycling endosomes ……....94

3.3.7 Expression of μ1A rescues trafficking of newly synthesized kAE1 to the plasma membrane ……....97

3.4 Discussion ……..101

4. Chapter four: Adaptor Protein - 1B regulates recycling of the kidney Anion Exchanger 1 in renal epithelial cells ……109

4.1 Introduction……110

4.2 Materials and Methods …….…..113

4.2.1 Plasmid construct and antibodies ……..113

4.2.2 Cell culture ……....113

4.2.3 Immunoprecipitation and western blotting ……...114

4.2.4 Proximity ligation assay ……....115

4.2.5 Peptide spot assay …….……116

4.2.6 Cell surface biotinylation ……..117

4.2.7 Cycloheximide treatment ……. 117

4.2.8 Phosphorylation experiment …….118

4.2.9 Competition between μ1 and GAPDH binding to kAE1 protein

……...119

4.2.10 Endocytosis experiment …….…..119

4.2.11 Caveolin colocalization with kAE1 …….121

4.2.12 Recycling experiment ……..121

4.2.13 Statistical Analysis …….….122

4.3 Results ……....122

4.3.1 kAE1 interaction with AP-1B ……...122

4.3.1.1 kAE1-WT is immunoprecipitated with μ1B in LLC-PK1 cells

……..122

4.3.1.2 kAE1 is in close proximity with μ1B protein …….123

4.3.1.3 kAE1-WT colocalizes with μ1B in the perinuclear region of LLC-PK1 cells …….126

4.3.1.4 AP-1B interacts with kAE1 via multiple binding sites

…….126

4.3.2 Factors that affect kAE1-WT and AP-1B interaction.

……129

4.3.2.1 Phosphorylation of the C-terminal tyrosine 904 does not affect kAE1 / AP-1B interaction ……..129

4.3.2.2 AP-1B binding to kAE1 displaces GAPDH interaction with kAE1 …….……131

4.3.3 The effect of μ1B expression on the amount of cell surface kAE1 at the steady state ……..……133

4.3.3.1 In non polarized LLC-PK1 cells, kAE1 is more abundant at the plasma membrane than kAE1 R901X mutant ……....133

4.3.3.2 In LLC-PK1 cells, the kAE1 R901X truncated mutant has a similar half-life as kAE1 WT ……..137

4.3.3.3 Expression of μ1B decreases cell surface amount of kAE1 WT and R901X mutant …….…137

4.3.4 The effect of μ1B on kAE1 endocytosis ……...142

4.3.4.1 kAE1 is endocytosed via a clathrin dependent pathway …….142

4.3.4.2 The amount of endocytosed carboxyl-terminal kAE1 mutant R901X is higher than kAE1 WT…….143

4.3.4.3 In the presence of μ1B, kAE1 is less efficiently endocytosed. ……..146

4.3.5 The effect of μ1B expression on kAE1 recycling …….....147

4.3.5.1 Carboxyl-terminal kAE1 R901X mutant recycles less efficiently to the plasma membrane than kAE1 WT ……147

4.3.5.2 Expression of μ1B in LLC-PK1 cells reduces the amount of recycled kAE1 WT but not that of kAE1 R90X mutant ……..…150

4.4 Discussion ……. 153

5. Chapter five: General discussion……...160

5.1 Introduction…….161

5.2 Validity of the cell models……..161

5.3 Studies in non-polarized epithelial cells……163

5.4 Role of the canonical YXXΦ motif for kAE1- R901X mutant's trafficking…….164

5.5 Functional consequence of kAE1 trafficking…….165

5.6 Transient versus stable transfections……..165

5.7 kAE1-WT and kAE1-R901X protein expression……..…166

6. Chapter six: Summary and future directions……..167

6.1 Summary…….168

6.2 Future directions…….169

7. References……....174

LIST OF FIGURES

Figure 1.1 Bicarbonate transporter families …….....5

Figure 1.2 AE1 topological model…….7

Figure 1.3 Nephron anatomy model…….…....16

Figure 1.4 Bicarbonate absorption at the proximal tubule ……..…17

Figure 1.5 Collecting duct cells model…….....21

Figure 1.6 Major steps of CCV formation from the donor to the acceptor compartment...

…….....32

Figure 1.7 The AP complexes…….…..34

Figure 1.8 The role of AP complexes in protein trafficking pathway…….…… 40

Figure 1.9 AP-1A interaction with kAE1…….41

Figure 2.1 kAE1 topological model……...…...46

Figure 2.2 SLC4A1-pFN21A cDNA……...….47

Figure 2.3 kAE1-HT protein is processed normally to complex oligosaccharides ….....54

Figure 2.4 kAE1-HT protein shows similar folding pattern to kAE1 protein …….…....55

Figure 2.5 HaloTag ligand binds specifically to kAE1–HT protein…….56

Figure 2.6 kAE1-HT is expressed at the plasma membrane of non-polarized and at the basolateral membrane of polarized MDCK cells …….….58

Figure 2.7 A new pool of kAE1-HT is synthesized 60 minutes after blocking pre-existing kAE1-HT proteins with O4 HT ligand…...……...59

Figure 2.8 kAE1-HT colocalizes with giantin one hour after synthesis and reaches the cell surface after a 3 hour chase time ……....61

Figure 2.9 Live cell imaging shows that kAE1-HT reaches the cell surface 3 hours after synthesis …….....64

Figure 2.10 kAE1-HT mutants reaches the cell surface except kAE1-HT R901X …....65

Figure 3.1 kAE1 binds to AP-1A, AP-1B and AP-3 adaptor complexes ……....83

Figure 3.2 kAE1-WT immunoprecipitates and colocalizes with the AP-1 adaptor complex …….…87

Figure 3.3 Knocking down μ1A affects the stability of kAE1 as well as trafficking of both cation-dependent mannose 6-phosphate receptor (CD-MPR) and kAE1 in MDCK cells……...…92

Figure 3.4 siRNA resistant μ1A stabilizes kAE1 in cells knocked down for μ1A and/or B……...…. 95

Figure 3.5 Newly synthesized kAE1 traffics in a μ1B-independent pathway and does not travel through recycling endosomes……....99

Figure 3.6 μ1A-HA allows newly synthesized kAE1 to reach the plasma membrane……102

Figure 4.1 μ1B interacts and colocalizes with both kAE1-WT and kAE1-R901X in the perinuclear region ……...124

Figure 4.2 AP-1B complex has multiple interaction sites on kAE1 protein……..127

Figure 4.3 Phosphorylation of tyrosine 904 does not impair μ1B HA interaction with kAE1……132

Figure 4.4 Expression of μ1B HA subunit displaces GAPDH interaction with kAE1 carboxyl-terminus ……..134

Figure 4.5 In non polarized LLC-PK1 cells, kAE1-WT is more abundant at the plasma membrane than kAE1-R901X mutant, but its surface expression decreases upon of μ1B expression ……...139

Figure 4.6 kAE1 is endocytosed via clathrin coated vesicles and colocalizes with endocytosed transferrin receptor……..144

Figure 4.7 kAE1-R901X mutant is endocytosed at a higher rate than kAE1 WT, but μ1B expression decreases both kAE1-WT and R901X endocytosis rates……..148

Figure 4.8 The kAE1 R901X mutant recycles less efficiently to the plasma membrane than kAE1-WT, and its recycling is independent of μ1B ……..…….151

Figure 5.1 Mutations in kAE1 tyrosine and dileucine motifs affect kAE1 processing and surface localization …….173

LIST OF TABLES

Table 1. 1 Diseases associated with abnormal kidney functions……...…...24

Table 2.1 Primer sequences used to introduce mutations in AE1 cDNA ……52

Table 4.1 Sequence of kAE1 peptides that interact with AP-1B by peptide spot assay ……..130

Table 6.1 Endocytosis and recycling of kAE1-WT and kAE1-R901X mutant in the presence and absence of μ1B…….….170

LIST OF ABBREVIATIONS

AE1	Anion exchanger
AMPA	α-amino-3-hydroxy-5-methyl-4-isoxazolepropionic acid receptor
AP	Adaptor protein
AQP	Aquaporin
CA	Carbonic anhydrase
CCD	Cortical collecting duct
CCV	Clathrin-coated vesicles
CD-MPR	Cation dependent mannose phosphate receptor
CFTR	Cystic fibrosis transmembrane conductance regulator
CHX	Cycloheximide
CI-MPR	Cation independent mannose phosphate receptor
CT	Connecting tubule
DAB	Diaminobenzidine
DAPI	4', 6-diamidino-2-phenylindole
DCT	Distal convoluted tubule
DIDS	4-4'Diisothiocyanatostilbene-2, 2'-disulfonic acid
dRTA	distal renal tubular acidosis
EE	Early endosomes
ER	Endoplasmic reticulum
ENaC	Epithelial sodium channel
FAM	Fluorescein amidite

GAPDH	Glyceraldehyde 3-phosphate dehydrogenase
GPA	Glycophorin A
HA	Hemagglutinin
HEK	Human embryonic kidney
H_2DIDS	4,4'-diisothiocyanodihydrostilbene-2,2'-disulfonic acid
HRP	Horseradish peroxidase
HS	Hereditary spherocytosis
HT	HaloTag
IC	Intercalated cell
IL-6ST	Interleukin 6 signal transducer
kAE1	Kidney anion exchanger 1
KD	Knockdown
KO	Knockout
LDLR	Low density lipoprotein receptor
LLC-PK1	Porcine kidney cell line (cell line of proximal tubular origin)
MDCK	Madin-Darby canine kidney
NBC (e/n)	Sodium bicarbonate co-transporters (electrogenic / electroneutral)
NHE	Sodium proton exchanger
ORF	Open reading frame
PCT	Proximal convoluted tubule
pRTA	Proximal renal tubular acidosis
RBC	Red blood cell
RE	Recycling endosomes

SAO	Southeast Asian Ovalocytosis
siRNA	Short interfering RNA
SITS	4-Acetamido-4'-isothiocyano-2, 2'-stilbene disulphonic acid
SLC	Solute Carriers
SNARE	N-ethylmaleimide-sensitive factor attachment protein receptor
TAL	Thick ascending limb
TARPs	Transmembrane AMPA receptor regulatory proteins
TfnR	Transferrin receptor
TGN	Trans-Golgi network
TMD	Transmembrane domains
TMR	Tetramethylrhodamine
VSVG	Vesicular stomatitis virus G
WT	Wild-type
YXXΦ	Y: Tyrosine, X, any amino acid, Φ: bulky hydrophobic amino acid

1. Chapter one: General Introduction

1.1. Thesis overview

This thesis investigated the role of adaptor protein 1 (AP-1) A and B complexes in trafficking of the kidney anion exchanger 1 (kAE1). This protein exchanges chloride for bicarbonate ions in kidney alpha-intercalated cells (IC), thus participating in renal acid-base homeostasis. AP-1A and B are protein complexes involved in basolateral membrane protein trafficking and recycling.

Herein, we showed that kAE1/AP-1A interaction is crucial for kAE1 localization and stability at the surface of epithelial cell. We also demonstrated for the first time an interaction between kAE1 and AP-1B. We found that AP-1B affects the amount of cell surface kAE1 by playing a role in kAE1 endocytosis and recycling.

The first chapter of my thesis is a general introductory chapter with two major parts: while the first part reviews the current knowledge on bicarbonate transporter families and their role in acid-base homeostasis specifically in the kidney, it also discusses in more details the current literature on anion exchanger 1 (AE1) protein and its renal isoform kidney AE1 (kAE1). The second part provides an overview of adaptor proteins and their role in proteins' trafficking and recycling, focusing specifically on the AP-1A and B complexes. Finally, the last section of the introduction will review published results about the interaction of kAE1 protein with AP-1A/B and other AP complexes.

This thesis follows a paper-based format, where the second, third and fourth chapters are the main chapters. Each has a specific introduction, materials and methods, results and discussion.

The second chapter characterizes the chimeric kAE1 protein fused to a HaloTag

(kAE1-HT) protein used to study kAE1 intracellular trafficking. Chapter three focuses on characterization of the physiological role of kAE1/AP-1A interaction in renal epithelial cells. The fourth chapter discusses the role of kAE1/AP-1B interaction on kAE1 trafficking, recycling and endocytosis. This chapter also describes for the first time kAE1 endocytosis. The fifth chapter is a general discussion chapter, focussing on the study limitations. The sixth chapter summarizes the main findings of this thesis and proposes future experimental directions.

1.2. Bicarbonate transporter role in acid - base homeostasis

The human body metabolizes ingested foods to produce energy and to perform different biological processes such as growth and reproduction. However, by-products such as carbon dioxide (CO_2) are generated during the energy production process from food metabolism (1,2). Accumulation of CO_2 increases blood acidity, which impairs physiological functions. To maintain optimal biological functions, the blood pH depends on the relative amount of CO_2 and HCO_3^- and must be strictly buffered. Carbonic anhydrase II (CAII) is a cytosolic enzyme that catalyzes the reversible hydration of carbon dioxide (1,2) as shown in the following equation:

$$\mathbf{CO_2 + H_2O \Leftrightarrow H_2CO_3 \Leftrightarrow HCO_3^- + H^+}$$

Unlike CO_2 that can diffuse through the plasma membrane, HCO_3^- movement across the plasma membrane occurs through anion exchangers, anion channels, and metal transporters (3). The Solute Carriers (SLC) of anion transporters are separated phylogenetically into two families: SLC4A and SLC26A (4). This first section discusses the two families of bicarbonate transporters and their respective roles in acid-base regulation.

The SLC4 family is divided into three groups: the electroneutral Na^+-independent Cl^- / HCO_3^- exchangers SLC4A1-3 (AE1-3), the electrogenic Na^+-coupled HCO3 cotransporters SLC4A4, 5 (NBCe1 and NBCe2), and the electroneutral Na^+-coupled HCO_3^- cotransporters SLC4A7, 8, 10 (NBCn1, NDCBE, NBCn2) respectively, and SLC4A9. The SLC4A6 is considered a pseudogene (5,6). The SLC4A11 is not reported to transport HCO_3^-. Rather, it is acts as borate (7) and water (8) transporter or Na^+/H^+ exchanger (8). Figure 1.1 summarizes the bicarbonate transporter families. The next sections will review the current general knowledge on the three groups of SLC4 family members.

1.2.1. Sodium-independent Cl^-/ HCO_3^- exchangers

1.2.1.1. AE1

Anion Exchanger 1 (also called Band 3) is encoded by the SLC4A1 gene and is the first and best characterized of the SLC4 family members (9). It is located at the plasma membrane of red blood cells (RBC), where it accounts for approximately 50 % of integral membrane proteins at the RBC plasma membrane (10). AE1 mediates the exchange of one Cl^- for one HCO_3^- ion. CO_2 produced by the cellular metabolism diffuses into the RBC where it is converted into H_2CO_3 and then HCO_3^- in a reaction catalyzed by cytosolic CAII (11). AE1 exchange activity is reversed in lungs. HCO_3^- that enters the RBC via AE1 is converted by CAII to CO_2 that in turn diffuses out of the RBC and is exhaled in the lungs (12). AE1 maintains pH homeostasis by transporting HCO_3^-. In addition, AE1 is capable of transporting different anions, including Br^-, F^-, and I^- but with less affinity than the HCO_3^- ion (13-15). Furthermore, AE1 can mediate the transport of divalent anions like SO_4^{2-} through allosteric interactions between subunits that modulate

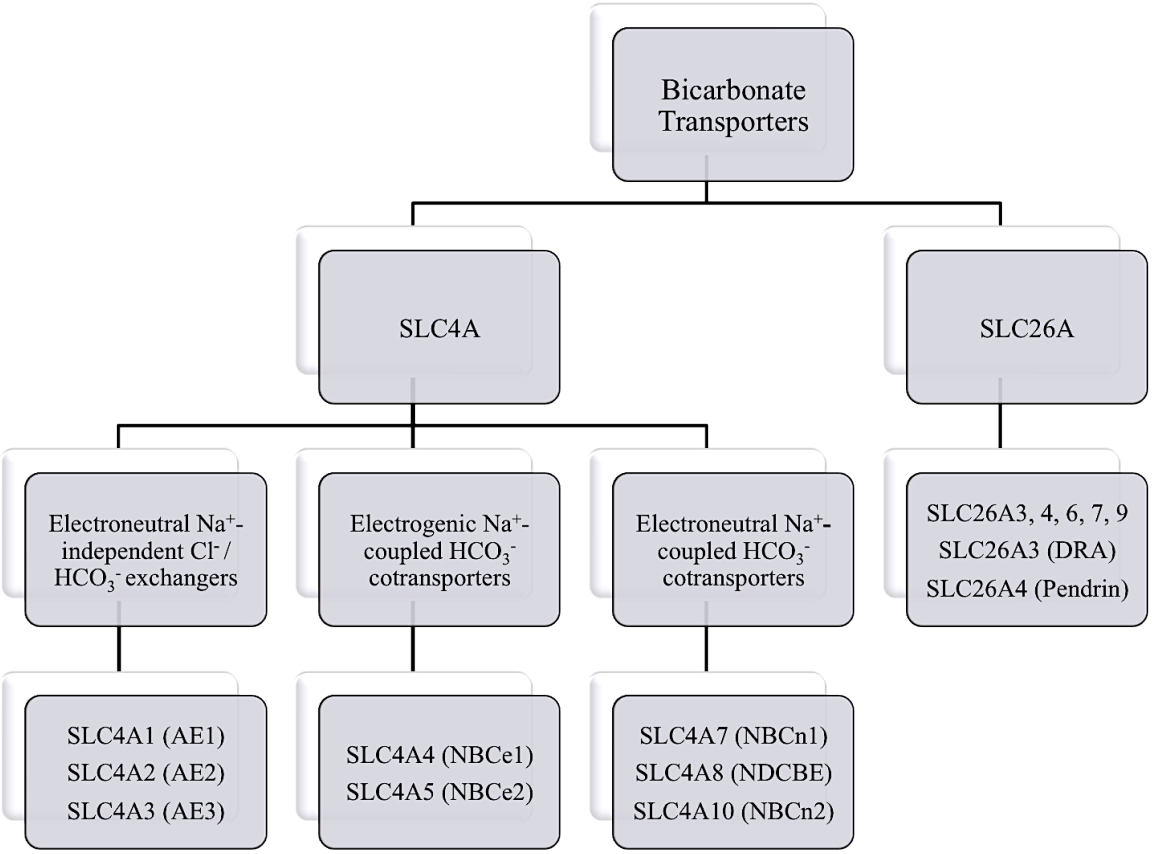

Figure 1.1: Bicarbonate Transporter families

the anion transport activity (16).

AE1 consists of 911 amino acids and is composed of two major domains: an amino-terminal (N-terminal) cytosolic domain (residues 1-360) and a carboxyl-terminal (C-terminal) membrane domain including a short cytosolic region (residues 872-911) (17). AE1 has a single N-glycosylation site at asparagine 642 in the fourth-extracellular loop of the protein (17-19) (Fig 1.2). Some organic anions like 4,4'-diisothiocyanostilbene-2, 2'-disulfonic acid (DIDS) inhibit the activity of AE1 protein by crosslinking lysine 539 and lysine 851 (20,21).

The N-terminus of AE1 controls the shape and deformability of RBC (22,23) via multiple interactions with deoxyhemoglobin (24), glycolytic enzymes like GAPDH (25,26), cytoskeletal proteins like ankyrin (27), protein 4.1 (28) and protein 4.2 (22). AE1 also interacts physically with Rhesus-associated glycoproteins (29). In addition, AE1 forms a complex with glycophorin A (GPA) known as Wright^{b} blood group antigen (30). Recently, AE1 binding to GPA was shown to affect AE1 activity and trafficking (31). On the other hand, AE1 C-terminal cytosolic domain binds to CAII enzyme, which increases the rate of HCO_3^- transport (11). The AE1 membrane domain (residues 361-911) carries out the anion exchange activity. The latest AE1 topological model proposed that AE1 is organized in 14 transmembrane domains (TMD) based on homology with *E.coli* UraA uracil permease (32). AE1 forms oligomers in RBC membrane, as it is present as dimeric (60 %) and tetrameric (40 %) protein complexes (33,34).

Two main physiological conditions are associated with mutations in the gene encoding AE1 protein: South East Asian Ovalocytosis (SAO) and Hereditary Spherocytosis (HS). SAO affects the RBC's oval shape and makes individuals with this condition resistant to

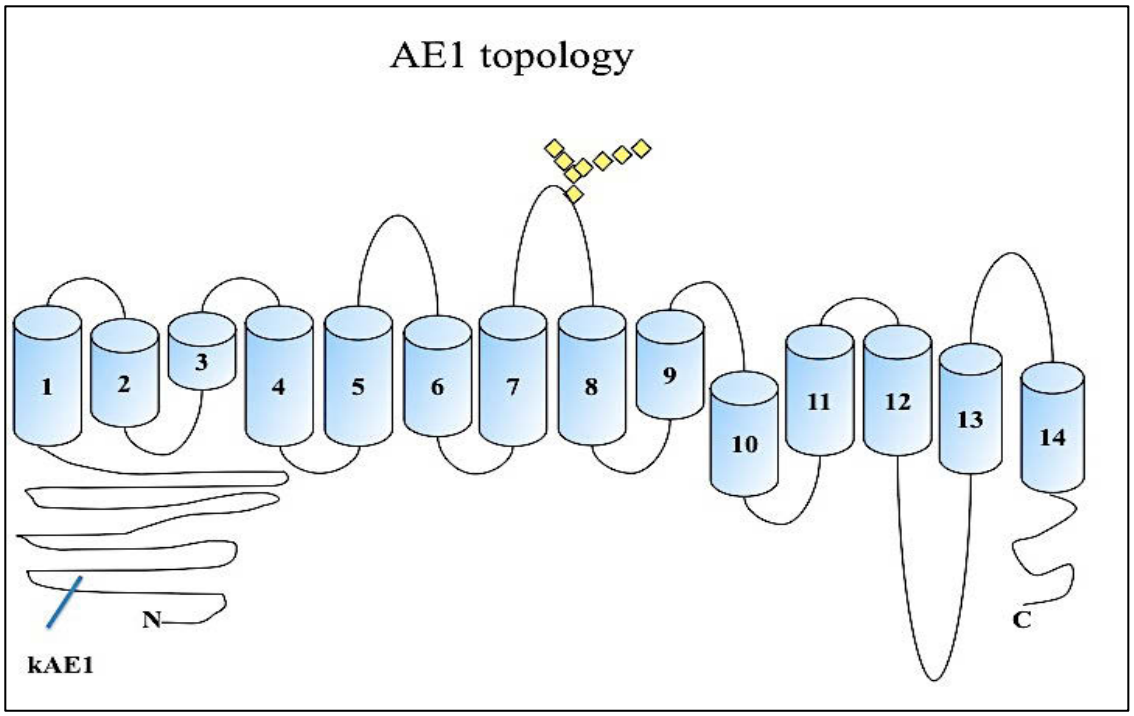

Figure 1.2: AE1 topological model. This model shows AE1 N- and C-termini with the 14 TMD (barrels). kAE1 is 65 amino acids shorter than AE1 (start of the kidney isoform is represented by the blue line). Yellow diamonds represents the N-oligosaccharides attached to the fourth extracellular loop. *The model based on Barneaud-Rocca D. topological model of AE1* (32).

malaria, as Plasmodium falciparum parasite cannot infect SAO-affected RBC (35). The condition results from the deletion of amino acids 400-408 in the first TMD, which impairs AE1 normal folding and anion transport activity (35,36).

HS results from dominant or recessive point mutations in the SLC4A1 gene (37). In HS patients, AE1 mutants are typically misfolded and prematurely degraded during RBC maturation (37). As a result, RBC become spheric, smaller, and more fragile than the regular RBC biconcave disk. HS RBC rupture easily, causing hemolytic anemia (37). HS is characterized by the presence of spherocytes, increased numbers of reticulocytes, splenomegaly, jaundice, and gallstones (38). Blood transfusion and splenectomy are the usual treatments to improve the life of HS patients (39). When dominant HS mutants were heterologously expressed in human embryonic kidney (HEK) 293 cells, they were misfolded and retained in the endoplasmic reticulum (ER) (37). In contrast, some recessive HS mutants reached the cell surface but were not functional. Mutations in other proteins that are connecting RBC surface to its cytoskeleton including spectrin, ankyrin and protein 4.2 can also cause HS disease (40,41).

Ae1$^{-/-}$ mice have fragile erythrocytes due to the absence of Ae1 protein; they developed severe anemia, cardiac hypertrophy, impaired cardiac function, and distal renal tubular acidosis (dRTA) (42,43).

1.2.1.2. kAE1

The kidney expresses a truncated form of AE1 that is 65 amino acids shorter at the N-terminus. This protein, called kidney AE1 (kAE1), results from the use of an alternative promoter in the SLC4A1 gene (44,45) (Fig 1.2). Similarly to AE1 function, kAE1 mediates the reabsorption of HCO_3^- in exchange for Cl^- (44,45). kAE1 is expressed

basolaterally in alpha-IC of the distal connecting tubule and the cortical collecting duct (CCD). Low amounts of kAE1 are also expressed in podocyte cells in the kidney (46,47). kAE1 protein forms dimers in kidney cells (48).

Because kAE1 lacks the first 65 amino acids compared to full length AE1, kAE1 functions differently than erythroid AE1. For instance, kAE1 does not bind to ankyrin (49). Instead, kAE1 binds kanadaptin protein and colocalizes with it at the intracellular vesicles (50). Kanadaptin is expressed in the kidney alpha IC, it may function as an adaptor protein mediating kAE1 trafficking in rabbit kidney alpha IC (50). Surprisingly, human kanadaptin and human kAE1 did not bind to each other in HEK 293 cells. Further studies showed that human kanadaptin is mainly localized in the nucleus, and is therefore unlikely to have a role in kAE1 biosynthesis and targeting in human (51). kAE1 also binds directly to adaptor protein 1A (AP-1A) μ subunit via the tyrosine motif Y_{904}DEV as shown by yeast two hybrid assay (52). Knockdown of this μ subunit of AP-1A (μ1A) in HEK 293 cells by short interfering RNA (siRNA) impaired kAE1 localization at the plasma membrane. AP family and their interaction with kAE1 will be discussed in more detail in the last section of the introduction (Page 47).

kAE1 also interacts with the glycolytic enzyme GAPDH through the D_{902}EYDE amino acid sequence (53). This binding is important for kAE1 trafficking to the cell surface as knockdown of GAPDH resulted in kAE1 intracellular retention in Madin-Darby canine kidney (MDCK) cells (53). Unlike AE1, kAE1 / GAPDH interaction does not affect GAPDH glycolytic activity and is not altered by phosphorylation (53), suggesting a different role for kAE1 / GAPDH interaction in the kidney. GAPDH may participate in intracellular membrane transport, fusion, microtubule bundling, and kinase

activity (54). In addition, GAPDH may be involved in cargo transport (55) and in the ER to Golgi transport through interaction with Rab2 and microtubules (56). GAPDH may participate in the forward trafficking of kAE1, since the knockdown of GAPDH decreased the cell surface kAE1 (53).

Two cytosolic kAE1 tyrosine residues, tyrosine 359 and 904 in the N- and C-termini, respectively, are phosphorylated (57) in response to hyperosmolarity, hypertonicity, or high extracellular bicarbonate concentration, which caused kAE1 internalization from the basolateral membrane. These findings support that alpha-IC may regulate kAE1 phosphorylation to adjust the amount of basolateral kAE1 under different physiological conditions (57).

Growing evidence suggests that kAE1 could play a role in maintaining cell membrane integrity in podocytes and alpha-IC. In podocytes, kAE1 binds to nephrin, a protein involved in the maintenance of the glomerular slit diaphragm (46,47). In HEK 293, MDCK cells and alpha-IC, kAE1 was reported to directly bind to integrin-linked kinase (ILK) protein, an actin binding protein. Via this interaction, ILK links kAE1 to the underlying actin cytoskeleton (58,59).

1.2.1.3. AE2 and AE3

AE2 and AE3 have a similar topological structure as AE1, with around 50 % sequence identity (60,61). The TMD of AE2 and AE3 consist of 14 TM segments with a difference in the length of the N-terminal cytoplasmic domain. AE2 has up to five N-terminal variants AE2 (a, b1, b2, c1, and c2) due to the presence of alternative promoters (60,62-64). AE2 is ubiquitously expressed in cells, with high abundance reported in the choroid plexus, gastric parietal cells, renal collecting duct, and thick ascending limb (65-67). *Ae2*$^{-}$

$^{-/-}$ mice are thin, weak and growth-retarded compared to wild type. They are also toothless; their stomach parietal cells are unable to produce acid thus revealing alkaline gastric contents. Most *Ae2* deficient mice died early at the time of weaning (68).

AE3 is expressed as two N-terminal variants: the full-length AE3 variant is expressed in the brain (69), retina (70) and smooth muscles (71). The shorter cardiac AE3 variant is expressed in the heart and retina (72). Alanine 867 to Aspartate (A867D) substitution in AE3 has been reported in patients with idiopathic generalized epilepsy. This AE3 mutant is functionally less active than AE3-WT, which likely affects the intracellular pH as well as the cell volume in brain cells (73,74). However, the AE3-A867D mutant had a similar expression pattern and was similarly regulated by PKA as AE3-WT protein (74).

Ae3$^{-/-}$ mice showed defects in brain, vision and hearing (75). These mice also showed reduced seizure threshold when induced by chemicals. Finally, *Ae3*$^{-/-}$ mice also have cardiac defects, as their cardiomyocytes show a reduced response to stimuli-induced hypertrophic growth (76).

1.2.2. Electrogenic Na^+ - HCO_3^- cotransporters

The electrogenic Na^+-coupled HCO_3^- cotransporters NBCe1 and NBCe2 cotransport Na^+ and HCO_3^- with a stoichiometry of 1 Na^+: 2 HCO_3^- or 1 Na^+: 3 HCO_3^- (77,78). NBCe1 is expressed as three variants (A, B, C), which are expressed in different tissues. NBCe1-A is expressed at the basolateral membrane of renal proximal tubule cells (79). NBCe1-B is expressed in pancreas (80) and heart (81) and NBCe1-C is expressed in rat brain (82). NBCe1-A will be discussed in the proximal renal tubular acidosis section (section 1.5.1).

NBCe2 is found as seven variants (a-g) (83,84). This protein is mainly expressed

in liver, testis, brain, kidney, heart, liver, spleen, small intestine and placenta (85,86). *Nbce2*$^{-/-}$ mice are hypertensive, present vision and neurological defects and develop renal metabolic acidosis (87,88).

1.2.3. Electroneutral Na^+ - HCO_3^- cotransporters

The electroneutral Na^+ - coupled HCO_3^- cotransporter NBCn1, which functions with a $1Na^+$: $1HCO_3^-$ stoichiometry, is expressed in the heart, skeletal muscles, spleen, testis, brain, lungs, liver, and in kidney thick ascending loop of Henle (6,89,90).

NBCn2 is expressed in the brain, where it exchanges HCO_3^- for Cl^- ions in a sodium-dependent manner, in addition to co-transporting Na^+ and HCO_3^- in a $1Na^+$: $1HCO_3^-$ stoichiometry (91). The *slc4a10* $^{-/-}$ mice exhibit a smaller brain ventricular volume and protection against epileptic seizures, supporting that NBCn2 participates in neural pH control and in the cerebrospinal fluid secretion (92).

The NDCBE electroneutral Na^+ - coupled HCO_3^- cotransporter, also called SLC4A8, has a 1 Na^+: 2 HCO_3^-: 1 Cl^- (inward/outward/inward) stoichiometry (93). It is expressed in the brain, (91,94) and beta-IC in the kidney cortical collecting duct (95). *Slc4a8*$^{-/-}$ mice have neurological defects, likely via mis-regulating presynaptic glutamate release (96).

1.2.4. SLC26 family

The SLC26 family of bicarbonate transporters consists of 11 members SLC26A1-11. SLC26A10 is a pseudogene (97). In contrast with SLC4 gene family, the function of SLC26 family is Na^+-independent with a broader range of anions transported than the SLC4 family. In addition to the HCO_3^- and Cl^- ions, SLC26 family members can transport I^-, SO_4^-, oxalate, formate, and glycolate and some SLC26 proteins behave as anion

channels. SLC26A3, 4, 6, 7, and 9 proteins are the only proteins from this family that transport HCO_3^- (98-100). The SLC26 family members share the same topological structure: they have both cytosolic N- and C-termini and 12 TMD. The SLC26 C-termini contain a STAS domain (Sulfate Transport and Anti-Sigma factor antagonist) (101), which regulates SLC26 protein interactions with other proteins like CFTR (102) and CAII (103).

The SLC26A3 (DRA) is apically expressed in colon, sweat glands, testis, enterocytes and epididymis (104). Mutations in the SLC26A3 gene cause congenital chloride diarrhea (104). SLC26A4 (also called Pendrin) is apically expressed in thyroid, inner ear, prostate, airway epithelial cells, as well as kidney beta-IC (105). Mutations in the SLC26A4 cause Pendred syndrome, which is discussed in more details in the Pendred syndrome section (1.5.2).

Another member of the SLC26 family, SLC26A7 has been linked to the dRTA disease (106). It is expressed basolaterally in thyroid, stomach, retina, olfactory epithelium, and alpha-IC (107). The SLC26A11 protein is expressed mainly in the kidney and brain and it functions as a Cl^- transporter.

1.3. Blood pH regulation

The control of intracellular and extracellular pH is of great importance for optimal physiological processes. The arterial blood pH should be strictly maintained within the range 7.35-7.45. A slight change in the plasma pH would sharply affect normal enzyme function and cause protein denaturation, which may lead to death (108,109).

A decrease in plasma pH (pH< 7.35) is called acidemia, reflects an increase in arterial $[H^+]$. Acidosis could originate from a respiratory defect where blood CO_2 partial

pressure (pCO_2) represents more than 5.7 kPa, or from a metabolic defect when arterial [HCO_3^-] decreases to less than 22 mM (110). A blood pH increase due to pCO_2 decreasing to less than 5.7 kPa or [HCO_3^-] higher than 26 mM is called alkalosis (110). Changes in pH are controlled by different strategies. Buffers can reversibly bind to hydrogen ion and therefore minimize pH changes (110). Extracellular buffers include bicarbonate and ammonia, whereas proteins and phosphate act as intracellular buffers (111).

If the extracellular buffers are unable to bind the excess of H^+, the lungs and kidneys will participate in elimination of excessive acid or base. A decrease in pH is sensed by arterial chemoreceptors and leads to increased respiration rate, which results in an increase of pO_2 and a decrease in pCO_2. The pulmonary response occurs over minutes to hours. It is about 50 to 75 % effective and does not completely normalize pH (108,109).

The renal response to acid-base imbalance is quite slow compared to the action of buffers or respiratory organs; it takes several days to adjust the amount of reabsorbed HCO_3^- or excreted H^+ (112-114). Renal response for acid-base imbalance in addition to bicarbonate reabsorption along the different nephron segments is discussed in the following section.

1.4. Renal response to acid base imbalance and bicarbonate reabsorption

Under normal circumstances, the kidneys filter approximately 4320 mEq / day of HCO_3^- (24 mEq/L X 180 L / day, where 180 L / day is the amount of filtered blood per day) (115). To completely reabsorb all the filtered bicarbonate, kidneys, must secrete 4320 mEq / day of hydrogen ions. Bicarbonate reabsorption occurs predominantly in the

proximal tubule (PT) (about 80 %) (114). The remaining HCO_3^- is reabsorbed in the thick ascending limb (TAL), the distal tubule (DT), and the cortical collecting duct (CCD) where urine is acidified to pH of 4.5 to 6, and the remaining HCO_3^- that escaped the PT is reabsorbed (Fig 1.3) (114,115).

The H^+ ions are buffered in the blood and are not filtered by the kidney as free ions. Secreted H^+ ions combine with urinary buffers to be excreted as titrable acids and ammonium, or combine with filtered HCO_3^- leading to HCO_3^- reabsorption (114).

1.4.1. Bicarbonate reabsorption in the PT

In the PT, H^+ ions are secreted by two mechanisms: via an apical Na^+-H^+ antiporter 3 (NHE3) and via H^+-ATPase (proton pump) (Fig 1.4) (114). Secreted H^+ ions are excreted by binding to buffers, such as HPO_4^{2-} and creatinine, or to NH_3 to form NH_4^+. Two-thirds of proximal HCO_3^- reabsorption occurs via H^+ secretion by NHE3, whereas the other third of HCO_3^- reabsorption occurs via the apical H^+-ATPase pump that secretes H^+ to the lumen (113,114,116).

Carbonic anhydrases play an important role in H^+ secretion and HCO_3^- reabsorption in PT cells (Fig 1.4) (117). H_2CO_3 is converted into CO_2 and H_2O by the membrane bound luminal CAIV, which is expressed along the PT. Luminal CO_2 enters the PT cells by diffusion (Fig 1.4) (118), and in presence of H_2O is converted into H^+ and HCO_3^- by cytosolic CAII enzyme (Fig 1.4) (119). The H^+ ions are secreted into the tubular lumen across the apical membrane via apical NHE3 or H^+-ATPase, where they bind to free HCO_3^- to form H_2CO_3 again (114,120,121). Intracellular HCO_3^- is reabsorbed through basolateral electrogenic symporter NBCe1 ($3HCO_3^-$: $1Na^+$) (Fig 1.4) (114). PT cells express high amounts of angiotensin II receptors (122). Angiotensin II is a

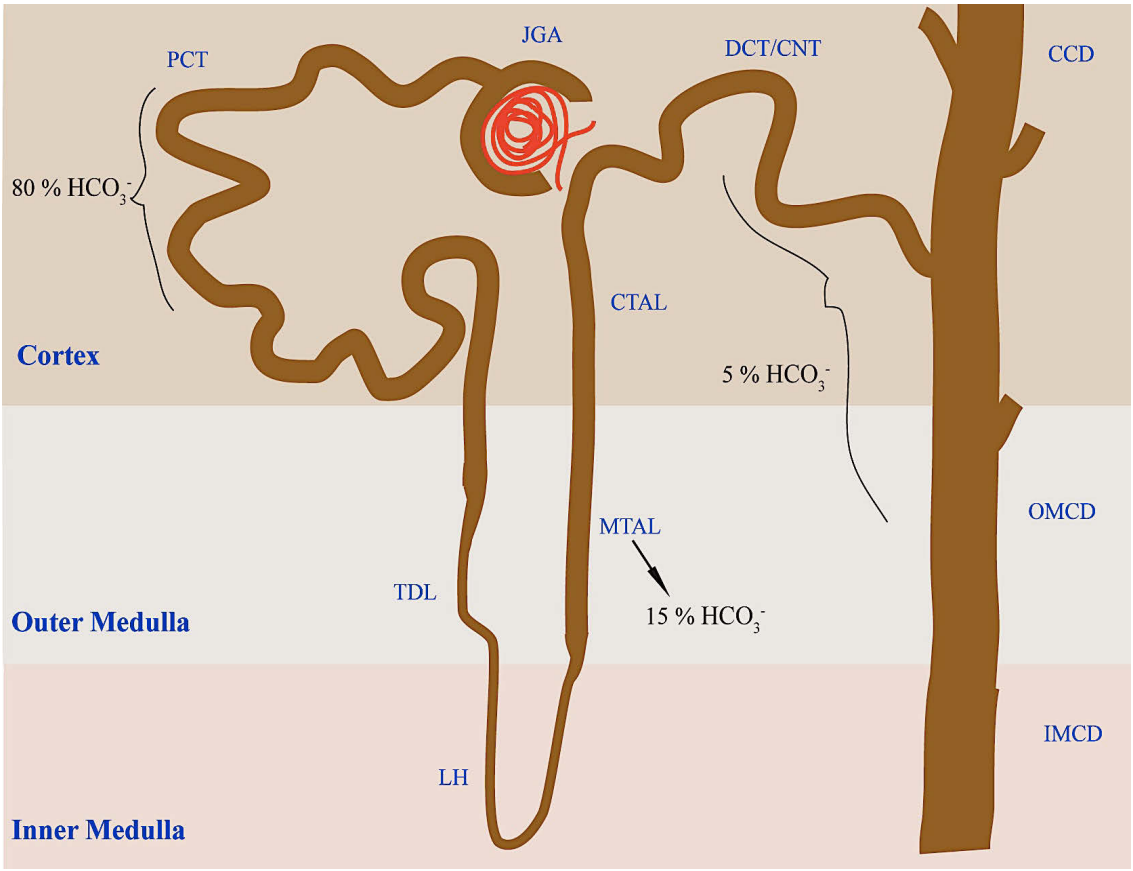

Figure 1.3: Nephron anatomy model. This model includes the fractional delivery of bicarbonate to the various nephron segments, which varies with an individual's diet; the shown percentages are based on a normal diet of healthy individual [5]. JGA: Juxtaglomerular Apparatus. PCT: proximal convoluted tubule, TDL: thin descending limb, LH: loop of Henle, MTAL: medullary thick ascending limb, CTAL: cortical thick ascending limb, DCT: distal convoluted tubule, CNT: connecting tubule, CCD: cortical collecting duct, OMCD: outer medullary collecting duct, IMCD: inner medullary collecting duct.

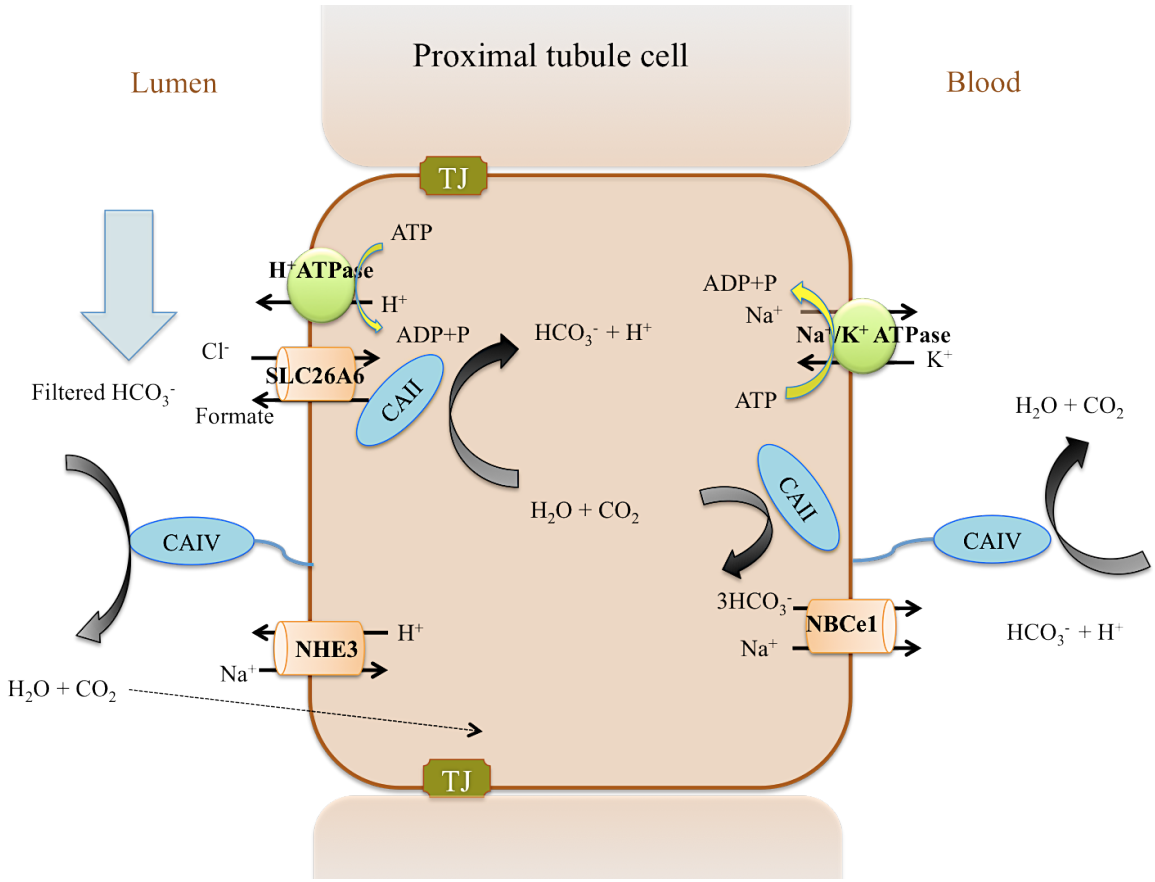

Figure 1.4: Bicarbonate absorption in the proximal tubule. The filtered HCO_3^- is converted in the lumen to H_2O and CO_2. The CO_2 diffuses through the apical membrane into the cell where it is converted again to HCO_3^- and H^+ by CAII. HCO_3^- is transported by basolateral NBCe1 to the blood along with Na^+. There the HCO_3^- is converted again by CAIV to H_2O and CO_2. TJ: Tight junctions, Modified from (121).

potent regulator of HCO_3^- reabsorption in this nephron segment (122). A low dose of angiotensin II has a stimulatory effect on the rate of HCO_3^- reabsorption, while high dose decreases the rate of HCO_3^- reabsorption (123).

1.4.2. Bicarbonate reabsorption in TAL

Around 15 % of the filtered HCO_3^- is reabsorbed via the thick ascending limb (TAL) of the loop of Henle (Fig 1.3) via the apical Na^+-H^+ exchanger NHE3 and H^+-ATPase and the basolateral NBCn1. This process is increased under metabolic acidosis and high sodium intake and inhibited under metabolic alkalosis conditions. (124-126).

1.4.3. Bicarbonate reabsorption in the DT and CCD

The DT and the CCD are also involved in acid-base homeostasis (127,128). The CCD fine-tunes HCO_3^- reabsorption and H^+ secretion. This segment is composed of two different cell types: principal cells that transport water, Na^+ and K^+, and IC, which mediate acid-base transport (Fig 1.5) (129). Principal cells are involved in sodium and water reabsorption via the apical epithelial sodium channel ENaC and aquaporin 2, respectively, and the basolateral Na^+/ K^+ ATPase (Fig 1.5) (130). At least three types of IC have been identified: alpha, beta and non-alpha, non-beta-IC (131,132).

Intercalated cells participate in acid-base homeostasis. They express high amounts of cytosolic CAII and are interspersed among the principal cells of the distal convoluted tubule (DCT), connecting tubule (CNT), and collecting duct (131,133). They are distinguished from other cell types by their positive staining for the vacuolar H^+-ATPase and CAII (133,134). Alpha-IC have a columnar shape with apical micro projections. These cells express kAE1 at their basolateral membrane and vacuolar H^+-ATPase is expressed at the apical side (Fig 1.5) (129,134).

Almost mirroring the alpha-IC, beta-IC display the opposite polarity, with the bicarbonate exchanger pendrin, (SLC26A4), located at the apical membrane and vacuolar H^+-ATPase at the basolateral membrane (Fig 1.5). With their squamous shape, beta-IC have a smooth apical surface, an organelle-free zone below the apical membrane, and cytoplasmic vesicles dispersed throughout the cells (131,132,135). Non-alpha, non-beta IC are mainly located in the CNT. These large cells express both pendrin and vacuolar H^+-ATPase at their apical membrane, and display a large number of mitochondria and intracellular vesicles (119,132). The function of non-alpha, non-beta IC is not known. The presence of apical vacuolar H^+-ATPase and bicarbonate transporter suggests that these cells could be involved in either proton or bicarbonate secretion or that they are an intermediate cell-type undergoing interconversion (119,131,132).

As in the PT cells, CO_2 enters the alpha-IC, where CAII catalyzes its hydration to produce one HCO_3^- and a proton H^+. The proton is pumped across the apical membrane via the vacuolar H^+-ATPase and the HCO_3^- ion is transported across the basolateral membrane by kAE1 protein (113,136). Therefore, the function of alpha-IC results in both net reabsorption of bicarbonate and concomitant proton secretion into the urine.

Also rich in CAII, beta-IC reabsorb protons via the basolateral vacuolar H^+-ATPase and excrete bicarbonate into the urine via the apical bicarbonate transporter pendrin (137). In addition to their role in HCO_3^- secretion, beta-IC are also involved in Na^+ reabsorption. Pendrin at the apical membrane of beta-IC cooperates with NDCBE (SLC4A8) for the net reabsorption of Na^+ and Cl^-, driven by HCO_3^- secretion and reabsorption as shown in Figure 1.5.

Metabolic acidosis develops when kidneys are unable to excrete the excess of acid produced daily (138). This can originate from defective proteins along the different nephron segments. The following section will briefly introduce disorders resulting from mutations in different proteins including renal bicarbonate transporters and will focus specifically on distal renal tubular acidosis, a disease caused by mutations on the SLC4A1 gene encoding AE1.

1.5. Diseases associated with acid – base imbalance

1.5.1. Proximal renal tubular acidosis (Type 2 RTA)

Proximal renal tubular acidosis (pRTA) is usually associated with Fanconi's syndrome, a disease of the PT, in which glucose, amino acids, uric acid, phosphate and bicarbonate are not reabsorbed from the urine (115,139). It is characterized with impaired HCO_3^- reabsorption in the PT, which causes metabolic acidosis, hyperchloremia,, hypokalemia, and with urine pH becoming more acidic with pH < 5.5 (Table 1.1) (115,139).

The NBCe1 protein (SLC4A4) co-transports sodium and bicarbonate at a ratio of 1:3 or 1:2 (77). NBCe1-A splice variant is expressed at the basolateral membrane of renal proximal tubule cells (Fig 1.3) (79). Mutations in SLC4A4 gene cause a defect in bicarbonate reabsorption in the renal PT and result in pRTA disease (140). In addition to impaired kidney function, the disease can be associated with growth and mental retardation, pancreatitis, ocular abnormalities, reduced bone density, and abnormal dentition (Table 1.1) (115). The WT NBCe1-A is located at the basolateral membrane of polarized MDCK I cells (141,142).

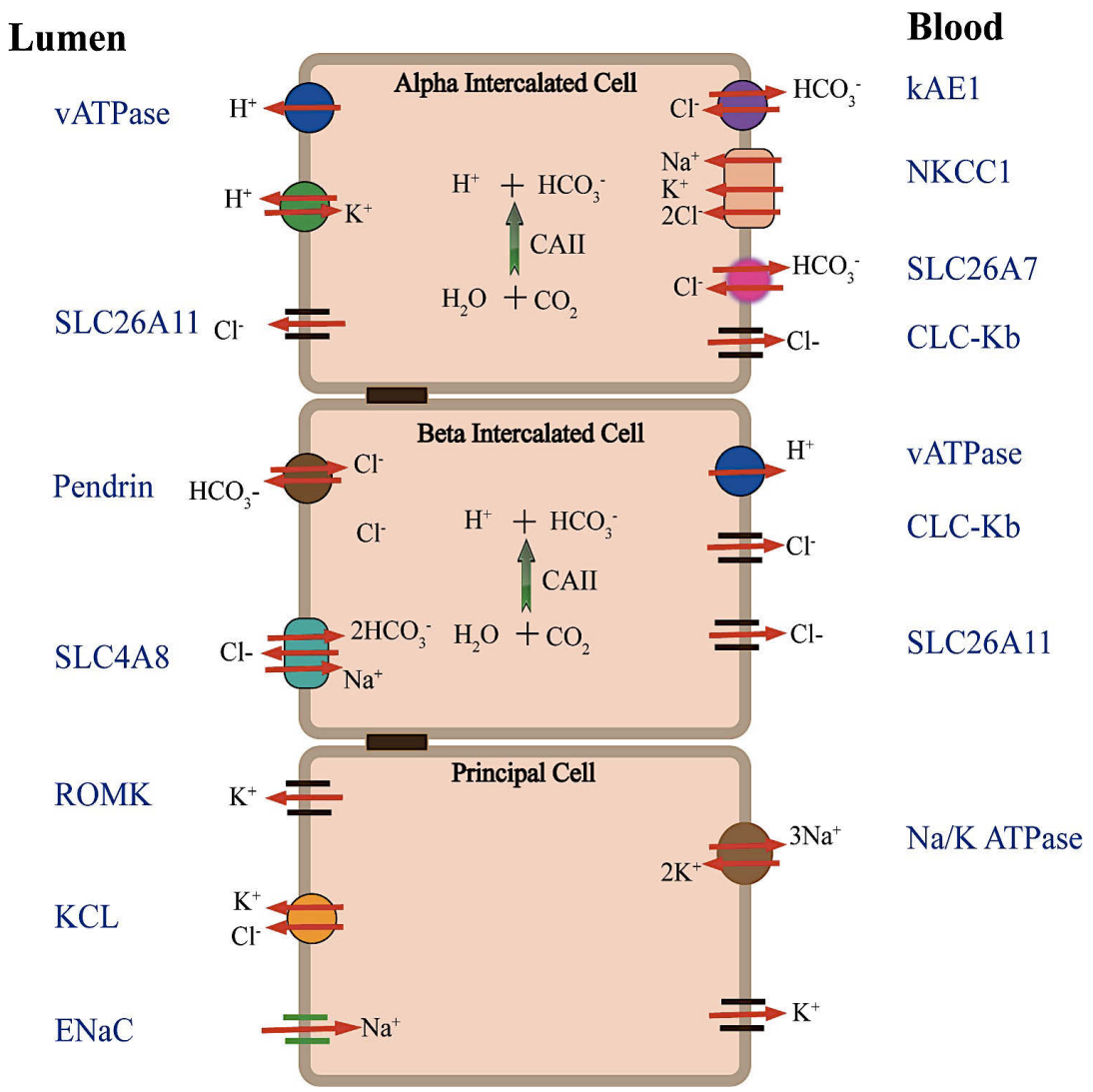

Figure 1.5: Collecting duct cell model. This model shows three CCD cell types with different proteins expressed in each cell type. *Alpha-IC* secrete protons into the lumen through the apical vacuolar H^+-ATPase proton pump and the H^+/K^+-ATPase, and reabsorb HCO_3^- in exchange for Cl^- through the basolateral kAE1. They also express the chloride/bicarbonate exchanger SLC26A7 at the basolateral membrane and the Cl^- channel SLC26A11 at the apical membrane. The Na^+-K^+-$2Cl^-$ cotransporter (NKCC1) is also expressed at the basolateral membrane of these cells, along with the chloride channel ClC-Kb. *Beta-IC* secrete HCO_3^- into the lumen through apical pendrin. Protons are

(Continued from figure 1.5)

effluxed into the blood through the basolateral vacuolar H^+-ATPase. These cells also express the ClC-Kb and SLC26A11 Cl^- channels at their basolateral membrane. At the apical membrane, pendrin's function is coupled to that of SLC4A8 to promote sodium and chloride reabsorption. *Principal cells* regulate ion homeostasis by expressing the epithelial sodium channel (ENaC), a K^+/Cl^- cotransporter (KCC), the renal outer medullary potassium (ROMK) channel in their apical plasma membrane, and the Na^+/K^+-ATPase at the basolateral membrane.

In contrast, the NBCe1-R881C mutant (a common mutation among the pRTA patients) is located at the endoplasmic reticulum (ER) (142). This correlates with data from *Xenopus* oocytes that demonstrated reduced functional activity of the R881C mutant owing to 40 % decreased expression at the plasma membrane of the oocytes.

1.5.2. Pendred syndrome

The symptoms found in pRTA patients are comparable to those observed in mice lacking NBCe1 (143). These *nbce1*$^{-/-}$ mice displayed severe metabolic acidosis, growth retardation, reduced plasma sodium, and abnormal dentition, all symptoms consistent with pRTA. However, no ocular or pancreatic defects were found in these mice (Table 1.1) (143). Pendrin is an anion exchanger encoded by the SLC26A4 gene. It is predominantly expressed in the thyroid, inner ear (cochlea), and kidney. Mutations in the pendrin gene result in a disease called Pendred syndrome, an autosomal recessive disorder characterized by goiter, hypothyroidism, and deafness (Table 1.1) (144). In kidneys, pendrin is expressed at the apical membrane of beta-IC and non-alpha, non-beta IC in the CCD (Fig 1.5) (144) and is responsible for secreting bicarbonate to the pro-urine in alkalotic conditions. It mediates the exchange of Cl^- ions for bicarbonate, sulfate, iodide, and formate (145). Deletion of the *Slc26a4* gene in mice affects secretion of bicarbonate *in vivo* and reduces the apical Cl^-/HCO_3^- exchanger activity in beta- and non alpha-, non beta-IC in the CCD (Table 1.1) (137). In addition, pendrin knockout mice display acidic

Table 1. 1 Diseases associated with abnormal kidney functions.

Protein	Disease	Mutated gene	Knockout mice symptoms	References
Kidney anion exchanger 1 (kAE1)	**Distal renal tubular acidosis (dRTA)** Metabolic acidosis, alkaline urine, hypokalemia, hyperchloremia, hypercalciurea, kidney stones, mild electrolyte imbalance	**SLC4A1**	Severe anemia, complete dRTA, increased serum osmolarity, decreased urine osmolarity, hypercalciuria, dehydration	(43)
v-H+-ATPase subunit B1	Recessive **dRTA** associated with deafness, hypokalemia and dehydration	**ATP6V1B1**	Mild metabolic acidosis	(146, 147)
v-H+-ATPase subunit a4	Recessive **dRTA** associated with deafness, hypokalemia and dehydration	**ATP6V0A4**	Deafness, dRTA accompanied by proximal tubule malfunction, proteinuria and phosphaturia	(148, 149)
SLC26A7	**dRTA**	**SLC26A7**	Complete dRTA, hypotension, failure to reabsorb chloride	(150)
Carbonic anhydrase II	Mixture of recessive **distal and proximal RTA**, can be associated with autosomal recessive osteopetrosis (increased bone density), growth failure, mental retardation and hearing impairment	**CA2**	Renal tubular acidosis symptoms, down-regulation of proteins involved in acid-base homeostasis in intercalated cells such as pendrin SLC26A7, pendrin and AE1	(151)
Pendrin	**Pendred syndrome** Goiter and hearing loss	**SLC26A4**	Renal inability to excrete the excess bicarbonate into the urine, deafness	(137, 152)
NBCe1	**Proximal renal tubular acidosis** Impaired HCO_3^- reabsorption in the PT, metabolic acidosis, hyperchloremia, hypokalemia, acidic urine pH	**SLC4A4**	Severe metabolic acidosis, growth retardation, reduced plasma sodium, and abnormal dentition	(115, 119, 139) (143)

urine, elevated serum bicarbonate, and an increase in urine ammonium excretion (137). However, patients with Pendred syndrome do not display metabolic alkalosis and renal symptoms.

1.5.3. Distal renal tubular acidosis (Type 1 RTA)

In distal renal tubular acidosis (dRTA), kidney alpha-IC are unable to excrete the excess of protons generated as a waste product of metabolism. Children suffering from dRTA have growth failure, present with vomiting and are dehydrated. Patients with dRTA display an increased plasma CO_2 concentration and chloride concentration (hyperchloremia) and a decrease in plasma potassium concentration (hypokalemia). Urine analysis shows an increase in urinary pH and calcium concentration (hypercalciuria) (Table 1.1) (153). The dRTA disease is treated by medications that correct acidemia like sodium bicarbonate, sodium citrate, and potassium citrate (154). If not treated early, dRTA leads to kidney stone formation and kidney failure (155).

Some individual present incomplete dRTA, characterized by an inability to acidify urine spontaneously or following an acute acid load, but without metabolic acidosis and with normal blood bicarbonate concentration on a normal diet. The dRTA symptoms typically appear after an acid challenge (156).

There are multiple origins for dRTA. It can be associated with or result from autoimmune diseases like Sjogren's syndrome, systemic lupus erythematosus, and rheumatoid arthritis (157), but the most common cause for dRTA is an inherited defect. Most dRTA patients inherit dominant or recessive mutations in genes encoding proteins expressed in alpha-IC of the kidney including kAE1 protein, vacuolar H^+-ATPase pump, CAII, and SLC26A7 (Table 1.1). This following section will only discuss hereditary

causes of dRTA.

1.5.3.1. Mutations in the SLC4A1 gene

The most common cause of dRTA is a dominant or recessive mutation in SLC4A1 gene that encodes for kAE1 protein (Table 1.1, Fig 1.5). Previous studies have characterized the effect of mutations in the SLC4A1 gene. MDCK and HEK 293 kidney cells have been used as mammalian cell models to study expression, function and trafficking of kAE1 mutants that cause dRTA. When kAE1-WT is heterologously expressed in MDCK cells, it is located at the plasma membrane of non-polarized and at the basolateral membrane of polarized MDCK cells, reflecting the normal localization of kAE1 in alpha-IC (158-160). When kAE1 mutants are expressed in these cells, they are either mistargeted to the apical membrane or retained either in the ER or the Golgi (37,158-160).

As kAE1 protein forms dimers in kidney cells (48), co-expression of dominant kAE1 mutant with kAE1-WT in MDCK cells resulted in intracellular retention of the kAE1-WT protein. In contrast, when kAE1 recessive mutants were co-expressed with kAE1-WT, the mutants' trafficking was rescued to the cell surface (48,156,158). This thesis focuses on dominant dRTA mutations within kAE1 cytosolic C-terminus. The various mutations within this short cytosolic domain are reviewed below.

KAE1-R901X (also called Band 3 Walton, R901STOP) mutation results in deletion of the last 11 amino acids of kAE1 (161). This mutant retains normal anion exchange activity in *Xenopus* oocytes but fails to localize at the surface of non-polarized MDCK cells (162) and HEK 293 cells (48). Studies in polarized MDCK and MDCK I (a highly polarized subtype of MDCK cells, resembling IC) cells showed that kAE1-R901X mutant is mistargeted to the apical membrane in polarized cells or traffics in a non-

polarized way depending on the degree of polarization of the cells (159,160). As described above, when kAE1-R901X was co-expressed with kAE1-WT to mimic the situation found in dRTA patients, the R901X mutant retained kAE1-WT protein intracellularly (159,163).

KAE1-M909T is another dominantly inherited dRTA mutant within kAE1 cytosolic C-terminus (164). It is located within the putative type II PDZ (PSD-95/Discs-large/ZO-1) interaction domain of kAE1 C-terminus (A_{908}MPV) (165,166). When kAE1-M909T was expressed in *Xenopus* oocyte, it showed normal anion exchange activity, indicating that the mutant is functional (164). When kAE1-M909T was expressed in polarized MDCK cells, it was located in both apical and basolateral membranes (164), supporting that dRTA results from insufficient amount of kAE1 protein at the basolateral membrane.

The compound **kAE1-A888L/D889X** point and deletion mutations are also dominantly inherited in dRTA patients (167). Additionally, dominant frameshift **kAE1-D905Gfs15** and duplication **kAE1-D905dup** dRTA mutations have been identified in kAE1 C-terminus (168,169). These mutants have not been studied in immortalized epithelial cells yet.

The above-described dRTA mutations result in alteration of kAE1 C-terminus that contains binding sites of various proteins including GAPDH (53), CAII (11) and AP-1A (170). These mutations also alter two important motifs, the tyrosine motif Y_{904}DEV and the putative type-II PDZ interaction domain A_{908}MPV (165,166). Tyrosine 904 can be phosphorylated and its phosphorylation state regulates the rate of internalization of kAE1 (57). These mutations likely impair protein interactions that are important for

kAE1 trafficking and localization at the plasma membrane, and consequently, with kAE1's function in bicarbonate reabsorption (52,53,159).

Unfortunately, no animal model is available where kidney AE1 but not erythroid AE1 is knocked out. Such an animal would allow investigations of dominant and recessive dRTA pathophysiology in more detail. Knockout mice lacking both eAe1 and kAe1 (*Ae1*$^{-/-}$) have high mortality rate shortly after birth and severe anemia that complicates further physiological studies. *Ae1*$^{-/-}$ mice develop spontaneous metabolic acidosis, alkaline urine, low blood pH, slightly increased blood chloride and phosphate levels, and reduced Cl^-/HCO_3^- exchange activity in the basolateral membrane of alpha-IC (Table 1.1) (43). WT and heterozygous *Ae1*$^{+/-}$ mice have no apparent defects in urine or blood parameters. Therefore, *Ae1*$^{-/-}$ mice represent a model for some cases of recessive dRTA where no kAE1 protein is present in alpha-IC (43).

1.5.3.2. Mutations in the vacuolar H^+-ATPase gene

Hereditary dRTA can also result from recessive mutations in either a4 or B1 subunits of the vacuolar H^+-ATPase (Fig 1.5) (171). Distal RTA originating from mutated a4 subunit can be associated with sensorineural deafness in addition to other dRTA symptoms (Table 1.1). As no such symptom is observed with mutated B1 subunit, it is proposed that B2 subunit compensates for the loss of B1 subunit, which results in a milder form of dRTA (172). B1 knockout mice do not develop spontaneous acidosis and have no hearing loss (146,147). In contrast, a4 knockout mice develop more severe dRTA phenotype associated with deafness, impaired sense of smell, hypocitraturia, and nephrocalcinosis (148,149).

1.5.3.3. Mutations in the SLC26A7 gene

SLC26A7 (SUT2) is another anion exchanger protein expressed basolaterally in alpha-IC (Fig 1.5), stomach gastric parietal cells and apically in endothelial cells (97). SLC26A7 protein exchanges Cl^- for HCO_3^- and OH^- and sulfate. *SLc26a7* knockout mice display complete dRTA, hypotension, and gastric hypochlorohydra (lack of stomach acid) (Table 1.1) (150). The absence of SLC26A7 protein is apparently not compensated by AE1 protein expression and vice-versa in alpha-IC, indicating that both exchangers are distinctly important for bicarbonate reabsorption in alpha-IC.

1.5.3.4. Mutations in the CAII gene

In addition to PT cells (Fig 1.4), cytosolic CAII is expressed in IC (Fig 1.5) and osteoclasts. Patients with CAII mutations develop a mixture of recessive distal and proximal RTA, in addition to osteopetrosis (increased bone density), growth failure, mental retardation, and hearing impairment (113,173,174). Mice lacking *car2,* the gene encoding CAII, develop renal tubular acidosis and show down regulation of proteins involved in acid-base homeostasis in IC cells including SLC26A7, pendrin and AE1 (Table 1.1) (151).

In summary, inherited dRTA results from dominant or recessive mutations in genes either encoding AE1, vacuolar H^+-ATPase, SLC26A7 or CAII. The severity and pathogenicity of dRTA differ from one individual to another and depends mainly on the mutated protein.

1.6. Membrane protein trafficking and endocytosis

Polarized epithelial cells have an uneven distribution of proteins embedded in the apical or basolateral membrane. The cell polarity is achieved by sorting newly synthesized proteins at the trans-Golgi network (TGN), and sorting endocytotic proteins in recycling

endosomes (175). Epithelial cells use distinct protein transport mechanisms to the apical and basolateral membrane. For example, in the TGN of MDCK cells, proteins are sorted into distinct transport vesicles for direct delivery to the apical and basolateral membranes (176). In contrast, in hepatocytes, apical proteins are transported to the basolateral membrane prior to their apical delivery (177). In Caco-2 intestinal epithelial cell line, proteins can be transported via both pathways (178).

1.6.1. Membrane proteins sorting signals in epithelial cells

Signals required for apical targeting include N- and O-glycans (179,180), glycosylphosphatidylinositol (GPI) lipid anchors (181), and protein domains with affinity to lipid rafts (182). The absence of these signals results in transport to the basolateral surface by default (183). Basolateral sorting signals are tyrosine YXXΦ, where X is any amino acid and Φ is a bulky hydrophobic amino acid, dileucine [D/E]XXXL[L/I] (175) and monoleucine motifs [EEDXXXXXL] (184-186) and [EEXXXL] (186).

1.6.2. Membrane proteins processing and trafficking in epithelial cells

Plasma membrane proteins are synthesized on the rough ER, where most of them undergo glycosylation by addition of high mannose oligosaccharides, which are used by the quality control machinery to monitor protein-folding (187,188). Only properly folded proteins can traffic to *cis*–Golgi via COPII coated vesicles, before proceeding forward through *medial*- and TGN. At the Golgi, the high mannose oligosaccharide is modified to complex oligosaccharide (187,188). From the TGN, membrane proteins travel through clathrin coated vesicles (CCV) to early endosomes (EE) or directly to the plasma membrane. Adaptor proteins are involved in CCV formation as they mediate the binding of cargo proteins to clathrin (Fig 1.6) (189,190). Proteins at the plasma membrane may be

endocytosed to common recycling endosomes (CRE) again via CCV. At the CRE, the proteins either recycle back to the plasma membrane or are targeted to other cellular organelles (191,192).

1.6.3. Membrane protein endocytosis

Endocytosis is the process by which membrane proteins (cargo) are internalized from the plasma membrane. Endocytosed proteins traffic back to the CRE or the TGN where they are sorted again and either returned back to the plasma membrane or to other cellular organelles (193). Depending on the type of cargo and molecular machinery driving the internalization process, there are several endocytosis pathways: clathrin-mediated endocytosis, caveolae / lipid raft mediated endocytosis, macropinocytosis, and phagocytosis (193). Clathrin-mediated endocytosis is the best-described type of endocytosis. It begins with clathrin recruitment by AP-2, which mediates assembly of the clathrin coat. The role of different AP-2 subunits in cargo selection will be detailed in the next section. Small GTPase dynamin mediates the fission of the budding clathrin-coated vesicle from the membrane (Fig 1.6) (194,195). Other proteins like synaptojanin, auxilin, Hsc70 uncoat the vesicle. After uncoating, the vesicle fuses with the sorting endosome from where endocytosed proteins either recycle back to the plasma membrane, or enter late endosomes, either via an endosomal carrier vesicle or direct maturation of the early endosome into a late endosome. The late endosome in turn fuses with a lysosome where digestion occurs due to the low luminal pH (196). Figure 1.6 summarizes the major steps of CCV vesicle formation from the donor compartment to the acceptor compartment. The next part will discuss AP and their role in protein trafficking.

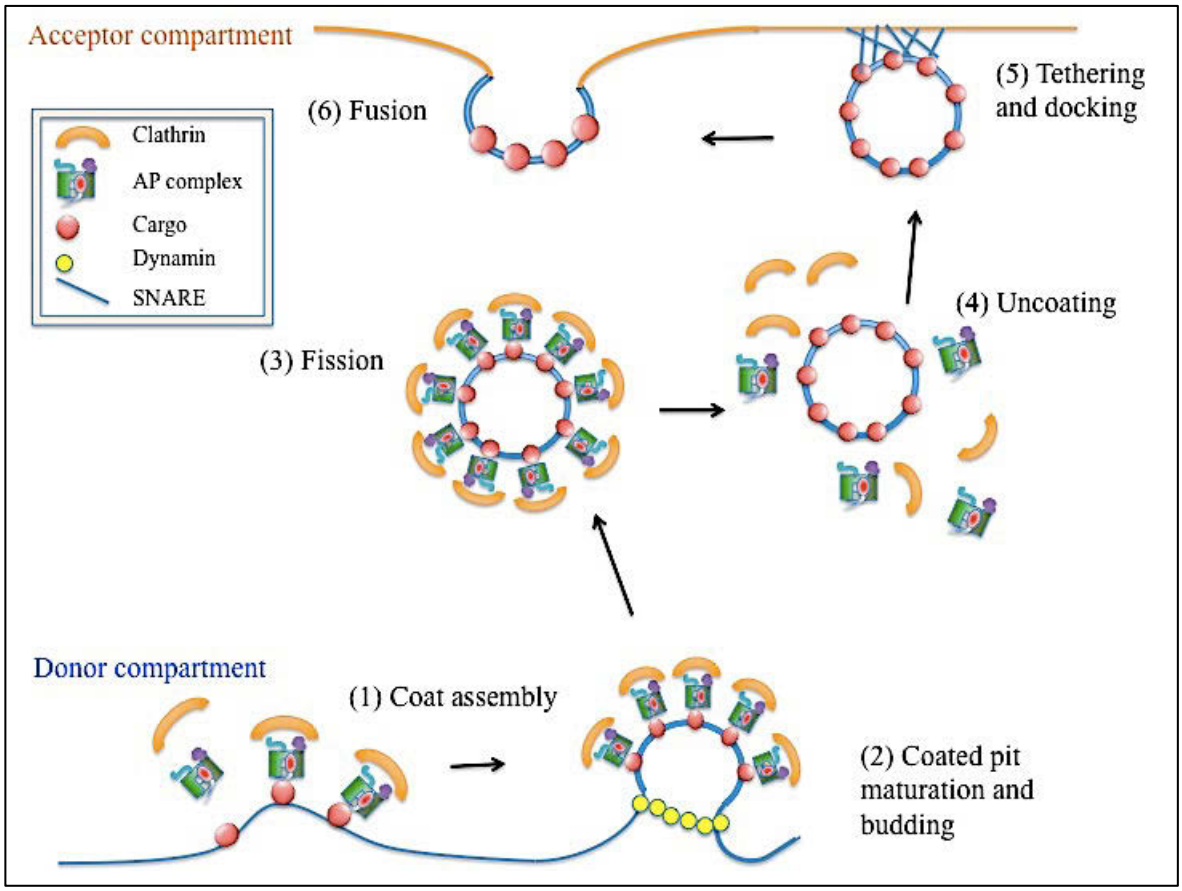

Figure 1.6: Major steps of CCV formation from the donor membrane to the acceptor membrane. (1) Adaptor proteins concentrate cargo proteins at the donor membrane and recruit clathrin to form CCV. (2) Once the vesicle buds, a dynamin small GTPase mediates the vesicle scission from the donor membrane. (3) The formed CCV travels toward the acceptor membrane. (4) The clathrin coat is removed from the vesicle. (5) Vesicles tethering and docking is a selective process with high fidelity mediated by SNARE proteins that ensure vesicle anchoring prior to vesicle fusion as in step (6).

1.7. Adaptor proteins and their role in protein trafficking

The AP complex family shares common conserved morphological and biochemical characteristics (197-199). At this date, five AP complexes have been identified in mammals (Fig 1.7). They play important roles in transport vesicle formation and cargo selection in post-Golgi trafficking pathways (Fig 1.6) (189,190). AP complexes bind to cargo proteins and facilitate their loading to budding vesicles from the donor membrane. This binding enhances the recruitment of clathrin to allow CCV formation that will transport cargo proteins towards the recipient membrane as described earlier (Fig 1.6) (200).

AP-1 and AP-3 exist in two forms: AP-1A and AP-3A are ubiquitously expressed in cells, while AP-1B and AP-3B are only expressed in epithelial cells and neurons, respectively (201). Each AP is composed of four adaptin subunits, two large adaptin subunits (β1-5 and γ,δ,α,ε, ζ), a medium (μ1-5) and one small (σ1-5) subunit (189,190)(Fig 1.7). Unlike other AP complexes, AP-4 and 5 are not associated with clathrin (202).

Each subunit in the AP complex performs a specific function within the complex. For example, one of the large subunits in each AP complex (γ,δ,α,ε,ζ) mediates binding to the target membrane (203). β-adaptins recruit clathrin to form CCV that mediate protein transport (204). The C-terminus of μ subunits are involved in cargo selection and recognize the YXXΦ motif on cargo proteins, while the N-terminus of the μ subunit binds to AP complex adaptins. During cargo protein recruitment, a linker in the μ subunit is phosphorylated, which results in a conformational change that exposes the C-terminus of the μ subunit to the cytosol and allows for cargo and membrane lipid binding (205).

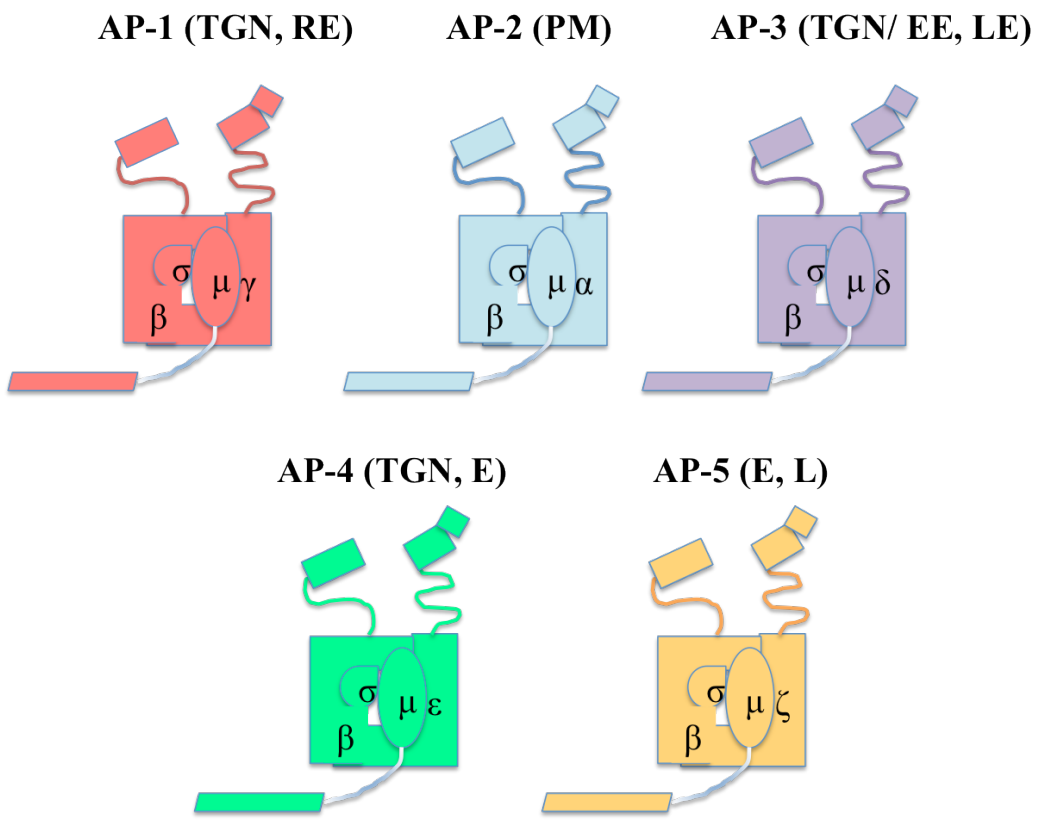

Figure 1.7: The AP complexes. AP complexes 1-5 share the same morphological characteristics; they are tetrameric proteins composed of two large subunits, (β1-5) and (γ, δ, α, ε, and ζ), a medium (μ1-5) and one small (σ1-5) subunit. AP-1 is expressed in the trans-Golgi network (TGN) and recycling endosomes (RE) and it is involved in polarized protein trafficking and recycling. AP-2 is expressed at the plasma membrane (PM) and is involved in endocytosis. AP-3 transports cargo proteins from TGN or early endosomes (EE) to late endosomes (LE). AP-4 may be involved in protein transport from the TGN. AP-5 is involved in the Endosomal (E) to lysosome (L) pathway.

The small σ subunit is involved in AP complex stability (201,203). The different AP complexes function and location will be discussed in the following sections.

1.7.1. Adaptor protein 1A/B

AP-1A complex is located at the TGN and in endosomes (Fig 1.8). It binds to PI_4P (Phosphatidylinositol 4 phosphate) and Arf1 small GTPase in the TGN, where it is involved in cargo protein transport to recycling endosomes and to the cell membrane (206,207). The membrane recruitment of AP-1A depends on PI_4P that is enriched at the TGN (208). AP-1B is also located at the TGN and in recycling endosomes, where it binds to $PI(3,4,5)P_3$ (Phosphatidylinositol 3, 4, 5 triphosphate) and Arf6 (209,210). Interestingly, $PI(3,4,5)P_3$ is important for AP-1B recruitment to recycling endosomes (209) as the absence of $PI(3,4,5)P_3$ from recycling endosomes leads to missorting of AP-1B dependent cargo to the apical membrane (209). AP-1B is involved in basolateral protein biosynthetic and recycling routes, and in cell polarity (165).

1.7.1.1. Adaptor protein 1A/B subunits

In addition to the AP-1 μ adaptin that has two isoforms μ1A and μ1B, γ subunit has also two isoforms (γ1 and γ2), and σ1 adaptin has three isoforms (σ1A, σ1B, and σ1C) (211). The focus of this section will be only on the μ1A and μ1B isoforms. AP-1 complex not only binds to cargo proteins through its μ subunit but also via γ and σ subunits that recognize tyrosine (YXXΦ) and di-leucine ([D/E]XXXL[L/I]) based sorting signal respectively (212,213). AP-1B is distinguished from AP-1A by the 50 kDa μ subunit only. μ1A and μ1B share 79 % amino acid identity (166).

1.7.1.2. Adaptor protein 1A/B function

In spite of this close homology, AP-1A and AP-1B have distinct functions in endosomal /

lysosomal sorting and basolateral membrane targeting (214). AP-1A mediates direct basolateral sorting of cargo proteins like kAE1 from the TGN (215). In contrast, AP-1B mediates basolateral sorting and recycling of cargo proteins from recycling endosomes (216).

The tissue specific AP-1B is expressed in epithelial kidney, intestine, salivary gland and lung cells (166). Interestingly, AP-1B is absent from specific epithelial cells such as kidney proximal tubule cells, retinal pigment epithelial cells and liver hepatic cells (217,218).

Additionally, AP-1A and B have different cargoes and functions. A previous study showed that neither can AP-1A substitute for AP-1B in basolateral transport of LDLR (AP-1B cargo specific protein) nor will AP-1B substitute for AP-1A in Furin (AP-1A cargo specific protein) trafficking (219). AP-1B sorts basolateral plasma membrane proteins like vesicular stomatitis virus G (VSVG) in both biosynthetic and recycling routes, and transferrin receptor (TfnR) in the biosynthetic route in non polarized cells (216).

1.7.1.3. Adaptor protein 1A/B diversity

The physiological importance of AP-1A and B has been studied in different organisms. Knocking out of any AP-1 adaptins in the *Nematode (Caenorhabditis elegans)* causes growth arrest at the embryonic stage, highlighting the importance of AP-1 complex in embryonic development (169,220,221).

Moreover, AP-1 acts early during cell differentiation of the external sensory organ of *Drosophila melanogaster* (222,223). AP-1A is a negative regulator of the Notch-mediated cell fate through regulation of basolateral sorting of Sanpodo (an

activator and a binding partner of Notch) in the sensory organ cells.

In Zebrafish (*Danio rerio*), three μ1 subunits (A, B, and C) are expressed. Unlike in mammals, Zebrafish μ1A is not ubiquitously expressed. Instead, it is only expressed in tissues where μ1B is absent, like the brain, skeletal muscles, eye, heart and testis (224,225). While Zebrafish μ1A and B have high homology to human μ1A and B, μ1C that is expressed only on Zebrafish showed 80 % sequence identity with human μ1A and B (225). The physiological importance of μ1A and B subunits in Zebrafish was addressed through the double Knockdown of μ1A/B. These animals showed severe defects in kidney function and developed cardiac edema (225).

1.7.1.4. Adaptor protein 1A/B knockout mice models

The role of AP-1 in mammals has been studied in knockout mice for several AP-1 subunits. A recent study showed that σ1B knockout mice developed lipodystrophy, a fatty tissue disorder characterized by a selective loss of body fat (226). The knockout of γ subunit is lethal at the embryonic stage E3.5 of development (227). μ1A knockout mice also die early at embryonic stage E13.5 (228). In μ1A knockout cells, the remaining subunits that normally form AP-1A complex fail to locate to the TGN (228). Further, cation-dependent mannose 6 phosphate receptor (CD-MPR) and cation independent MPR (CI-MPR), which are both cargo proteins that exit the TGN via AP-1, fail to recycle back from endosomes to the TGN, and instead accumulate in endosomes, indicating that in absence of μ1A, retrograde transport to the TGN is blocked (228).

The role of μ1B in maintaining cell polarity is emphasized in μ1B knockout mice. In contrast with μ1A, μ1B knockout mice survive after birth. These mice show growth retardation, polarity defect in the intestinal epithelial cells, and the majority die by

the age of eight weeks (229). μ1B basolateral cargo proteins like EphB2, LDLR and E-cadherin are mis-localized in μ1B knockout mice (185,198,230). Apical proteins such as villin were also mis-localized in μ1B knockout mice intestine causing apical-basolateral conversion. This resulted in the formation of ectopic microvilli like structure at the basolateral sites, suggesting an involvement of μ1B in intestine apical proteins sorting (229). Cytokine receptor proteins like interleukin 6 signal transducer (IL-6st) and the poly-immunoglobulin receptor (pIgR) were also mislocalized in μ1B knockout mice intestine, which resulted in immunocompromised mice highly susceptible to bacterial infections (231).

1.7.2. Adaptor protein 2

AP-2 mediates the formation of CCV that transport endocytosed proteins from the plasma membrane to early endosomes (Fig 1.8) (232) (233). AP-2 is recruited to the plasma membrane via the binding of μ and α subunits to PIP_2 (Phosphatidylinositol 4,5-bisphosphate) (234). The μ2 subunit of AP-2 is responsible for cargo selection, it binds to the endocytosis signal YXXØ, and to α and σ2 that recognizes the dileucine [DE]xxxL[LI] motif (235,236). AP-2 also acts as a cargo protein receptor to selectively sort transmembrane proteins including TfnR and some lysosomal-associated membrane proteins (237) (238). μ2 knockout mice die before the E3.5 blastocyst stage (239), suggesting that AP-2 complex is essential for early embryonic development

1.7.3. Adaptor protein 3 A/B

AP-3A transports cargo proteins from TGN or early endosomes to late endosomes, multivesicular bodies or lysosomes (Fig 1.8) (189) (232) (240). AP-3B is expressed in neurons, where it is involved in the formation and release of exocytic organelles (241).

1.7.4. Adaptor protein 4

The role of AP-4 is still unclear at the physiological and molecular levels. AP-4 is conserved in mammals and higher eukaryotes but not in lower eukaryotes like nematodes and fruit fly (238). It mediates the transport of certain lysosomal proteins from TGN to lysosomes (Fig 1.8) and might be involved in the basolateral transport of LDLR in polarized epithelial cells (189). The AP-4 β *(AP4B1)* knockout mice developed abnormalities in neurons. The axon terminal regions of neurons were swollen and contain autophagosomes that are rich with AMPA receptor and its regulatory protein (TARPs). The TARP protein trafficking is regulated by the AP-4 protein (242) On the other hand, AP-4 ε *(AP4E1)* knockout female mice developed significant abnormalities in their hearts (243).

1.7.5. Adaptor protein 5

The recently identified AP complex, AP-5 is involved in late endosomal to lysosomal transport pathway (Fig 1.8) (202). This complex does not bind to clathrin but binds to SPG11 and 15, two proteins mutated in patients with hereditary spastic paraplegia which have a structure similar to clathrin (190).

1.8. The role of adaptor proteins in regulating kAE1 trafficking

The importance of AP-1A in kAE1 trafficking was first reported by Sawasdee and colleagues who showed by yeast two-hybrid assay that the C-terminal of kAE1 interacts with the μ1A subunit via Y_{904}DEV motif (52). The interaction between kAE1 and μ1A subunit was confirmed by immunoprecipitation and immunofluorescence colocalization in HEK 293 cells (Figure 1.9) (52). The effect of the interaction between μ1A and kAE1 trafficking and surface localization was investigated by knocking-down endogenous μ1A.

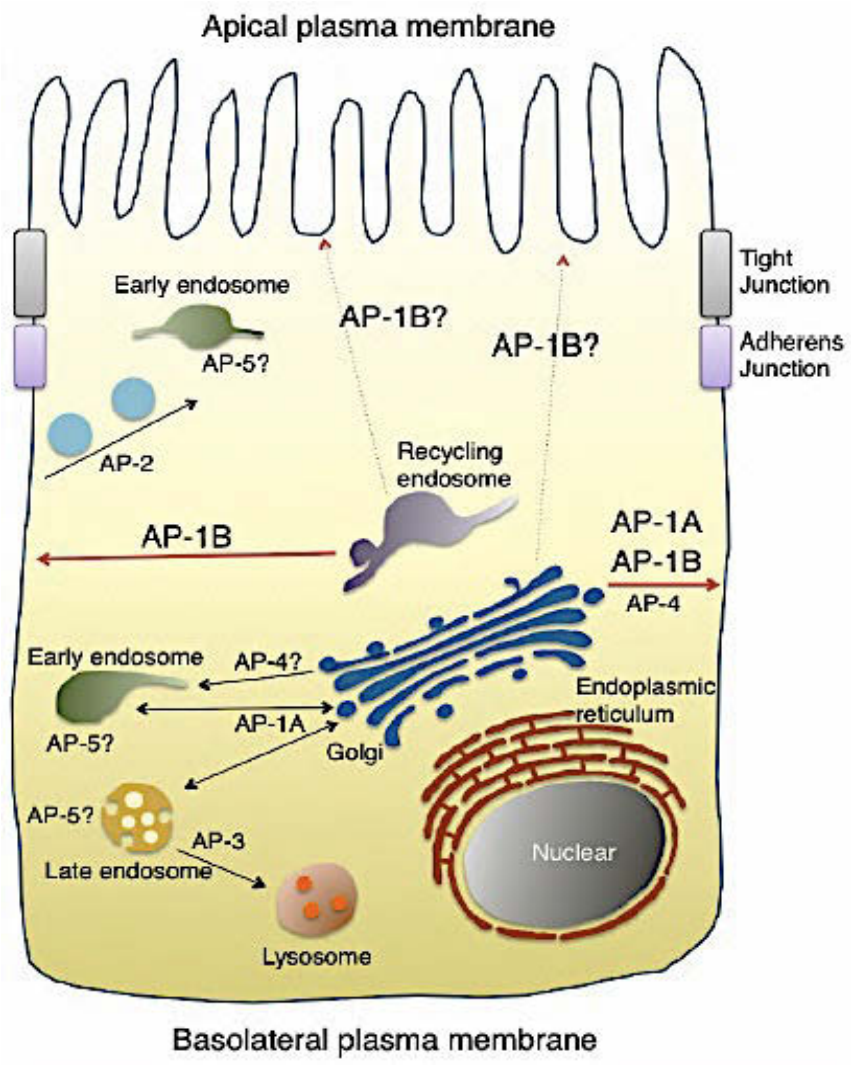

Figure 1.8: The role of AP in protein trafficking pathway. AP-1A is localized at the TGN and endosomes and regulates TGN-endosomal and TGN-basolateral membrane pathways. The epithelium-specific AP-1B localizes at the TGN and recycling endosomes and controls polarized sorting to the basolateral membrane. AP-1B may be indirectly involved in apical protein sorting. AP-2 is recruited to the plasma membrane to regulate endocytosis. AP-3 regulates the endosomal and the lysosomal trafficking pathways. AP-4 is involved in the TGN-endosomal and the TGN-basolateral plasma membrane pathways. AP-5 localizes in late endosome. This cartoon is adapted from (244).

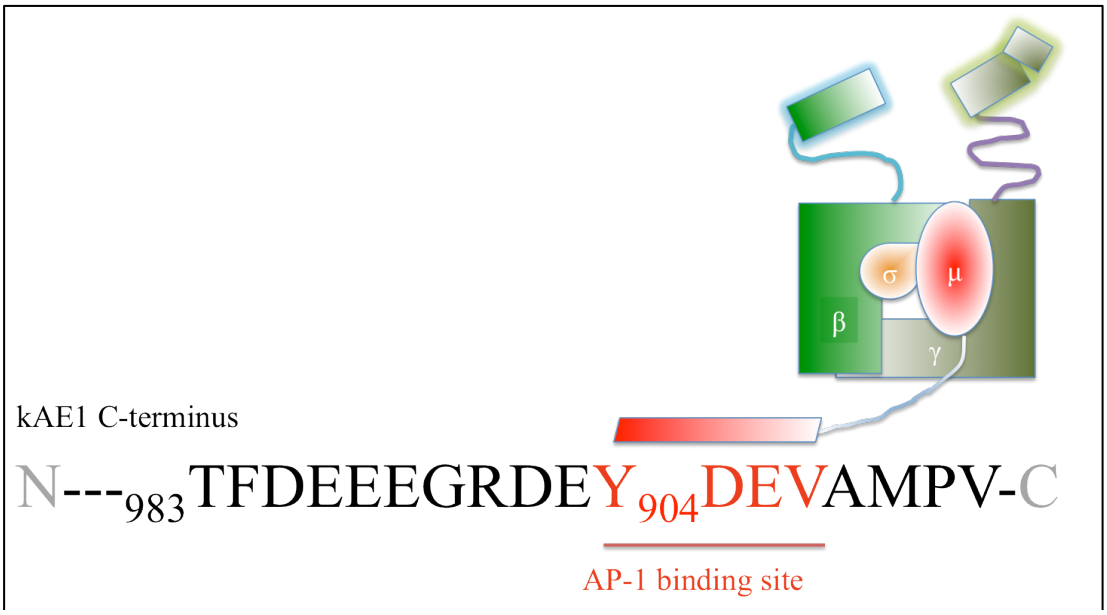

Figure 1.9: AP-1A interaction with kAE1. AP-1A interacts with kAE1 C–terminus via the Y_{904}DEV tyrosine motif. Letters in black and red represent amino acids composing kAE1 C-terminus; letters in grey represent the N- and C-termini of kAE1.

The knockdown of μ1A in HEK 293 cells reduced kAE1 surface localization and resulted in its intracellular accumulation (52). The same group later showed that cell surface expression of kAE1 is reduced after knockdown the μ subunit of either AP-1A, 3, or 4 complexes in polarized and non-polarized MDCK cell (245).

1.9. Thesis hypothesis

AP-1A/B interaction with kAE1 is crucial for kAE1 residency at the basolateral membrane in polarized epithelial cell. Lack of proper interaction between AP-1A/B and kAE1 affects kAE1 trafficking and surface expression, and causes dRTA.

1.10. Thesis objectives

- To devise new experimental tools to examine the trafficking of kAE1 in living cells.
- To investigate the physiological role of kAE1 and AP-1A interaction in kAE1 protein trafficking in an epithelial environment.
- To study the physiological role of kAE1 and AP-1B interaction in kAE1 trafficking, endocytosis and recycling in epithelial cells.
- To characterize kAE1 endocytosis and recycling pathways.

2. Chapter two: kAE1 HaloTag as a tool to study kAE1 trafficking in MDCK cells

2.1. Introduction

Adding epitope tags to proteins makes the detection and the purification process easier and more efficient. Epitope tags like hemaglutinin (HA) or myc (derived from c-myc gene) are useful for immunoblotting, immunoprecipitation, protein purification and immunofluorescence assays (156,215). However, the use of such epitope tags can be difficult in live cell imaging because the plasma membrane of the cell is not permeable to antibodies used to detect the tagged protein. The kAE1 protein we use in the laboratory is either HA- or myc-tagged at residue 557 on the third extracellular loop (246,247). To detect kAE1 HA/myc tagged proteins, cells need to be fixed and permeablized so anti-HA or anti-myc antibodies can enter the cell and label kAE1 protein, which restrict their use to fixed cells only.

To study kAE1 trafficking and interaction with AP-1 complexes in different cellular compartments in living cells, we used kAE1 fused to a 33 kDa HaloTag (HT) protein at its amino-terminus (Fig 2.1). HT is a modified haloallkane dehalogenase designed to covalently and irreversibly binds to synthetic ligands. Ligands can be fluorescently tagged, can be linked to agarose beads, and can be membrane permeable or impermeable. Examples of ligands are O4 block (non fluorescent), fluorescent carboxytetramethylrhodamine (TMR) (red), Fluorescein amidite (FAM) (green), and Coumarin (blue) (www.promega.ca/products/pm/halotag-technology/halotag-technology) (248,249). HT linked to agarose beads (Halolink resin) is also useful for pulling down chimeric proteins for purification purposes (248,249). HT ligands bind specifically and irreversibly to Halo-tagged proteins either in solutions, in living cells, or in chemically fixed cells (248). To study the physiological effect of the interaction between kAE1 and

AP-1 complexes, we obtained and first characterized the amino-terminally tagged kAE1 with HT protein. This chapter describes the characterization of kAE1 protein fused to HT protein as a tool to study kAE1 trafficking and interaction with AP-1A in MDCK cells. Initial studies showed by western blotting and DIDS/SITS inhibitors binding that HT addition to kAE1 N-terminus does not affect kAE1 trafficking and normal cellular processing like glycosylation and normal folding processes. Second, immunofluorescence techniques revealed that HT addition does not affect kAE1 trafficking and basolateral expression in polarized MDCK cells. Finally, I used immunofluorescence and live cell imaging to demonstrate the possibility of using kAE1 HT to follow a newly synthesized pool of kAE1 protein to the cell surface.

2.2. Materials and methods

2.2.1. kAE1 HaloTag construct

The kAE1-HT in pFN21A plasmid (clone name PFN21AB8562, Flexi ORF Clone FXC03789) was purchased from the Kazusa DNA Research Institute (associated with Promega, Madison WI). This construct contains the HT protein fused to the amino terminus of human kAE1 cDNA that was inserted between the *SgfI* restriction site (5′) and *PmeI* restriction site (3′) (Fig 2.2).

2.2.2. kAE1 deglycosylation

MDCK cells (3 X 10^6) were either transfected with 5 µg of pcDNA3-kAE1 cDNA that was expressed in cells as kAE1 protein, or with pFN21A-kAE1 cDNA

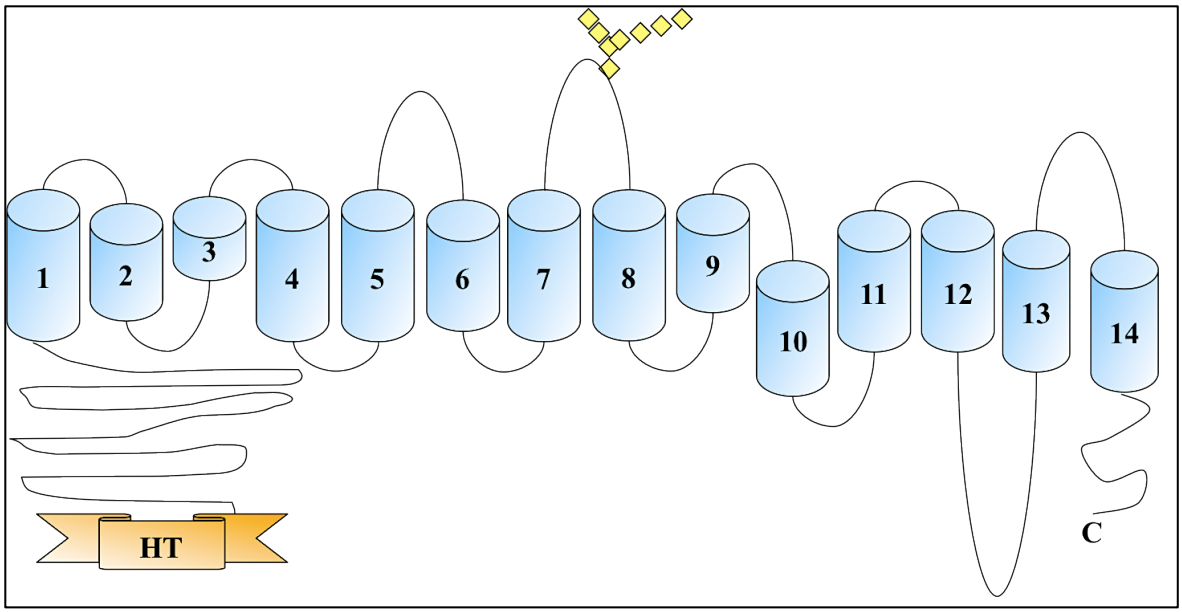

Figure 2.1: kAE1-HT topological model. kAE1 is a transmembrane glycoprotein that contains 14 transmembrane segments. Both N- and C- termini are cytoplasmic, with an N-glycosylation site in the 4th extracellular loop. HaloTag (HT) protein was fused in frame to the kAE1 N- terminus. (32).

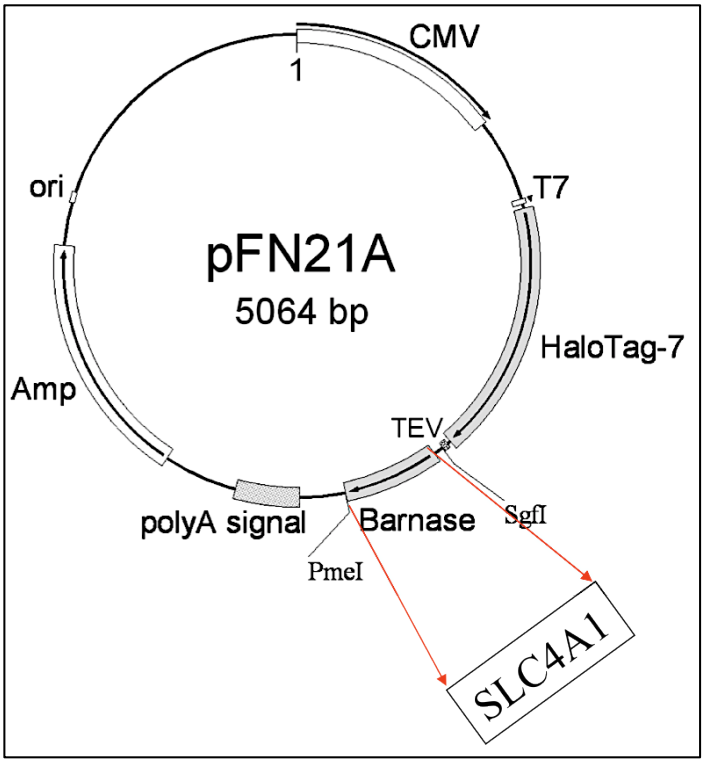

Figure 2.2: SLC4A1-pFN21A cDNA. SLC4A1 open reading frame (ORF) was introduced into pFN21A HaloTag flexi vector to express a kAE1-HT chimeric protein. SLC4A1 ORF replaced the Barnase CDS gene using Sgf I and Pme I restriction enzymes. The abbreviations in the pFN21A plasmid stand for: CMV promoter. T7 RNA polymerase promoter. HaloTag-7 CDS. TEV protease recognition sequence. Sgf I recognition site. Barnase CDS. Pme I recognition site. SV40 late polyadenylation signal, beta-lactamase (Amp) CDS, ColE1-derived plasmid replication origin (Kazusa DNA Research Institute).

that resulted in kAE1 HT protein chimera expression. Transfection was performed using the NEON electroporation system (1400-V pulse voltage, 20-ms pulse width, and 3 pulses) (Invitrogen). The cells were lysed in PBS buffer (1.37 mM NaCl, 0.027 mM KCl, 0.1 mM Na_2HPO_4, and 0.018 mM KH_2PO_4, pH 7.2-7.4) containing 1 % Triton X-100 and protease inhibitors (1 μg / ml aprotinin, 2 μg / ml leupeptin, 1 μg / ml pepstatin A, and 100 μg / ml PMSF) at 4 °C. 100 μl of the cell lysates were digested with 1 μl (1000 U) of two enzymes: endoglycosidase-H (New England BioLabs), which cleaves high mannose oligosaccharides from kAE1 protein, and peptide N-glycanase F (New England BioLabs), which cleaves N-glycans from glycoproteins (156). Proteins in the samples were analyzed by SDS-PAGE followed by immunoblot using mouse anti C-terminus AE1 primary antibody (provided by Dr. Reinhart Reithmeier, University of Toronto), then with rabbit anti-HT primary antibody (Promega).

2.2.3. Immunofluorescence

MDCK cells (1 X 10^5) were transfected with 1 μg pFN21A-kAE1 cDNA to express kAE1-HT protein using NEON electroporation. The following day, the cells were incubated with 50 nM TMR-HT ligand (red) or 50 nM FAM-HT (green) for 10 min at 37 °C. The cells were then washed with 1 ml medium without phenol red three times for 5, 5, and 15 min. Cells were fixed with 4 % paraformaldehyde (PFA) in PBS, permeabilized with 0.2 % Triton X-100 in PBS, and blocked with 1 % BSA in PBS. Mouse anti-AE1 C-terminus antibody (IVF12) followed by Alexa 488 coupled secondary antibody (green) was used to detect kAE1 protein. To detect surface kAE1, fixed but non-permeabilized cells were incubated with Bric 6 (International Blood Group Reference Laboratory, Bristol, UK) antibody followed by Cy3 (red) coupled secondary antibody. For

experiments conducted in polarized MDCK cells, MDCK cells transiently expressing kAE1-HT protein were grown on coverslips for five days until they reached confluency. The cells were then incubated with 50 nM TMR-HT (red) for 10 min at 37 °C, then washed with cold media without phenol red at 4 °C for 5, 5, and 15 min before fixation and mounting on glass slides.

2.2.4. Pulse chase experiment

To detect newly synthesized kAE1-HT proteins, MDCK cells transiently expressing kAE1-HT protein were incubated with 10 μM O4 block-HT ligand (non fluorescent) for 1 h at room temperature (RT) to covalently bind all of the pre-existing kAE1-HT protein (later referred as "block"). The cells were then washed four times (3 min) with PBS and incubated at 37 °C for different chase times (0, 30, 45, 60 min) in DMEM:F12 media without phenol red (Gibco, life technology). The cells were incubated with 50 nM TMR-HT (red) for 10 min at 37 °C in order to stain the newly synthesized kAE1 protein. The cells were then fixed with 4 % PFA in PBS, permeabilized with 0.2 % Triton X-100 in PBS and blocked with 1 % BSA in PBS, prior to incubation with mouse anti-AE1 antibody (1:500 dilution) followed by anti-rabbit Alexa 488 (green) (1:500 dilution) coupled secondary antibody to detect total kAE1.

To colocalize newly synthesized kAE1 with organelle markers, MDCK cells transiently expressing kAE1-HT protein were incubated with 10 μM HT-O4 block ligand (non-fluorescent) for 1 h. Cells were washed four times (3 min) with PBS, then incubated at 37 °C for 1 h to synthesize new kAE1-HT protein. The newly synthesized proteins were labeled with 50 nM of TMR-HT ligand (red) for 10 min at 37 °C. Then the cells were incubated at 37 °C for 3 h chase time in warm DMEM:F12 media without phenol

red. Cells were fixed with 4 % PFA in PBS, permeabilized with 0.2 % Triton X-100 in PBS and blocked with 1 % BSA in PBS and were incubated with rabbit anti-giantin antibody (1:500 dilution) followed with anti-rabbit Alexa 488 (green) coupled secondary antibody (1:500 dilution).

2.2.5. SITS Affi-gel binding assay

MDCK cells expressing either kAE1 or kAE1 HT were lysed in PBS containing 1 % Triton X-100 and protease inhibitors (1 μg / ml aprotinin, 2 μg / ml leupeptin, 1 μg / ml pepstatin A, and 100 μg / ml PMSF) buffer at 4 °C. The lysates were spun down to precipitate the insoluble materials and 100 μl of supernatant was incubated with 50 μl 4-acetamido-4'-isothiocyanatostilbene-2, 2'-disulfonic acid (SITS)-Affi gel in the presence or absence of 1 mM free H_2 4,4'-diisothiocyanatostilbene, 2, 2'-disulfonic acid (H_2DIDS) for 15 min at 4 °C in 850 μl binding buffer (0.1% $C_{12}E_8$, 228 mM sodium citrate, pH 7.1). The gel beads were washed three times with the binding buffer and bound proteins were eluted with Laemmli buffer. kAE1 and kAE1 HT were detected on SDS-PAGE using mouse anti C-terminus AE1 and rabbit anti-HT primary antibodies.

2.2.6. kAE1-HT mutant preparation

Site-directed mutagenesis was performed using Quick change II site-directed mutagenesis kit (Stratagene), according to the manufacturer's instructions. The presence of mutations was confirmed by automated sequencing (TAGC, The Applied Genomic Core, University of Alberta). Primer sequences used to prepare kAE1-HT Y904A, Y904F, V907A, and R901X mutants are shown on Table (2.1).

2.2.7. Imaging of kAE1-HT expressing cells

Fixed and live cells were imaged using an inverted confocal microscope IX81 (Olympus, Japan), equipped with a Nipkow spinning-disk optimized by Quorum Technologies and a 100 X objective. Scanning speed and laser intensity were adjusted to avoid photobleaching of the fluorophores and damage to the cells. The microscope is equipped with a microenvironmental chamber to maintain physiological conditions during long-term experiments.

2.3. Results

2.3.1. kAE1-HT protein is expressed as a 129 kDa protein in SDS-PAGE and carries complex oligosaccharides

kAE1 protein migrates on SDS-PAGE gel as two main bands: kAE1 carrying high mannose oligosaccharides (lower band), and kAE1 carrying complex oligosaccharides (upper band) (158). To verify kAE1-HT protein expression and examine its glycosylation pattern, MDCK cell lysates either expressing kAE1 or kAE1-HT proteins were either digested with endoglycosidase-H (which cleaves high mannose oligosaccharides from kAE1 protein) or peptide N-glycanase F (which cleaves N-glycans from glycoproteins). Immunoblot results (Fig 2.3) show that kAE1-HT protein is expressed at the expected molecular weight of 129 kDa. Additionally, digestion with peptide N-glycanase F enzyme causes a band shift to a lower molecular weight, indicating that kAE1 HT carries complex N-oligosaccharides and is processed normally in MDCK cells.

2.3.2. kAE1-HT protein is properly folded in MDCK cells

To verify that HT addition to kAE1 N-terminus does not affect kAE1 protein folding, I determined the ability of kAE1-HT to bind stilbene disulfonate inhibitor SITS that is covalently bound to Affi-gel resin in the presence or absence of an excess of free

Table 2.1 Primer sequences used to prepare mutations in kAE1 cDNA

AE1 Mutations	Forward primer (5′-3′)	Reverse primer (5′-3′)
Tyr904Ala	AAGGTCGGGATGAAGCCGACGAAGTGGCCA	TGGCCACTTCGTCGGCTTCATCCCGACCTT
Tyr904Phe	GGTCGGGATGAATTCGACGAAGTGGC	GCCACTTCGTCGAATTCATCCCGACC
Val907Ala	GAATACGACGAAGCGGCCATGCCTGTG	CACAGGCATGGCCGCTTCGTCGTATTC
Arg901Stop	GAGGAGGAAGGTTAAGATGAATACGAC	GTCGTATTCATCTTAACCTTCCTCCTC

inhibitor (1 mM H_2DIDS). SITS inhibitor was previously shown to specifically bind to properly folded AE1 (37,250). Results in Figure 2.4 show that kAE1-HT protein binds to SITS and H_2DIDS inhibitors as kAE1 protein, indicating that kAE1-HT is properly folded in MDCK cells.

2.3.3. HT ligands bind specifically to kAE1-HT protein

Next, we verified the specificity of HT ligands to kAE1-HT proteins. Immunofluorescence was performed on MDCK cells expressing kAE1-HT as described in the Materials and Methods section. As shown on Figure 2.5, labeling with TMR HT ligand (red) and an antibody against the C-terminus of AE1 (green) shows colocalization between kAE1-HT staining and kAE1 C-terminus staining (yellow) compared to control (non-transfected MDCK cells), indicating that HT ligand staining is specific to kAE1-HT protein.

2.3.4. KAE1-HT is expressed at the plasma membrane of non-polarized MDCK cells and at the basolateral membrane of polarized MDCK cells

To determine whether kAE1-HT is expressed at the plasma membrane, intact MDCK cells expressing kAE1-HT were incubated with FAM-HT ligand, then washed and fixed without permeabilization. The cells were incubated with Bric 6 antibody that recognizes a kAE1 extracellular epitope (251), followed by anti-mouse Cy3 (red) coupled secondary antibody. Figure 2.6 A shows that kAE1 extracellular staining colocalizes with FAM HT (yellow).

To ensure that HT addition to kAE1 N-terminus does not affect kAE1 localization in polarized epithelial cells, MDCK cells expressing kAE1-HT were grown

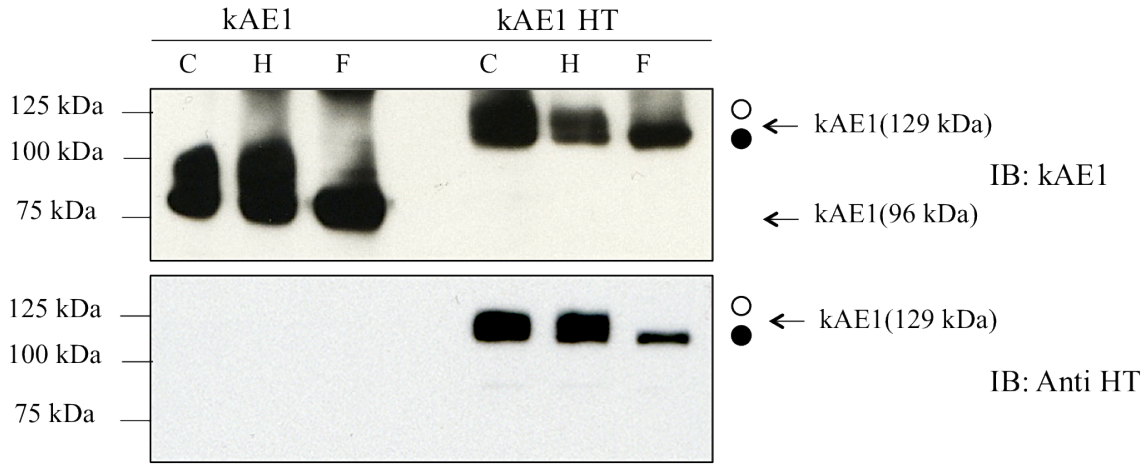

Figure 2.3: kAE1-HT protein is processed normally to complex oligosaccharides. MDCK transfected with either pCDNA3-kAE1 or pFN21A-kAE1 HT cDNAs were lysed and digested with endoglycosidase-H or peptide N-glycanase F enzymes. The samples were loaded on 8 % SDS-PAGE gel. *C* lane corresponds to total cell lysates, *H* lane shows lysate digested with endoglycosidase-H, *F* lane indicates cell lysate digested with Peptide N-glycanase F. The upper blot was incubated with mouse anti-AE1 antibody; the lower blot was incubated with rabbit anti-HT antibody. KAE1-HT protein migrates as a 129 kDa band, whereas wild type kAE1 migrate as a 96 kDa band. Open circle corresponds to kAE1 carrying complex oligosaccharides, and filled circle indicates kAE1 carrying high mannose oligosaccharides.

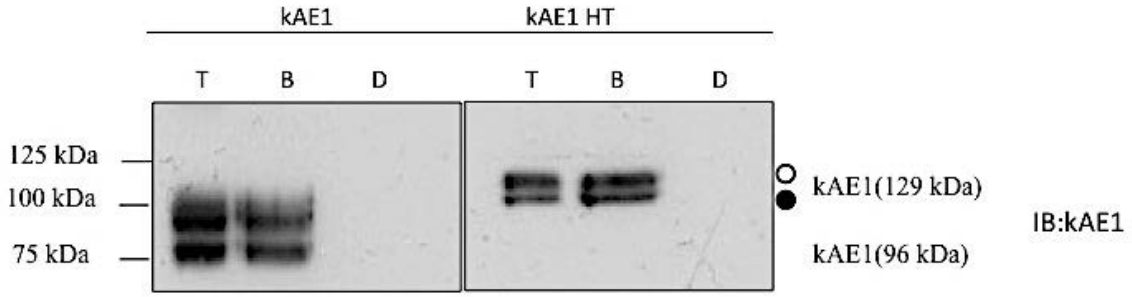

Figure 2.4: kAE1 HT protein has a folding pattern similar to kAE1 protein. Cell lysates from MDCK cells expressing either kAE1 or kAE1 HT were incubated with SITS Affi-gel in presence or absence of 1 mM H_2DIDS. Total cell lysates (T), SITS bound fractions in the absence (B) or presence (D) of H_2DIDS were loaded on 8 % SDS- PAGE gels. kAE1 was visualized by immunoblot, using an anti AE1 -N terminal antibody followed by anti-rabbit antibody coupled to horseradish peroxidase. Open circle corresponds to kAE1 carrying complex oligosaccharides, and filled circle indicates kAE1 carrying high mannose oligosaccharides.

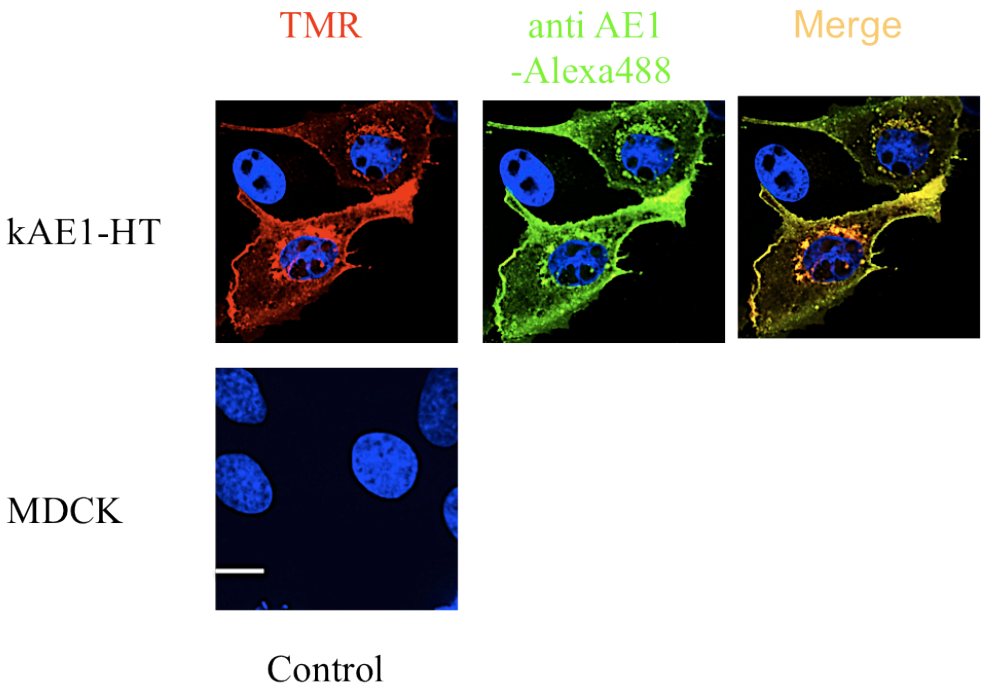

Figure 2.5: HaloTag ligand TMR binds specifically to kAE1–HT protein. MDCK cells expressing kAE1-HT protein or non-transfected were incubated with 50 nM of TMR-HT ligand (red) for 10 min at 37 °C before they were washed and fixed. The cells were then incubated with mouse anti-AE1 C-terminus antibody followed by Alexa 488 coupled secondary antibody (green). kAE1-HT staining colocalizes with anti-AE1 C-terminus staining (yellow). Blue staining shows nuclear staining with 4',6-diamidino-2-phenylindole (DAPI). Bar = 10 μm.

on semi-permeable Transwell polycarbonate filters for five days until they became polarized, and the cells were incubated with TMR HT ligand.

Immunofluorescence results (Figure 2.6 B) show that kAE1-HT is expressed at the basolateral membrane of MDCK cells. However, some intracellular accumulation of kAE1-HT was noticed in cells, which could be due to the over-expression of kAE1-HT by transient transfection, where multiple copies of kAE1 HT encoding cDNA could have entered the transfected cells. This could overwhelm the cell machinery and slow down protein processing. Importantly, this intracellular accumulation disappears when transfected cells are grown for 48 hours after transfection and before fixation, instead of 24 hours.

2.3.5. A new pool of kAE1–HT protein is synthesized 60 min after "blocking"

To test how long a new pool of kAE1 HT protein would take to be synthesized, MDCK cells expressing kAE1-HT protein were incubated with 10 μM O4 block-HT ligand (non-fluorescent) for 1 h at RT to block all of the pre-existing kAE1-HT protein. The cells were then washed and incubated at 37 °C for 0, 30, 45 or 60 min chase times. Newly synthesized kAE1 HT was detected using TMR-HT (red) and total kAE1 in green using mouse anti-AE1 antibody. Results in Figure 2.7 show that a 60 min incubation post-blocking is enough to detect a pool of newly synthesized kAE1. Next, pulse chase and live cell imaging experiments were performed to follow the new pool of kAE1 to the cell surface.

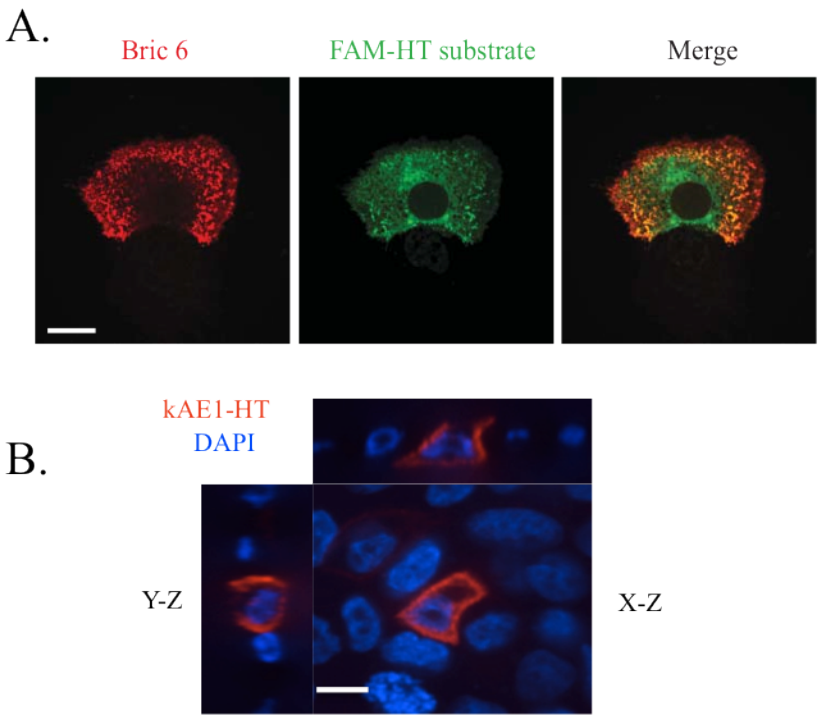

Figure 2.6: kAE1-HT is expressed at the plasma membrane of non polarized and at the basolateral membrane of polarized MDCK cells *A*. MDCK cells expressing kAE1-HT were stained with 50 nM FAM-HT substrate (green) then washed, fixed and incubated with Bric 6 antibody followed by anti-mouse antibody coupled to Cy3 (red) before mounting the coverslip on slides. Samples were examined using an Olympus spinning disk confocal microscope and a 100 X objective. ***B.*** Polarized MDCK expressing kAE1-HT, stained in red with TMR-HT substrate, cells. Blue staining indicates nuclear staining with DAPI. Bar =10 μm.

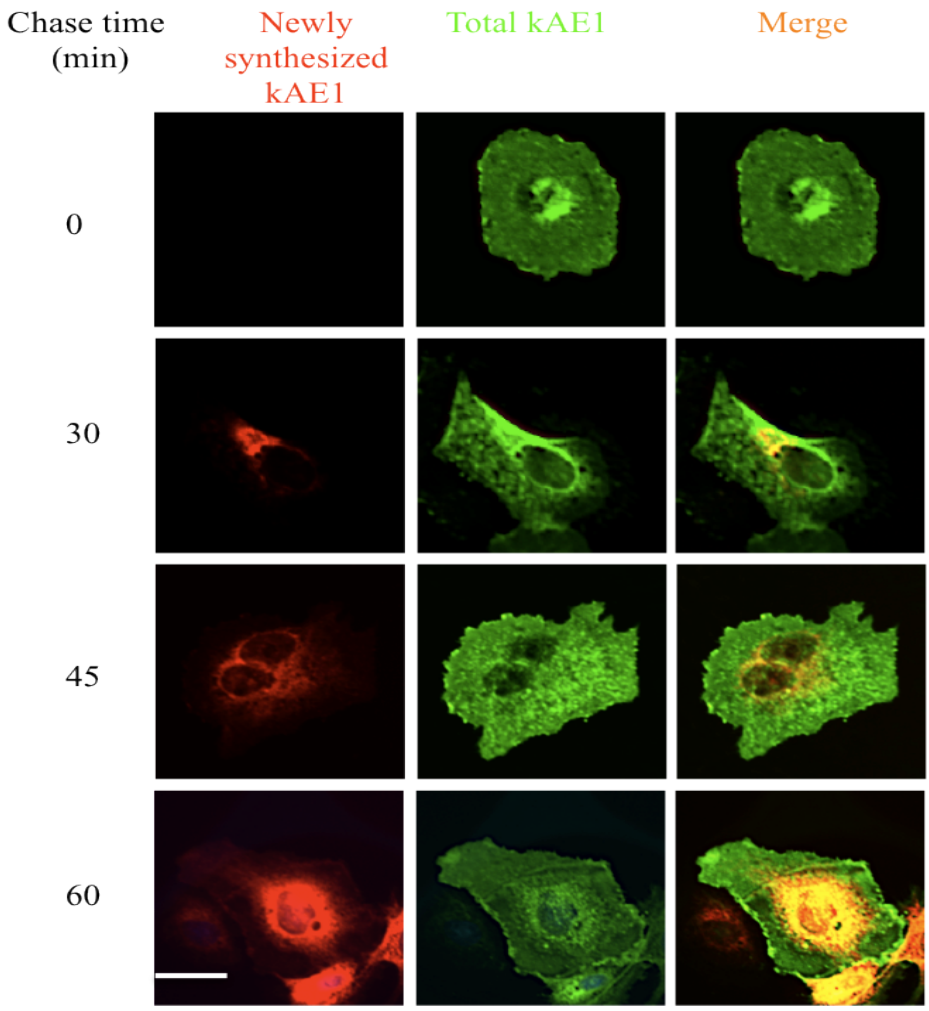

Figure 2.7: A new pool of kAE1-HT is synthesized 60 minutes after blocking pre-existing kAE1 HT proteins with O4 HT ligand. MDCK cells expressing kAE1-HT protein were incubated with 10 μM O4 HT block ligand (non fluorescent) for 1 h at RT. The cells were then washed and incubated at 37 °C for different chase times (0, 30, 45, 60 min). Newly synthesized kAE1 HT proteins were stained with 50 nM TMR-HT (red) for 10 min at 37 °C. The cells were fixed and permeabilized before incubation with mouse anti-AE1 antibody followed by anti-mouse Alexa 488 (green) coupled secondary antibody to detect total kAE1. Bar =10 μm.

2.3.6. Newly synthesized kAE1–HT protein colocalizes with giantin one hour after synthesis and reaches plasma membrane after three hours

The previous experiment indicated that a detectable new pool of kAE1 was formed after 1 h chase time. The following "pulse-chase" and live cell imaging experiments were performed in MDCK cells to determine how long newly synthesized kAE1-HT needs to reach the plasma membrane.

2.3.6.1. Pulse chase experiment

MDCK cells expressing kAE1-HT protein were incubated with HT-O4 ligand to block all pre-existing kAE1 HT protein. The cells were then incubated at 37 °C for 1 hour to allow synthesis of new kAE1-HT protein, and were stained with TMR HT ligand to label newly synthesized kAE1-HT protein. The excess of unbound ligand was washed and cells were re-incubated at 37 °C for different chase times (Fig 2.8) until kAE1 was detected at the plasma membrane. Cells were finally fixed, permeabilized, and stained with an antibody against giantin, a marker of the Golgi (Fig 2.8A). The cells chased for 3 hours were fixed and incubated with mouse anti-Bric 6 antibody followed with anti-mouse Alexa 488 (green) coupled secondary antibody (Fig 2.8 B). Results show that kAE1-HT protein colocalizes with giantin after a 1 h chase and reaches the plasma membrane after a 3-hour chase.

2.3.6.2. Live cell imaging

This experiment determined whether it is possible to use live cell imaging to follow kAE1 trafficking to the cell surface. MDCK cells expressing kAE1-HT were incubated with HT-O4 block ligand to block all pre-existing kAE1-HT protein. The cells were incubated at 37 °C for 1 h to allow synthesis of new kAE1-HT protein, and were stained

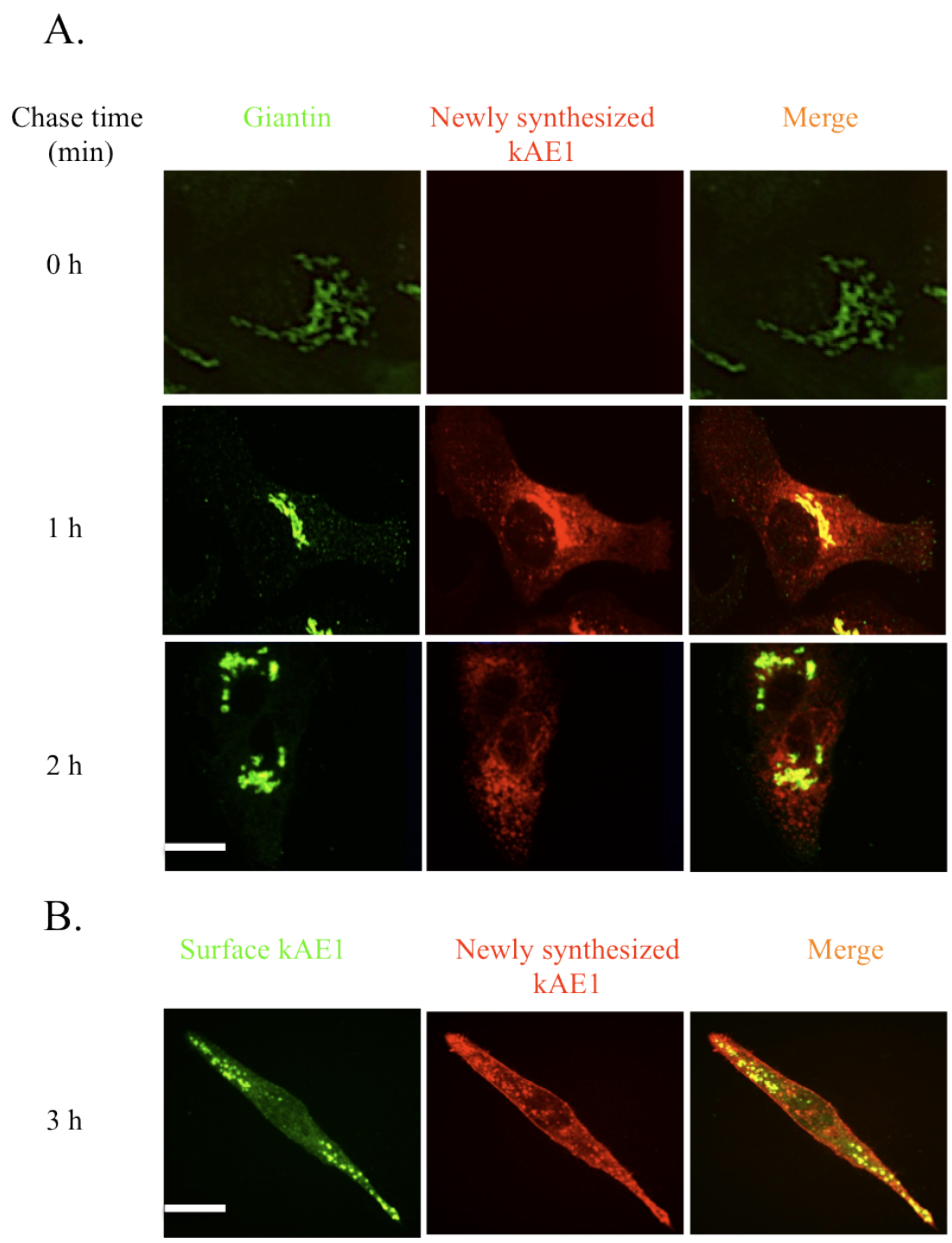

Figure 2.8: kAE1-HT colocalizes with giantin 1 h after synthesis and reaches the cell surface after a 3 h chase. MDCK cells expressing kAE1-HT protein were incubated with 10 μM HT-O4 ligand for 1 h to block all the pre-existing kAE1-HT proteins. The cells were incubated at 37 °C for 1 h to synthesize new kAE1-HT protein followed by 50 nM TMR-HT ligand (red) for 10 min at 37 °C to label newly synthesized kAE1 protein.

(Continued from figure 2.8)

A. Cells were re-incubated at 37 °C for 0, 1, and 2 h chases. They were then fixed, permeabilized, blocked and incubated with rabbit anti-giantin antibody followed with anti-rabbit Alexa 488 (green) coupled secondary antibody. ***B.*** To detect surface kAE1, following a 3 h chase, the cells were fixed and incubated with mouse anti-Bric 6 antibody followed with anti-mouse Alexa 488 (green) coupled secondary antibody. Bar =10 μm.

with TMR HT ligand to label newly synthesized kAE1-HT protein. The excess of unbound ligand was washed and cells were incubated at 37 °C in warm medium to perform live cell imaging using confocal microscopy. The microscope was set up to take images at fixed time intervals (images shown for 0, 30, 60, 120, 150, 180 min). Results in Figure 2.9 show that kAE1-HT is detected at the plasma membrane after a 3 hour chase as indicated by the white arrows.

2.3.7. kAE1 – HT mutants reach the cell surface of non-polarized MDCK cells

Once we have ensured that kAE1-HT chimera behaves in a similar way to kAE1, we wondered whether kAE1-HT mutants would show the same localization as kAE1 mutants that do not contain the HT epitope. kAE1 C-terminal mutants are retained intracellularly in non-polarized MDCK cells and apically mistargeted when expressed in polarized MDCK cells (159). In order to determine the effect of the HT epitope on kAE1 subcellular localization, four different mutants were prepared in the kAE1 HT background: kAE1-R901X, Y904A, Y904F and V907A (Table 2.1). Figure 2.10 shows that in non-permeabilized cells, all the prepared mutants were able to reach the cell surface (green staining) except kAE1 R901X, which was mostly retained intracellularly. This localization is consistent with previous results obtained using constructs that do not contain the HT epitope of non-polarized cells but not the polarized MDCK cells (159,160).

2.4. Discussion

To study kAE1 protein trafficking and interaction with AP-1 in epithelial cells, we purchased a construct where the 33 kDa engineered HaloTag cDNA has been fused to the

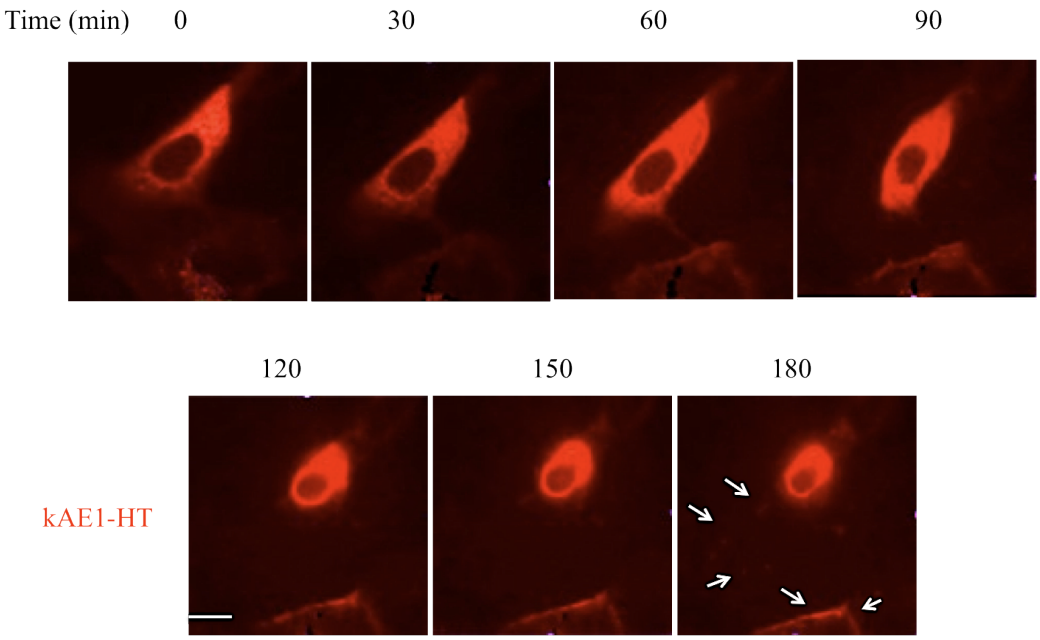

Figure 2.9: kAE1 HT reaches the cell surface after 3 h of live cell imaging. MDCK cells expressing kAE1-HT protein were incubated with 10 μM HT-O4 ligand for 1 h to block all the pre-existing kAE1-HT protein. The cells were incubated at 37 °C for 1 h to synthesize new kAE1-HT protein followed with 50 nM TMR-HT ligand (red) for 10 min at 37 °C to label newly synthesized kAE1 HT protein. Cells were incubated in warm medium (DMEM:F12 without phenol red) to perform live cell imaging using a confocal microscope. Images were taken every 10 min for 3 hours (images shown for 0, 30, 60, 120, 150, 180 min). White arrows point to kAE1 that has reached the cell surface. Bar =10 μm.

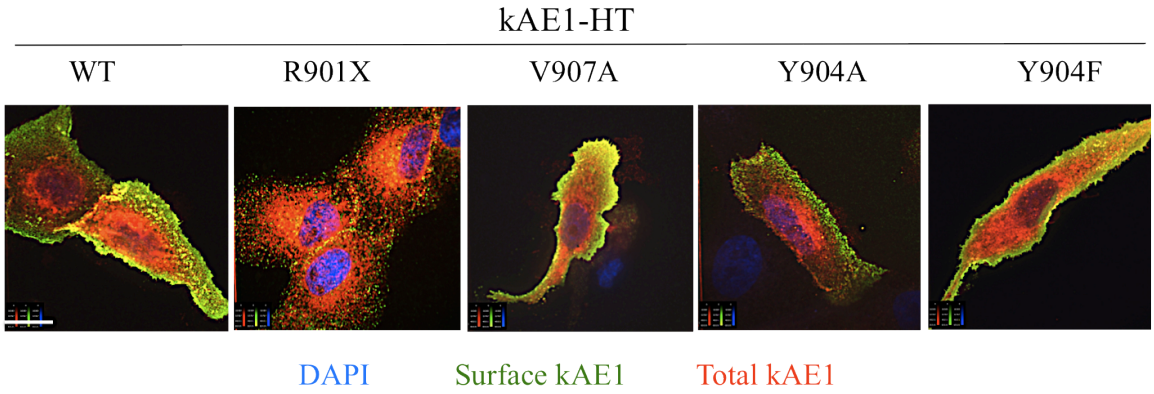

Figure 2.10: kAE1-HT mutants reach the cell surface except kAE1-HT R901X. MDCK cells expressing either kAE1-HT protein WT or mutants were incubated with 50 nM of TMR-HT substrate (red) then washed, fixed and incubated with Bric 6 antibody followed by anti-mouse antibody coupled to Alexa 488 (green) before mounting the coverslip on slides. Yellow staining indicates colocalization between total kAE1 and surface kAE1. Samples were examined, using an Olympus spinning disk confocal microscope and a 100 X objective. Blue staining indicates nuclear staining with DAPI. Bar = 10 μm.

amino-terminus of kAE1 cDNA. Halo-Tagged chimeric proteins have the advantage of binding covalently, rapidly, and irreversibly to different HT ligands that are not toxic to the cells (248). Importantly, some synthetic HT ligands are plasma membrane-permeant, so they can be added to live or fixed cells to allow studies of labeled proteins in living cells (248,249). HaloTag technology has successfully been used to study peroxisome formation and turn over dynamics of peroxisomes in mammalian cells (252). It was also used to study cell signaling and trafficking pathway of proteins, like the voltage-gated K^+ channel (hERG/KCNH2) (248), X-linked inhibitor of apoptosis (XIAP) associated factor 1 (253), and human B1 integrin (254).

The addition of epitopes to proteins may affect proteins' function and trafficking. The HT protein has a molecular weight (33 kDa) close to that of the GFP protein (27 kDa). The addition of a GFP epitope to kAE1 N-terminus did not affect kAE1 targeting or function (255). Therefore, we hypothesized that a protein of similar molecular weight fused to kAE1 N-terminus may not affect kAE1 targeting or function either. Importantly, proteins fused to a HT protein can be selectively and irreversibly detected using different cell permeant HT-ligands in living cells (248). We used these ligands in the following chapter to discriminate between preexisting and newly synthesized kAE1 proteins.

In this study, immunoblotting revealed that kAE1-HT is processed in a similar way to kAE1 in renal epithelial cells, as it acquires complex oligosaccharides when processed from the ER to the Golgi apparatus (Figure 2.3). kAE-HT binds to the stilbene disulfonate competitive inhibitors SITS/H_2DIDS to the same extent as kAE1 without HT fusion using SITS Affi-gel resin (Figure 2.4). These findings suggest that addition of HT

does not affect kAE1-WT and mutant proteins' processing and folding, suggesting that HT does not interfere with normal kAE1 protein function.

Immunofluorescence results showed that the majority of kAE1-HT is expressed at the cell surface of non-polarized MDCK cells (Figure 2.5 A) and at the basolateral membrane of polarized MDCK cells (Figure 2.5 B), indicating that addition of HT to kAE1 N-terminus does not affect normal kAE1 localization at the surface of renal epithelial cells. However, Figures 2.5 and 2.7 show that at steady-state or even three hours after initiating protein synthesis, there is a substantial amount of intracellular retained kAE1-HT, in addition to cell surface protein. This suggests that addition of HT to kAE1 protein somehow slightly alters processing of the protein. It is possible that addition of the HT slightly destabilizes the folding of the newly synthesized kAE1-HT protein and delays its processing. Another possibility could be due to the over-expression of kAE1-HT by transient transfection, where many copies of cDNA encoding kAE1-HT were introduced into the transfected cells. This could overwhelm the cell machinery and slow down protein processing. As indicated earlier, the intracellular accumulation disappears when the transfected cells were grown for 48 hours post-transfection or until polarization as in Figure 2.6 B.

We took advantage of the covalent bond between kAE1-HT and plasma membrane permeant, fluorescent HT ligand to perform a kAE1-HT protein imaging experiment in living MDCK cells (248). A similar approach enabled live cell imaging to visualize spatial separation and real-time trafficking of proteins like B1-integrin (254) and p65-HT (248). Pulse chase experiments with fixed (Figure 2.8) or living (Figure 2.9) cells demonstrated that a new pool of kAE1-HT protein was synthesized after a 60 min

chase time and localized in the Golgi apparatus. Further, incubation of MDCK for 3 hour was enough to show a cell surface-like staining.

We finally verified that the fusion of HT to kAE1 N-terminus does not affect the previously-described trafficking patterns of kAE1-R901X, Y904A, Y904F or V907A carboxyl-terminal mutants. Compared to kAE1-HT WT, all the described mutants were able to reach the cell surface except kAE1-HT R901X, which was retained intracellularly in MDCK cells. These mutants have been stably expressed and studied in polarized MDCK I cells. kAE1 Y907A was localized at the basolateral membrane similarly to kAE1 WT (159). Unlike our findings for kAE1-HT Y904F and Y904A mutants in non polarized MDCK cells, kAE1 Y904A was mistargeted to the apical membrane (160) while kAE1 Y904F was retained intracellularly in polarized MDCK I cells (159). In agreement with previous findings, kAE1 R901X is either retained intracellularly or traffics in a non-polarized way to the apical membrane in polarized MDCK I cells (159,160). We found that kAE1-HT R901X was retained intracellularly in non-polarized MDCK cells.

In summary, this study showed that kAE1-HT protein is normally folded and trafficked to the basolateral membrane in polarized MDCK cells. Also, kAE1-HT is a suitable tool to study kAE1 protein trafficking in living cells. The next chapter describe how kAE1-HT proteins can be used to study the physiology of interaction between kAE1 and AP-1A in MDCK cells.

3. Chapter three: Adaptor protein 1A complex regulates intracellular trafficking of the kidney Anion Exchanger 1 in Epithelial cells

3.1. Introduction

Newly synthesized glycoproteins whose final destination is the plasma membrane traffic through the Golgi to the TGN from which they can reach the plasma membrane either directly by constitutive secretion or indirectly via early endosomes and even RE (175,256). Typical cargoes that traffic directly from the TGN to the plasma membrane include FcII-B2 receptor and a mutant low density lipoprotein receptor (LDLR-Y18A) (257). In contrast, examples of cargos trafficking through RE prior to reaching the plasma membrane are vesicular stomatitis virus glycoprotein (VSVG) or a truncated version of LDLR (LDLR-CT27) (256,257). In the TGN, cargoes are loaded into trafficking vesicles via the interaction of canonical motifs (di-leucine based or YXXΦ) in their cytoplasmic domain with adaptor proteins, which in turn bind to clathrin to form clathrin-coated vesicles (189). Four types of adaptor protein complexes (AP) AP-1 to AP-4, have been identified, each consisting of two large subunits, one medium subunit and one small subunit. AP-1, AP-3 and AP-4 localize to the TGN and endosomes (258). A recently described fifth adaptor protein complex localizes in late endosomes and does not appear to associate with clathrin, a feature shared with AP-4 and possibly AP-3 (202).

AP-1 is responsible for tethering the interaction between clathrin and cargo proteins that exit the TGN *en route* to endosomes. Two forms of AP-1 have been described: AP-1A is ubiquitously expressed (208) while AP-1B expression is restricted to polarized epithelial cells (165) and is targeted to common RE (209). The classical cargo protein of AP-1A is the cation-dependent mannose 6-phosphate receptor 46 (CD-MPR 46), a type I transmembrane glycoprotein that recycles between the TGN and endosomes (259). Knocking-out μ1A adaptin proved to be embryonic lethal in mice but in derived

mouse embryonic fibroblasts, CD-MPR 46 was mislocalized to endosomes and lysosomal enzymes were missorted to secretions (228).

Recently, it was reported that in HEK 293 cells, kAE1 interacts with the μ-1A adaptin of AP-1A adaptor, via a $Y_{904}DEV_{907}$ canonical motif within kAE1 cytoplasmic carboxyl-terminal domain (52). In order to gain greater insights into this interaction, we have characterized the physiological role of this interaction in renal epithelial cells. Human kidney AE1, encoded by the *SLC4A1* gene, is a membrane glycoprotein that exchanges bicarbonate for chloride at the basolateral membrane of renal alpha IC (136). Naturally occurring mutations in the *SLC4A1* gene can lead to dRTA disease (36), which is characterized by metabolic acidosis, metabolic bone disease, failure to thrive and nephrolithiasis or nephrocalcinosis. *SLC4A1* mutations associated with dRTA (dRTA mutations hereon) can be either dominantly or recessively inherited. One dominant dRTA mutation, R901X truncates the last 11 amino acids of kAE1. When expressed in epithelial MDCK cells, this mutant protein was mis-localized either to both basolateral and apical membrane or exclusively at the apical membrane, depending on the degree of polarization of the cells (159,160). Interestingly, when expressed in porcine LLC-PK1 cells that lack endogenous AP-1B but contain endogenous AP-1A, kAE1-WT protein was still located at the basolateral membrane demonstrating that AP-1B is not required for basolateral targeting of kAE1-WT protein (160). The machinery regulating the normal processing of kAE1 in epithelial cells is undetermined and it remains unclear whether failure of this machinery to interact with kAE1 results in dRTA. We hypothesize that in kidney cells, interaction with AP-1A via μ1A adaptin is crucial for proper basolateral membrane targeting of kAE1-WT protein, and that mis-sorting of the kAE1-R901X

dRTA mutant could be due to the deletion of an YXXΦ motif located within the last 11 residues of the AE1 protein.

In this report, we first confirmed the interaction between kAE1 and μ1A adaptor protein in MDCK cells using co-immunoprecipitation with endogenous or heterologously expressed μ1A. In addition, we present evidence that kAE1 also binds to μ1B and μ3 proteins from adaptor complex AP-1B and AP-3, respectively. In agreement with these results, we found that kAE1 protein and μ1A and/or B proteins co-localize in intracellular vesicles in IC of mouse kidney sections and co-immunoprecipitate from a mouse kidney homogenate. Moreover, in MDCK cells where endogenous μ1A was the predominant isoform to be knocked-down, kAE1 protein was prematurely degraded via a lysosomal pathway and kAE1 was no longer detectable at the plasma membrane. In MDCK cells, reintroducing siRNA resistant μ1A allowed proper targeting of newly synthesized kAE1 to the cell surface. Thus, these data highlight a novel role for AP-1A in normal processing of kAE1 in epithelial cells. Finally, our results show that newly synthesized kAE1 does not traffic through RE prior to reaching the cell surface in cells that contain endogenous AP-1A. These findings suggests that *(i)* AP-1A is the primary adaptor complex required for kAE1 processing to the plasma membrane; and *(ii)* AP-1B can partially compensate for the absence of AP-1A in kAE1 normal trafficking. Together, our results demonstrate that AP-1 adaptor complexes are crucial for normal targeting of newly synthesized kAE1 to the cell surface of renal epithelial cells.

3.2. Materials and Methods

3.2.1. Recombinant plasmid constructs and antibodies

The pFB-Neo plasmid construct containing human kAE1 WT cDNA with a HA or myc epitope in position 557 (in the third extracellular loop) were previously described (158,246). The constructs encoding human μ1A-HA and μ1B-HA were provided by Dr. Heike Folsch (Northwestern University) and those encoding VSVG protein were kindly provided by Dr. Paul Melancon (University of Alberta). The kAE1 HT in pFN21A plasmid (reference # FHC11947) was purchased from the Kazusa DNA research institute (associated with Promega Corp., Madison WI, USA). This construct contains the HT protein fused to the amino terminus of human kAE1 cDNA that was inserted between the SgfI restriction site (5') and PmeI restriction site (3'). This construct does not contain an HA epitope.

The rabbit polyclonal antibody that detects both dog μ1A and μ1B adaptor proteins was generously provided by Dr. Linton Traub (University of Pittsburgh) and is not suitable for immunofluorescence experiments. The rabbit polyclonal antibody that detects μ1A from murine kidney homogenates was provided by Dr. Peter Schu (University of Goettingen) and is not suitable for immunoprecipitations or immunofluorescence (personal communication). Mouse antibody against epsilon adaptin (# 612018) and goat antibody against μ 3 adaptor protein (sc-46771) were purchased from BD transduction laboratories and Santa Cruz Biotechnologies, respectively. The mouse antibody against gamma-adaptin subunit was purchased from BD Transduction Laboratories (San Jose, USA). The rabbit polyclonal antibody detecting murine AE1 was provided by Dr. Sebastian Frische (Aarhus University) and is not suitable for western-blots (260). A mouse monoclonal antibody against AE1 developed by Dr. Jennings was obtained from the Developmental Studies Hybridoma Bank developed under the auspices

of the NICHD and maintained by the University of Iowa, Department of Biology, Iowa City, IA 52242. Bric 6 antibody that detects an exofacial epitope of kAE1 was purchased from the International Blood Group Reference Laboratory, Bristol, UK). Goat antibody detecting mouse AE1 (C-17) was purchased from Santa Cruz (Santa Cruz Biotech. Santa Cruz, USA). Mouse monoclonal anti-HA and mouse anti-myc antibodies were purchased from Covance (Covance Inc., Princeton); rat anti-HA antibody was purchased from Roche (Roche Diagnostics, Basel, Switzerland); Mouse monoclonal antibody against MPR was purchased from Abcam (Abcam, Cambridge, USA).

3.2.2. Cell culture

MDCK (CCL-34), LLC-PK1 (CL-101) and HEK 293T (CRL-11268) cells were purchased from the American Type Culture Collection (ATCC, Manassas, USA) and MDCK cells expressing kAE1-WT were prepared according to methods previously described (158). Briefly, HEK 293 cells were transfected with p-VPack-GP, p-VPack-VSV-G and pFB-Neo-kAE1-HA557 WT or mutant plasmids using FuGENE 6 (Roche Applied Science, Indianapolis, IN, USA). Cell culture supernatants containing infectious viral particles were added to dividing MDCK cells complemented with 8 mg / ml of polybrene (Sigma-Aldrich Canada Ltd., Oakville, ON, Canada). After 24 hours incubation, an heterogenous population of MDCK cells expressing kAE1 was selected with 1 mg / ml geneticin (Sigma-Aldrich Canada Ltd., Oakville, ON, Canada). MDCK or LLC-PK1 cells were also transiently transfected using the Neon transfection system (Invitrogen, Inc. Burlington, Canada), following the manufacturer's instructions. For immunofluorescence experiments, $1*10^6$ cells were transfected with 2 to 6 mg of cDNA, and for immunoprecipitation experiments, $3 * 10^6$ cells were transfected with 24 mg of

cDNA. Both LLC-PK1 and MDCK cells were transfected using 1400 V pulse voltage, 20 ms pulse width and 3 pulses.

3.2.3. Immunoprecipitation

MDCK cells expressing kAE1-HA557 WT were lysed in PBS containing 1 % Triton X-100 and protease inhibitors ((aprotinin 1mg/ml, leupeptin 2 mg/ml, pepstatin A 1 mg/ml, and PMSF 100 mg/ml). Aliquots of the cell lysates were saved as total fraction, the remaining cell lysates were incubated with rabbit anti-μ 1A/B or with rat anti-HA antibodies, followed by precipitation with Protein G-sepharose (Thermo Scientific, Rockford, USA). The bound proteins were eluted with Laemmli buffer before detection by Western blot using either a mouse anti-HA antibody followed by an anti-mouse antibody coupled to HRP, rabbit anti- μ1A/B anti-rabbit antibody followed by an anti-rabbit antibody coupled to HRP, mouse anti-gamma adaptin antibody followed by an anti-mouse antibody coupled to HRP or mouse anti-actin antibody followed by an anti-mouse antibody coupled to HRP. Alternatively, proteins in cell lysates were immunoprecipitated with a rabbit anti-myc antibody and detected using the mouse anti-HA antibody.

Kidney from PBS-perfused mouse kidneys were freshly dissected and extracts were prepared in PBS (pH 7.5), 1 mM EDTA, 1 % Triton X-100 and protease inhibitors at 4 °C. The PBS perfusion allowed the removal of a majority of red blood cells that would contain extensive amounts of erythroid AE1. After removing insoluble materials with two low speed centrifugations (15000 Xg for 10 min), an aliquot of the Triton soluble extract (60 μg of proteins) was saved while the remaining lysate (3 mg of total proteins) was pre-cleared with protein G beads, prior to immunoprecipitation with 5 μl of

goat anti-AE1 antibody (Santa Cruz C-17). The eluted proteins were detected on Western-blot using a rabbit anti- μ1A antibody. All experiments were performed in compliance with the animal ethics board at the University of Alberta, Health Sciences Section (protocol 576).

3.2.4. Immunocytochemistry

MDCK cells expressing kAE1-HA557 WT were grown on glass coverslips, fixed with 4 % paraformaldehyde, permeabilized with 0.3 % Triton X-100 and blocked with 1 % BSA. Cells were then incubated with mouse anti-HA antibody and rabbit polyclonal anti-gamma adaptin antibody or rat anti-HA and mouse anti-CD-MPR antibodies. Secondary antibodies were donkey anti-mouse or donkey anti-rat antibodies coupled to Cy3 (Jackson Immunoresearch, West Grove, PA, USA) and goat anti-mouse antibody coupled to Alexa 488 (Molecular Probes, Carlsbad, CA, USA). Nuclei were stained with DAPI (1 μg / ml) in PBS or water for 5 min (Sigma Aldrich). Samples were examined using an Olympus IX81 microscope equipped with a Nipkow spinning-disk optimized by Quorum Technologies (Guelph, ON, Canada) and a 100 X lens.

For immunohistochemistry experiments, formalin fixed, paraffin-embedded 2 mm thick mouse kidney sections were baked overnight at 60 °C, dewaxed in xylene and hydrated in decreasing concentrations of alcohol in distilled water. Sections were heated to retrieve antigen in TEG buffer at pH 9 (10 mM Tris, 0.5 mM EGTA, pH 9.0) for 20 minutes before blocking then immunostained with mouse anti-gamma adaptin and rabbit anti-AE1 antibodies (1:500) in PBS, followed by anti-mouse antibody coupled to Cy3 and anti-rabbit antibody coupled to Alexa 488 (1:500) in PBS. The sections were examined with the Olympus IX81 microscope described above and a 20 X objective.

3.2.5. Knockdown of Canine µ1A adaptin with siRNA duplexes

Sub-confluent MDCK cells (2 X 10^5 cells per well) expressing kAE1-HA557 WT, grown in 6-well plates, were transiently transfected with either 200 nM of canine-specific siRNA duplexes targeting dog µ1A adaptin (5'- GGTCCGAGGGCATCAAGTA) or 200 nM of control siRNA targeting luciferase (Dharmacon Inc. Lafayette, CO, USA) using 12 µl of OLIGOFectamine (Invitrogen, Inc. Burlington, Canada) resuspended in opti-MEM reduced serum medium (Invitrogen, Carlsbad, CA, USA) (protocol provided by Dr. Ashley Toye, Bristol University). Four hours later, the cell culture medium was replaced by DMEM-F12 containing 10 % fetal bovine serum, 0.5 % penicillin / streptomycin and 1 mg / ml geneticin to maintain expression of kAE1-HA557 WT protein. Transfected cells were grown for 48 h or 72 h at 37 °C before lysis in PBS containing 1 % Triton X-100 and protease inhibitors. Approximately 20 % of the cells died after 72 h incubation with siRNA against canine µ1A, but not with siRNA against luciferase. After lysing cells, 7 µg of total proteins were loaded per lane on an 8 % SDS-PAGE gel. After transfer to a nitrocellulose membrane, the samples were incubated with mouse anti-HA antibody, rabbit anti- µ1A/B antibody and mouse anti-actin antibody, followed by anti-mouse and anti-rabbit secondary antibodies coupled to HRP. After visualization by enhanced chemiluminescence, intensities of the bands of interest were compared using densitometric analysis with Image J software. Alternatively, after 48 h or 72 h incubation post-transfection in 6-well plates containing glass coverslips, cells were fixed with 4 % paraformaldehyde, permeabilized with 0.2 % Triton X-100 and blocked with 1 % BSA. Cells were then incubated with rat anti-HA antibody and mouse anti-CD-MPR antibody. Secondary antibodies were donkey anti-rat antibodies coupled to Cy3 and donkey anti-

mouse antibody coupled to Cy5 (Jackson Immunoresearch). Nuclei were stained with DAPI. Samples were examined using an Olympus IX81 microscope equipped with a Nipkow spinning-disk optimized by Quorum Technologies (Guelph, ON, Canada) and a 100 X objective. There is a 3 bases mismatch between our μ1A siRNA and canine μ1B, 10 bases mismatch between our μ1A siRNA and canine μ3 and 10 bases mismatch between μ1A siRNA and canine μ4 from AP-4.

3.2.6. Expression of siRNA resistant μ1A in μ1A/B siRNA transfected cells

MDCK cells (1 X 10^6 cells) expressing kAE1-HA557 WT were transiently transfected with 5 μg of either pcDNA3 empty vector or μ1A HA cDNA in the pCDNA3 vector using the NEON system. 24 hours later, 200 nM of either canine-specific siRNA duplexes targeting dog μ1A protein or control siRNA targeting luciferase were transfected using the protocol described in the above paragraph. Forty-eight hours later, the cells were lysed and kAE1 and μ1A were both detected by western-blot using a mouse anti-HA antibody followed by anti mouse antibody coupled to HRP. μ1A HA was detectable by western-blot after up to 72 hours post transfection and 5 μg of μ1A HA cDNA was the minimum amount required for maximal expression of μ1A HA protein for this number of cells (data not shown). To calculate the amount of rescued kAE1, intensities of the respective bands were measured using the Image J software. We normalized the intensities of kAE1 to the internal control actin, and then compared the percentage of kAE1 band in μ1A/B siRNA cells to kAE1 in luciferase siRNA cells in each condition (pcDNA3, μ1A HA or μ1B HA transfected cells).

3.2.7. Recycling endosomes inactivation and immunolocalization

To inactivate RE, we adapted the RE inactivation protocol from (261). MDCK cells ($1X10^6$ cells per well) were transiently transfected with 2 μg of cDNA encoding kAE1-HT and 2 μg of cDNA encoding VSVG fused to the green fluorescent protein, using the NEON system. The cells were then placed in 6 well plates with glass coverslips in CO_2-independent culture medium (Invitrogen) supplemented with 10 % FBS and incubated for 2 hours at 37 °C to allow them to re-attach to the glass coverslip, prior to their transfer to 19 °C. The following day, the activity of pre-existing kAE1 HT proteins was blocked by incubating cells with 500 nM of coumarin-HT substrate (Promega) for 1 h at 19 °C in a starving DMEM-F12 medium (containing no serum or antibiotics) to deplete transferrin (Tfn). After 3 washes with PBS for 5, 5 and 10 minutes on ice, cells were incubated with 0.01 mg / ml of transferrin-HRP (Tfn-HRP, Accurate Biochemical, US Biological) at 19 °C in the starving medium for 2 hours. During the last 20 minutes of incubation, 50 nM of TMR-HT substrate was directly added to the medium to allow labeling of newly synthesized proteins. Cells were then washed three times with PBS, twice with an ice-cold solution containing 150 mM NaCl and 20 mM citric acid, pH 5 to remove the remaining cell surface Tfn-HRP. RE were then inactivated by incubating the cells on ice for 1 h with 0.1 mg / ml DAB and either 0.025 % H_2O_2 or PBS (as a control condition) in the dark. After 2 washes with PBS containing 1 % BSA, the medium was replaced by warm DMEM-F12 medium containing 10 % FBS and 10 μg / ml of cycloheximide and transferred to 30 °C for 0 (no chase) or 3 hours to release proteins from the TGN and allow their trafficking to the cell surface. Cells were then fixed with 4 % paraformaldehyde, permeabilized with 0.2 % Triton X-100, blocked with 1 % BSA and incubated with rabbit anti-GFP antibody followed by anti-rabbit antibody coupled to

Alexa 488. Samples were examined using an Olympus IX81 microscope equipped with a Nipkow spinning-disk optimized by Quorum Technologies and a 100 X objective. For counting cells, random pictures were taken using a 20 X objective on the same microscope and two individuals independently counted the percentage of cells transfected with kAE1 that had kAE1 cell surface staining as well as the number of cells transfected with VSVG that displayed VSVG cell surface staining.

3.2.8. Pulse chase like experiment

MDCK cells were transfected with siRNA against either luciferase or fluorescein-labeled siRNA against μ1A/B as described in the paragraph entitled "Knock-down of canine μ1A adaptin with siRNA duplexes". Twenty-four hours later, the cells were transfected with kAE1-HT and either μ1A HA, μ1B HA or pCDNA3 vector as a control using the NEON system. Forty-eight hours after this second transfection (72 hours after the first transfection), pre-existing kAE1 HT proteins were blocked with 500 nM of coumarin-HT substrate, and cells were incubated at 37°C for 30 minutes to allow synthesis of new kAE1-HT. The newly synthesized kAE1-HT were then either stained with TMR-HT (red) or FAM-HT (green) substrate (50 nM) and either immediately fixed (no chase) or incubated at 37 °C for 3 hours to allow trafficking of the protein (3 h chase). Cells were then fixed with 4 % paraformaldehyde, permeabilized with 0.2 % Triton X-100, blocked with 1 % BSA and incubated with mouse anti-HA antibody to detect μ1A HA or μ1B HA. Slides were examined using an Olympus IX81 microscope equipped with a Nipkow spinning-disk optimized by Quorum Technologies and a 100 X objective.

3.2.9. Statistical analysis

Experimental results are summarized as mean ± SEM. All statistical comparisons were made using unpaired Student's *t* test. A *P* value less than 0.05 was considered significant.

3.3. Results

3.3.1. μ1A and B subunits bind to kAE1 in epithelial cells

Recently, the C - terminus of the AE1 was found to interact with μ1A subunit from adaptor complex 1A, using a yeast two-hybrid assay (52). We aimed to determine the significance of this interaction in renal epithelial cells. In MDCK cells, we first confirmed that human kAE1 interacted with endogenous canine μ1A by immunoprecipitation in renal epithelial cells. We immunoprecipitated kAE1-WT (246) expressed in MDCK cells with rat anti-HA antibody and blotted the samples with rabbit anti-μ1A/B antibody, mouse anti-gamma adaptin or mouse anti-actin antibodies as a negative control (Fig 3.1 A). In MDCK epithelial cells, kAE1 protein migrates as two main bands: the upper band corresponds to proteins carrying complex oligosaccharide (open circle) and the lower band corresponds to kAE1 carrying high mannose oligosaccharide (closed circle) as shown on Figure 3.1 A and B. On Figure 3.1 A, we show that kAE1, endogenous μ1A/B and gamma adaptin, but not actin are present in the same protein complex in MDCK cell lysates.

To clarify whether kAE1 can specifically bind to μ1A and / or B isoform, we transiently co-expressed kAE1 carrying a myc epitope (kAE1 myc) (158) and either μ1A HA or μ1B HA in MDCK cells and examined whether they interact. As seen in Figure 1 B, we observed that both μ1A and μ1B co-immunoprecipitated with kAE1 from MDCK cells transiently expressing either human μ1A or μ1B carrying a HA epitope (μ1A HA or

μ1B HA). This result indicates that kAE1 can be located in the same protein complex as either μ1A or μ1B in epithelial cells.

To confirm our previous findings, we transiently expressed kAE1-WT in LLC-PK1 cells that were shown to lack the endogenous μ1B (166). In these cells, we were also able to detect co-immunoprecipitation between kAE1-WT and γ-adaptin (which is only part of the AP-1A complex, since these cells are lacking endogenous μ1B) as well as with μ1A adaptin, but no co-immunoprecipitation with actin (data not shown). These results confirm that kAE1-WT can interact with AP-1A adaptor protein complex.

3.3.2. kAE1 protein co-immunoprecipitates with AP-3 but not with AP-4 adaptor protein complex

Since AP-1A recognizes the same YXXΦ motif on cargo proteins as the other clathrin associated adaptors (189), we asked whether other adaptors also interact with kAE1. Specifically, we tested the interaction of kAE1 with AP-4, which is involved in trafficking of basolateral membrane proteins (262). We also determined whether AP-3A, which localizes in the TGN and endosomes, interacts with kAE1 (189). Figure 3.1 C and D show that in MDCK cells, kAE1 co-immunoprecipitates with AP-3 μ but not with AP-4 ε adaptin. Since AP-3A is involved in trafficking of cargo proteins to the lysosome, we hypothesize that kAE1 interacts with this adaptor complex on its way to degradation.

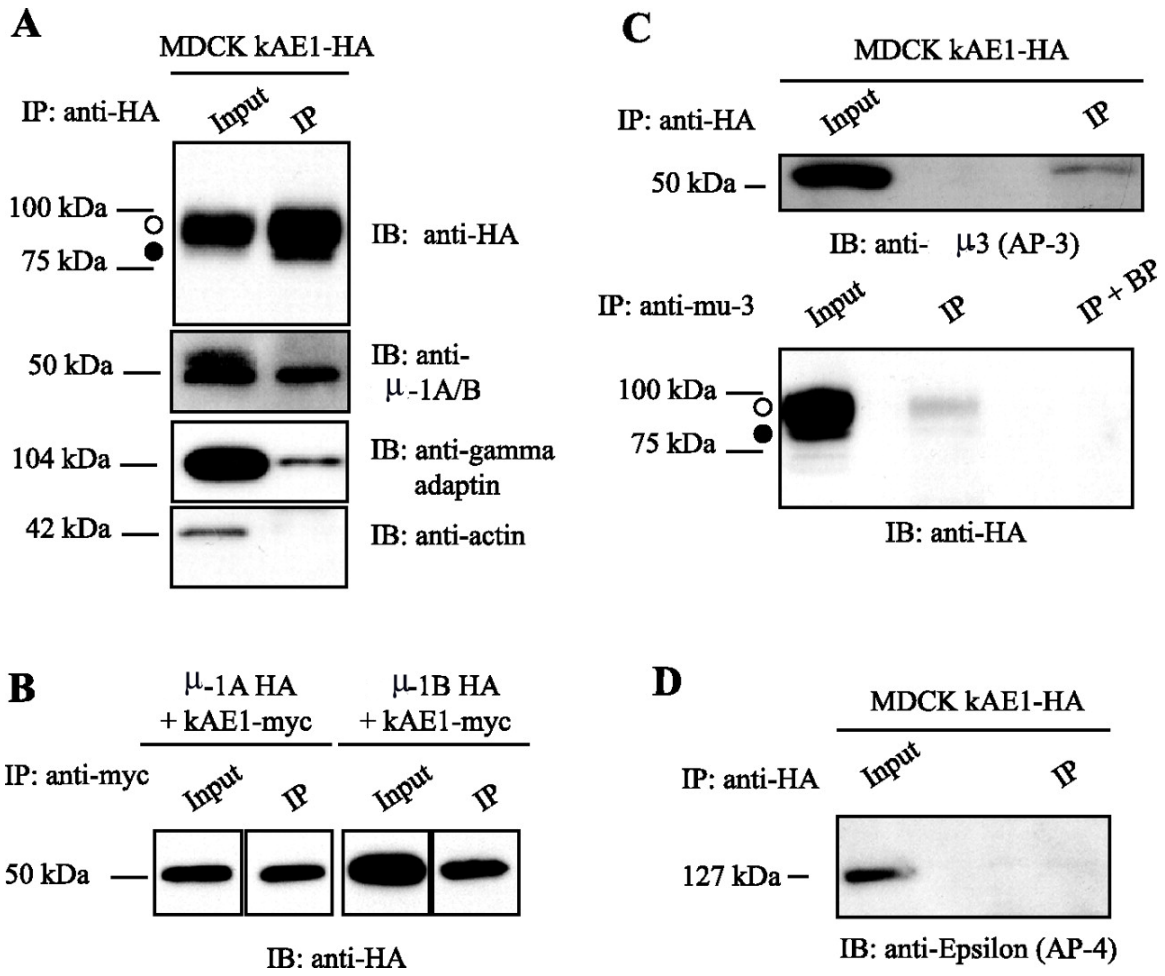

Figure 3.1: kAE1 binds to AP-1A, AP-1B and AP-3 adaptor complexes.

A. Madin-Darby canine kidney cells (MDCK) expressing kAE1-WT were lysed and proteins were either directly resolved on SDS-PAGE (input) or immunoprecipitated (IP) with rat anti-hemagglutinin (HA) antibody before the SDS-PAGE. After proteins were transferred to nitrocellulose membranes, samples were blotted with mouse anti-HA antibody, rabbit anti-subunit μ1A/B antibody, mouse anti-gamma adaptin antibody, or mouse anti-actin antibody followed by anti-mouse horseradish peroxidase (HRP) or anti-rabbit HRP antibodies. Open circle corresponds to kAE1 carrying complex oligosaccharides, and filled circle indicates kAE1 carrying high mannose oligosaccharides. ***B***. MDCK cells expressing kAE1 WT carrying a myc epitope and either

(Continued from figure 3.1)

μ1A-HA or μ1B-HA was lysed, and proteins were either directly loaded on an 8 % SDS-PAGE (input) or immunoprecipitated with mouse anti-myc antibody. μ subunits present in the same protein complex were detected with a rat anti-HA antibody followed by an anti-rat antibody coupled to HRP. ***C***. MDCK cells expressing kAE1-WT were lysed. 20 μg of protein was directly loaded on an 8 % SDS-PAGE. Three aliquots containing each 500 μg of protein present in the remaining lysate were prepared. Proteins in each aliquot were either immunoprecipitated with a rat anti-HA antibody (Fig. 1 **D**, **top**) or with goat anti-μ3 adaptor protein antibody (**bottom**) before SDS-PAGE. After proteins were transferred on nitrocellulose membranes, samples were blotted with goat anti- μ3 adaptor protein or mouse anti-HA antibodies. IB, immunoblot; BP, immunoprecipitating antibody was preincubated with the immunogenic peptide before incubation with the cell lysate. ***D***. MDCK cells expressing kAE1-WT were lysed, and 500 μg of protein was immunoprecipitated with rat anti-HA antibody followed by SDS-PAGE. After transfer, the proteins were detected with a mouse anti-ε adaptor protein antibody. Blots represent 3 independent experiments.

3.3.3. KAE1 protein colocalizes with AP-1A and /or B in mouse kidney sections and coimmunoprecipitates with µ1A from mouse kidney homogenates

If the interaction between kAE1 protein and µ1A occurs *in vivo*, we expect that both proteins co-localize to some extent in the same cells. We thus tested this in IC of murine kidney. Since AP-1A is ubiquitous and AP-1B adaptor complex is present in cortical collecting ducts (217), it is likely that both kAE1 and AP-1A and B adaptor complexes are expressed in the same cells. In the absence of an antibody specifically detecting µ1A subunit that would work in immunofluorescence, we opted to detect the gamma-adaptin subunit present in AP-1A and AP-1B complexes. Mouse kidney sections were incubated with a rabbit polyclonal antibody that specifically recognizes mouse kAE1 protein (stained in green) and with a mouse anti-gamma-adaptin antibody (stained in red) (Fig 3.2 A). In contrast with sections incubated with secondary antibodies only (data not shown), the antibody against kAE1 detected the protein in alpha-IC (the other cells in the tubular section being beta-IC, non-alpha, non-beta IC and principal cells that do not express kAE1) and showed a clear predominant basolateral staining as well as a discrete vesicular intracellular staining. The anti-gamma-adaptin antibody displayed a perinuclear staining, consistent with the previously described localization of AP-1 complexes in the TGN (228). In the insets (Fig 2 A, bottom panels), a higher magnification of intracellular red and green staining shows co-localization of both mouse endogenous kAE1 protein with endogenous gamma-1 subunit of the AP-1 complex in a vesicular-like pattern,

supporting that kAE1 and AP-1A and/or B complexes can co-localize in the same cell compartment in mouse kidney sections.

We next determined whether endogenous kAE1 could physically interact with endogenous μ1A in mouse kidney homogenates. As seen in Figure 3.2 B, immunoprecipitated kAE1 pulled down a protein with the same molecular weight as endogenous μ1A strongly suggesting that the two proteins interact *in vivo*. We were unable to perform the reciprocal immunoprecipitation, as the rabbit anti- μ 1A antibody used in this experiment is not suitable for immunoprecipitations or immunofluorescence. Nevertheless, this immunoprecipitation performed with kidney homogenates confirms that kAE1 and μ1A physically interact *in vivo.*

3.3.4. KAE1 is degraded in μ1A/B knocked- down MDCK cells

To determine whether μ1A protein is important for kAE1 sorting, we designed dog-specific siRNA duplexes, transiently transfected sub-confluent MDCK cells expressing kAE1-WT protein with either μ1A specific siRNA or control siRNA against luciferase (Fig 3.3 A) and detected endogenous μ1A/B, kAE1 and actin proteins by immunoblot. Densitometric comparison of the immunoblot bands indicated that there was no change in the amount of endogenous μ1A/B proteins in cells transfected with siRNA against luciferase after 48 h or 72 h incubation. In contrast, we observed a 40 ± 4 % (n = 3, ± SEM) reduction of endogenous μ1A/B proteins after 48 h incubation post-transfection with siRNA against μ1A, and a 50 ± 13 % (n = 3, ± SEM) reduction after 72 h incubation.

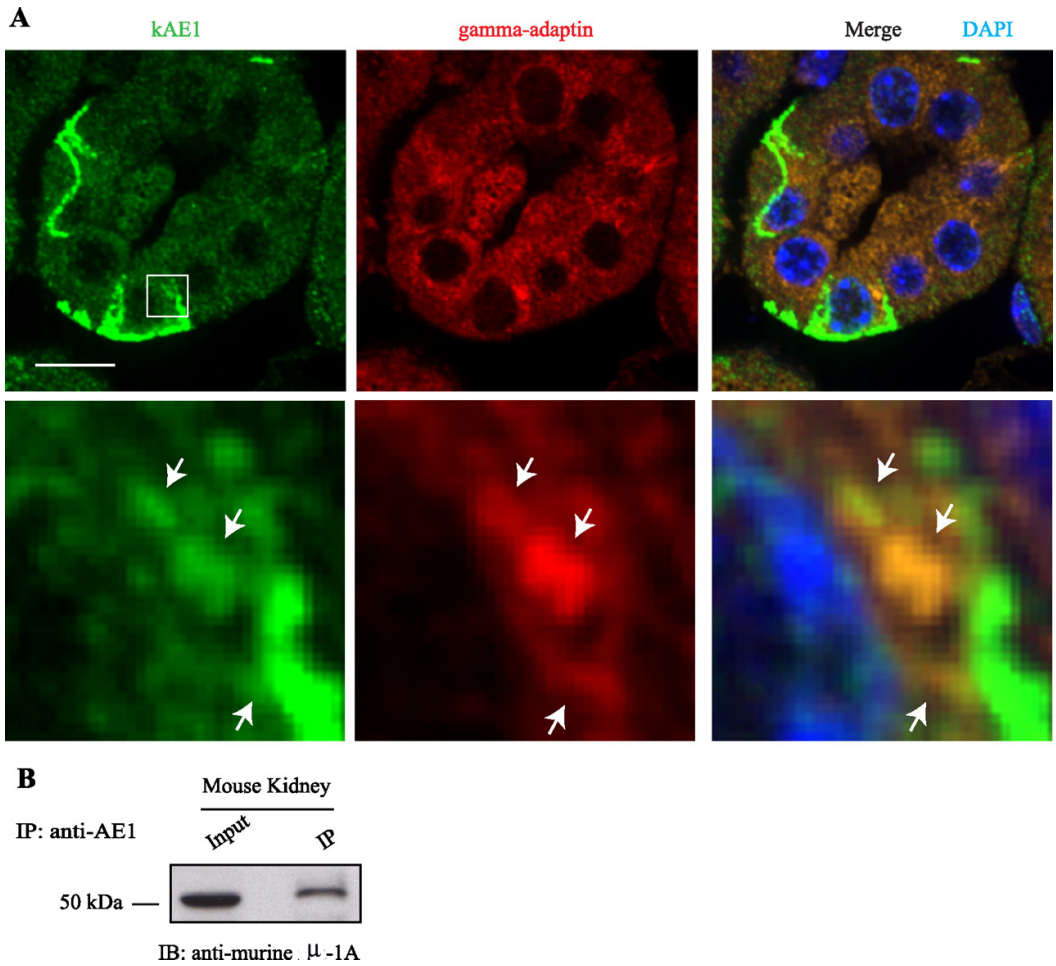

Figure 3.2: kAE1 WT immunoprecipitates and colocalizes with the AP-1 adaptor complex. ***A***. paraffin-embedded 2 µm thick mouse kidney sections were submitted to heat-induced antigen retrieval before blocking and incubation with rabbit anti-kAE1 antibody and mouse anti-gamma adaptor subunit. Slides were then incubated with anti-rabbit antibody coupled to Alexa 488 (green) and anti-mouse antibody coupled to Cy3 (red), followed by nuclear staining with DAPI (blue). Samples were examined using an Olympus spinning disk confocal microscope and a 100 X objective. **Bottom**: enlargement of the region contained in the white square in the above picture. Note that only few cells, that correspond to alpha IC, show basolateral membrane staining of kAE1. Non-stained cells are likely beta, and non-alpha non-beta IC, and principal cells.

(Continued from figure 3.2)

White arrows indicate the location of overlapping red and green staining. Bars =10 μm. ***B***. kidney homogenate was prepared from freshly dissected mouse kidneys and either directly loaded on an 8 % gel or immunoprecipitated with a goat anti-AE1 antibody. Coimmunoprecipitated endogenous μ1A proteins were detected with a rabbit anti-murine μ1A antibody.

Importantly, the rabbit anti μ1A/B antibody detects both μ1A and μ1B (263) proteins, therefore, the 40 % and 50 % reduction represent the reduction in both μ1A and B together. μ1A is 79 % identical to μ1B (166,264) thus, although the siRNA we designed presents 3 bases out of 19 mismatching with μ1B mRNA, we performed a quantitative RT-PCR to determine the respective amount of endogenous μ1A or B mRNAs remaining in cells knocked-down with siRNAs against μ1A, relative to cells treated with siRNAs against luciferase. Quantitative RT-PCR indicated that 48 hours post-transfection, there was 63 ± 3 % (n = 7, ± SEM) endogenous μ1B and only 38 ± 4 % (n = 7, ± SEM) endogenous μ1A mRNAs remaining in cells transfected with siRNAs against μ1A. Concomitant with this significant decrease of endogenous μ1A/B mRNA and proteins, our immunoblot showed an abrupt decrease (43 ± 5 % (n = 3, ± SEM)) in the amount of kAE1-WT protein after 48 h incubation and an 81 ± 5 % (n = 3, ± SEM) decrease of kAE1 protein amount after 72 h (Fig 3.3 A and B). No change of endogenous amount of housekeeping protein actin was observed in any of these conditions. The quick disappearance of kAE1 in MDCK cells where μ1A and to a lesser extent μ1B were knocked down suggests mis-sorting and premature degradation of kAE1 in these cells.

To determine the respective role of μ1A or μ1B knock down on kAE1 stability, we specifically knocked down endogenous μ1B using a previously published siRNA sequence (216) (Fig 3.3 C). Interestingly, this siRNA was reported to knock down 90 % of endogenous μ1B protein in MDCK cells but increased μ1A protein levels by a 1.5 to 2 factor without altering μ1A mRNA levels. Accordingly, we were unable to detect a significant decrease of μ1A and B proteins using the non-discriminating rabbit antibody against μ1A/B. However, although RT-PCR results indicated that endogenous μ1B

mRNA was knocked down by 80 ± 2 % (n = 3, ± SEM), consistently with data previously published, there was only a 21 ± 5 % (n = 3, ± SEM) decrease of steady-state kAE1 protein in these cells after normalizing the intensity of kAE1 bands to the internal control actin. These results indicate that the knock down of either μ1A or μ1B results in decreased expression of kAE1.

To confirm these findings, we investigated the sub-cellular location of kAE1 WT protein in cells where μ1A and to a lesser extent μ1B were knocked-down by immunostaining. MDCK cells expressing kAE1-WT were transiently transfected with siRNA against μ1A or luciferase and grown for 48 or 72 hours prior to detecting kAE1 (red staining) and CD-MPR (green staining) (Fig 3.3 D). CD-MPR binds to newly synthesized hydrolases carrying mannose-6-phosphate in the TGN and target them to endosomes before they reach their final destination in lysosomes (259). AP-1A interacts with CD-MPR via the μ1A subunit. In MDCK cells transfected with siRNA against luciferase and incubated for either 48 or 72 h, kAE1 WT protein (red) localized predominantly at the plasma membrane, and CD-MPR was located in a perinuclear compartment, likely the TGN. In contrast, 48 h after transfection with siRNA against μ1A, the staining from kAE1 WT protein was dramatically decreased and plasma membrane staining was no longer detected (Fig 3.3 D). In the same cells, the CD-MPR TGN marker (green) showed a diffuse, non - perinuclear staining, in agreement with previous findings in $\mu1A^{-/-}$ mouse embryonic fibroblasts (228). Seventy-two hours post-transfection, there was almost no more red staining corresponding to kAE1 protein in the three cells transfected with siRNA against μ1A (as verified using fluorescein dye attached to the siRNA, data not shown) (white stars, Fig 3.3 D). In these three cells, CD-

MPR also showed diffuse staining in the periplasm, but the top cell that was not transfected displayed normal plasma membrane red staining for kAE1 protein and normal perinuclear staining of CD-MPR. These data are consistent with the degradation of kAE1-WT protein in MDCK cells expressing reduced levels of μ1A/B.

3.3.5. Expression of human μ1A-HA and μ1B-HA rescues kAE1 stability in μ1A/B siRNA transfected cells

Since RT-PCR results indicated that the siRNAs we used were not exclusively specific to canine μ1A but also significantly knock down μ1B, we determined what effect siRNA resistant human μ1A or μ1B proteins expression would have on kAE1 stability in cells knocked down for endogenous canine μ1A/B. Figure 3.4 A shows that human μ1A HA and μ1B HA proteins are unaffected by the μ1A/B siRNAs since there is no significant decrease of human μ1A HA or μ1B HA in cells either transfected with siRNA against luciferase or against canine μ1A/B. Furthermore, in μ1A/B siRNA transfected cells, 80 ± 6 % (n = 4, ± SEM) of kAE1 was detected after expressing human μ1A-HA while only 67 ± 7 % (n = 4, ± SEM) kAE1 was present after pcDNA3 transfection (see materials and methods for detailed calculation) (Fig 3.4 B). Similarly, 86 ± 6 % (n = 4, ± SEM) of kAE1 was detectable after transfection with human μ1B HA in the μ1A/B siRNA transfected cells. These findings indicate that transfection with siRNA resistant human μ1A or μ1B stabilizes kAE1 in μ1A/B siRNA transfected cells. Thus, both μ1A and μ1B are involved in the stability of kAE1 at the steady state in epithelial cells.

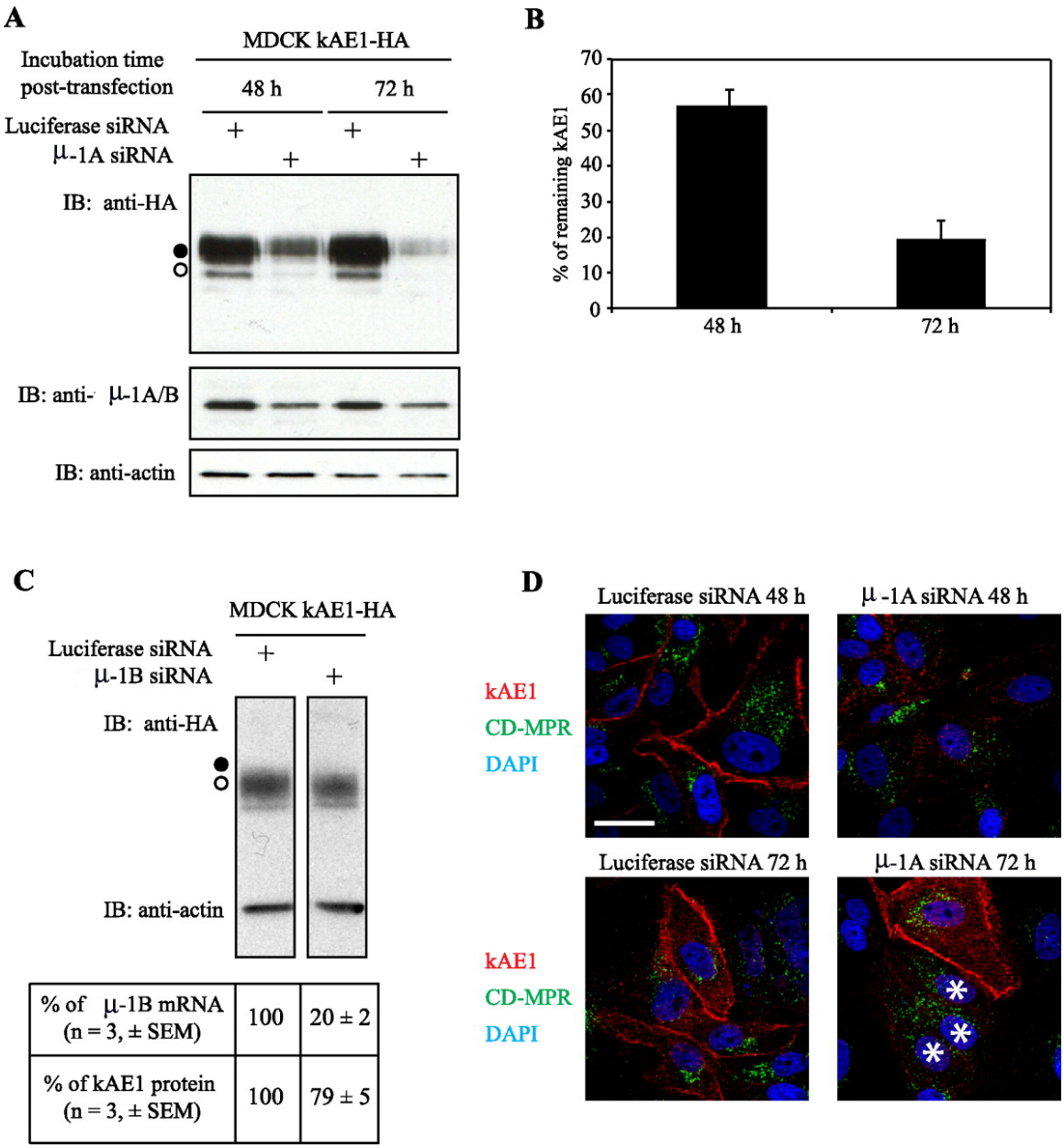

Figure 3.3: Knocking down μ1A affects the stability of kAE1 as well as trafficking of cation-dependent mannose 6-phosphate receptor (CD-MPR) and kAE1 in MDCK cells. ***A.*** MDCK cells expressing kAE1 WT were transiently transfected with either 200 nM of canine-specific siRNA duplexes targeting μ1A or 200 nM of control siRNA targeting luciferase and grown for 24, 48, or 72 h. Cell lysates (7 μg of proteins) were loaded on SDS-PAGE gel and proteins were examined by Western blotting using mouse

(Continued from figure 3.3)

anti-HA antibody, rabbit anti- μ1A/B antibody that detects the endogenous μ1A and μ1B proteins, and mouse anti-actin antibody, followed by anti-mouse and anti-rabbit secondary antibodies coupled to HRP. Blot represents 3 independent experiments. ***B***. histogram representing the percentage of kAE1 remaining in cells transfected with siRNA against μ1A, 48 or 72 h after transfection, after normalization to amount of actin. Amounts were calculated by densitometric analysis of 3 independent experiments, including the 1 presented on **A**. Intensity of the bands was measured using the Image J software. Error bars correspond to means ±SE. ***C***. MDCK cells expressing kAE1-WT were transfected three times at 72-h intervals with 200 nM of siRNA against μ1B using the NEON transfection system according to a previously published protocol (19). Seventy-two hours after the third transfection, 15 μg of proteins in the cell lysates were immunoblotted with anti-μ1A/B, anti-actin or anti-HA antibodies. Table indicates the percentage of endogenous μ1B mRNA quantified by RT-PCR (**n** = 3), and the percentage of remaining kAE1 protein in these cells (**n** =3). **D**: 48 or 72 h posttransfection, cells grown on glass coverslips were fixed, permeabilized and blocked before incubation with rat anti-HA antibody and mouse anti-CD-MPR antibody. Secondary antibodies were donkey anti-rat antibodies coupled to Cy3 (red) and donkey anti-mouse antibody coupled to Cy5. Nuclei were stained with DAPI (blue). For the purpose of this figure, Cy5 staining (corresponding to μ1A) is here shown in green. White stars indicate the location of 3 cells transfected with the siRNA against μ1A. Images represent 3 separate experiments.

3.3.6. In presence of AP-1A, newly synthesized kAE1 does not traffic through recycling endosomes

AP-1B, which is predominantly located in RE, is required for basolateral trafficking of some newly synthesized membrane proteins such as VSVG (256). Since kAE1-WT binds to both AP-1A and AP-1B, we wondered whether AP-1B is necessary for newly synthesized kAE1 to reach the plasma membrane in renal epithelial cells. Since kAE1 reaches the basolateral membrane in polarized LLC-PK1 cells (159 and our own data,160), we suspected that this hypothesis would be wrong. Nevertheless, we asked whether newly synthesized kAE1 traffics to the plasma membrane when RE, which contain AP-1B, are inactivated.

We obtained a construct encoding a chimeric protein where the modified haloallcane dehalogenase haloTag (HT) protein (Promega) is fused to the kAE1 amino terminus (kAE1-HT). We first confirmed that this fusion protein is properly targeted to the plasma membrane and to the basolateral membrane of polarized MDCK cells, despite some intracellular retention of the fusion protein (Fig 3.5 A). The HT system allows studying trafficking of a single pool of proteins, using pulse-chase-like protocols with multiple membrane-permeant, fluorescent HT substrates. We transiently co-transfected MDCK cells with VSVG, which traffics through RE on its way to the plasma membrane (256), and kAE1 WT HT protein in MDCK cells. After transfection, we stopped trafficking of newly synthesized VSVG in the Golgi by incubating the cells at 19 °C for 18 hours. We then blocked all pre-existing kAE1-HT with a first coumarin-HT ligand, labeled newly synthesized kAE1-HT with a TMR (red) fluorescent HT substrate and allowed its trafficking to the Golgi at 19 °C. We inactivated RE using transferrin coupled

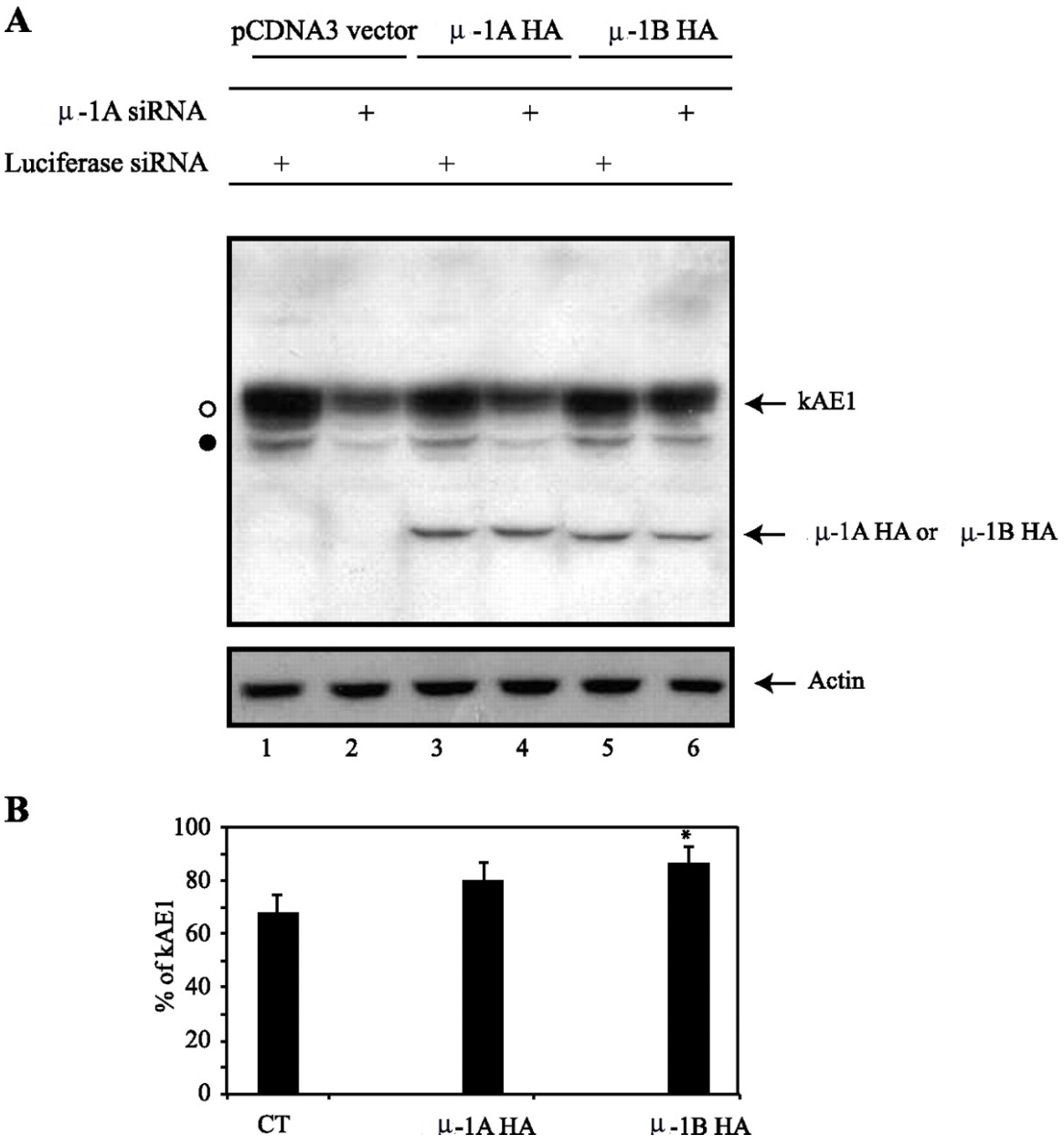

Figure 3.4: siRNA resistant μ1A stabilizes kAE1 in cells knocked down for μ1A and/or B. ***A***. MDCK cells expressing kAE1 WT were transiently transfected with either 5 μg of μ1A HA, μ1B HA or pCDNA3 as control. Twenty-four hours later, cells were transfected with 200 nM of siRNA targeting μ1A or 200 nM of control siRNA targeting luciferase and grown for 48 h. Cell lysates (20 μg of proteins) were loaded on SDS-

(Continued from figure 3.4)

PAGE gel, and proteins were detected by immunoblotting using mouse anti-HA antibody and mouse anti-actin antibody. Blot represents 3 independent experiments. ***B***. Histogram representing the percentage of kAE1 present in cells transfected with siRNA against μ1A or luciferase and either subsequently transfected with pCDNA3 vector, μ1A HA or μ1B HA. Amounts were calculated by densitometric analysis of 4 independent experiments; see EXPERIMENTALPROCEDURES for calculation details. Intensity of the bands was measured, using the Image J software. Error bars correspond to means **±** SE. ***P** < 0.05 vs. control.

to horseradish peroxidase (Tfn-HRP) (see methods for details) and then released trafficking of proteins from the TGN by transferring cells from 19 °C to 30 °C for 0 (no chase) or 3 hours (3 hours chase). This protocol was adapted from (256) and exploits the reaction catalyzed by HRP, which forms an insoluble precipitate with DAB and H_2O_2. We then immunolocalized VSVG (green), the kAE1-HT being already labeled with the red fluorescent substrate in side views (X-Z sections) of the cells (Fig 3.5 B). If newly synthesized kAE1 traffics through AP-1B positive RE prior to reaching the plasma membrane, it should be retained intracellularly in inactivating conditions, along with VSVG. In contrast, if kAE1 traffics independently from AP-1B positive RE, the RE inactivation should only retain VSVG intracellularly without affecting kAE1 cell surface localization. As seen in Figure 3.5 B, in contrast with control conditions, kAE1 was detected at the plasma membrane in cells where VSVG was retained intracellularly due to RE inactivation. We observed that after 3 h chase in control conditions (active recycling endosomes), 81 % (n = 121) of the kAE1 transfected cells displayed kAE1 at the cell surface and 76 % (n = 83) of VSVG transfected cells showed VSVG at the plasma membrane. In contrast, when RE were inactivated, 75 % (n = 86) of the kAE1-transfected cells displayed kAE1 at the cell surface while only 45 % (n = 86) of VSVG transfected cells showed VSVG at the plasma membrane. This result indicates that newly synthesized kAE1 does not traffic through RE prior to reaching the plasma membrane and suggest that kAE1 preferentially use another adaptor protein complex than AP-1B.

3.3.7. Expression of μ1A rescues trafficking of newly synthesized kAE1 to the plasma membrane

Our previous data strongly suggest that, when AP-1A is present, AP-1B is not involved in trafficking of newly synthesized kAE1 to the plasma membrane. Since kAE1 does not interact with the TGN-located AP-4 adaptor complex that is involved in basolateral targeting of some proteins (262), we hypothesized that AP-1A may be involved in targeting of newly synthesized kAE1 to the plasma membrane.

To test this hypothesis, MDCK cells with knocked down μ1A/B were transfected with kAE1-HT and either human μ1A HA, μ1B HA or the empty vector. Forty eight hours later, we performed a pulse-chase like experiment as follows: pre-exisiting kAE1-HT proteins were first blocked with coumarin-HT substrate, and newly synthesized proteins were stained with TMR (red) fluorescent HT substrate and either allowed to traffic for 0 or 3 hours (3 hours chase) at 37 °C (Fig 3.6). After fixation, cells were examined using a confocal microscope. Cells transfected with the fluorescein coupled siRNA displayed green labeling and expression of μ1A HA or μ1B HA was confirmed using a mouse anti-HA antibody coupled to Cy5. To better assess plasma membrane targeting, we took multiple sections in the z-axis through the cell and show X-Z views of kAE1 staining. Figure 3.6 showed that kAE1 is detectable at the plasma membrane of cells where μ1A HA was transfected. In this experiment, 88 % of the cells (n = 9) that were transfected with kAE1, μ1A/B siRNA and μ1A HA displayed cell surface kAE1. As seen in the "μ1B HA" representative images on Figure 6, only 53 % of the cells rescued with μ1B HA (n = 15) displayed cell surface kAE1 while the remaining 47 % showed intracellular retention of kAE1. This last finding suggests that μ1B can partially compensate for the absence of μ1A, in agreement with previously published works (206). Based on these results, we propose that μ1A from AP-1A adaptor

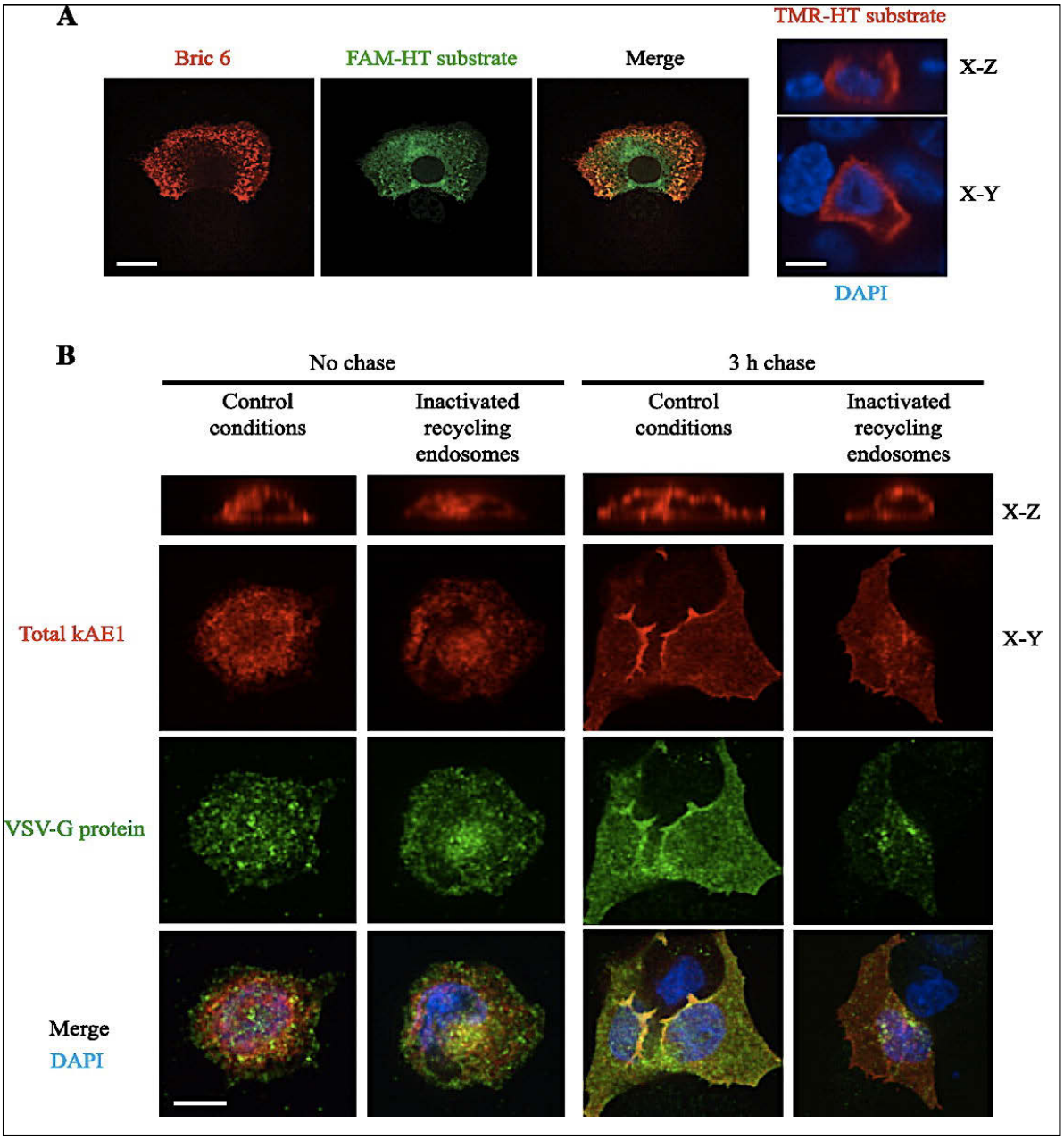

Figure 3.5: Newly synthesized kAE1 traffics in a µ1B independent pathway and does not travel through recycling endosomes. ***A.*** 24 h after transfection in MDCK cells, kAE1-HT was stained with 50 nM of FAM-HT substrate (green) for 10 min at 37 °C. After 3 washes for 5, 5, and 10 min with culture medium without FBS or antibiotics on ice, cells were fixed, blocked with 1 % BSA, and incubated with Bric 6 antibody

(Continued from figure 3.5)

followed by anti-mouse antibody coupled to Cy3 (red) before being mounted the coverslip on slides. Samples were examined using an Olympus spinning disk confocal microscope and a 100 X objective. Note that Bric 6 antibody recognizes an extracellular epitope of kAE1 on these nonpermeabilized cells. **Right**: kAE1-HT expression, stained in red with TMR HT substrate, in polarized MDCK cells. Blue staining indicates nuclear staining with DAPI. Bar = 10 μm. ***B***. MDCK cells were transiently transfected with cDNAs encoding VSVG and kAE1-HT, and newly synthesized proteins were blocked in the Golgi by incubating cells at 19 °C (see EXPERIMENTAL PROCEDURES for details). After blocking all the preexisting kAE1 with a first HT substrate, newly synthesized kAE1-HT was stained with TMR-HT substrate (red) and allowed to traffic to the Golgi by incubating cells at 19 °C. During that incubation, Tfn-HRP was added to the medium at 19°C to allow its accumulation in RE. RE were then either inactivated as described in EXPERIMENTAL PROCEDURES ("inactivated recycling endosomes") or kept intact ("control conditions"). Newly synthesized proteins were then released from the Golgi by incubation at 30 °C for 0 or 3 h before fixation. VSVG protein was detected using an anti-GFP antibody (green), and total kAE1 is stained in red. Samples were examined using an Olympus spinning disk confocal microscope and a X 100 objective. Blue staining corresponds to DAPI nuclear staining. Yellow staining indicates colocalization between red and green colors. Bar =10 μm.

complexes facilitates kAE1 targeting to the plasma membrane of non-polarized epithelial cells.

3.4. Discussion

The physical interaction between kAE1 carboxyl-terminus, via a canonical tyrosine / aspartate / glutamate / valine (YDEV) sequence, and μ1A protein from the adaptor complex 1A was recently reported (52). In our study, we characterized the novel interaction between kAE1 protein and μ subunits from the AP-1 adaptor complexes in a physiologically relevant model cell line, the renal epithelial MDCK cells. In this cell line, kAE1 protein behaves similarly as when expressed in renal IC: kAE1 protein is properly folded (156), and traffics to the basolateral membrane (158-160). When expressed in porcine LLC-PK1 cell line that is devoid of endogenous μ1B, kAE1-WT was also predominantly located at the basolateral membrane (159,160). In both MDCK and LLC-PK1 cells, we were able to co-immunoprecipitate heterologously expressed kAE1 WT with endogenous μ1A and/or B and with endogenous gamma adaptin, indicating that kAE1-WT physically interacts with AP-1 adaptor protein complexes. In addition, in MDCK cells, we show that kAE1-WT immunoprecipitates with heterologously expressed μ1A HA and μ1B HA subunits. Using siRNA knock down, we confirmed that AP-1 adaptor complexes are required for normal stability of kAE1 in MDCK cells (Fig 3.3).

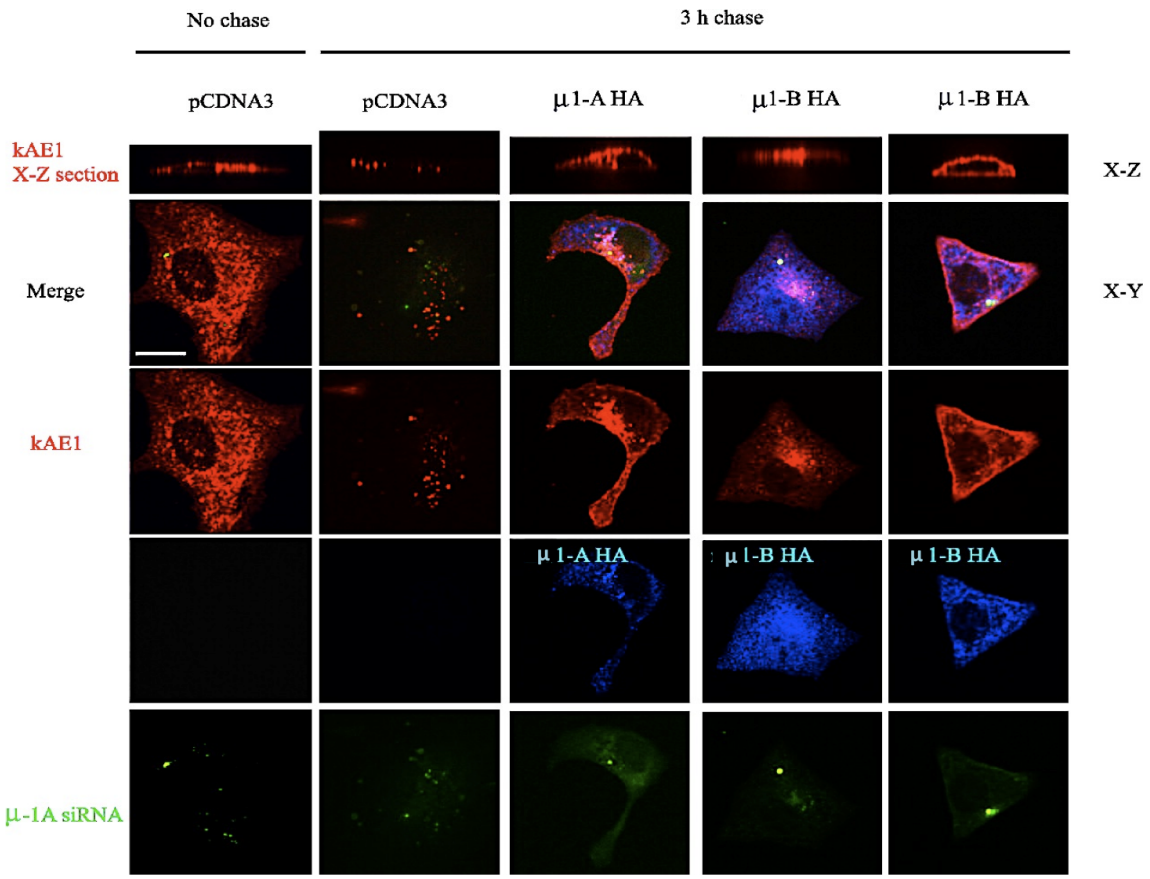

Figure 3.6: μ1A HA allows newly synthesized kAE1 to reach the plasma membrane. μ1A HA allows newly synthesized kAE1 to reach the plasma membrane. MDCK cells were transfected with siRNA against luciferase or fluorescein-labeled siRNA against μ1A/B. Twenty-four hours later, the cells were transfected with kAE1-HT and either μ1A HA, μ1B HA, or pCDNA3 vector as a control. Forty-eight hours after this second transfection, preexisting kAE1-HT proteins were blocked with coumarin-HT substrate, and cells were incubated at 37 °C for 30 min to allow synthesis of new kAE1-HT. Newly synthesized kAE1-HT were then stained with TMR-HT substrate and incubated at 37 °C for 0 (no chase) or 3 h to allow trafficking of the protein. Cells were then fixed, permeabilized, blocked with 1 % BSA, and incubated with mouse anti-HA antibody to

(Continued from figure 3.6)

detect μ1A HA or μ1B HA. Slides were examined using an Olympus IX81 microscope equipped with a Nipkow spinning-disk optimized by Quorum Technologies and a X 100 objective. Bar = 10 μm. Top: kAE1-HT localization on side (X-Z) views of the cells. Green staining corresponds to cells transfected with the μ1A/B siRNA, blue staining indicates the location of human μ1A HA or μ1B HA, and red staining corresponds to cells expressing kAE1-HT; Two right columns correspond to the 2 phenotypes observed with cells rescued with μ1B HA.

Furthermore, introducing siRNA resistant human μ1A or μ1B stabilized kAE1 in these cells (Fig 3.4). In support of these findings, we were able to co-immunoprecipitate kAE1 with μ1A from freshly dissected mouse kidneys (Fig 3.2 B) and we observed a co-localization of endogenous kAE1 and AP-1A and/or B in intracellular vesicles of mouse kidney sections (Fig 3.2 A). Thus, our results strongly support that AP-1A is required for processing of the polytopic basolateral protein kAE1 to the plasma membrane in renal epithelial cells. Although further work is needed in polarized epithelial cells, our results highlight the unsuspected key role of AP-1A adaptor complex for targeting of this basolateral membrane protein. Our results are in agreement with recent findings from Gravotta and colleagues who showed that AP-1A is involved in basolateral targeting of membrane proteins and that AP-1B can partially compensate for the absence of AP-1A (206). Of note, had our μ1A/B siRNA been exclusively specific to μ1A subunit, we would likely have been unable to see any effect on kAE1 protein stability as endogenous μ1B may have compensated for the loss of endogenous μ1A.

Interestingly, only AP-3A μ but not AP-4 ε was also found to co-immunoprecipitate with kAE1 (Fig 3.1 C and D). AP-4 is located in subdomains of the TGN and is involved in basolateral targeting of LDL receptor or MPR46 but not of TfnR in epithelial cells (262). The lack of interaction of kAE1 with AP-4 ε suggests that the AP-4 adaptor is not involved in kAE1 targeting to the plasma membrane. Nevertheless, we cannot exclude an interaction via other AP-4 subunits such as the μ subunit that binds to cargo proteins (205). AP-3A is ubiquitously expressed and is found in the TGN and in endosomes. We hypothesize that endocytosed kAE1, targeted for lysosomal degradation, traffics via AP-3A positive endosomes.

μ1B from AP-1B protein complex was found to physically interact with kAE1 protein. Since both kAE1 and AP-1B are expressed in epithelial cells (166), such interaction between kAE1 and AP-1B was not surprising. AP-1B is involved in the targeting of some basolateral membrane proteins such as VSVG to the basolateral membrane (256): newly synthesized VSVG proteins exit the TGN and within a few minutes, enter transferrin-positive RE prior to reaching the cell surface. Therefore, we tested whether AP-1B, which colocalizes with TfnR (219), is also involved in kAE1 targeting to the plasma membrane by inactivating TfnR-positive RE (Fig 3.5). We found that inactivating RE did not affect cell surface trafficking of newly synthesized kAE1 to the cell surface, in contrast with trafficking of VSVG. Thus, newly synthesized kAE1 protein, a protein normally expressed in epithelial IC, traffics to the basolateral membrane in a fashion independent of the epithelial-specific μ1B adaptor protein. Since in MDCK cells, endocytosed kAE1 co-localizes with TfnR (our own unpublished data), a protein that co-localizes with AP-1B adaptor complex (219), we hypothesize that endocytosed kAE1 interacts with AP-1B in transferrin receptor-positive RE. Indeed, plasma membrane kAE1 may be constitutively endocytosed and targeted to recycling endosomes where it may interact with AP-1B protein complex prior to returning to the cell surface. This hypothesis is consistent with the clear stabilization of kAE1 after expression of siRNA resistant μ1B in cells where endogenous μ1A and B were knocked down (Fig 3.4), but remains contradictory with the predominant basolateral targeting of kAE1 at the basolateral membrane of LLC-PK1 cells. One would expect that if AP-1B is required for proper recycling of endocytosed kAE1 to the basolateral membrane, kAE1

would either be prematurely degraded or apically mistargeted in polarized LLC-PK1 cells.

The physical interaction of kAE1 with μ1A from adaptor complex 1A was more unexpected. To date, AP-1A has been reported to be important for CD-MPR trafficking between the TGN and endosomes (228). In agreement with our findings, two recent works reported the key role of AP-1A for basolateral targeting of various membrane proteins (206,265), suggesting that AP-1A may play an under-estimated role for normal processing of a wide number of basolateral membrane proteins. In our study, we observed that kAE1 is destabilized and degraded via a lysosomal pathway in cells where μ1A and to a lesser extent μ1B were knocked down (data not shown) and that expression of siRNA resistant μ1A restored stability of the protein (Fig 3.4). This last finding confirms that AP-1A is important for kAE1 stability and trafficking. It also suggests that kAE1 is degraded via specific mechanisms that differ from CD-MPR, which is not rapidly degraded when mis-sorted in μ1A-deficient cells (228).

Our results from Figure 6 suggest that μ1B can occasionally compensate for the absence of μ1A for kAE1 processing. This is in agreement with the compensatory action of AP-1B in absence of AP-1A for sorting of mannose 6-phosphate receptors and coxsackie and adenovirus receptor (265,266); however, the clear rescue of kAE1 trafficking in μ1A HA transfected cells strongly suggest that μ1A is the major adaptor complex involved in kAE1 processing. Thus, the role of the interaction between kAE1 and AP-1B remains unclear and will require further investigations. Interestingly, kAE1 is not the only protein reported to traffic to the basolateral membrane in a μ1B independent way. Like kAE1, the Na^+, K^+-ATPase that resides at the basolateral membrane of epithelial cells, also

traffics in an AP-1B independent way to the basolateral membrane of MDCK cells. The identity of adaptor proteins involved in the Na^+, K^+-ATPase pump trafficking remains to be elucidated (261).

In addition to adaptor proteins, the carboxyl-terminus of kAE1 is the site of interaction with other proteins (267). Recently, GAPDH was also reported to interact with the D_{902}EYDE motif in the kAE1 carboxyl terminal domain, which includes tyrosine 904 from the $Y_{904}DEV_{907}$ motif that interacts with μ1A protein (53). The $Y_{904}DEV_{907}$ motif contains tyrosine 904 that can be phosphorylated and its phosphorylation status determines whether the protein remains at the plasma membrane or undergoes endocytosis (57). Further studies will be needed to investigate whether binding of GAPDH affects the interaction of the carboxyl terminus of kAE1 with adaptor proteins and whether these overlapping interactions are part of a regulatory mechanism for kAE1 targeting to the cell surface.

Two dRTA patients have been reported to carry mutations that cause carboxyl-terminal truncations of kAE1 protein by 11 (R901X) or 23 (A888L/D889X) amino acids (167,268). The kAE1 R901X mutant either mis-trafficked to both basolateral and apical membranes in polarized MDCK cells or exclusively to the apical membrane in highly polarized MDCKI cells (159,160). We postulate that mis-trafficking of the R901X mutant and possibly of the A888L/D889X mutant cause dRTA due to the lack of interaction with μ1 subunits from adaptor protein complexes 1A or B, and perhaps with GAPDH. This would result in loading of newly synthesized kAE1 proteins in the wrong trafficking vesicles *en route* to the apical membrane instead of the basolateral membrane.

It is possible that the phosphorylation status of this tyrosine potentially regulates kAE1 interaction with μ1A adaptin.

All together, our study strongly supports that AP-1A regulates normal trafficking of newly synthesized kAE1 to the plasma membrane. Further studies are required to fully understand the respective physiological role of AP-1A and B on stability and polarized trafficking of newly synthesized or endocytosed kAE1 to the basolateral membrane of type-A IC in the kidney and the consequences of its mis-sorting on the development of dRTA.

4. Chapter four: Adaptor Protein - 1B regulates recycling of the kidney Anion Exchanger 1 in renal epithelial cells

4.1. Introduction

Plasma bicarbonate is the predominant extracellular buffer minimizing changes in extracellular pH. Alpha and beta-IC in the renal collecting duct participate directly in the maintenance of plasma bicarbonate. In polarized alpha-IC, the concomitant activity of at least three protein ensure proper bicarbonate reabsorption to the blood: cytosolic carbonic anhydrase II, apical H^+-ATPase and basolateral kAE1 that is encoded by the SLC4A1 gene (136). Other proteins such as SLC26A7 or SLC26A11 may also play a role in this process. When mutated, the gene encoding basolateral kAE1 either induces dominant or recessive dRTA, a disease characterized by metabolic acidosis, hypokalemia, nephrocalcinosis and failure to thrive in children (269). kAE1 dRTA mutants are usually mis-trafficked either to the endoplasmic reticulum, to the Golgi or to the apical membrane instead of the normal basolateral membrane (136).

A growing number of either point or frameshift mutations in the SLC4A1 gene that cause dRTA affect the cytosolic C-terminus of kAE1 (168,169,268,270). The integrity of the carboxyl terminus plays a crucial role for normal kAE1 targeting to the cell surface as truncation of the last five amino acids is enough to reduce cell surface abundance of kAE1 by 50 % in HEK 293 cells (246). The C-terminal domain of kAE1 physically interacts with cytosolic CAII, thus providing a functional metabolon that directly provides the exchanger with one of its substrate (11,271,272). The cytosolic C-terminus of kAE1 also interacts with the β subunit of Na^+/K^+ ATPase pump in alpha-IC (273), this interaction being important for kAE1 residency at the basolateral membrane (273). In addition, the C-terminal domain of kAE1 encompasses the phosphorylatable tyrosine 904 (57) that is part of a canonical tyrosine based YXXΦ. Phosphorylation of

the tyrosine 904 residue is important for kAE1 residency at the basolateral membrane in polarized MDCK cells (57). Moreover, tyrosine 904 also participates in kAE1 interaction with GAPDH in both kidneys and MDCK cells (53) as well as in the interaction with adaptor proteins (52).

Adaptor protein complexes comprise five heterotetrameric members which provide an anchor between cargo proteins and clathrin to form CCV (274). These physical interactions involve various canonical motifs within cytoplasmic domains of cargo proteins, ranging from canonical tyrosine-based motif YXXΦ, di-leucine motifs or acidic motifs (211,212,275). AP-1 complexes exist as two isoforms, A and B. The ubiquitously expressed AP-1A is thought to mediate basolateral polarity (206) while the epithelial-specific AP-1B is involved in post-endocytic recycling to the basolateral membrane (276). AP-2 mediates the internalization of coated-pits from the plasma membrane and AP-3 targets cargo proteins to the lysosome. AP-4 also participates to basolateral targeting of some cargo proteins (262). The most recently described AP-5 is involved in endosomal sorting (202). AP-1 is a tetramer protein composed of four subunits, two large subunits (one β and one γ), a medium μ and one small σ subunit.

The C-terminus of kAE1 interacts with the μ1A subunit of AP-1A protein complex through the canonical tyrosine motif Y_{904}DEV (52,215). Interestingly, the interaction site on kAE1 C-terminus is either disrupted or missing in most of the reported C-terminal mutants that cause dRTA. The first reported dRTA mutant affecting the C-terminus of kAE1, kAE1-R901X, was shown to traffic either to the apical membrane or to both apical and basolateral membranes of MDCK cells, depending on the polarization degree of the cells (159,160) The engineered kAE1 Y904A/V907A double mutant

lacking the AP-1A binding site localizes exclusively to the apical membrane of MDCK cells [15]. Our work showed that AP-1A is essential for proper plasma membrane trafficking of newly synthesized kAE1 protein (215). This work found that kAE1 not only co-immunoprecipitates with the ubiquitous AP-1A but also with the epithelial specific AP-1B (215).

The epithelial specific AP-1B sorts basolateral proteins including VSVG along its biosynthetic route and the TfnR along both its biosynthetic and recycling routes in MDCK cells (216). LDLR is another known cargo protein that needs μ1B for recycling: when μ1B was knocked down in MDCK cells, LDLR was mistargeted to the apical membrane (216). When LDLR and TfnR were expressed in the porcine kidney epithelial cell line LLC-PK1, which lacks μ1B, they were both mistargeted to the apical membrane (276). Thus, AP-1B protein complex plays a specific role in sorting basolateral membrane proteins in their biosynthetic and recycling routes.

kAE1 was rapidly degraded and did not reach the cell surface in MDCK cells that were knockdown for the endogenous μ1A and to less extent μ1B by siRNA (215). When either human μ1A or B was expressed in the knocked down cells, they stabilized and partially rescued kAE1 trafficking to the cell surface (215). Based on these previous findings, we aimed to identify the physiological role of the kAE1 and AP-1B interaction. We hypothesized that the interaction between kAE1 and μ1B is important for kAE1 recycling in renal epithelial cells. According to our hypothesis, AP-1B would be important to maintain adequate amount of kAE1 at the basolateral membrane to efficiently reabsorb bicarbonate back into the blood. Herein, we examined the effect of

μ1B heterologous expression on kAE1-WT and R901X mutant's cell surface expression, endocytosis and recycling in LLC-PK1 cells that are devoid of μ1B.

4.2. Materials and Methods

4.2.1. Plasmid construct and antibodies

The pCDNA3 plasmid constructs containing human kAE1-WT and R901X cDNA with a hemagglutinin (HA) or myc epitope in position 557 (in the third extracellular loop) were used to express kAE1 protein in the transfected cell lines. We used the Quick change II site-directed mutagenesis kit (Stratagene) or Q5 Site directed mutagenesis (New England Biolabs), according to the manufacturer's instructions and confirmed the mutations by automated sequencing. The constructs encoding human μ1A-HA and μ1B-HA were provided by Dr. Heike Folsch (Northwestern University). The mouse monoclonal antibody against the HA epitope was purchased from Covance (Covance, Princeton, NJ). The mouse monoclonal and the rabbit polyclonal antibodies that detect myc epitope were purchased from Cell signaling, or from Santa Cruz Biotechnology respectively. Rabbit polyclonal antibody against the Na^+/K^+ ATPase was purchased from Cell signaling. Rat anti HA antibody was purchased from Roche (Roche Diagnostics). Anti-AE1 antibodies were provided by Drs. Reinhart Reithmeier (University of Toronto) and Joe Casey (University of Alberta), Bric 155 antibody was purchased from the International Blood Group Laboratory; the anti-phosphotyrosine 904 antibody was a kind gift from Dr. Ashley Toye (Bristol University). The anti-GAPDH antibody was purchased from Millipore.

4.2.2. Cell culture

MDCK (CCL-34), LLC-PK1 (CL-101), and HEK 293T (CRL-11268) cells were purchased from the American Type Culture Collection (ATCC). LLC-PK1 cells expressing kAE1-WT

were prepared according to methods previously described (247). Briefly, HEK 293 cells were transfected with p-VPack-GP, p-VPack-VSV-G, and pFB-Neo-kAE1-HA557 WT, pFB-Neo-kAE1-myc557 WT or mutant plasmids using XtremeGENE9 (Roche Applied Science). Cell culture supernatants containing infectious viral particles were added to dividing LLC-PK1 cells complemented with 8 μg / ml of polybrene (Sigma-Aldrich). After 24-hours incubation, a heterogenous population of LLC-PK1 cells expressing kAE1 was selected with 3 mg / ml geneticin (Sigma-Aldrich). The cells were further maintained in DMEM: F12 containing 10 % FBS, 3 mg / ml geneticin, 1 mg / ml penicillin/streptomycin. For immunofluorescence experiment, 50 % confluent LLC-PK1 cells were transfected with 1 μg cDNA and 4 μl XtremeGENE 9.

4.2.3. Immunoprecipitation and western blotting

Confluent LLC-PK1 cells expressing μ1B-HA and pCDNA3 empty vector or μ1B HA and kAE1-myc WT or R901X mutant were lysed in PBS containing 1 % Triton X-100 and protease inhibitors (1 μg / ml aprotinin, 2 μg / ml leupeptin, 1 μg / ml pepstatin A, and 100 μg / ml PMSF). Protein concentration was measured using BCA assay (Pierce). A fraction of the cell lysate (15 μg) was saved as total lysate; the remaining cell lysates were incubated with 4 μl rabbit anti AE1 N-terminus antibody (provided by Dr. Reinhart Reithmeier, University of Toronto) at 4 °C on rocker for 2 hours. Forty microliters of protein G-Sepharose beads (Thermo Scientific, Rockford, IL) were added to each sample for 1 hour at 4 °C on rocker to pull down the antibody. The bound proteins were eluted from the beads with 40 μl Laemmli buffer and detected by immunoblotting with mouse anti-myc and mouse anti-HA antibodies overnight at 4 °C. The blots were further incubated with anti-mouse secondary antibody coupled to horseradish peroxidase (HRP) for 1 hour at room

temperature. Enhanced chemiluminescence (ECL western blotting substrate from Thermo Scientific, or ECL prime western blotting detection reagent from GE Healthcare) was used after to detect proteins. Relative band intensities were determined using the freeware Image J.

4.2.4. Proximity ligation assay

Semi confluent LLC-PK1 cells were seeded on coverslips and transfected with empty vector and μ1B as a negative control, kAE1-WT myc and CAII as a positive control, and with kAE1 myc and μ1B HA. The following day the cells were fixed with 4 % paraformaldehyde (PFA), then quenched with 50 mM NH_4Cl, and permeabilized with 0.2 % Triton X-100. The slides were then blocked in 5 % donkey serum (Jackson Immunoscience, Jackson Immuno Research Europe Ltd, Suffolk, UK), 2 mg / ml salmon sperm (Sigma), 5 mg / ml bovine serum albumin (Sigma) and 2 mM cysteine (Sigma) in TBS-Tween (TBST) with 5 mM EDTA (Sigma) for 30 min in humidifying chamber at 37 °C. The samples were then incubated with the appropriate combination of primary antibodies mouse anti-HA and rabbit anti-myc or rabbit anti-CAII diluted 1:50 in blocking solution for 1 hour at 37 °C. After washing, the slides were incubated with Duolink PLA Rabbit MINUS and PLA Mouse PLUS proximity probes (Olink Bioscience, Uppsala, Sweden) and proximity ligation was performed using the Duolink detection reagent kit (Olink Bioscience) according to the manufacturer's protocol. High resolution images were acquired using the 60 X oil immersion objective on an Angstrom Illumination system (Quorum Technologies Inc.) equipped with OptiGrid structured illumination (Qioptiq), excitation and emission filter wheels (Ludl Electronic Products) and the Flash 4.0 camera (Hamamatsu). The Angstrom and associated hardware are mounted to the 100 % sideport on a DMI6000 (Leica

Microsystems), fully motorized inverted microscope. All hardware was controlled with Metamorph software (Molecular Devices).

4.2.5. Peptide spot assay

Fifteen amino acid long kAE1 peptides, covering the entire human kAE1 sequence were synthesized on cellulose membranes (277). Each peptide overlapped by 12 residues with the adjacent peptide. A positive control peptide was included based on the published interacting site of μ1B with the VSVG protein (HTKKRQIYTDIEMNR) (257,278). The negative control consisted in a 15 amino acid poly-alanine peptide. Two membranes containing exactly the same peptides were first blocked with 3 % skim milk in 1X TBST buffer (50mM Tris HCL, 150mM NaCl, 0.1%Tween 20, pH 7.4) for 4 hours at room temperature with gentle shaking. LLC-PK1 cells stably expressing μ1B HA and grown to confluency in two 15 cm dishes were lysed in PBS containing 1 % Triton X-100 and protease inhibitors (1 μg / ml aprotinin, 2 μg / ml leupeptin, 1 μg / ml pepstatin A, and 100 μg / ml PMSF) and 3 ml of either lysis buffer or cell lysate containing a total of 6.75 mg of protein were added overnight to membrane 1 and 2, respectively, at 4 °C. The membranes were washed 4 times for 15 min with TBST buffer and incubated with a rat anti-HA primary antibody overnight at 4 °C, washed and incubated with a secondary anti-rat HRP antibody for 1 hour at room temperature. The membrane blots were developed using a scanner developer (In-Vivo FPro Carestream Imaging system). Results were analyzed using Image J freeware analysis program. The intensity of each spot on membrane 1 was subtracted from the intensity of the corresponding spot on membrane 2, and the average intensity of negative controls spots on membrane 2 was subsequently subtracted from the corrected value of each spot on the same membrane. This double correction approach ensured that only the strongest signals were

taken into account. As AP-1B is a cytosolic protein complex, interaction sites within transmembrane segments and extracellular loops were excluded, based on the topological model from (32).

4.2.6. Cell surface biotinylation

Confluent LLC-PK1 cells expressing kAE1-WT or R901X were transfected with pCDNA3 empty vector or μ1B HA. Twenty-four hours after transfection the cells were incubated twice with EZ-Link Sulfo-NHS-SS-Biotin reagent (1 mg / ml) (Pierce) at 4 °C for 15 min in borate buffer (10 mM Boric acid, 145 mM NaCl, 7.2 mM KCl, 1.8 mM $CaCl_2$, pH 9). The excess of biotin was quenched with 100 mM glycine in PBS four times for 1 min each wash. The cells were lysed in 300 μl TNT lysis buffer (50 mM Tris-HCl, 150 mM NaCl, 1 % Triton X-100, 0.2 % SDS, 1 μg / ml aprotinin, 2 μg / ml leupeptin, 1 μg / ml pepstatin A, and 100 μg / ml PMSF). Ten percent of the lysate was kept as total lysate and the remaining was incubated with 100 μl streptavidin agarose resin (Thermo Scientific) for 1 hour at 4 °C. Cell surface proteins were eluted with 50 μl Laemmli buffer that contained 15 % beta-mercaptoethanol. Samples were immunoblotted with a mouse anti-HA antibody to detect both kAE1 WT and μ1B proteins. Relative band intensities were determined using the freeware Image J. To quantify the ratios of surface kAE1, we considered that amounts loaded in "Total kAE1" fraction only represented 1/9 of the amount incubated with avidin beads.

4.2.7. Cycloheximide treatment

Confluent LLC-PK1 cells expressing kAE1-WT HA transfected with pCDNA3 empty vector or μ1B HA. Twenty-four hours after transfection, the cells were treated with 10 μg / ml cycloheximide (Fluka) for 0, 4, 8, 24 hours, the cells were then lysed in PBS containing

1 % Triton X-100 and protease inhibitors. Protein concentration was measured using BCA assay (Pierce). Samples were loaded on SDS-PAGE and mouse anti-HA was used for immunoblotting to detect both kAE1 WT and μ1B HA proteins. Relative band intensities were determined using the freeware Image J.

4.2.8. Phosphorylation experiment

Two groups of MDCK cells (3 X 10^6 each) were either transfected with 5 μg cDNA encoding kAE1-myc and μ1A HA or kAE1-myc and μ1B HA using the NEON electroporation system (Invitrogen) (1400-V pulse voltage, 20-ms pulse width, and 3 pulses). Twenty four hours after transfection, one group of cells were treated with 200 μM pervanadate in warm DMEM:F12 media for 30 min at 37 °C, the other group was kept as control (warm media only). The cells were lysed with 500 μl phosphatase inhibitor lysis buffer (0.05 % Triton X-100, 10 mM HEPES, 100 mM NaCl, 14 mM beta - mercaptoethanol, 0.5 mM EGTA, $MgCl_2$, PhosSTOP Phosphatase Inhibitor Cocktail Tablets (Roche), 100 nM Calyculin A (Sigma), pH 7.5). Protein concentrations were measured using BCA assay. A 20 μg aliquot of the total cell lysate was kept as the total fraction. The remaining lysate (1 mg) was divided into two parts: one immunoprecipitated with 3 μl mouse anti myc antibody and the other with 3 μl mouse anti Bric 155 antibody for 2 hours at 4 °C, followed by 40 μl protein G-Sepharose. The bound proteins were eluted with 50 μl Laemmli buffer and phosphorylated kAE1 was immunoblotted with an antibody raised against phosphorylated tyrosine 904 overnight at 4 °C. Total kAE1 was detected by a rabbit anti-AE1 N-terminus antibody (provided by Dr. Joe Casey, University of Alberta), μ1A or μ1B HA proteins were detected by rat anti-HA antibody. The stock solution of pervanadate contained 200 mM sodium orthovanadate in PBS and 3 % (W/W) H_2O_2, the mixture was

incubated for 15 min at room temperature in the dark. This concentrated pervanadate solution was diluted to 200 μM in DMEM:F12 medium supplemented with 10 % FBS. This diluted pervanadate solution was added to cells for 30 min at 37 °C.

4.2.9. Competition between μ1 and GAPDH binding to kAE1 protein

Two groups of MDCK cells (3 X 10^6 each) were transfected with 2 μg of kAE1-myc and 5 μg pCDNA3 empty vector cDNA or with 2 μg of kAE1-myc and 5 μg μ1A HA or μ1B HA cDNA using the NEON electroporation system. Twenty-four hours after transfection, the cells were lysed and fractions containing fifteen-μg of proteins were kept as total cell lysate. Proteins in the remaining lysate (approximately 300 μg) were immunoprecipitated with 3 μl rabbit anti kAE1-myc antibody for 2 hours at 4 °C, followed by 40 μl protein G-Sepharose for an hour at 4 °C. Eluted protein were analyzed by immunoblotting. μ1A HA or μ1B HA were detected with rat anti-HA antibody overnight at 4 °C. Mouse anti-GAPDH antibody was added for 15 min at room temperature to detect the endogenous GAPDH protein. Relative band intensities were determined using the freeware Image J.

4.2.10. Endocytosis experiment

Semi confluent LL-CPK1 cells were transfected with total of 1 μg of kAE1-myc and pCDNA3 as control or with kAE1-myc and μ1B cDNA using 4 μl X-tremeGENE 9 transfection reagent (Roche). Twenty-four hours later, the cells were incubated with mouse anti-myc antibody for 45 min on ice. The antibody was washed three times with cold PBS, before incubation with warm DMEM:F12 medium at 37 °C for 20 minutes to induce endocytosis. An acid-wash was performed with a citrate buffer (40 mM citric acid, 100 mM KCl, 135 mM NaCl, pH 1.5), which was added to the cells for 10 min on ice to wash out non-endocytosed antibodies. The cells were then fixed with 4 % PFA for 10 minutes on ice,

permeabilized with 0.2 %, Triton-X 100 for 15 min, blocked with 1 % bovine serum albumin (BSA) for 20 min before incubation with the secondary antibody anti-mouse Alexa 488 (Invitrogen) to detect endocytosed kAE1-myc. Rat anti-HA antibody was added for 20 minutes followed by anti rat Cy3 to detect μ1B HA. Mouse anti myc antibody was added again for 20 minutes followed by anti mouse Dylight 649 secondary antibody to detect total kAE1. 4', 6-diamidino-2-phenylindole (DAPI) was used to stain the nucleus.

To inhibit endocytosis with Dynasore, semi-confluent LLC-PK1 cells stably expressing kAE1-myc were incubated at 37 °C in DMEM: F12 medium without FBS for 1 hour for serum starvation to promote the intake of Transferrin-Alexa 488 conjugate (Life technology). The cells were incubated with mouse anti-myc antibody for 45 minutes on ice, prior to three washes with cold PBS. The cells were incubated with Dynasore hydrate (120 μM) (Sigma, Cat no. D7G93) and Transferrin-Alexa 488 conjugate (10 μg / ml) in DMEM: F12 medium without FBS for 20 minutes at 37 °C to induce endocytosis. After three washes, citrate buffer was added for 10 minutes on ice to wash out the non-endocytosed antibodies. Then endocytosis experiment proceeded as described above. Colocalization between kAE1-myc and Tfn-Alexa 488 was measured using Pearson's colocalization coefficient Fiji freeware. High resolution images were acquired using the 60 X oil immersion objective on an Angstrom Illumination system (Quorum Technologies Inc.) equipped with OptiGrid structured illumination (Qioptiq), excitation and emission filter wheels (Ludl Electronic Products) and the Flash 4.0 camera (Hamamatsu). The Angstrom and associated hardware are mounted to the 100 % sideport on a DMI6000 (Leica Microsystems), fully motorized inverted microscope. All hardware was controlled with Metamorph software (Molecular Devices). For quantification of endocytosed kAE1 protein,

fluorescence intensities were measured using Volocity Imaging analysis program (Perkin Elmer). The ratios shown in histograms for endocytosed kAE1 represents (endocytosed / total) for each cell from three independent experiments.

4.2.11. Caveolin colocalization with kAE1

Semi confluent LLC-PK1 cells were transfected with kAE1 myc and pCDNA3 as control or with kAE1-myc and Caveolin-YFP using FuGENE 6 transfection reagent (Roche) as described for the 12-well plate 0.5 µg cDNA: 3µl FuGENE 6 reagent. Twenty-four hours after transfection the cells were incubated with mouse anti-myc antibody diluted in DMEM:F12 medium for 45 minutes on ice. After three washes with cold PBS, the cells were incubated with warm DMEM:F12 medium at 37 °C for 20 minutes to induce endocytosis as described above. Anti-mouse Cy3 antibody was used to detect endocytosed kAE1. Total kAE1 was detected by mouse anti-myc antibody followed by anti-mouse antibody coupled to Dylight 649 for 20 minutes. DAPI was added to detect the nuclei. Colocalization between kAE1-myc and Caveolin was measured using Pearson's colocalization coefficient with Fiji freeware analysis program.

4.2.12. Recycling experiment

Semi confluent LLC-PK1 cells were transfected with both kAE1-myc and pCDNA3 as control or with kAE1-myc and µ1B HA. Twenty-four hours later, the cells were incubated with mouse anti-myc antibody for 45 minutes on ice, followed by three washes with cold PBS. Warm DMEM:F12 medium was added and cells were incubated at 37 °C for 20 minutes to induce endocytosis. After an acid-wash with citrate buffer at pH 1.5 on ice to remove non-endocytosed antibodies, the cells were incubated again with warm DMEM:F12 medium for 80 min at 37 °C to induce protein recycling then fixed at 4 °C with 4 % PFA.

The cells were blocked with 1 % BSA and incubated with goat anti mouse secondary antibody coupled to Alexa 488 to detect the recycled proteins. The cells were next permeabilized, blocked again and incubated with rat anti-HA antibody followed by anti-rat Cy3 antibody to detect μ1B HA. Mouse anti-myc antibody followed by anti-mouse Dylight 649 secondary antibody detected non-recycled kAE1. DAPI was used after to stain the nuclei. Samples were examined using an Olympus IX81 microscope equipped with a Nipkow spinning-disk optimized by Quorum Technologies (Guelph, ON, Canada) and a 100 lens. For the quantification of recycled kAE1 protein, the image colors intensities were measured using Volocity imaging program (Perkin Elmer). The ratios shown in histograms for recycled kAE1 represents (Recycled / total) for each cell from three independent experiments.

4.2.13. Statistical Analysis

All the experiments were repeated at least three times. Results are expressed as mean values ± standard error of the mean (SE). All statistical comparisons were made using unpaired student t-test. $P < 0.05$ was considered significant.

4.3. Results

4.3.1. KAE1 interaction with AP-1B

4.3.1.1. kAE1-WT is immunoprecipitated with μ1B in LLC-PK1 cells

The interaction between kAE1 and AP-1A was originally identified using a yeast two-hybrid assay and the carboxyl-terminal tail of AE1 as bait (52). In our previous work, we confirmed that kAE1 immunoprecipitates with μ1A as well as with μ1B in MDCK cells (215). As the carboxyl-terminus of kAE1 contains a potential canonical YXXΦ adaptor protein binding site ($Y_{904}DEV_{907}$) (52), we hypothesized that μ1B interacts with kAE1 via

this site. To test this hypothesis, we examined the interaction with the truncated kAE1-R901X that is missing the last 11 amino acids [15]. To confirm that kAE1 and μ1B interact with each other, we transiently transfected LLC-PK1 cells (that do not express endogenous μ1B (276)) with μ1B and kAE1, both carrying HA epitopes. We immunoprecipitated kAE1-WT or R901X using anti kAE1 N-terminus antibody, and immunoblotted the membrane with mouse anti-HA antibody to detect both kAE1 and μ1B. As seen on Figure 4.1 A, kAE1 protein migrates as two main bands in LLC-PK1 cells: the top band corresponds to proteins carrying complex oligosaccharide (open circle) and the bottom band corresponds to kAE1 carrying high mannose oligosaccharide (closed circle) (158). In agreement with our previous findings (215), these results show that μ1B co-immunoprecipitates with kAE1 in LLC-PK1 cells (Fig 4.1 A). These results confirm our previous results supporting a physical interaction between AP-1B and kAE1 protein.

4.3.1.2. kAE1 is in close proximity with μ1B protein

To confirm that kAE1-WT and AP-1B are in close proximity to interact with μ1B in the cells, a proximity ligation assay was performed (279). In this assay, if the two proteins of interest are within 30 to 40 nm distance from each other, a specific, red signal is detected by fluorescence microscopy (280). In our experiment, LLC-PK1 were transiently transfected with empty vector and μ1B HA as a negative control, kAE1-WT myc and CAII as a positive control, or with kAE1-WT or R901X myc and μ1B HA. Cells were then incubated with rabbit anti-myc antibody to detect kAE1 and mouse anti-HA to detect μ1B, and proximity ligation was performed using the Duolink detection reagent kit according to the manufacturer's protocol.

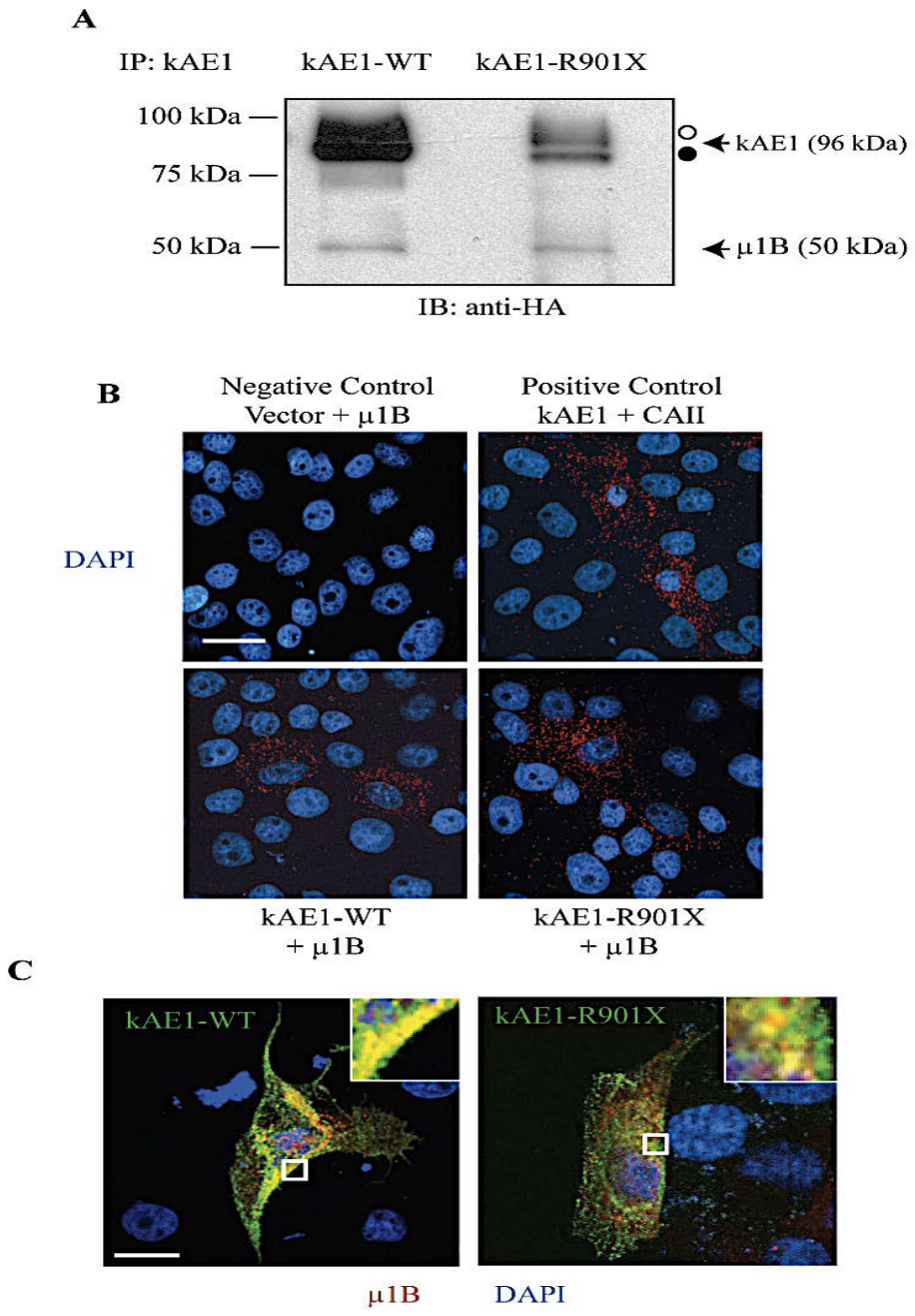

Figure 4.1: μ1B interacts and colocalizes in the perinuclear region with both kAE1-WT and kAE1-R901X truncated mutant in LLC-PK1 cells. ***A.*** LLC-PK1 cells expressing kAE1-WT HA or mutant were transfected with μ1B HA cDNA, kAE1 was immunopreciptated with anti kAE1 N-terminus antibody before immunoblotting with mouse anti-HA antibody to detect kAE1 and μ1B proteins. Open circle corresponds to

(Continued from figure 4.1)

kAE1 carrying complex oligosaccharides, and filled circle indicates kAE1 carrying high mannose oligosaccharides. μ1B migrates as a 50 kDa band. ***B***. For the proximity ligation assay, LLC-PK1 cells were transiently transfected with empty vector and μ1B as a negative control, kAE1-WT and CAII as a positive control, and with kAE1 WT or R901X and μ1B. Red dots appear when the two proteins are in close proximity to each other. Nuclei were stained with DAPI (blue). ***C.*** immunofluorescence experiment showing colocalization between kAE1 carrying a myc epitope and μ1B HA. Twenty-four hours post transient transfection, LLC-PK1 cells expressing kAE1 and μ1B were fixed, permeabilized and blocked before incubation with an anti myc antibody to detect kAE1 followed by secondary anti mouse antibody coupled to Alexa 488. Subsequently, cells were incubated with rat anti-HA antibody to detect μ1B followed by secondary anti-rat antibody coupled to Cy3 (red). This sequential staining avoids cross reactivity of the anti-mouse secondary antibody on the rat primary antibody. Nuclei were stained with DAPI (blue). Bar = 10 μm. The inset shows a zoomed region of the cell showing yellow staining (colocalization).

Red fluorescent dots were detected in the positive control and in cells expressing kAE1-WT and mutants and μ1B but not in the negative control sample (Fig 4.1 B). These results indicate that kAE1-WT and R901X, are in close proximity to AP-1B mu proteins and support our immunoprecipitation results.

4.3.1.3. KAE1-WT colocalizes with μ1B in the perinuclear region of LLC-PK1 cells

To further determine whether kAE1 and μ1B colocalize in the same organelle in cells, we performed immunofluorescence. LLC-PK1 cells were transiently transfected with kAE1-WT myc or kAE1 R901X myc and with μ1B HA cDNAs. KAE1 protein was detected using mouse anti-myc antibody (Fig 4.1 C, green) and rat anti-HA primary antibody (red) to detect μ1B HA by immunostaining. Our results show that AP-1B and kAE1-WT or mutant colocalize in the perinuclear region as shown by the yellow signal (Fig 4.1 C), confirming that kAE1-WT or mutant are in close proximity to μ1B in renal epithelial cell.

4.3.1.4. AP-1B interacts with kAE1 via multiple biding sites

As the expected C-terminal binding site for μ1B was either deleted or mutated in kAE1-R901X mutant, we did not expect to see interactions or colocalization between μ1B and kAE1-R901X proteins. However, Figure 1 shows that μ1B interacts and colocalizes with kAE1 mutant. Therefore, we determined whether μ1B interacts with kAE1 via binding sites other than kAE1 carboxyl-terminus. To test this hypothesis, we performed a peptide spot assay (Fig 4.2). Fifteen amino acid long peptides were synthesized on two nitrocellulose membranes that were subsequently incubated either with lysis buffer as a control (membrane 1) or with a μ1B HA expressing LLC-PK1 cell lysate (membrane 2). The membranes were then incubated with anti-HA antibody and appropriate HRP-coupled

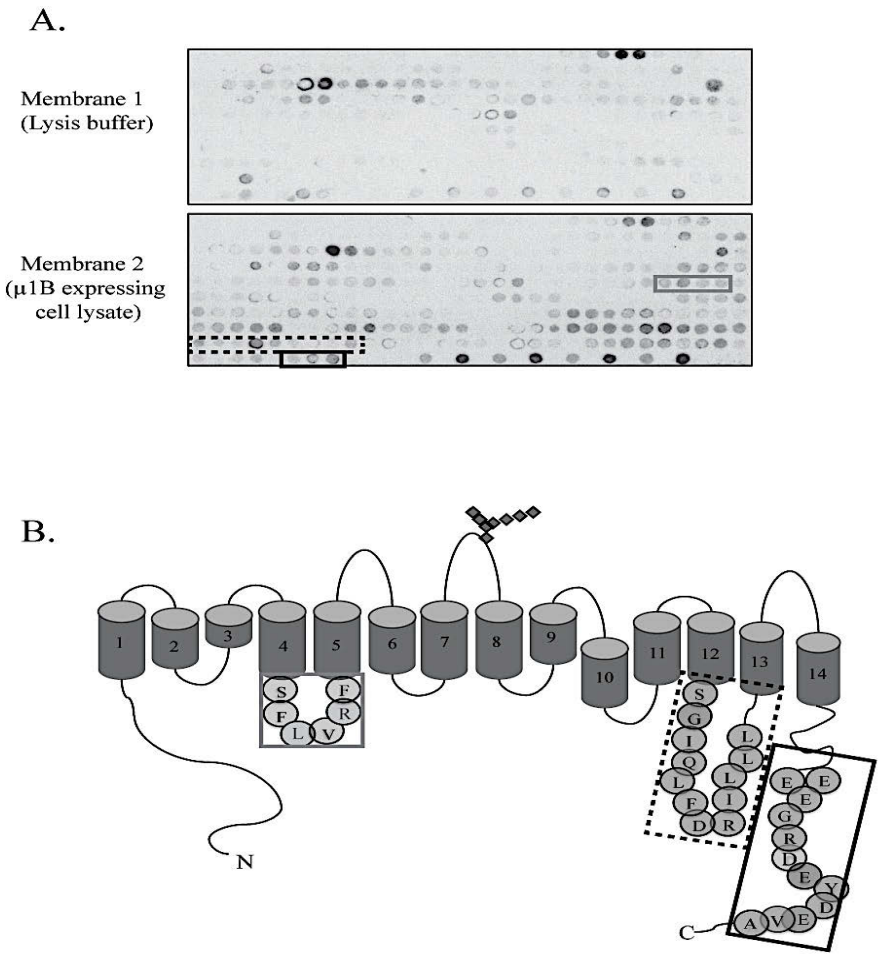

Figure 4.2: AP-1B complex has multiple interaction sites on kAE1 protein

A. Nitrocellulose membranes containing overlapping peptides (15 amino acid per peptide) encompassing the entire kAE1 protein sequence were either incubated with lysis buffer only (membrane 1) or a cell lysate from LLC-PK1 cells expressing μ1B HA (membrane 2). The two membranes were then blocked and incubated with a rat anti-HA antibody followed by an anti-rat antibody coupled to HRP, to detect μ1B. Each spot corresponds to one of the overlapping peptides. The intensity of each spot was measured using Image J freeware. ***B.*** Topological model of kAE1 (modified from (32)) showing the sites of AP-1B interaction to kAE1 peptides with AP-1B complex. The sites of interaction represent the amino acid sequence that overlap within the peptide spots.

(Continued from figure 4.2)

Barrels represent transmembrane domains; grey diamonds represents the N-glycosylation attached to the fourth extracellular loop.

secondary antibody to detect HA antibody-interacting spots by immunoblotting. The binding sites within the transmembrane domains and the extracellular loops were excluded since μ1B is an intracellular membrane protein. After corrections for negative controls (see materials and methods for details), we confirmed that μ1B complex interacts with the carboxyl-terminus of kAE1 (Table 4.1, peptides 9 and 11). Interestingly, in contrast with peptides 9 and 11, no binding was found for peptide 10, suggesting that residues downstream of C-terminal alanine 908 may stabilize the binding. We identified several other binding sites in addition to the carboxyl-terminal Y_{904}DEV motif (Table 4.1 & Fig 4.2). Specifically, the S_{510}FLVRF sequence within the second intracellular loop (between transmembrane domains 4 and 5) and the sequence T_{796}SLSGIQLFDRILLL within the sixth intracellular loop (between transmembrane domains 12 and 13) showed the strongest signals, supporting the existence of additional binding sites of μ1B to kAE1. Overall, these results support that AP-1B interacts with kAE1 via the Y_{904}DEV binding motif and suggest additional binding sites within the second and sixth cytosolic loops.

4.3.2. Factors that affect kAE1-WT and AP-1B interaction

4.3.2.1. Phosphorylation of the C-terminal tyrosine 904 does not affect kAE1 / AP-1B interaction

In kAE1 cytosolic carboxyl-terminal domain, tyrosine 904 is phosphorylated in MDCK cells (57). As our results support the interaction between AP-1B and the carboxyl-terminus of kAE1, we next tested the effect of kAE1 phosphorylation on kAE1-μ1B binding. MDCK cells stably expressing kAE1 WT myc were transiently transfected with μ1B HA and either kept in control conditions or treated for 30 minutes with pervanadate to promote accumulation of phosphorylated kAE1 within the cells, following the protocol from

Table 4.1: Sequence of kAE1 peptides that interact with AP-1B by peptide spot assay. ICL corresponds to intracellular loop. C-ter corresponds to carboxyl-terminus of kAE1.

Peptide number	Peptide sequence	Band intensity after correction for negative controls and spot-specific background	Location in kAE1 secondary structure
1	V_{501}VLVVAFEG**SFLVRF**	434.3	ICL2
2	V_{504}VAFEG**SFLVRF**ISR	1837.3	ICL2
3	F_{507}EG**SFLVRF**ISRYTQ	100.7	ICL2
4	**S_{510}FLVRF**ISRYTQEIF	144.3	ICL2
5	F_{792}LYMGVTSL**SGIQLF**	587.8	ICL6
6	M_{795}GVTSL**SGIQLFDRI**	1191.5	ICL6
7	**T_{798}SLSGIQLFDRILLL**	567.3	ICL6
8	**L_{810}LL**FKPPKYHPDVPY	455.2	ICL6
9	A_{891}KATFD**EEEGRDEYD**	12.9	C-ter
10	**E_{897}EEGRDEYDEVAMPV**	798.7	C-ter

Williamson and colleagues (57). KAE1 proteins were immunoprecipitated with either an anti-myc or a Bric155 antibody that recognizes the carboxyl-terminus of kAE1. Eluted proteins were detected either with anti-myc antibody or an antibody that specifically detects phosphorylated tyrosine 904 (57), and anti-HA antibody to detect co-immunoprecipitated μ1B HA. Figure 4.3 A shows that in conditions when tyrosine 904 was phosphorylated (Fig 3 A, lane 6), μ1B HA still co-immunoprecipitated with kAE1, supporting that the phosphorylation status of this tyrosine does not dramatically impair the interaction between kAE1 and μ1B HA subunit. Of note, tyrosine 904 phosphorylation did not affect the interaction between kAE1 and μ1A either (Fig 4.3 B, lane 12). When kAE1 was immunoprecipitated with Bric155, which specifically detects kAE1 carboxyl-terminus, pervanadate treatment sharply, reduced the amount of immunoprecipitated protein (compare Figure 3, lanes 3 and 4 and lanes 9 and 10), supporting that tyrosine 904 phosphorylation impairs the interaction with Bric155 antibody. In absence of pervanadate, Bric155 immunoprecipitated predominantly non-phosphorylated kAE1 protein as seen by the absence of a band in lanes 3 and 9 (top blots), suggesting that at the steady-state kAE1 tyrosine 904 is mostly non-phosphorylated. As μ1A and μ1B binding sites on $Y_{904}DEV_{907}$ amino acids overlap with the GAPDH interaction site (D_{902}EYDEV) (53). We next tested whether μ1B and GAPDH are competing for the same or an overlapping interaction site on kAE1.

4.3.2.2. AP-1B binding to kAE1 displaces GAPDH interaction with kAE1

kAE1 protein physically interacts with GAPDH (53) via the carboxyl-terminal D_{902}EYDE motif, which encompasses the binding site for μ1A that was reported by Saswadee and

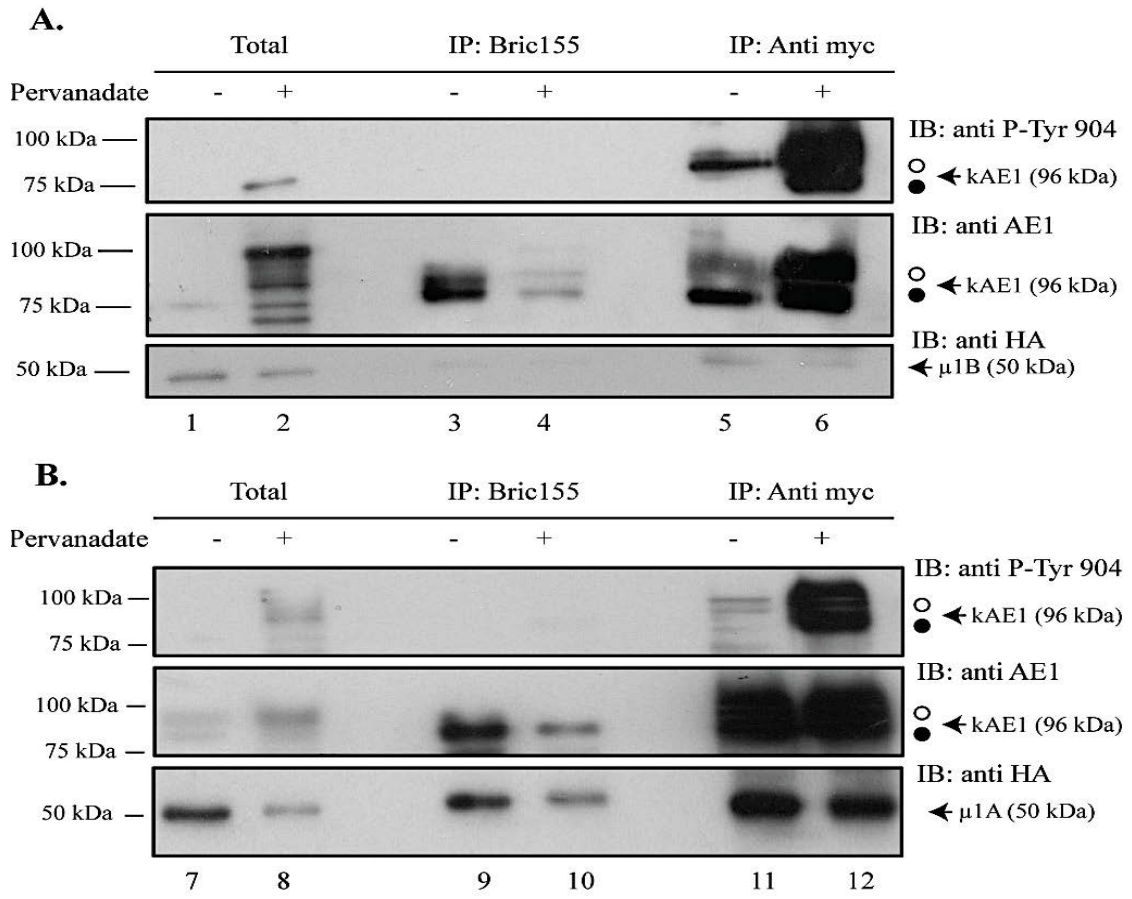

Figure 4.3: Phosphorylation of tyrosine 904 does not impair µ1A HA or µ1B HA interaction with kAE1. MDCK cells co-expressing kAE1-WT myc and **µ1A HA (A) or µ1B HA (B)** were either kept in control conditions or treated with pervanadate for 30 minutes prior to cell lysis and imunoprecipitation of kAE1 proteins. Eluted proteins were resolved by immunoblot and identified, using an anti-HA antibody to detect µ1B HA and µ1A HA , an anti-kAE1 antibody to detect kAE1 and anti-phospho-tyrosine 904 antibody to detect phosphorylated kAE1. The difference of band intensities in immunoblots with anti-HA antibodies (A and B) results from the difference in the exposure times of the films but rather than a difference in protein expression level. Open circle corresponds to kAE1 carrying complex oligosaccharides, and filled circle indicates kAE1 carrying high mannose oligosaccharides. This is a typical experiment out of 3 independent experiments.

colleagues (52). We thus asked whether binding of kAE1 to the μ1B subunit of AP-1B complex impedes binding to GAPDH. To answer this question, kAE1 WT-myc stably expressing MDCK cells were transiently transfected with vector cDNA or cDNA encoding for μ1B HA. In MDCK cells that express endogenous μ1A and μ1B, kAE1 interacts with μ1B (215). KAE1 protein was then immunoprecipitated and eluted proteins were detected with anti-myc antibody (to detect kAE1), anti-HA antibody (to detect μ1B) and anti-GAPDH antibody to detect endogenous GAPDH (Fig 4.4). Heterologous expression of μ1B HA displaced GAPDH interaction with kAE1 as seen by the decreased band intensity of GAPDH in Figure 4.4 A (compare lane 3 to lane 1). Similar observations were made with the μ1A isoform (lane 2, Fig 4.4 A). Quantification of the relative band intensities from a minimum of 4 independent experiments confirmed that only 44 ± 7 % (n = 5, ± SEM) and 28 ± 7 % (n = 4, ± SEM) of GAPDH co-immunoprecipitated with kAE1 protein after expression of μ1A and μ1B subunits, respectively (Fig 4.4 B). These experiments indicate that GAPDH and adaptor protein complexes AP-1A and B compete for the same binding site on kAE1 carboxyl-terminus.

4.3.3. The effect of μ1B expression on the amount of cell surface kAE1 at the steady state

4.3.3.1. In non-polarized LLC-PK1 cells, kAE1 is more abundant at the plasma membrane than kAE1 R901X mutant

To better understand the physiological role of μ1B in kAE1 trafficking, we quantitatively characterized phenotypic differences between kAE1-WT and carboxyl-terminal mutants in LLC-PK1 cells that do not express endogenous μ1B (165). We first asked whether carboxyl-terminal kAE1 mutants have a similar abundance to kAE1-WT at the cell surface.

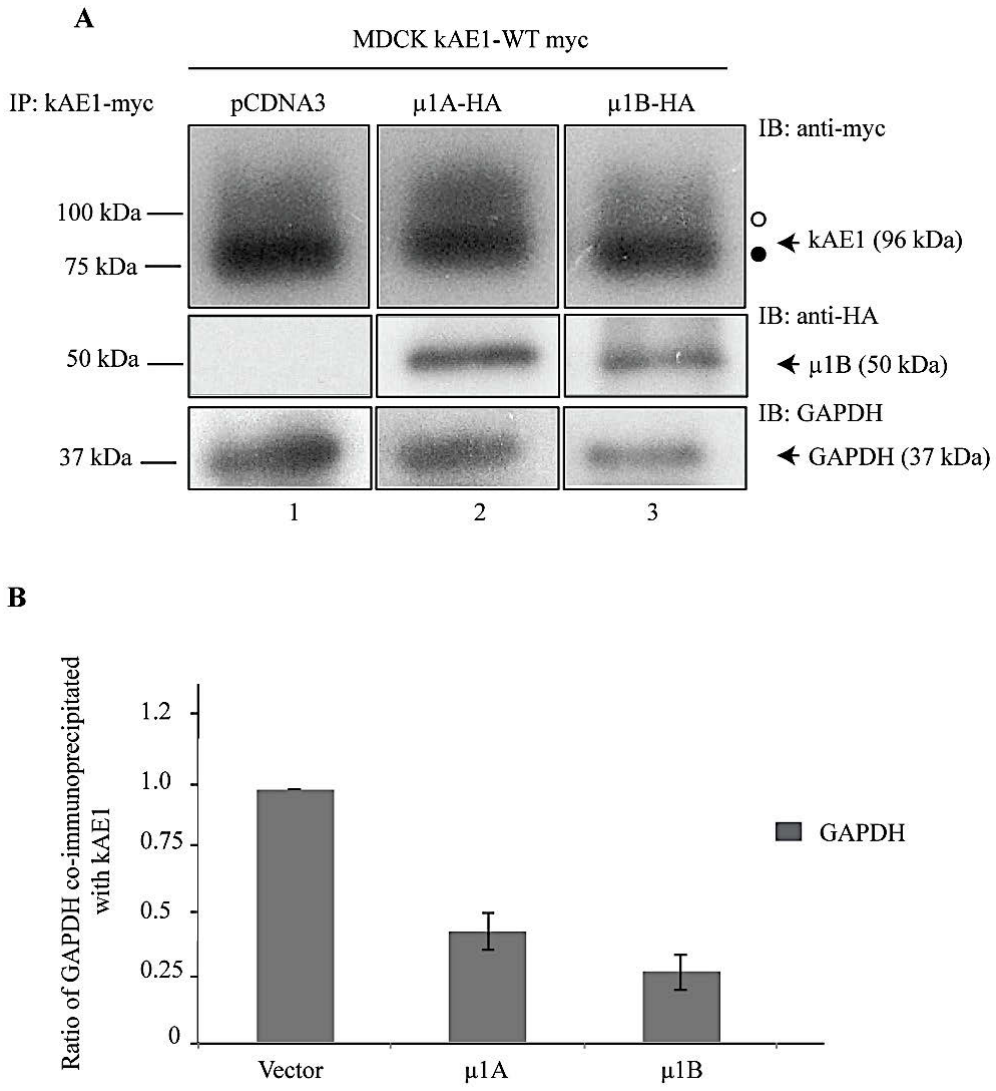

Figure 4.4: Expression of µ1B HA subunit displaces GAPDH interaction with kAE1 carboxyl-terminus. ***A.*** MDCK cells stably expressing kAE1-WT myc were either transfected with vector cDNA, pcDNA3-encoding µ1A HA or µ1B HA. Twenty-four hours after transfection, cells were lysed and kAE1 was immunoprecipitated with a rabbit anti-myc antibody. Proteins were immunoblotted using anti-myc antibody (to detect kAE1), anti-HA antibody (to detect µ1A or B HA) and anti-GAPDH antibody. The blot corresponds to one experiment from at least three independent experiments ***B.*** GAPDH and kAE1 band intensities were measured using Image J software and the ratio of GAPDH band

(Continue from figure 4.4)

intensity in the absence of μ1A or μ1B HA (vector) and after the expression of either μ1A or μ1B HA was measured. Error bars correspond to standard errors of the mean, from a minimum of 3 independent experiments.

In MDCK cells, kAE1-WT is predominantly located at the plasma membrane in non-polarized cells and at the basolateral membrane of polarized MDCK cells (159,160,247). In contrast, kAE1-R901X is predominantly found intracellularly in non-polarized MDCK cells but is found at the apical membrane when the cells are polarized.

To determine the amount of cell surface kAE1-WT and R901X mutant at the steady state, two experimental approaches were used: cell surface biotinylation and immunofluorescence. Plasma surface abundance was first determined in LLC-PK1 cells expressing kAE1-WT HA or R901X HA mutant, using EZ-Link Sulfo-NHS-SS-biotinylation reagent (Fig 4.5 A). Eluted streptavidin fractions were analyzed by immunoblot with mouse anti-HA antibody to detect kAE1-WT and mutant. Immunoblot results showed that kAE1-WT is more abundant at the cell surface than kAE1-R901X mutant (Fig 4.5 A). Densitometric quantification of cell surface kAE1 relative to total kAE1 protein showed that the ratio of cell surface kAE1-WT is significantly higher than kAE1-R901X (0.19 ± 0.01 % (n=3; ± SE) versus 0.15 ± 0.01 (n=3; ± SE), respectively) (Fig 4.5 B dark bars).

Immunofluorescence was used to confirm our biotinylation findings (Fig 4.5 C). Non-polarized LLC-PK1 cells were transiently transfected with μ1B HA cDNA and either kAE1-WT myc or kAE1-R901X myc mutant. To detect surface kAE1, fixed but non-permeabilized cells were incubated with anti-myc primary antibody followed by Alexa 488 (green) secondary antibody. After permeabilization, intracellular kAE1 was detected by incubating cells again with anti-myc antibody followed by a secondary antibody coupled to Dylight 649 (blue). The green fluorescence intensity measured using Volocity software reflected the amount of cell surface kAE1 and was normalized to the blue fluorescence

intensity (total kAE1). We found significantly less kAE1-R901X mutant at the cell surface compared with kAE1 WT as Figure 4.5 D shows that the ratio of cell surface kAE1-R901X mutant was 0.37 ± 0.06 (n=3; ± SE), which is 60 % less than kAE1-WT (0.94 ± 0.11 %, n=3; ± SE) at the steady state (Fig 4.5 D, dark bars). These results confirm that kAE1-R901X mutant is less abundant at the plasma membrane than kAE1 WT. This decrease could originate from a decreased processing of newly synthesized kAE1, from increased internalization rate of kAE1-R901X or slow recycling of kAE1-R901X.

4.3.3.2. In LLC-PK1 cells, the kAE1 R901X truncated mutant has a similar half-life as kAE1 WT

We next determined whether the mutant is more rapidly degraded than kAE1-WT. LLC-PK1 cells expressing kAE1-WT or mutant were incubated with the protein synthesis inhibitor cycloheximide for up to 24 hours and the relative amount of kAE1 remaining in the samples was determined by immunoblotting (Fig 4.5 E). We observed a slight reduction in kAE1-R901X half-life to 15.5 hours, compared with kAE1-WT (17 hours). Similar results were obtained in MDCK cells (281). To investigate the effect of μ1B on kAE1 half-life, the experiment was repeated with LLC-PK1 cells expressing kAE1-WT or mutant and transiently transfected with either vector or μ1B (Fig 4.5 E). Expression of human μ1B in these cells did not significantly affect the half-life of either kAE1-WT or R901X.

4.3.3.3. Expression of μ1B decreases cell surface amount of kAE1 WT and R901X mutant

AP-1B is located in common recycling endosomes and is necessary for recycling of basolateral membrane proteins (282). We therefore next determined whether expression of μ1B affects the amount of kAE1 proteins at the plasma membrane. To investigate the effect

of μ1B in these cells, we heterologously expressed human μ1B in LLC-PK1 cells (which do not express μ1B endogenously), a strategy known to restore a functional AP-1B complex in these cells (165,263,283). As AP-1A and AP-1B only differ in their μ subunit, expression of μ1B subunit in these cells is enough to create *de novo* AP-1B complexes. LLC-PK1 cells expressing kAE1-WT or R901X mutant and transiently transfected with μ1B cDNA or vector were first submitted to cell surface biotinylation. As shown on (Fig 4.5 A & B), cells expressing μ1B displayed a reduced ratio of cell surface kAE1-WT over total kAE1-WT (0.15 ± 0.01) compared to kAE1-WT expressing cells transfected with vector only (0.19 ± 0.01). A similar result was obtained with cells expressing kAE1-R901X (0.09 ± 0.01 compared with 0.15 ± 0.01 in absence of μ1B). Therefore, expression of μ1B significantly reduced the relative amount of cell surface kAE1-WT and kAE1-R901X.

A similar trend was obtained by immunofluorescence (Fig 4.5 C & D). Cells expressing kAE1-WT or R901X and transiently transfected with vector only or μ1B cDNA were stained for cell surface kAE1 (green), total kAE1 (blue) and μ1B expression (red). Consistent with cell surface biotinylation results, comparison of the ratio of surface kAE1 over total kAE1 by immunofluorescence showed that μ1B expression significantly decreased the amount of surface kAE1-WT by 8 fold (0.94 ± 0.11 versus 0.12 ± 0.01), and R901X by two fold (0.37 ± 0.07 versus 0.17 ± 0.02).

This decrease could have three origins: expression of μ1B could *(i)* reduce the amount of newly synthesized kAE1-WT protein that reaches the cell surface, *(ii)* accelerate the rate of endocytosis of kAE1-WT; or *(iii)* reduce the amount of recycled kAE1-WT to the cell surface. We showed earlier (215) that expression of μ1B in MDCK cells knocked

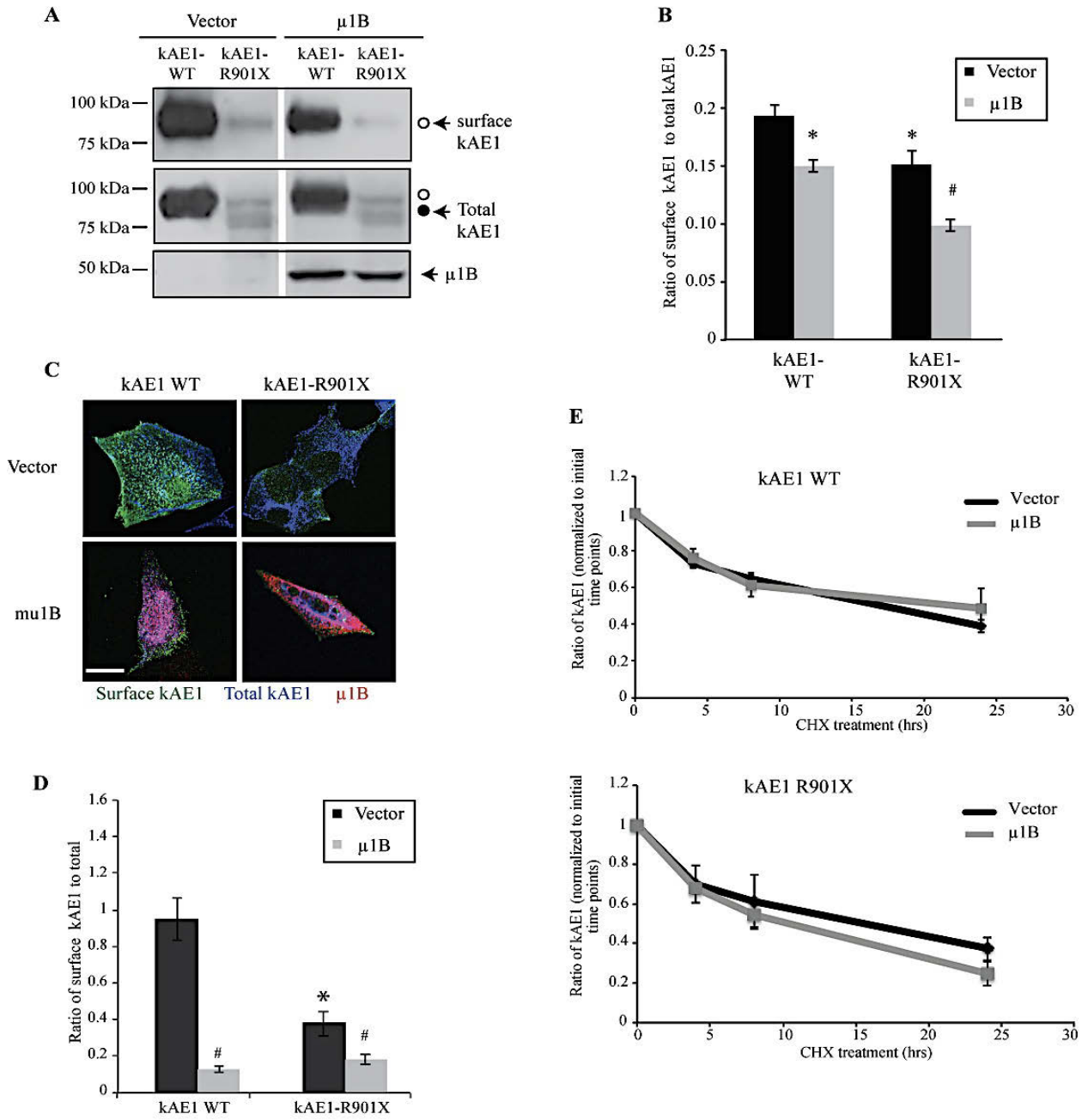

Figure 4.5: **In non-polarized LLC-PK1 cells, kAE1-WT is more abundant at the plasma membrane than the kAE1-R901X mutant, but its surface expression decreases upon μ1B expression.** ***A***. Cell surface biotinylation: confluent LLC-PK1 cells stably expressing kAE1 WT-HA were transiently transfected with empty vector or μ1B

(Continued from figure 4.5)

HA cDNA. Twenty-four hours after transfection, the cells were incubated with membrane impermeable EZ-Link Sulfo-NHS-SS-Biotin reagent; the cells were lysed and incubated with streptavidin resin. Surface proteins were eluted from the beads with Laemmli reagent and immunoblotted with mouse anti HA antibody to detect kAE1 and μ1B. ***B.*** Histogram showing the ratio of surface kAE1 to total kAE1 in cells were transfected with kAE1-WT or R901X mutant and either μ1B or empty vector. Band intensities were determined by densitometric analysis (using Image J freeware) of more than three independent experiments, taking into account that "Total kAE1" fractions correspond to 1/9 of the kAE1 amount used in "Surface kAE1" fractions. $^{*}P < 0.05$ versus kAE1-WT or R901X-expressing cells transfected with vector only, $^{\#}P < 0.05$ versus the same kAE1-expressing cells transfected with μ1B. Error bars correspond to means ± SE. ***C.*** Immunofluorescence experiment of LLC-PK1 cells showing surface kAE1 in the presence and absence of μ1B: LLC-PK1 cells grown on glass coverslips and expressing kAE1 and μ1B were fixed and incubated with mouse anti-myc antibody to detect surface kAE1 followed by a secondary antibody coupled to Alexa 488 (green). The cells were then permeabilized and incubated with rat anti-HA antibody to detect μ1B HA followed by a secondary antibody coupled to Cy3 (red). Total kAE1 was detected with an anti-myc antibody followed by a secondary antibody coupled to Dylight 649 (blue). Bar = 10 μm. ***D.*** Histogram representing the ratio of green fluorescence intensity (surface kAE1) to blue fluorescence intensity (total kAE1) in LLC-PK1 cells that were transfected with kAE1-WT and mutant with either μ1B or empty vector. Fluorescence intensities for at least 50 cells for each condition from 3 independent experiments were measured using

(Continued from figure 4.5)

Volocity Image analysis program. Error bars correspond to means ± SE. *$P < 0.05$ versus kAE1-WT or R901X expressing cells transfected with vector only, $^{\#}P < 0.05$ versus the same kAE1-expressing cells transfected with μ1B. ***E.*** The carboxyl-terminal truncated mutant has a similar half-life as kAE1-WT: LLC-PK1 cells stably expressing kAE1-WT HA or R901X mutant were transiently transfected with cDNA encoding μ1B HA or vector. Twenty-four hours later, cells were treated with the protein synthesis inhibitor cyclohexamide (CHX) for 0, 4, 8 or 24 hours. Remaining kAE1 proteins were detected by immunoblot with a mouse anti-HA antibody. Band intensities were analyzed by densitometric analysis, using the Image J software from more than 3 independent experiments, error bars correspond to means ± SE. The relative amount of kAE1 was normalized to the intensity of the band at initial time point.

down for endogenous μ1A and μ1B increased cell surface trafficking of newly synthesized kAE1-WT protein and increased the stability of total kAE1. We therefore considered the first hypothesis unlikely. Thus, we first tested the hypothesis that expression of μ1B accelerates the rate of kAE1 endocytosis.

4.3.4. The effect of μ1B on kAE1 endocytosis

4.3.4.1. KAE1 is endocytosed via a clathrin dependent pathway

We first examined kAE1 endocytosis pathway as it is not characterized (193,284). We performed two sets of experiments for this characterization: in the first set, we asked whether endocytosed kAE1 colocalizes with endocytosed TfnR, which is well known to be endocytosed via a clathrin-dependent pathway (216). As a control, we used dynasore, an inhibitor of dynamin-dependent endocytosis that blocks Tfn endocytosis (285). The second set determined whether endocytosed kAE1 colocalizes with endocytosed caveolin protein, which is known to be endocytosed in a clathrin-independent pathway (286,287).

For the first set of experiments, serum starved LLC-PK1 cells expressing kAE1 myc were incubated with mouse anti-myc antibody on ice to label cell surface kAE1. Cells were then incubated with Dynasore or vehicle and Tfn-Alexa Fluor 488 conjugate for 20 min at 37 °C. Cells were then washed with a citrate buffer at pH 1.5 to remove antibodies remaining at the cell surface (Fig 4.6 A). Cells were fixed, permeabilized, and endocytosed kAE1 proteins were detected with anti-mouse secondary antibody coupled to Cy3 fluorophore (red). Total kAE1 expression was detected by re-adding mouse anti-myc antibody followed by anti-mouse secondary antibody coupled to Dy649 (blue). Representative pictures on Fig 4.6 B (compare columns 1 and 2) show that Dynasore inhibited endocytosis of both kAE1 and Tfn, as neither red (kAE1) nor green (Tfn) was

observed after acid wash. In absence of Dynasore (Fig 4.6 B column 1), kAE1 and Tfn colocalized in a perinuclear compartment, likely in recycling endosomes (216). Colocalization measurements between kAE1 and Tfn using Pearson's colocalization coefficient showed that kAE1 and Tfn colocalize to some extent (Fig 4.6 C).

In the second set of experiments, LLC-PK1 cells expressing kAE1 myc and Caveolin-YFP were incubated with mouse anti-myc antibody followed by anti mouse Cy3 (red) to detect endocytosed kAE1 (Fig 4.6 B, column 3). Colocalization measurement showed that endocytosed kAE1 did not colocalize with caveolin protein (Fig 4.6 C). As these previous experiments support that kAE1 is endocytosed in a clathrin-dependent pathway, we next determined whether kAE1-WT is endocytosed at the same rate as the carboxyl-terminal truncated kAE1-R901X mutant.

4.3.4.2. The amount of endocytosed carboxyl-terminal kAE1 mutant R901X is higher than kAE1-WT

As we were unable to efficiently remove the biotinylation reagent remaining at the cell surface in living cells in endocytosis experiments, we used immunofluorescence to quantitatively compare the relative amount of kAE1 protein endocytosed, by taking advantage of the extracellular myc epitope that has been added to the third extracellular loop of kAE1 (247).

After incubation with anti-myc antibody on intact LLC-PK1 cells expressing kAE1-WT or kAE1-R901X, and incubation at 37 °C to promote endocytosis of the protein, we were able to efficiently remove the antibody attached to kAE1 proteins that remained at the cell surface by performing an acid-wash of the cells for 10 minutes at 4 °C (Fig 4.6 A). To perform endocytosis experiments, the cells were incubated with anti-myc antibody at 4

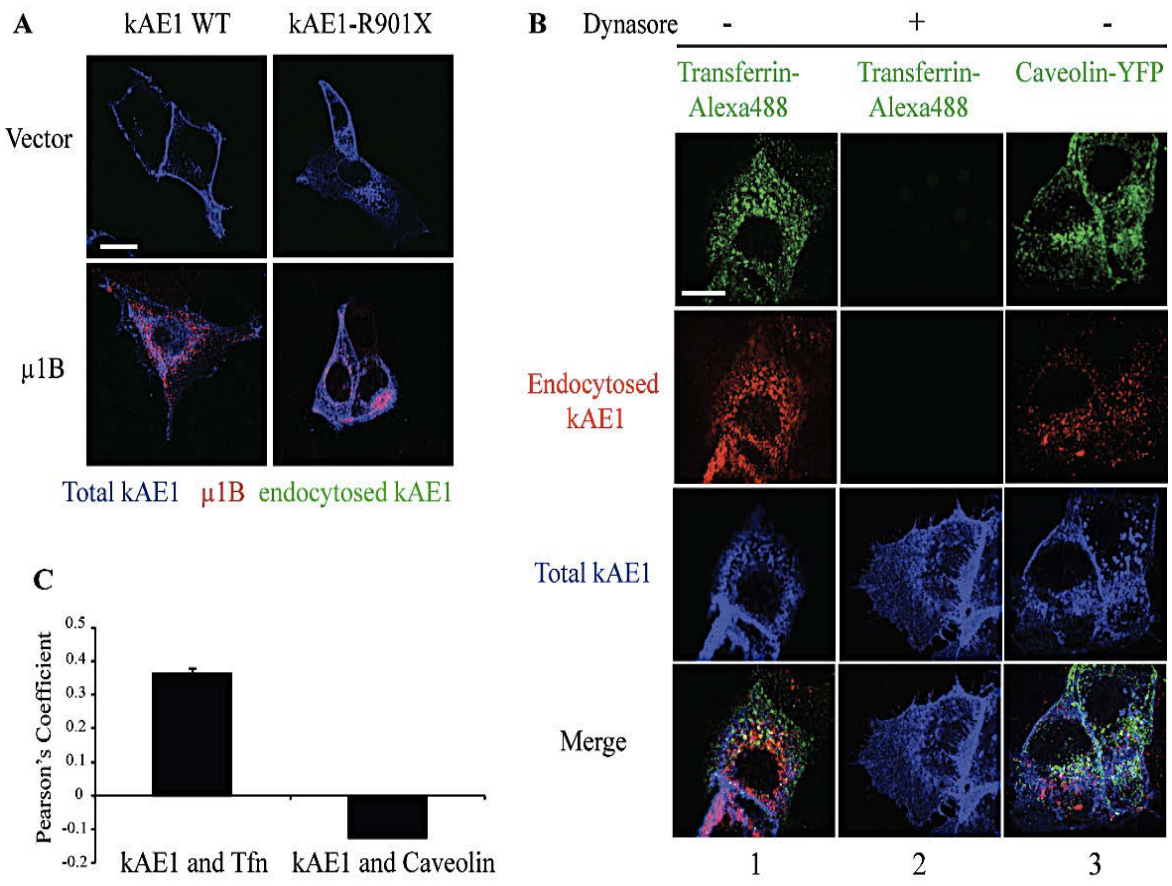

Figure 4.6: kAE1 is endocytosed via clathrin coated vesicles and colocalizes with endocytosed transferrin receptor. ***A.*** As a control for the efficacy of the acid wash, LLC-PK1 cells expressing kAE1 myc and μ1B HA were incubated with mouse anti-myc antibody on ice. The cells were then acid washed, fixed, and incubated with a secondary antibody coupled to Alexa 488 (green). After permeabilization, the cells were incubated with rat anti-HA antibody followed by anti-rat antibody coupled to Cy3 (red) to detect μ1B. Mouse anti-myc antibody followed by secondary antibody coupled to Dy649 (blue) was finally added to detect total kAE1. Bar = 10 μm. ***B.*** Immunostaining experiment showing that endocytosed kAE1 colocalizes with transferrin receptor but not with caveolin. In columns 1 & 2, intact LLC-PK1 cells expressing kAE1-myc were transferrin-depleted before incubation with mouse anti myc antibody on ice, then with dynasore hydrate and

(Continued from figure 4.6)

Tfn-Alexa Fluor 488 conjugate at 37°C for 20 minutes. The cells were then fixed and permeablized before incubation with secondary antibody coupled to Cy3 (red) to detect endocytosed kAE1 protein. Samples were next incubated with the same anti-myc antibody followed by secondary antibody coupled to Dylight 649 (blue) to detect the intracellular kAE1-myc. In column 3, LLC-PK1 cells were transfected with kAE1-myc and Caveolin-YFP. Twenty-four hours after transfection, the cells were incubated with an anti-myc antibody followed by a secondary antibody coupled to Cy3 (Red) to detect the endocytosed kAE1. ***C.*** Histogram showing the average Pearson's Coefficient values for colocalization between kAE1 and transferrin receptor or kAE1 and Caveolin for a minimum of 50 cells. Error bars correspond to means ± SE.

°C for 45 minutes. Then, the cells were washed from the excess of antibody and transferred to 37 °C for 20 minutes (visible amount of endocytosed kAE1). After removing the antibody remaining at the cell surface with an acid-wash, cells were fixed, permeabilized and endocytosed proteins were detected with a secondary antibody coupled to Alexa 488 (green). Intracellular kAE1 protein was subsequently detected using the same primary antibody and a differently labeled secondary antibody (blue). Using this procedure, we first established that incubation of the cells for 20 minutes at 37 °C was sufficient to detect endocytosed kAE1-WT proteins after acid-wash (Fig 4.7 A, first row). Comparison of endocytosed kAE1-WT, and R901X using Volocity Image analysis software showed that the ratio of kAE1-R901X internalized after a 20 minute incubation at 37 °C was slightly but significantly higher than that of kAE1-WT (0.19 ± 0.01 versus 0.14 ± 0.01 (n=3; ± SE), respectively) in non polarized LLC-PK1 cells. (Fig 4.7 B black bars), The slightly higher amount of endocytosed kAE1 R901X than kAE1-WT could explain the lower abundance of kAE1-R901X at the steady state compared to WT.

Overall, these experiments support that kAE1 is endocytosed via a clathrin-dependent pathway and that endocytosed kAE1 colocalizes with Tfn. As *(i)* AP-1B is a clathrin adaptor complex that tethers cargo proteins to clathrin-coated recycling vesicles (166), and *(ii)* endocytosed kAE1 will likely be recycled to the plasma membrane, we next asked whether AP-1B plays a role in kAE1 endocytosis and recycling machinery.

4.3.4.3. In the presence of μ1B, kAE1 is less efficiently endocytosed

We next tested whether there is a difference in kAE1 internalization in presence or absence of μ1B subunit. As seen on Figure 4.7 A, we not only observed a decrease in number but also in apparent size of green intracellular vesicles. To quantify this effect, we used

Volocity image analysis software to measure the ratio of fluorescence intensity seen in the green channel (endocytosed kAE1) relative to the blue fluorescence intensity (total kAE1) to normalize for kAE1 protein expression in approximately 50 LLC-PK1 cells from 3 independent experiments either transfected with μ1B (red channel) or empty vector. This quantification revealed a dramatic decrease of green fluorescence in cells expressing kAE-WT or R901X and μ1B, compared with cells that were transfected with the vector only. The fluorescence intensity ratio decreased from 0.14 ± 0.01 in absence of μ1B to 0.07 ± 0.01 in cells expressing μ1B and kAE1 WT. Similar results were obtained for kAE1-R901X with a ratio decreasing from 0.19 ± 0.01 to 0.12 ± 0.01 (Fig 4.7 B black versus light grey bars). Therefore, unexpectedly, μ1B expression decreased significantly the amount of endocytosed kAE1-WT and R901X. We next asked whether μ1B expression also affects the amount of recycled kAE1 in LLC-PK1 cells.

4.3.5. The effect of μ1B expression on kAE1 recycling

4.3.5.1. Carboxyl-terminal kAE1-R901X mutant recycles less efficiently to the plasma membrane than kAE1-WT

To determine whether kAE1-R901X is less abundant at the plasma membrane because it is less efficiently recycled back to the plasma membrane, we incubated intact LLC-PK1 cells expressing kAE1-WT or R901X with anti-myc antibody for 45 minutes at 4 °C, prior to washing and transferring the cells to 37 °C for 20 minutes to allow protein endocytosis. After an acid-wash to remove proteins remaining at the cell surface, we re-incubated the cells at 37 °C for an additional 80 minutes to allow endocytosed kAE1 protein to recycle back to the plasma membrane. After washing, cells were fixed and recycled proteins were detected by adding a green secondary antibody. Cells were next permeabilized and total

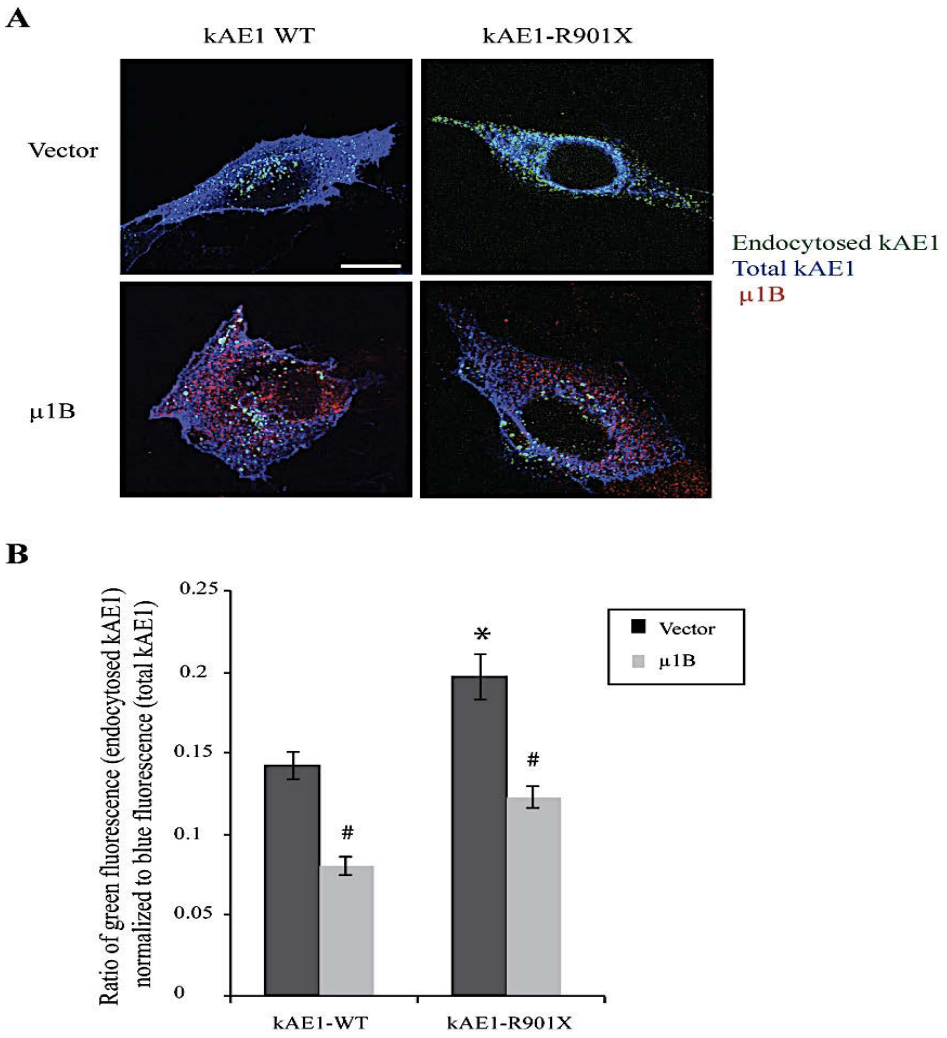

Figure 4.7: kAE1-R901X mutant is endocytosed at a higher rate than kAE1-WT, but μ1B expression decreases both kAE1 WT and R901X endocytosis rates. ***A.*** LLC-PK1 cells transfected with kAE1-myc and pCDNA3 as control or with kAE1-myc and μ1B HA cDNA were incubated with an anti-myc antibody on ice. The cells were incubated with a 37 °C medium to induce endocytosis, prior to fixation, permeabilization, and incubation with a secondary antibody coupled to Alexa 488 (green). μ1B HA was detected with a rat anti HA antibody and a secondary antibody coupled to Cy3 (red) and total kAE1 with an anti myc

(Continued from figure 4.7)

antibody coupled to Dylight 649 (blue) ***B.*** Histogram representing the ratio of endocytosed kAE1 to total kAE1 in cells expressing kAE1-WT or R901X mutant and either μ1B or empty vector. Fluorescence intensities were measured using Volocity image analysis program for at least 50 cells for each condition from 3 independent experiments. Error bars correspond to means ± SE. *$P < 0.05$ versus kAE1-WT or R901X expressing cells transfected with vector only, $^{\#}P < 0.05$ versus the same kAE1-expressing cells transfected with μ1B.

kAE1 proteins were detected by re-incubating with anti-myc antibody, detected with a blue secondary antibody (Fig 4.8 A). By normalizing green fluorescence intensities corresponding to recycled kAE1-WT or R901X, to that of the blue fluorescence corresponding to total kAE1, we determined the ratio of recycled kAE1 proteins after 80 minutes. As seen on Figure 4.8 B (dark bars), kAE1-R901X mutant recycled significantly less efficiently to the cell surface than kAE1-WT (0.66 ± 0.03 versus 0.88 ± 0.05, respectively). This impaired recycling may contribute to the lower cell surface abundance of kAE1 mutants compared to kAE1-WT in non-polarized LLCPK cells.

4.3.5.2. Expression of μ1B in LLC-PK1 cells reduces the amount of recycled kAE1 WT but not that of kAE1 R90X mutant

We next wondered whether expression of μ1B would affect the recycling rate of kAE1-WT or R901X mutant. To answer this question, we performed endocytosis and recycling experiments in LLC-PK1 cells expressing kAE1-WT or kAE1-R901X mutant and transfected with either μ1B or empty vector (Fig 4.8 A, lower row). Expression of μ1B did not significantly alter the recycling rate of kAE1-R901X mutant (Fig 4.8 B, light grey bars). This result indicates that μ1B is not involved in kAE1-R901X mutant recycling, and importantly, rules out that the μ1B effects observed on kAE1 trafficking originate from a non-specific overwhelming of the processing machinery upon expression of μ1B. In contrast, we observed a 30 % decrease in the recycling rate of kAE1-WT upon expression of μ1B (from 0.88 ± 0.05 to 0.58 ± 0.03). Thus, as expected, recycling of the carboxyl-terminal kAE1 R901X mutant is independent of μ1B, while kAE1-WT recycling was inhibited by μ1B expression in LLC-PK1 cells.

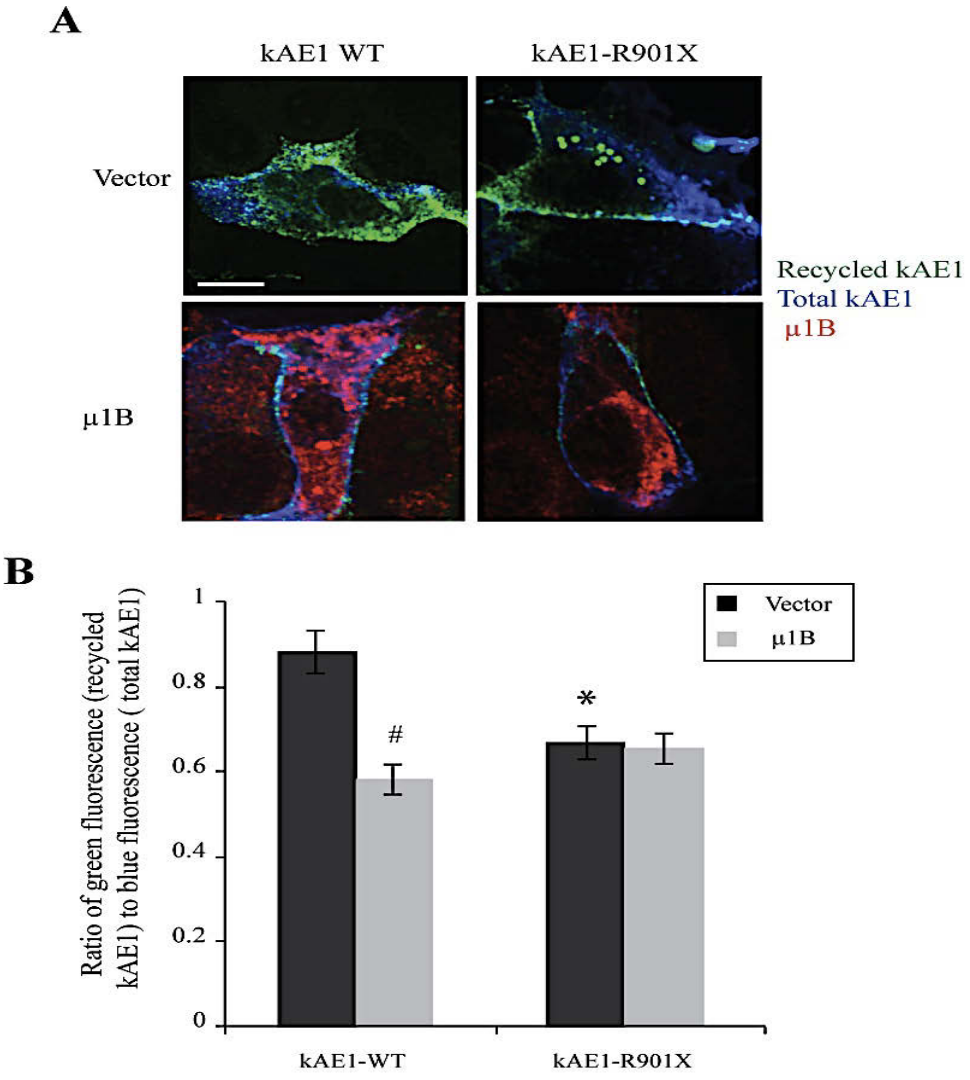

Figure 4.8: The kAE1-R901X mutant recycles less efficiently to the plasma membrane than kAE1-WT, and its recycling is independent of μ1B. ***A.*** LLCPK1 cells transfected with kAE1 myc and vector as control or with kAE1 myc and μ1B HA cDNA were incubated with an anti-myc antibody on ice. The cells were incubated with a warm medium for 20 minutes to induce endocytosis, acid washed and reincubated with warm media for 80 minutes to induce protein recycling. The cells were then fixed and incubated with secondary antibody coupled to Alexa 488 (green) to detect recycled protein. Cells were then

(Continued from figure 4.8)

permeablized before incubation with rat anti HA antibody followed by secondary antibody coupled to Cy3 to detect μ1B HA (red). Mouse anti-myc antibody was added again followed by secondary antibody Dylight 649 to detect the total kAE1 (blue). ***B.*** Histogram representing the ratio of recycled kAE1 to total in cells were transfected with kAE1-WT and mutants and either μ1B or empty vector. Fluorescence intensities for at least 25 cells for each condition from 3 independent experiments were measured using Volocity image analysis program, see statistical analysis for more details. Error bars correspond to means ± SE. *$P < 0.05$ versus kAE1- WT or R901X expressing cells transfected with vector only, $^{\#}P < 0.05$ versus the same kAE1-expressing cells transfected with μ1B.

4.4. Discussion

AP-1A and epithelial AP-1B tetrameric complexes share the small and two large subunits. These two complexes only differ by their medium subunit, μ1A for AP-1A and μ1B for AP-1B. Both AP-1A and AP-1B regulate basolateral trafficking of cargo proteins (216). However, the respective functions of these two complexes are a matter of debate in the current literature. Original studies pointed toward a different sub-cellular localization of the two complexes, with AP-1A mostly localized at the trans-Golgi network and AP-1B predominantly located in recycling endosomes (206,219,263). However, the absence of one AP-1 complex could be compensated by the presence of the other (206,266). More recent data supported that AP-1B sorts basolateral cargo proteins that are not efficiently recognized by AP-1A (288). In animals, μ1B is required for protein sorting and polarization of mouse intestinal cells, as lack of this subunit in these cells causes cell proliferation, hyperplasia and mistargeting of E-cadherin / beta-catenin complex (229). Both AP-1A and AP-1B interact with kAE1 protein (215). In the current work, we confirmed that AP-1B binds to kAE1 and that binding is important for kAE1 endocytosis and recycling in LLC-PK1 cells. We performed our experiments in porcine epithelial LLC-PK1 cells that are devoid of endogenous AP-1B complex (263,283). Understanding the physiological role of this adaptor complex for kAE1 trafficking would ideally require studies conducted in polarized epithelial cells. However, we were unable to obtain properly polarized LLC-PK1 cells expressing sufficient amounts of kAE1, and we therefore pursued our experiments with non-polarized LLC-PK1 cells.

First, we showed that μ1B immunoprecipitated and colocalized with kAE1-WT and kAE1-R901X mutant in LLC-PK1 cells (Fig 4.1). This result confirmed our previous

finding that both AP-1A and μ1B co-immunoprecipitate with kAE1 WT in MDCK cells (215). As μ1A binds to kAE1 via the C-terminal Y_{904}DEV motif (52) and μ1B binds to canonical tyrosine motifs YXXΦ (289), we assumed that μ1B binds to kAE1 via the same Y_{904}DEV motif. Interestingly, our results indicate that deletion of Y_{904}DEV motif did not abolish the interaction between kAE1 and μ1B (Fig 4.1). However, in contrast to kAE1-WT, recycling of kAE1-R901X mutant was clearly independent of μ1B expression in LLC-PK1 cells, supporting a role for kAE1 C-terminus in protein recycling. These results point toward additional binding sites in kAE1 to AP-1B.

To determine whether μ1B interacts with kAE1 via different binding sites, we conducted a peptide spot assay, using peptides covering the human kAE1 sequence and a μ1B expressing cell lysate or a lysis buffer as control (Fig 4.2 & Table 4.1). We found that in addition to the kAE1 C-terminal E_{897}EEGRDEYDEV sequence that includes the Y_{904}DEV motif, μ1B also interacted with kAE1 S_{510}FLVR sequence in the second cytosolic loop and with S_{799}GIQLFDRILLL sequence within the sixth cytosolic loop of kAE1. Importantly, this assay was not designed to identify a direct interaction between kAE1 and μ1B, as it was performed with whole cell lysates expressing epitope tagged μ1B subunit. While the S_{510}FLVR sequences has never been reported before as interacting motif with adaptor complexes, the E_{897}EEGRDEY_{904}DEV contains a typical acidic cluster signal and a YXXΦ motif known to interact with the μ1 adaptin (212). D_{805}RILLL is another typical (D/E)XXXL(L/I) motif known to interact with β1- and γ-σ1 subunits within the AP-1 complex (211,290). Together, our results suggest that kAE1 interacts via a combination of interacting sites with various subunits of the AP-1B complex. These

results reconcile our findings with previous data that showed no direct interaction between kAE1 and the μ1B subunit (245).

Phosphorylation of tyrosine 904, within the Y_{904}DEV binding motif to μ1B, induces internalization of cell surface kAE1 (57), and the DEY_{904}DEV motif within kAE1 C-terminus also interacts with GAPDH (53). Thus, we next determined whether phosphorylation of tyrosine 904 could alter kAE1/AP-1B interaction. Upon pervanadate treatment to induce phosphorylation (57), we found that binding of kAE1 to AP-1B was similar to control conditions, supporting that phosphorylation of tyrosine 904 did not affect kAE1/AP-1B interaction in MDCK cells. Of note, this phosphorylation did not affect kAE1/AP-1A interaction either (Fig 4.3). Interestingly, our results demonstrate that phosphorylation of tyrosine 904 does not disrupt kAE1/GAPDH interaction as previously shown (53). They also infer that AP-1B and GAPDH are competing for the same interaction site on kAE1 (Fig 4.4), as expressing μ1B or μ1A decreased the binding of kAE1 to endogenous GAPDH (53). This finding together with our peptide spot assay results support that AP-1B binds to kAE1 via the C-terminal Y_{904}DEV motif. Interestingly, a recent report showed that μ1B does not directly interact with kAE1 protein (245). This seeming contradiction may be explained by the interaction of kAE1 with AP-1B via other subunits than μ1B, such as β1 and γ, σ1 as explained by the interaction of subunits within the AP-1B complex (211,290). Indeed, we do not have evidence supporting that the interaction between kAE1 and AP-1B occurs directly via the μ1 subunit.

To understand the physiological role of a kAE1 interaction with AP-1B, we first expressed kAE1-WT or R901X mutant in LLC-PK1 cells that are devoid of endogenous

AP-1B (283), and characterized kAE1 WT and mutant protein's behavior. Both biotinylation and immunofluorescence results showed that kAE1-WT is more abundant at the plasma membrane of LLC-PK1 cells than mutants (Fig 4.5 A, C). Importantly, the two experimental approaches provided very different ratio of cell surface protein amounts. This discrepancy is likely due to an incomplete release of biotinylated proteins after elution, or in a difference in accessibility of the biotinylation reagent or antibody to the epitope or primary amine at the surface of the cells. Nevertheless, both approaches showed the same trend with a significant decrease in cell surface kAE1 after μ1B expression. In agreement with our results, kAE1-WT was predominantly located at the plasma membrane in non-polarized MDCK cells and at the basolateral membrane of polarized MDCK cells (159,160,247). In contrast, kAE1-R901X was found predominantly intracellularly in non-polarized MDCK cells but was apically located in polarized MDCK cells. Our results could reflect three scenarios: *(i)* kAE1-R901X mutant is less efficiently processed which would likely result in premature degradation, *(ii)* kAE1 R901X mutant is endocytosed faster than kAE1-WT, or *(iii)* kAE1-R901X mutant is recycled less efficiently than kAE1-WT to the plasma membrane. As shown in Figure 4.5 E, the half-lives of kAE1-WT and R901X were not different in LLC-PK1 cells, indicating that the reduced amount of kAE1-R901X at the cell surface was not due to accelerated turnover of the mutant.

To test the possibility that kAE1 mutants are endocytosed faster than kAE1-WT, we first briefly characterized the human kAE1-WT endocytosis pathway. We observed that kAE1 is constitutively endocytosed in a dynamin-dependent pathway and that endocytosed kAE1 colocalizes with the TfnR, a protein known to accumulate in recycling

endosomes after clathrin-mediated endocytosis (Fig 4.6) (291). In agreement with our findings, in erythroleukemia K562 cells and in HEK 293 cells, murine erythroid AE1 is also endocytosed in a clathrin dependent pathway and colocalizes with the TfnR after 20 minutes (292).

We found that the rate of kAE1 R901X endocytosis is higher than that of kAE1-WT (Fig 4.7). The kAE1-R901X mutant is truncated at the last 11 amino acids, a part which contains three important motifs, the Y_{904}DEV canonical interaction motif with adaptor proteins, the D_{902}EYDE motif that interacts with GAPDH, and the putative PDZ1-binding domain A_{908}MPV, which may be responsible for kAE1 apical mistargeting in polarized cells (159,164,293). The instability and the rapid endocytosis of kAE1-R901X may be due to the absence of one or several of the above described motifs. Consistent with this, we observed that the absence of the last 11 amino acids of kAE1 influences the endocytosis rate of kAE1 protein. Finally, we found that kAE1-R901X mutant recycled less efficiently to the plasma membrane than kAE1-WT (Fig 4.8). Together, our data support that the C-terminal kAE1-R901X mutant is endocytosed at a higher rate and recycled less efficiently to the plasma membrane. This pattern may reflect the activity of the peripheral quality-control machinery, which was previously shown to prematurely degrade other kAE1 mutants that had escaped the endoplasmic reticulum of MDCK cells (294).

We next examined the effect of μ1B expression on kAE1-WT and the C-terminal kAE1-R901X mutant in LLC-PK1 cells. Using immunofluorescence and cell surface biotinylation, we found that upon expression of μ1B, relative kAE1 cell surface expression decreased significantly in LLC-PK1 cells expressing both kAE1-WT and

kAE1-R901X mutant (Fig 4.5 B & D). Previous work (215) has shown that AP-1A interacts with the kAE1 Y_{904}DEV motif (52) and that this interaction is important for newly synthesized kAE1 trafficking to the cell surface (215). In light of these previous findings and knowing that LLC-PK1 cells express endogenous AP-1A (283), it is possible that kAE1-R901X mutant is less efficiently processed to the plasma membrane due to an inefficient interaction with μ1A. Alternatively, the R901X truncation is also predicted to disrupt the GAPDH binding site composed of the D_{902}EYDE motif in kAE1 (53). This motif overlaps with the μ1A and B binding sites. Knock-down of GAPDH resulted in intracellular retention of kAE1 protein (53), consistent with GAPDH also regulating kAE1 intracellular trafficking.

Expression of μ1B in LLC-PK1 cells significantly decreased the amount of endocytosed kAE1-WT and kAE1-R901X (Fig 4.7). This finding was unexpected, as AP-1B is not known to be involved in endocytosis (276), but it supports a destabilization of the endocytosis machinery upon expression of μ1B in LLC-PK1 cells. Interestingly, the amount of recycled kAE1 WT also decreased by a third upon expression of μ1B in LLC-PK1 cells (Fig 4.8). However, μ1B expression had no effect on kAE1-R901X recycling rate, supporting that the truncation of the last 11 amino acids is enough to abolish the effect of μ1B on kAE1 recycling. This finding also supports that the effects of μ1B on kAE1 trafficking are not originating from overwhelming of the cellular processing machinery. The fact that kAE1-WT efficiently recycled back to the plasma membrane in LLC-PK1 cells that do not express endogenous μ1B support that these cells have an alternative recycling mechanism.

We chose to perform these experiments in LLC-PK1 cells because they do not express endogenous μ1B and are thus devoid of AP-1B complex (165). Therefore, heterologous expression of μ1B was expected to restore functional AP-1B complexes as previously shown (165), and based on the role of AP-1B in protein recycling, to increase the recycling rate of kAE1-WT protein. Unexpectedly, μ1B expression in LLC-PK1 cells significantly decreased the recycling rate of kAE1-WT but did not affect that of the mutant (Fig 4.8). This unexpected decreased recycling rate of kAE1-WT upon expression of μ1B may originate from the use of non-polarized LLC-PK1 cells that could behave differently compared with polarized cells (206,216).

Despite our repeated attempts to test the effect of μ1B expression on kAE1-WT and mutant's endocytosis and recycling in polarized LLC-PK, we were unable to keep the levels of kAE1 and μ1B expression high enough to be detected by immunofluorescence. Overall, our results show that expression of μ1B affects kAE1 WT endocytosis and recycling, but not that of the truncated kAE1-R901X dRTA mutant. This finding provides a possible mechanism for dRTA pathophysiology, where in polarized collecting duct epithelial cells, kAE1-R901X may be unable to properly interact with μ1B and therefore, is mistargeted to the apical membrane.

5. Chapter five: General discussion

5.1. Introduction

This PhD thesis discussed the role the AP-1A and B on kAE1 protein trafficking and recycling in epithelial cells. This general discussion will focus on limitations and alternative approaches that could have been used to complement our studies.

5.2. Validity of the cell models

Our study of the effect of μ1A expression on kAE1 trafficking used MDCK cells. The MDCK epithelial cell line was derived from canine kidney cortex in 1958 (295) MDCK cells are considered a prototypical model of epithelial cells because of their ability to polarize and form tight junctions that separate the apical from the basolateral compartment (229). We chose MDCK cells for the following reasons: *1)* when kAE1 is expressed in MDCK cells, it is located at the basolateral membrane mimicking its physiological location in alpha-IC (247), *2)* when heterologously expressed in MDCK cells, kAE1 exchanges chloride for bicarbonate, as described in red blood cells (296,297) demonstrating that MDCK cells are a good model of renal epithelial cells, *3)* MDCK cells do not express endogenous kAE1*, 4)* MDCK cells have been widely used to study the behavior of many membrane proteins that are implicated in human diseases. For example, MDCK cells have been used to investigate the polarized expression and trafficking of WT and ΔF508 CFTR mutant and for validation of novel therapeutic compounds for treatment of cystic fibrosis (298). In the case of kAE1, several studies have used MDCK cells to investigate kAE1-WT trafficking and phosphorylation (57), the behavior of different disease-causing point and truncation kAE1 mutants (159,160) or the role of chemical chaperones to rescue mis-trafficking and function of these mutants (296,297). The fact that in MDCK cells, kAE1 is properly localized at the basolateral

membrane and is functional support that these cells have the machinery needed for kAE1 to behave as in its physiological environment, alpha-IC.

The effect of μ1B expression on kAE1 endocytosis and recycling was studied in LLC-PK1 cells. LLC-PK1 cells are porcine kidney epithelial cells, derived from proximal tubules (299) and they are naturally devoid of μ1B (276). LLC-PK1 cells get polarized and form tight junctions as in alpha-IC, but they have a low trans-epithelial electrical resistance, typical of proximal tubular cells. In agreement with previously published data (160), when expressed in polarized LLC-PK1 cells, kAE1 is located at the basolateral membrane. This cell line has also been widely used to study the role of μ1B in trafficking of a number of membrane proteins such as LDLR and VSVG proteins (216).

However, neither MDCK nor LLC-PK1 cells originate from the collecting duct and truly mimic intercalated cells. The collecting duct contains at least four types of cells, including alpha, beta, non-alpha non-beta intercalated cells and principal cells (134). This nephron segment is the only one that contains such a heterogenous population of cells. Importantly, depending on the acid-base status, intercalated cells can convert from beta to alpha-IC (129). This unique plasticity is very likely lost in cultured renal epithelial cells, which further limits the validity of the cell lines. Additionally, MDCK cells have been cultured for more than 40 years and are very likely to have lost many epithelial characteristics of renal epithelial cells. The best cell model to investigate kAE1 trafficking is alpha-IC, where kAE1, μ1A and μ1B are endogenously expressed. One cell line that would more closely resemble the physiological environment of kAE1 is the mouse inner medullary collecting duct (mIMCD) cell line (300). However, this cell line does not express endogenous kAE1 protein and kAE1 has to be exogenously expressed in

order to study its trafficking. This suggests that although originating from the collecting duct, this cell line has lost some characteristics of intercalated cells. Moreover, mIMCD cell are not as well characterized as MDCK and LLC-PK1 cells, which limits the number of biological tools (antibodies, etc) we can use. Consequently, MDCK and LLC-PK1 cells were the cells of choice to perform our studies.

5.3. Studies in non-polarized epithelial cells

As μ1B is involved in polarized recycling of membrane proteins (216), our experiments investigating the role of μ1B in kAE1 trafficking and recycling should have been performed in polarized cells. However, for several reasons, we were unable to perform these experiments in polarized cells. In the third chapter, when we knocked down the endogenous μ1A/B using canine μ1A/B siRNA, we noticed that 72 hours after knockdown, around 20 % of the cells detached, which made it difficult to do further studies on polarized cells.

In the fourth chapter, LLC-PK1 cells were used to study the role of μ1B in kAE1 endocytosis and recycling. The cells were transiently transfected with kAE1 and μ1B cDNA and grown for 3-5 days to reach polarization. Unfortunately, we were unable to find conditions where cells reached full polarization and maintained enough kAE1 and μ1B protein expression to study kAE1 protein endocytosis and recycling. Alternatively, we tried to stably co-express kAE1 and μ1B in LLC-PK1 cells. The cells were transfected with infectious viral particles first to express kAE1 protein, then transiently transfected to express μ1B protein. Once again however, our attempts to co-express kAE1 and μ1B proteins were unsuccessful as we were unable to find cell co-expressing kAE1 and μ1B in the same cells. Importantly, kAE1 expression has already been reported

to affect MDCK cell polarization by affecting the integrity of their tight junctions (159). This finding could explain our difficulties in expressing sufficient amounts of kAE1 and μ1B in polarized cells.

5.4. Role of the canonical YXXΦ motif for kAE1- R901X mutant's trafficking

In the fourth chapter of this thesis, we compared the trafficking and recycling of kAE1-WT with that of the truncated kAE1-R901X mutant. As mentioned earlier in this thesis, this mutant lacks the last 11 amino acids of kAE1 protein, which include two important motifs, the Y_{904}DEV and the putative type II PDZ domain A_{908}MPV (165,166). In our discussion, we focused on the loss of AP-1 binding sites to explain the differences in steady-state cell surface expression, endocytosis, and recycling between kAE1-WT and the kAE1-R901X. However, these differences could either originate from the absence of Y_{904}DEV motif, the PDZ type II binding domain or both. The kAE1 PDZ type II binding domain could play a role in kAE1 membrane targeting and retention. The truncation mutant kAE1-V911stop in the PDZ type II binding domain caused an increase in the intracellular level of kAE1, but the mutant predominantly localized at the basolateral membrane (159). Further, the kAE1 M909T dRTA mutant affects the PDZ type II interaction domain (A_{908}MPV) (164). This mutation converts the type II PDZ domain (X-Φ- X-Φ-) into a type I PDZ domain (X- S/T-X-V/L) (164). Trafficking of this mutant mimics that of the kAE1-R901X mutant, as it is found at both the apical and basolateral membranes when expressed in polarized MDCK cells (164).

To discriminate between the role of the PDZ domain and adaptor protein domain on kAE1 trafficking, endocytosis and recycling, one should use kAE1 specifically deleted

or mutated on either the Y_{904}DEV motif or the PDZ domain. Previously studied mutations such as Y904A, Y904F, and Y904A/V907A would be the best controls to compare the importance of the Y_{904}DEV for kAE1 trafficking and recycling (159).

5.5. Functional consequence of kAE1 trafficking

Although this thesis focused on a chloride/bicarbonate transporter, we do not provide evidence of kAE1 function in our work. In fact, the function of most mutants studied here has already been investigated. However, kAE1 protein can perform its physiological function only if it reaches the cell surface, and kAE1 mutations that affect its trafficking affect its function as well. For example, kAE1-R901X and M909T dRTA mutants are retained intracellularly or mistargeted to the apical membrane (159,160,164). When expressed in *Xenopus* oocytes, these mutants are functional and retained the same Cl^- transport activity as kAE1-WT (162,164). However, a question that remains un-answered is whether intracellular retention of kAE1 mutants affects the intracellular acid-base status or vesicular pH. Indeed, a number of sodium-proton exchangers are physiologically expressed in the membrane of endosomes or lysosomes where they participate in vesicular acidification (301). It is thus possible that by transporting bicarbonate and chloride, intracellularly retained kAE1 mutants alter physiological lysosomal degradation or endoplasmic reticulum pH, although this has never been investigated. Further functional studies will thus be needed to compare the effect of kAE1-WT or mutants expression on vesicular pH.

5.6. Transient versus stable transfections

In this work, MDCK were transiently transfected, using electroporation, and LLC-PK1 cells, using XtremeGENE transfection reagent with cDNA coding for different kAE1-

WT or mutant proteins. Although transient transfection is a very efficient way to heterologously express a protein in cells, it often results in its over-expression, which can be overwhelming for the cell machinery. This over-expression can result in abnormal intracellular accumulation of the protein and misleading colocalization results within intracellular compartments. For best results, our experiments should have been performed in MDCK and LLC-PK1 cell lines stably expressing kAE1-WT and mutants with either μ1A or μ1B proteins.

5.7. kAE1-WT and kAE1-R901X protein expression

In the fourth chapter of this thesis, the trafficking and recycling behaviors of kAE1-WT and kAE1-R901X mutant were compared. kAE1-WT or mutant protein were transiently expressed in LLC-PK1 cells using the same amount of cDNA encoding kAE1-WT and kAE1-R901X mutant. However, kAE1-WT expression level was repeatedly noticed to be higher than kAE1-R901X mutant despite using the same amount of cDNA. This difference could reflect a less efficient protein synthesis for kAE1-R901X, compared to the WT. Importantly; this difference could have affected our conclusions on recycling and endocytosis of kAE1 proteins, where we assumed a similar protein expression after transfection. To circumvent this problem, the amount of transfected cDNA encoding kAE1-WT and kAE1-R901X proteins should have been adjusted to perform our experiments with the same initial amount of protein.

6. Chapter six: Summary and future directions

6.1. Summary

The purpose of this study was to investigate the physiological role of kAE1 interaction with AP-1A and B. We assumed that *(i)* this interaction is crucial for kAE1 residency at the basolateral membrane in polarized epithelial cell, and *(ii)* the lack of proper interaction between AP-1A and/or B and kAE1 affects kAE1 trafficking and surface expression, and may cause dRTA disease. My thesis work confirmed most of these hypotheses and improved our current knowledge of kAE1 interaction with AP-1A protein complex. The first part of this thesis confirmed the interaction between kAE1 and AP-1A in immortalized cells (MDCK cells) and tissue homogenates (mouse kidney cells) by immunoprecipitation and immunofluorescence colocalization. The knock down of the endogenous μ1A/B in MDCK cells by siRNA reduced the amount of kAE1 at the cell surface and resulted in kAE1 degradation. Interestingly, the stability and localization of kAE1 at the cell surface were restored by expressing human siRNA-resistant μ1A or μ1B in MDCK cells knock down for endogenous μ1A/B. We showed that newly synthesized kAE1 proteins traffic directly to the cell surface without traveling through recycling endosomes and that both μ1A and μ1B are important for normal kAE1 trafficking. Reciprocal immunoprecipitation confirmed an interaction between kAE1 and AP-1B.

The second main part of this thesis focused on studying the role of kAE1 interaction with AP-1B in kAE1 endocytosis and recycling. This interaction was confirmed by immunoprecipitation, immunofluorescence, and proximity ligation assay in kidney epithelial cells. We identified multiple interaction sites of AP-1B on kAE1 protein by peptide spot assay, which explained the persistent interaction between AP-1B and kAE1-R901X mutant. kAE1 endocytosis pathway was investigated for the first time in this thesis,

and appeared to be dynamin- and clathrin-dependent. The kAE1-R901X mutant was endocytosed faster and recycled slower than kAE1-WT. Surprisingly, μ1B expression in LLC-PK1 cells that lack endogenous μ1B reduced the amount of cell surface kAE1-WT at the steady state. This decrease correlated with an increased rate of kAE1 endocytosis and decreased rate of recycled kAE1-WT. Unlike that of kAE1-WT, kAE1-R901X recycling was independent from μ1B expression. Table 6.1 compares endocytosis and recycling pattern of kAE1-WT and kAE1-R901X mutant in the presence and absence of μ1B. These data lead to the proposal that the apically mistargeted kAE1-R901X dRTA mutant fails to recycle back to the basolateral membrane due to its inability to properly interact with AP-1B.

6.2. Future directions

In this thesis, the physiological relevance of kAE1 and AP-1A/B interaction was investigated in non-polarized epithelial cells. However, to exactly mimic the physiological situation in alpha intercalated cells, one should conduct these interaction studies in polarized kidney epithelial cells. Despite their common use as models for collecting duct cells, MDCK and LLC-PK1 cells are not originally collecting duct cells, but instead were either derived from the proximal tubule (302,303) or a mixture of kidney epithelial cells (295). A collecting duct cell line that endogenously expresses kAE1 and AP- 1A or B would be the most suitable model to mimic the situation *in vivo*.

Table 6.1 Endocytosis and recycling of kAE1-WT and kAE1-R901X mutant in the presence and absence of μ1B.

μ1B	-	-	+	+
Condition	**kAE1-WT**	**kAE1-R901X**	**kAE1-WT**	**kAE1-R901X**
Steady state	++++	++	++	+
Endocytosis	++	++++	+	++
Recycling	+++	++	++	(no Change)

In this project we identified multiple interaction sites of AP-1B on kAE1 protein by peptide spot assay. This assay did not determine which adaptin(s) of the AP-1B complex is involved in this interaction. Further, it is possible that more than one binding site for the same adaptin exists within kAE1 protein, as kAE1 protein form dimers (48). In my work, I have used a cell lysate expressing exogenous μ1B, which is enough to form a functional AP-1B complex using the endogenous γ1, β1, and σ1 adaptins (189,201) To determine which subunit(s) of the tetrameric AP-1 complex directly interacts with kAE1, pure AP-1B adaptin subunits should be incubated with kAE1 peptides spotted on cellulose membranes.

More investigation needs to be done on the binding motifs between kAE1 and AP-1B that we have identified in addition to the expected canonical tyrosine (Y_{904}DEV) motif. We identified a binding to a dileucine (D_{806}RILLL**)** motif, to the acidic cluster E_{897}EEGRDEYD within kAE1 C-terminus and to the S_{510}FLVRF motif in the second intracellular loop of kAE1 (Table 4.1). It will be interesting to mutate these motifs and test the effect of these mutations on kAE1 trafficking and function and interaction with AP-1B.

Both the dileucine (D_{806}RILLL**)** in the 6th kAE1 intracellular loop and the tyrosine (Y_{904}DEV) motifs in kAE1 C-terminus are important for kAE1 trafficking and localization at the plasma membrane. Our preliminary unpublished data indicate that quadruple mutations in both motifs DRIL[L_{810}L/AA] and [Y_{904}/A]DE[V_{907}/A] affect kAE1 normal processing to complex oligosaccharide as shown by immunoblotting (Figure 5.1 A, lane 4). The double mutations affect also kAE1 surface localization as immunofluorescence showed that the kAE1 quadruple mutant is retained intracellularly,

unlike kAE1 with mutations in either the dileucine or tyrosine motif (Figure 5.1 B). These data suggest that the tyrosine and dileucine motifs within kAE1 protein are synergically required for the normal processing and localization of kAE1 at the cell surface.

More experiments need to be performed in order to explore the importance of these two motifs. Cell surface biotinylation, binding to SITS/DIDS inhibitors, functional assay, and the mutants expression in polarized cells experiments will answer more questions regarding the role of tyrosine and dileucine motifs in kAE1 protein trafficking, folding, and function in chloride/ bicarbonate exchange activity.

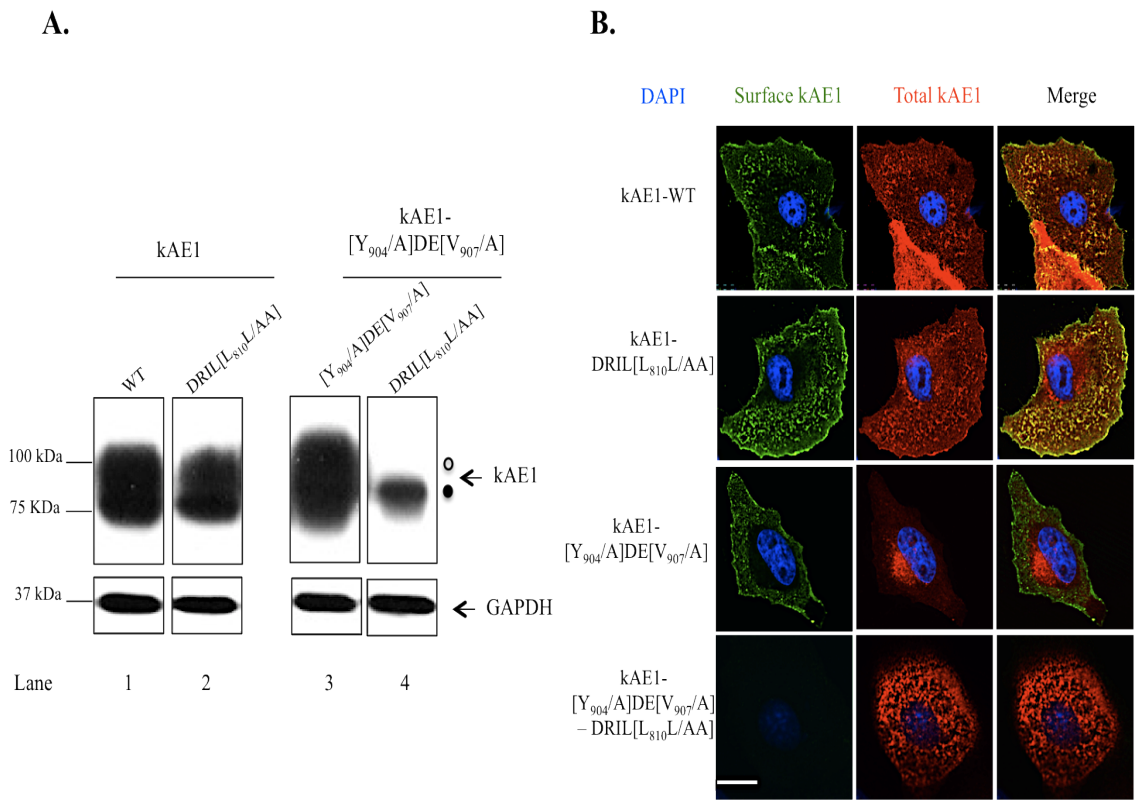

Figure 5.1 Mutations in kAE1 tyrosine and dileucine motifs affect kAE1 processing and surface localization. MDCK cells were transiently transfected with kAE1-WT, and kAE1 mutants DRIL[L_{810}L/AA], [Y_{904}/A]DE[V_{907}/A] and the quadruple mutant DRIL[L_{810}L/AA], [Y_{904}/A]DE[V_{907}/A]. ***A.*** The cells were lysed and lysate proteins separated on SDS-PAGE, then transferred to nitrocellulose and incubated with anti-HA and anti-GAPDH antibodies to detect both kAE1 and GAPDH (loading control) respectively. Open circle corresponds to kAE1 carrying complex oligosaccharides, and filled circle indicates kAE1 carrying high mannose oligosaccharides. ***B.*** Cells were fixed and incubated with anti-HA antibody followed by secondary antibody coupled to Alexa 488 (green). The cells were then permeabilized and incubated again with anti HA primary antibody followed by Cy3 (red) coupled secondary antibody. Nuclei were stained with DAPI (blue). Bar = 10 μm.

7. References

1. Supuran, C. T., Di Fiore, A., and De Simone, G. (2008) Carbonic anhydrase inhibitors as emerging drugs for the treatment of obesity. *Expert opinion on emerging drugs* **13**, 383-392
2. Boron, W. F., Endeward, V., Gros, G., Musa-Aziz, R., and Pohl, P. (2011) Intrinsic CO_2 permeability of cell membranes and potential biological relevance of CO_2 channels. *Chemphyschem : a European journal of chemical physics and physical chemistry* **12**, 1017-1019
3. Nebert, D. W., Galvez-Peralta, M., Hay, E. B., Li, H., Johansson, E., Yin, C., Wang, B., He, L., and Soleimani, M. (2012) ZIP14 and ZIP8 zinc/bicarbonate symporters in Xenopus oocytes: characterization of metal uptake and inhibition. *Metallomics : integrated biometal science* **4**, 1218-1225
4. Wain, H. M., Lush, M. J., Ducluzeau, F., Khodiyar, V. K., and Povey, S. (2004) Genew: the Human Gene Nomenclature Database, 2004 updates. *Nucleic Acids Res* **32**, D255-257
5. Romero, M. F., Chen, A. P., Parker, M. D., and Boron, W. F. (2013) The SLC4 family of bicarbonate HCO_3^- transporters. *Molecular aspects of medicine* **34**, 159-182
6. Choi, I. (2012) SLC4A transporters. *Current topics in membranes* **70**, 77-103
7. Park, M. H., Lee, K. S., Huh, M. J., and Lee, S. H. (2004) Early development of auditory performance in implanted infants and children with EARS-K in korea. *Cochlear implants international* **5 Suppl 1**, 120-124
8. Vilas, G. L., Loganathan, S. K., Liu, J., Riau, A. K., Young, J. D., Mehta, J. S., Vithana, E. N., and Casey, J. R. (2013) Transmembrane water-flux through SLC4A11: a route defective in genetic corneal diseases. *Hum Mol Genet* **22**, 4579-4590
9. Kopito, R. R., and Lodish, H. F. (1985) Primary structure and transmembrane orientation of the murine anion exchange protein. *Nature* **316**, 234-238
10. Fairbanks, G., Steck, T. L., and Wallach, D. F. (1971) Electrophoretic analysis of the major polypeptides of the human erythrocyte membrane. *Biochemistry* **10**, 2606-2617
11. Vince, J. W., and Reithmeier, R. A. (1998) Carbonic anhydrase II binds to the carboxyl terminus of human band 3, the erythrocyte $C1^-/HCO_3^-$ exchanger. *The Journal of biological chemistry* **273**, 28430-28437
12. Reithmeier, R. A. (2001) A membrane metabolon linking carbonic anhydrase with chloride/bicarbonate anion exchangers. *Blood Cells Mol Dis* **27**, 85-89
13. Lambert, A., and Lowe, A. G. (1978) Chloride/bicarbonate exchange in human erythrocytes. *The Journal of physiology* **275**, 51-63
14. Passow, H. (1986) Molecular aspects of band 3 protein-mediated anion transport across the red blood cell membrane. *Reviews of physiology, biochemistry and pharmacology* **103**, 61-203
15. Knauf, P. A., Ship, S., Breuer, W., McCulloch, L., and Rothstein, A. (1978) Asymmetry of the red cell anion exchange system. Different mechanisms of reversible inhibition by N-(4-azido-2-nitrophenyl)-2-aminoethylsulfonate (NAP-

taurine) at the inside and outside of the membrane. *The Journal of general physiology* **72**, 607-630
16. Salhany, J. M. (2004) Slow transitions between two conformational states of band 3 (AE1) modulate divalent anion transport and DBDS binding to a second site on band 3 which is activated by lowering the pH (pK approximately 5.0). *Blood Cells Mol Dis* **32**, 372-378
17. Tanner, M. J., Martin, P. G., and High, S. (1988) The complete amino acid sequence of the human erythrocyte membrane anion-transport protein deduced from the cDNA sequence. *The Biochemical journal* **256**, 703-712
18. Lux, S. E., John, K. M., Kopito, R. R., and Lodish, H. F. (1989) Cloning and characterization of band 3, the human erythrocyte anion-exchange protein (AE1). *Proceedings of the National Academy of Sciences of the United States of America* **86**, 9089-9093
19. Li, J., Quilty, J., Popov, M., and Reithmeier, R. A. (2000) Processing of N-linked oligosaccharide depends on its location in the anion exchanger, AE1, membrane glycoprotein. *The Biochemical journal* **349**, 51-57.
20. Jennings, M. L., and Nicknish, J. S. (1985) Localization of a site of intermolecular cross-linking in human red blood cell band 3 protein. *The Journal of biological chemistry* **260**, 5472-5479
21. Okubo, K., Kang, D., Hamasaki, N., and Jennings, M. L. (1994) Red blood cell band 3. Lysine 539 and lysine 851 react with the same H_2DIDS (4,4'-diisothiocyanodihydrostilbene-2,2'-disulfonic acid) molecule. *The Journal of biological chemistry* **269**, 1918-1926
22. Low, P. S. (1986) Structure and function of the cytoplasmic domain of band 3: center of erythrocyte membrane-peripheral protein interactions. *Biochim Biophys Acta* **864**, 145-167.
23. Willardson, B. M., Thevenin, B. J., Harrison, M. L., Kuster, W. M., Benson, M. D., and Low, P. S. (1989) Localization of the ankyrin-binding site on erythrocyte membrane protein, band 3. *The Journal of biological chemistry* **264**, 15893-15899
24. Walder, J. A., Chatterjee, R., Steck, T. L., Low, P. S., Musso, G. F., Kaiser, E. T., Rogers, P. H., and Arnone, A. (1984) The interaction of hemoglobin with the cytoplasmic domain of band 3 of the human erythrocyte membrane. *The Journal of biological chemistry* **259**, 10238-10246.
25. Campanella, M. E., Chu, H., and Low, P. S. (2005) Assembly and regulation of a glycolytic enzyme complex on the human erythrocyte membrane. *Proceedings of the National Academy of Sciences of the United States of America* **102**, 2402-2407
26. Ercolani, L., Brown, D., Stuart-Tilley, A., and Alper, S. L. (1992) Colocalization of GAPDH and band 3 (AE1) proteins in rat erythrocytes and kidney intercalated cell membranes. *Am J Physiol* **262**, F892-896
27. Chang, S. H., and Low, P. S. (2003) Identification of a critical ankyrin-binding loop on the cytoplasmic domain of erythrocyte membrane band 3 by crystal structure analysis and site-directed mutagenesis. *The Journal of biological chemistry* **278**, 6879-6884
28. Lombardo, C. R., Willardson, B. M., and Low, P. S. (1992) Localization of the protein 4.1-binding site on the cytoplasmic domain of erythrocyte membrane band 3. *The Journal of biological chemistry* **267**, 9540-9546.

29. Bruce, L. J., Beckmann, R., Ribeiro, M. L., Peters, L. L., Chasis, J. A., Delaunay, J., Mohandas, N., Anstee, D. J., and Tanner, M. J. (2003) A band 3-based macrocomplex of integral and peripheral proteins in the RBC membrane. *Blood* **101**, 4180-4188
30. Telen, M. J., and Chasis, J. A. (1990) Relationship of the human erythrocyte Wrb antigen to an interaction between glycophorin A and band 3. *Blood* **76**, 842-848
31. Williamson, R. C., and Toye, A. M. (2008) Glycophorin A: Band 3 aid. *Blood Cells Mol Dis* **41**, 35-43
32. Barneaud-Rocca, D., Etchebest, C., and Guizouarn, H. (2013) Structural model of the anion exchanger 1 (SLC4A1) and identification of transmembrane segments forming the transport site. *The Journal of biological chemistry* **288**, 26372-26384
33. Alper, S. L., Vandorpe, D. H., Peters, L. L., and Brugnara, C. (2008) Reduced DIDS-sensitive chloride conductance in *Ae1*$^{-/-}$ mouse erythrocytes. *Blood Cells Mol Dis* **41**, 22-34
34. Romero, M. F., Fulton, C. M., and Boron, W. F. (2004) The SLC4 family of HCO_3^- transporters. *Pflugers Arch* **447**, 495-509
35. Kuma, H., Abe, Y., Askin, D., Bruce, L. J., Hamasaki, T., Tanner, M. J., and Hamasaki, N. (2002) Molecular basis and functional consequences of the dominant effects of the mutant band 3 on the structure of normal band 3 in Southeast Asian ovalocytosis. *Biochemistry* **41**, 3311-3320
36. Wrong, O., Bruce, L. J., Unwin, R. J., Toye, A. M., and Tanner, M. J. (2002) Band 3 mutations, distal renal tubular acidosis, and Southeast Asian ovalocytosis. *Kidney Int* **62**, 10-19
37. Quilty, J. A., and Reithmeier, R. A. (2000) Trafficking and folding defects in hereditary spherocytosis mutants of the human red cell anion exchanger. *Traffic* **1**, 987-998
38. An, X., and Mohandas, N. (2008) Disorders of red cell membrane. *Br J Haematol* **141**, 367-375
39. Bolton-Maggs, P. H., Stevens, R. F., Dodd, N. J., Lamont, G., Tittensor, P., King, M. J., and General Haematology Task Force of the British Committee for Standards in, H. (2004) Guidelines for the diagnosis and management of hereditary spherocytosis. *Br J Haematol* **126**, 455-474
40. Gallagher, P. G., and Forget, B. G. (1997) Hematologically important mutations: band 3 and protein 4.2 variants in hereditary spherocytosis. *Blood Cells Mol Dis* **23**, 417-421
41. Perrotta, S., Gallagher, P. G., and Mohandas, N. (2008) Hereditary spherocytosis. *Lancet* **372**, 1411-1426
42. Alvarez, B. V., Kieller, D. M., Quon, A. L., Robertson, M., and Casey, J. R. (2007) Cardiac hypertrophy in anion exchanger 1-null mutant mice with severe hemolytic anemia. *American journal of physiology. Heart and circulatory physiology* **292**, H1301-1312
43. Stehberger, P. A., Shmukler, B. E., Stuart-Tilley, A. K., Peters, L. L., Alper, S. L., and Wagner, C. A. (2007) Distal renal tubular acidosis in mice lacking the AE1 (band3) Cl^-/HCO_3^- exchanger (slc4a1). *J Am Soc Nephrol* **18**, 1408-1418

44. Alper, S. L., Kopito, R. R., Libresco, S. M., and Lodish, H. F. (1988) Cloning and characterization of a murine band 3-related cDNA from kidney and from a lymphoid cell line. *The Journal of biological chemistry* **263**, 17092-17099
45. Brosius, F. C., 3rd, Alper, S. L., Garcia, A. M., and Lodish, H. F. (1989) The major kidney band 3 gene transcript predicts an amino-terminal truncated band 3 polypeptide. *The Journal of biological chemistry* **264**, 7784-7787
46. Wu, F., Saleem, M. A., Kampik, N. B., Satchwell, T. J., Williamson, R. C., Blattner, S. M., Ni, L., Toth, T., White, G., Young, M. T., Parker, M. D., Alper, S. L., Wagner, C. A., and Toye, A. M. Anion Exchanger 1 Interacts with Nephrin in Podocytes. *J Am Soc Nephrol*
47. Satchwell, T. J., Bell, A. J., Pellegrin, S., Kupzig, S., Ridgwell, K., Daniels, G., Anstee, D. J., van den Akker, E., and Toye, A. M. (2011) Critical band 3 multiprotein complex interactions establish early during human erythropoiesis. *Blood* **118**, 182-191
48. Quilty, J. A., Cordat, E., and Reithmeier, R. A. (2002) Impaired trafficking of human kidney anion exchanger (kAE1) caused by hetero-oligomer formation with a truncated mutant associated with distal renal tubular acidosis. *The Biochemical journal* **368**, 895-903
49. Ding, Y., Casey, J. R., and Kopito, R. R. (1994) The major kidney AE1 isoform does not bind ankyrin (Ank1) in vitro. An essential role for the 79 NH2-terminal amino acid residues of band 3. *The Journal of biological chemistry* **269**, 32201-32208
50. Chen, J., Vijayakumar, S., Li, X., and Al-Awqati, Q. (1998) Kanadaptin is a protein that interacts with the kidney but not the erythroid form of band 3. *The Journal of biological chemistry* **273**, 1038-1043
51. Kittanakom, S., Cordat, E., Akkarapatumwong, V., Yenchitsomanus, P. T., and Reithmeier, R. A. (2004) Trafficking defects of a novel autosomal recessive distal renal tubular acidosis mutant (S773P) of the human kidney anion exchanger (kAE1). *The Journal of biological chemistry* **39**, 40960-40971.
52. Sawasdee, N., Junking, M., Ngaojanlar, P., Sukomon, N., Ungsupravate, D., Limjindaporn, T., Akkarapatumwong, V., Noisakran, S., and Yenchitsomanus, P. T. (2010) Human kidney anion exchanger 1 interacts with adaptor-related protein complex 1 mu1A (AP-1 mu1A). *Biochemical and biophysical research communications* **401**, 85-91
53. Su, Y., Blake-Palmer, K. G., Fry, A. C., Best, A., Brown, A. C., Hiemstra, T. F., Horita, S., Zhou, A., Toye, A. M., and Karet, F. E. (2011) Glyceraldehyde 3-phosphate dehydrogenase is required for band 3 (anion exchanger 1) membrane residency in the mammalian kidney. *Am J Physiol Renal Physiol* **300**, F157-166
54. Sirover, M. A. (1999) New insights into an old protein: the functional diversity of mammalian glyceraldehyde-3-phosphate dehydrogenase. *Biochim Biophys Acta* **1432**, 159-184
55. Chen, J., Wu, M., Sezate, S. A., Matsumoto, H., Ramsey, M., and McGinnis, J. F. (2008) Interaction of glyceraldehyde-3-phosphate dehydrogenase in the light-induced rod alpha-transducin translocation. *Journal of neurochemistry* **104**, 1280-1292

56. Tisdale, E. J., Azizi, F., and Artalejo, C. R. (2009) Rab2 utilizes glyceraldehyde-3-phosphate dehydrogenase and protein kinase C{iota} to associate with microtubules and to recruit dynein. *The Journal of biological chemistry* **284**, 5876-5884
57. Williamson, R. C., Brown, A. C., Mawby, W. J., and Toye, A. M. (2008) Human kidney anion exchanger 1 localisation in MDCK cells is controlled by the phosphorylation status of two critical tyrosines. *Journal of cell science* **121**, 3422-3432
58. Wu, C., and Dedhar, S. (2001) Integrin-linked kinase (ILK) and its interactors: a new paradigm for the coupling of extracellular matrix to actin cytoskeleton and signaling complexes. *The Journal of cell biology* **155**, 505-510
59. Keskanokwong, T., Shandro, H. J., Johnson, D. E., Kittanakom, S., Vilas, G. L., Thorner, P., Reithmeier, R. A., Akkarapatumwong, V., Yenchitsomanus, P. T., and Casey, J. R. (2007) Interaction of integrin-linked kinase with the kidney chloride/bicarbonate exchanger, kAE1. *The Journal of biological chemistry* **282**, 23205-23218
60. Alper, S. L., Stewart, A. K., Chernova, M. N., Zolotarev, A. S., Clark, J. S., and Vandorpe, D. H. (2006) Anion exchangers in flux: functional differences between human and mouse SLC26A6 polypeptides. *Novartis Foundation symposium* **273**, 107-119; discussion 119-125, 261-104
61. Romero, M. F. (2005) Molecular pathophysiology of SLC4 bicarbonate transporters. *Current opinion in nephrology and hypertension* **14**, 495-501
62. Stewart, A. K., Kerr, N., Chernova, M. N., Alper, S. L., and Vaughan-Jones, R. D. (2004) Acute pH-dependent regulation of AE2-mediated anion exchange involves discrete local surfaces of the NH2-terminal cytoplasmic domain. *The Journal of biological chemistry* **279**, 52664-52676
63. Stewart, A. K., Kurschat, C. E., Burns, D., Banger, N., Vaughan-Jones, R. D., and Alper, S. L. (2007) Transmembrane domain histidines contribute to regulation of AE2-mediated anion exchange by pH. *American journal of physiology. Cell physiology* **292**, C909-918
64. Stewart, A. K., Chernova, M. N., Shmukler, B. E., Wilhelm, S., and Alper, S. L. (2002) Regulation of AE2-mediated Cl- transport by intracellular or by extracellular pH requires highly conserved amino acid residues of the AE2 NH2-terminal cytoplasmic domain. *The Journal of general physiology* **120**, 707-722
65. Stuart-Tilley, A., Sardet, C., Pouyssegur, J., Schwartz, M. A., Brown, D., and Alper, S. L. (1994) Immunolocalization of anion exchanger AE2 and cation exchanger NHE1 in distinct adjacent cells of gastric mucosa. *Am J Physiol* **266**, C559-568
66. Alper, S. L., Stuart-Tilley, A. K., Biemesderfer, D., Shmukler, B. E., and Brown, D. (1997) Immunolocalization of AE2 anion exchanger in rat kidney. *Am J Physiol* **273**, F601-614
67. Jiang, L., Chernova, M. N., and Alper, S. L. (1997) Secondary regulatory volume increase conferred on Xenopus oocytes by expression of AE2 anion exchanger. *Am J Physiol* **272**, C191-202
68. Gawenis, L. R., Ledoussal, C., Judd, L. M., Prasad, V., Alper, S. L., Stuart-Tilley, A., Woo, A. L., Grisham, C., Sanford, L. P., Doetschman, T., Miller, M. L., and

Shull, G. E. (2004) Mice with a targeted disruption of the AE2 Cl^-/HCO_3^- exchanger are achlorhydric. *The Journal of biological chemistry* **279**, 30531-30539

69. Kudrycki, K. E., Newman, P. R., and Shull, G. E. (1990) cDNA cloning and tissue distribution of mRNAs for two proteins that are related to the band 3 Cl^-/HCO_3^- exchanger. *The Journal of biological chemistry* **265**, 462-471
70. Kobayashi, S., Morgans, C. W., Casey, J. R., and Kopito, R. R. (1994) AE3 anion exchanger isoforms in the vertebrate retina: developmental regulation and differential expression in neurons and glia. *The Journal of neuroscience : the official journal of the Society for Neuroscience* **14**, 6266-6279
71. Brosius, F. C., 3rd, Pisoni, R. L., Cao, X., Deshmukh, G., Yannoukakos, D., Stuart-Tilley, A. K., Haller, C., and Alper, S. L. (1997) AE anion exchanger mRNA and protein expression in vascular smooth muscle cells, aorta, and renal microvessels. *Am J Physiol* **273**, F1039-1047
72. Linn, S. C., Kudrycki, K. E., and Shull, G. E. (1992) The predicted translation product of a cardiac AE3 mRNA contains an N terminus distinct from that of the brain AE3 Cl^-/HCO_3^- exchanger. Cloning of a cardiac AE3 cDNA, organization of the AE3 gene, and identification of an alternative transcription initiation site. *The Journal of biological chemistry* **267**, 7927-7935
73. Sander, T., Toliat, M. R., Heils, A., Leschik, G., Becker, C., Ruschendorf, F., Rohde, K., Mundlos, S., and Nurnberg, P. (2002) Association of the 867Asp variant of the human anion exchanger 3 gene with common subtypes of idiopathic generalized epilepsy. *Epilepsy research* **51**, 249-255
74. Vilas, G. L., Johnson, D. E., Freund, P., and Casey, J. R. (2009) Characterization of an epilepsy-associated variant of the human Cl^-/HCO_3^- exchanger AE3. *American journal of physiology. Cell physiology* **297**, C526-536
75. Hentschke, M., Wiemann, M., Hentschke, S., Kurth, I., Hermans-Borgmeyer, I., Seidenbecher, T., Jentsch, T. J., Gal, A., and Hubner, C. A. (2006) Mice with a targeted disruption of the Cl^-/HCO_3^- exchanger AE3 display a reduced seizure threshold. *Molecular and cellular biology* **26**, 182-191
76. Sowah, D., Brown, B. F., Quon, A., Alvarez, B. V., and Casey, J. R. (2014) Resistance to cardiomyocyte hypertrophy in ae3-/- mice, deficient in the AE3 Cl^-/HCO_3^- exchanger. *BMC cardiovascular disorders* **14**, 89
77. Gross, E., Hawkins, K., Pushkin, A., Sassani, P., Dukkipati, R., Abuladze, N., Hopfer, U., and Kurtz, I. (2001) Phosphorylation of Ser(982) in the sodium bicarbonate cotransporter kNBC1 shifts the HCO_3^- : Na^+ stoichiometry from 3 : 1 to 2 : 1 in murine proximal tubule cells. *The Journal of physiology* **537**, 659-665
78. Gross, E., and Kurtz, I. (2002) Structural determinants and significance of regulation of electrogenic Na^+/HCO_3^- cotransporter stoichiometry. *American journal of physiology. Renal physiology* **283**, F876-887
79. Schmitt, B. M., Biemesderfer, D., Romero, M. F., Boulpaep, E. L., and Boron, W. F. (1999) Immunolocalization of the electrogenic Na^+/HCO_3^- cotransporter in mammalian and amphibian kidney. *Am J Physiol* **276**, F27-38
80. Abuladze, N., Lee, I., Newman, D., Hwang, J., Boorer, K., Pushkin, A., and Kurtz, I. (1998) Molecular cloning, chromosomal localization, tissue distribution,

and functional expression of the human pancreatic sodium bicarbonate cotransporter. *The Journal of biological chemistry* **273**, 17689-17695

81. Choi, I., Romero, M. F., Khandoudi, N., Bril, A., and Boron, W. F. (1999) Cloning and characterization of a human electrogenic Na^+-HCO_3^- cotransporter isoform (hhNBC). *Am J Physiol* **276**, C576-584
82. Bevensee, M. O., Schmitt, B. M., Choi, I., Romero, M. F., and Boron, W. F. (2000) An electrogenic Na^+/HCO_3^- cotransporter (NBC) with a novel COOH-terminus, cloned from rat brain. *American journal of physiology. Cell physiology* **278**, C1200-1211
83. Sassani, P., Pushkin, A., Gross, E., Gomer, A., Abuladze, N., Dukkipati, R., Carpenito, G., and Kurtz, I. (2002) Functional characterization of NBC4: a new electrogenic sodium-bicarbonate cotransporter. *American journal of physiology. Cell physiology* **282**, C408-416
84. Virkki, L. V., Wilson, D. A., Vaughan-Jones, R. D., and Boron, W. F. (2002) Functional characterization of human NBC4 as an electrogenic Na^+/HCO_3^- cotransporter (NBCe2). *American journal of physiology. Cell physiology* **282**, C1278-1289
85. Pushkin, A., Abuladze, N., Newman, D., Lee, I., Xu, G., and Kurtz, I. (2000) Two C-terminal variants of NBC4, a new member of the sodium bicarbonate cotransporter family: cloning, characterization, and localization. *IUBMB life* **50**, 13-19
86. Pushkin, A., Abuladze, N., Newman, D., Lee, I., Xu, G., and Kurtz, I. (2000) Cloning, characterization and chromosomal assignment of NBC4, a new member of the sodium bicarbonate cotransporter family. *Biochim Biophys Acta* **1493**, 215-218
87. Groger, N., Vitzthum, H., Frohlich, H., Kruger, M., Ehmke, H., Braun, T., and Boettger, T. (2012) Targeted mutation of SLC4A5 induces arterial hypertension and renal metabolic acidosis. *Hum Mol Genet* **21**, 1025-1036
88. Kao, L., Kurtz, L. M., Shao, X., Papadopoulos, M. C., Liu, L., Bok, D., Nusinowitz, S., Chen, B., Stella, S. L., Andre, M., Weinreb, J., Luong, S. S., Piri, N., Kwong, J. M., Newman, D., and Kurtz, I. (2011) Severe neurologic impairment in mice with targeted disruption of the electrogenic sodium bicarbonate cotransporter NBCe2 (Slc4a5 gene). *The Journal of biological chemistry* **286**, 32563-32574
89. Cooper, D. S., Saxena, N. C., Yang, H. S., Lee, H. J., Moring, A. G., Lee, A., and Choi, I. (2005) Molecular and functional characterization of the electroneutral Na^+/HCO_3^- cotransporter NBCn1 in rat hippocampal neurons. *The Journal of biological chemistry* **280**, 17823-17830
90. Cooper, D. S., Lee, H. J., Yang, H. S., Kippen, J., Yun, C. C., and Choi, I. (2006) The electroneutral sodium/bicarbonate cotransporter containing an amino terminal 123-amino-acid cassette is expressed predominantly in the heart. *Journal of biomedical science* **13**, 593-595
91. Chen, L. M., Kelly, M. L., Parker, M. D., Bouyer, P., Gill, H. S., Felie, J. M., Davis, B. A., and Boron, W. F. (2008) Expression and localization of Na-driven Cl^-/HCO_3^- exchanger (SLC4A8) in rodent CNS. *Neuroscience* **153**, 162-174

92. Jacobs, S., Ruusuvuori, E., Sipila, S. T., Haapanen, A., Damkier, H. H., Kurth, I., Hentschke, M., Schweizer, M., Rudhard, Y., Laatikainen, L. M., Tyynela, J., Praetorius, J., Voipio, J., and Hubner, C. A. (2008) Mice with targeted Slc4a10 gene disruption have small brain ventricles and show reduced neuronal excitability. *Proceedings of the National Academy of Sciences of the United States of America* **105**, 311-316
93. Grichtchenko, II, Choi, I., Zhong, X., Bray-Ward, P., Russell, J. M., and Boron, W. F. (2001) Cloning, characterization, and chromosomal mapping of a human electroneutral Na^+- driven Cl^-/HCO_3^- exchanger. *The Journal of biological chemistry* **276**, 8358-8363
94. Chen, L. M., Haddad, G. G., and Boron, W. F. (2008) Effects of chronic continuous hypoxia on the expression of SLC4A8 (NDCBE) in neonatal versus adult mouse brain. *Brain research* **1238**, 85-92
95. Jacques, T., Picard, N., Miller, R. L., Riemondy, K. A., Houillier, P., Sohet, F., Ramakrishnan, S. K., Busst, C. J., Jayat, M., Corniere, N., Hassan, H., Aronson, P. S., Hennings, J. C., Hubner, C. A., Nelson, R. D., Chambrey, R., and Eladari, D. (2013) Overexpression of pendrin in intercalated cells produces chloride-sensitive hypertension. *J Am Soc Nephrol* **24**, 1104-1113
96. Leviel, F., Hubner, C. A., Houillier, P., Morla, L., El Moghrabi, S., Brideau, G., Hassan, H., Parker, M. D., Kurth, I., Kougioumtzes, A., Sinning, A., Pech, V., Riemondy, K. A., Miller, R. L., Hummler, E., Shull, G. E., Aronson, P. S., Doucet, A., Wall, S. M., Chambrey, R., and Eladari, D. (2010) The Na^+-dependent chloride-bicarbonate exchanger SLC4A8 mediates an electroneutral Na^+ reabsorption process in the renal cortical collecting ducts of mice. *J Clin Invest* **120**, 1627-1635
97. Alper, S. L., and Sharma, A. K. (2013) The SLC26 gene family of anion transporters and channels. *Molecular aspects of medicine* **34**, 494-515
98. Moseley, R. H., Hoglund, P., Wu, G. D., Silberg, D. G., Haila, S., de la Chapelle, A., Holmberg, C., and Kere, J. (1999) Downregulated in adenoma gene encodes a chloride transporter defective in congenital chloride diarrhea. *Am J Physiol* **276**, G185-192
99. Ohana, E., Yang, D., Shcheynikov, N., and Muallem, S. (2009) Diverse transport modes by the solute carrier 26 family of anion transporters. *The Journal of physiology* **587**, 2179-2185
100. Shcheynikov, N., Yang, D., Wang, Y., Zeng, W., Karniski, L. P., So, I., Wall, S. M., and Muallem, S. (2008) The Slc26a4 transporter functions as an electroneutral $Cl^-/I^-/HCO_3^-$ exchanger: role of Slc26a4 and Slc26a6 in I^- and HCO_3^- secretion and in regulation of CFTR in the parotid duct. *The Journal of physiology* **586**, 3813-3824
101. Aravind, L., and Koonin, E. V. (2000) The STAS domain - a link between anion transporters and antisigma-factor antagonists. *Curr Biol* **10**, R53-55
102. Ko, S. B., Zeng, W., Dorwart, M. R., Luo, X., Kim, K. H., Millen, L., Goto, H., Naruse, S., Soyombo, A., Thomas, P. J., and Muallem, S. (2004) Gating of CFTR by the STAS domain of SLC26 transporters. *Nat Cell Biol* **6**, 343-350

103. Alvarez, B. V., Vilas, G. L., and Casey, J. R. (2005) Metabolon disruption: a mechanism that regulates bicarbonate transport. *The EMBO journal* **24**, 2499-2511
104. Wedenoja, S., Pekansaari, E., Hoglund, P., Makela, S., Holmberg, C., and Kere, J. (2011) Update on SLC26A3 mutations in congenital chloride diarrhea. *Human mutation* **32**, 715-722
105. Scott, D. A., Wang, R., Kreman, T. M., Sheffield, V. C., and Karniski, L. P. (1999) The Pendred syndrome gene encodes a chloride-iodide transport protein. *Nature genetics* **21**, 440-443
106. Xu, J., Song, P., Nakamura, S., Miller, M., Barone, S., Alper, S. L., Riederer, B., Bonhagen, J., Arend, L. J., Amlal, H., Seidler, U., and Soleimani, M. (2009) Deletion of the chloride transporter slc26a7 causes distal renal tubular acidosis and impairs gastric acid secretion. *The Journal of biological chemistry* **284**, 29470-29479
107. Vincourt, J. B., Jullien, D., Kossida, S., Amalric, F., and Girard, J. P. (2002) Molecular cloning of SLC26A7, a novel member of the SLC26 sulfate/anion transporter family, from high endothelial venules and kidney. *Genomics* **79**, 249-256
108. Van Slyke, D. D. (1966) Some points of acid-base history in physiology and medicine. *Ann N Y Acad Sci* **133**, 5-14
109. Holmes, O. (1993) *Human acid-base physiology : a student text*, 1st ed., Chapman & Hall Medical, London ; New York
110. Lu, Y. S. (1985) [Arterial blood-gas and acid-base balance in hypertensive diseases of pregnancy: an analysis of 121 cases]. *Zhonghua fu chan ke za zhi* **20**, 215-217, 253
111. Garrett, R. H., and Grisham, C. M. (2000) Biochimie. *Annales de biologie clinique* **58**, 767-768
112. Pappas, C. A., and Koeppen, B. M. (1992) Electrophysiological properties of cultured outer medullary collecting duct cells. *Am J Physiol* **263**, F1004-1010
113. Alper, S. L. (2002) Genetic diseases of acid-base transporters. *Annu Rev Physiol* **64**, 899-923
114. Koeppen, B. M. (2009) The kidney and acid-base regulation. *Advances in physiology education* **33**, 275-281
115. Laing, C. M., Toye, A. M., Capasso, G., and Unwin, R. J. (2005) Renal tubular acidosis: developments in our understanding of the molecular basis. *The international journal of biochemistry & cell biology* **37**, 1151-1161
116. Lorenz, J. N., Schultheis, P. J., Traynor, T., Shull, G. E., and Schnermann, J. (1999) Micropuncture analysis of single-nephron function in NHE3-deficient mice. *Am J Physiol* **277**, F447-453
117. Lucci, M. S., Tinker, J. P., Weiner, I. M., and DuBose, T. D., Jr. (1983) Function of proximal tubule carbonic anhydrase defined by selective inhibition. *Am J Physiol* **245**, F443-449
118. Boron, W. F. (2006) Acid-base transport by the renal proximal tubule. *J Am Soc Nephrol* **17**, 2368-2382
119. Sly, W. S., and Hu, P. Y. (1995) Human carbonic anhydrases and carbonic anhydrase deficiencies. *Annual review of biochemistry* **64**, 375-401

120. Purkerson, J. M., Kittelberger, A. M., and Schwartz, G. J. (2007) Basolateral carbonic anhydrase IV in the proximal tubule is a glycosylphosphatidylinositol-anchored protein. *Kidney Int* **71**, 407-416
121. Purkerson, J. M., and Schwartz, G. J. (2007) The role of carbonic anhydrases in renal physiology. *Kidney Int* **71**, 103-115
122. Liu, F. Y., and Cogan, M. G. (1989) Angiotensin II stimulates early proximal bicarbonate absorption in the rat by decreasing cyclic adenosine monophosphate. *J Clin Invest* **84**, 83-91
123. Wang, T., and Chan, Y. L. (1990) Mechanism of angiotensin II action on proximal tubular transport. *The Journal of pharmacology and experimental therapeutics* **252**, 689-695
124. Capasso, G., Unwin, R., Rizzo, M., Pica, A., and Giebisch, G. (2002) Bicarbonate transport along the loop of Henle: molecular mechanisms and regulation. *Journal of nephrology* **15 Suppl 5**, S88-96
125. Capasso, G., Unwin, R., Ciani, F., De Santo, N. G., De Tommaso, G., Russo, F., and Giebisch, G. (1994) Bicarbonate transport along the loop of Henle. II. Effects of acid-base, dietary, and neurohumoral determinants. *J Clin Invest* **94**, 830-838
126. Capasso, G., Unwin, R., Ciani, F., De Tommaso, G., Vinciguerra, M., Russo, F., and De Santo, N. G. (1994) The effect of acute metabolic alkalosis on bicarbonate transport along the loop of Henle. The role of active transport processes and passive paracellular backflux. *Pflugers Arch* **429**, 44-49
127. Buerkert, J., Martin, D., Trigg, D., and Simon, E. (1983) Effect of reduced renal mass on ammonium handling and net acid formation by the superficial and juxtamedullary nephron of the rat. Evidence for impaired reentrapment rather than decreased production of ammonium in the acidosis of uremia. *J Clin Invest* **71**, 1661-1675
128. DuBose, T. D., Jr., Pucacco, L. R., Lucci, M. S., and Carter, N. W. (1979) Micropuncture determination of pH, PCO_2, and total CO_2 concentration in accessible structures of the rat renal cortex. *J Clin Invest* **64**, 476-482
129. Schwartz, G. J., Barasch, J., and Al-Awqati, Q. (1985) Plasticity of functional epithelial polarity. *Nature* **318**, 368-371
130. Wall, S. M., and Weinstein, A. M. (2013) Cortical distal nephron Cl^{-} transport in volume homeostasis and blood pressure regulation. *American journal of physiology. Renal physiology* **305**, F427-438
131. Kim, J. K., Kim, S. J., Kim, Y. C., So, I., and Kim, K. W. (1999) Influence of extracellular Na^{+} removal on cytosolic Ca_2^{+} concentration in smooth muscle cells of rabbit cerebral artery. *Journal of smooth muscle research = Nihon Heikatsukin Gakkai kikanshi* **35**, 135-145
132. Teng-umnuay, P., Verlander, J. W., Yuan, W., Tisher, C. C., and Madsen, K. M. (1996) Identification of distinct subpopulations of intercalated cells in the mouse collecting duct. *J Am Soc Nephrol* **7**, 260-274
133. Schuster, V. L., and Stokes, J. B. (1987) Chloride transport by the cortical and outer medullary collecting duct. *Am J Physiol* **253**, F203-212
134. Madsen, K. M., and Tisher, C. C. (1986) Structural-functional relationship along the distal nephron. *Am J Physiol* **250**, F1-15

135. Satlin, L. M. (1999) Regulation of potassium transport in the maturing kidney. *Seminars in nephrology* **19**, 155-165
136. Cordat, E., and Casey, J. R. (2009) Bicarbonate transport in cell physiology and disease. *The Biochemical journal* **417**, 423-439
137. Amlal, H., Petrovic, S., Xu, J., Wang, Z., Sun, X., Barone, S., and Soleimani, M. (2010) Deletion of the anion exchanger Slc26a4 (pendrin) decreases apical Cl^- /HCO_3^- exchanger activity and impairs bicarbonate secretion in kidney collecting duct. *American journal of physiology. Cell physiology* **299**, C33-41
138. Edwards, S. L. (2008) Pathophysiology of acid base balance: the theory practice relationship. *Intensive & critical care nursing : the official journal of the British Association of Critical Care Nurses* **24**, 28-38; quiz 38-40
139. Ring, T., Frische, S., and Nielsen, S. (2005) Clinical review: Renal tubular acidosis--a physicochemical approach. *Critical care* **9**, 573-580
140. Morris, R. C., Jr. (1969) Renal tubular acidosis. Mechanisms, classification and implications. *N Engl J Med* **281**, 1405-1413
141. Li, H. C., Szigligeti, P., Worrell, R. T., Matthews, J. B., Conforti, L., and Soleimani, M. (2005) Missense mutations in Na^+/HCO_3^- cotransporter NBC1 show abnormal trafficking in polarized kidney cells: a basis of proximal renal tubular acidosis. *American journal of physiology. Renal physiology* **289**, F61-71
142. Toye, A. M., Parker, M. D., Daly, C. M., Lu, J., Virkki, L. V., Pelletier, M. F., and Boron, W. F. (2006) The human NBCe1-A mutant R881C, associated with proximal renal tubular acidosis, retains function but is mistargeted in polarized renal epithelia. *American journal of physiology. Cell physiology* **291**, C788-801
143. Gawenis, L. R., Bradford, E. M., Prasad, V., Lorenz, J. N., Simpson, J. E., Clarke, L. L., Woo, A. L., Grisham, C., Sanford, L. P., Doetschman, T., Miller, M. L., and Shull, G. E. (2007) Colonic anion secretory defects and metabolic acidosis in mice lacking the NBC1 Na^+/HCO_3^- cotransporter. *The Journal of biological chemistry* **282**, 9042-9052
144. Everett, L. A., Glaser, B., Beck, J. C., Idol, J. R., Buchs, A., Heyman, M., Adawi, F., Hazani, E., Nassir, E., Baxevanis, A. D., Sheffield, V. C., and Green, E. D. (1997) Pendred syndrome is caused by mutations in a putative sulphate transporter gene (PDS). *Nature genetics* **17**, 411-422
145. Frische, S., Kwon, T. H., Frokiaer, J., Madsen, K. M., and Nielsen, S. (2003) Regulated expression of pendrin in rat kidney in response to chronic NH_4Cl or $NaHCO_3$ loading. *American journal of physiology. Renal physiology* **284**, F584-593
146. Dou, H., Finberg, K., Cardell, E. L., Lifton, R., and Choo, D. (2003) Mice lacking the B1 subunit of H+ -ATPase have normal hearing. *Hearing research* **180**, 76-84
147. Finberg, K. E., Wagner, C. A., Bailey, M. A., Paunescu, T. G., Breton, S., Brown, D., Giebisch, G., Geibel, J. P., and Lifton, R. P. (2005) The B1-subunit of the H^+ ATPase is required for maximal urinary acidification. *Proceedings of the National Academy of Sciences of the United States of America* **102**, 13616-13621
148. Hennings, J. C., Picard, N., Huebner, A. K., Stauber, T., Maier, H., Brown, D., Jentsch, T. J., Vargas-Poussou, R., Eladari, D., and Hubner, C. A. (2012) A mouse model for distal renal tubular acidosis reveals a previously unrecognized

role of the V-ATPase a4 subunit in the proximal tubule. *EMBO molecular medicine* **4**, 1057-1071
149. Norgett, E. E., Golder, Z. J., Lorente-Canovas, B., Ingham, N., Steel, K. P., and Karet Frankl, F. E. (2012) Atp6v0a4 knockout mouse is a model of distal renal tubular acidosis with hearing loss, with additional extrarenal phenotype. *Proceedings of the National Academy of Sciences of the United States of America* **109**, 13775-13780
150. Sun, X., and Petrovic, S. (2008) Increased acid load and deletion of AE1 increase Slc26a7 expression. *Nephron. Physiology* **109**, p29-35
151. Lewis, S. E., Erickson, R. P., Barnett, L. B., Venta, P. J., and Tashian, R. E. (1988) N-ethyl-N-nitrosourea-induced null mutation at the mouse Car-2 locus: an animal model for human carbonic anhydrase II deficiency syndrome. *Proceedings of the National Academy of Sciences of the United States of America* **85**, 1962-1966
152. Yoon, J. S., Park, H. J., Yoo, S. Y., Namkung, W., Jo, M. J., Koo, S. K., Park, H. Y., Lee, W. S., Kim, K. H., and Lee, M. G. (2008) Heterogeneity in the processing defect of SLC26A4 mutants. *J Med Genet* **45**, 411-419
153. Shayakul, C., and Alper, S. L. (2000) Inherited renal tubular acidosis. *Current opinion in nephrology and hypertension* **9**, 541-546
154. Morris, R. C., Jr., and Sebastian, A. (2002) Alkali therapy in renal tubular acidosis: who needs it? *J Am Soc Nephrol* **13**, 2186-2188
155. Buckalew, V. M., Jr. (1989) Nephrolithiasis in renal tubular acidosis. *The Journal of urology* **141**, 731-737
156. Cordat, E., and Reithmeier, R. A. (2006) Expression and interaction of two compound heterozygous distal renal tubular acidosis mutants of kidney anion exchanger 1 in epithelial cells. *American journal of physiology. Renal physiology* **291**, F1354-1361
157. Wrong, O. M., Feest, T. G., and MacIver, A. G. (1993) Immune-related potassium-losing interstitial nephritis: a comparison with distal renal tubular acidosis. *The Quarterly journal of medicine* **86**, 513-534
158. Cordat, E., Kittanakom, S., Yenchitsomanus, P. T., Li, J., Du, K., Lukacs, G. L., and Reithmeier, R. A. (2006) Dominant and recessive distal renal tubular acidosis mutations of kidney anion exchanger 1 induce distinct trafficking defects in MDCK cells. *Traffic* **7**, 117-128
159. Toye, A. M., Banting, G., and Tanner, M. J. (2004) Regions of human kidney anion exchanger 1 (kAE1) required for basolateral targeting of kAE1 in polarised kidney cells: mis-targeting explains dominant renal tubular acidosis (dRTA). *Journal of cell science* **117**, 1399-1410
160. Devonald, M. A., Smith, A. N., Poon, J. P., Ihrke, G., and Karet, F. E. (2003) Non-polarized targeting of AE1 causes autosomal dominant distal renal tubular acidosis. *Nature genetics* **33**, 125-127
161. Jarolim, P., Rubin, H. L., Liu, S. C., Cho, M. R., Brabec, V., Derick, L. H., Yi, S. J., Saad, S. T., Alper, S., Brugnara, C., and et al. (1994) Duplication of 10 nucleotides in the erythroid band 3 (AE1) gene in a kindred with hereditary spherocytosis and band 3 protein deficiency (band 3PRAGUE). *J Clin Invest* **93**, 121-130

162. Toye, A. M., Bruce, L. J., Unwin, R. J., Wrong, O., and Tanner, M. J. (2002) Band 3 Walton, a C-terminal deletion associated with distal renal tubular acidosis, is expressed in the red cell membrane but retained internally in kidney cells. *Blood* **99**, 342-347.
163. Toye, A. M., Williamson, R. C., Khanfar, M., Bader-Meunier, B., Cynober, T., Thibault, M., Tchernia, G., Dechaux, M., Delaunay, J., and Bruce, L. J. (2008) Band 3 Courcouronnes (Ser667Phe): a trafficking mutant differentially rescued by wild-type band 3 and glycophorin A. *Blood* **111**, 5380-5389
164. Fry, A. C., Su, Y., Yiu, V., Cuthbert, A. W., Trachtman, H., and Karet Frankl, F. E. (2012) Mutation conferring apical-targeting motif on AE1 exchanger causes autosomal dominant distal RTA. *J Am Soc Nephrol* **23**, 1238-1249
165. Folsch, H., Ohno, H., Bonifacino, J. S., and Mellman, I. (1999) A novel clathrin adaptor complex mediates basolateral targeting in polarized epithelial cells. *Cell* **99**, 189-198
166. Ohno, H., Tomemori, T., Nakatsu, F., Okazaki, Y., Aguilar, R. C., Foelsch, H., Mellman, I., Saito, T., Shirasawa, T., and Bonifacino, J. S. (1999) Mu1B, a novel adaptor medium chain expressed in polarized epithelial cells. *FEBS letters* **449**, 215-220
167. Cheidde, L., Vieira, T. C., Lima, P. R., Saad, S. T., and Heilberg, I. P. (2003) A novel mutation in the anion exchanger 1 gene is associated with familial distal renal tubular acidosis and nephrocalcinosis. *Pediatrics* **112**, 1361-1367
168. Shao, L., Xu, Y., Dong, Q., Lang, Y., Yue, S., and Miao, Z. (2010) A novel SLC4A1 variant in an autosomal dominant distal renal tubular acidosis family with a severe phenotype. *Endocrine* **37**, 473-478
169. Zhang, Z., Liu, K. X., He, J. W., Fu, W. Z., Yue, H., Zhang, H., Zhang, C. Q., and Zhang, Z. L. (2012) Identification of two novel mutations in the SLC4A1 gene in two unrelated Chinese families with distal renal tubular acidosis. *Archives of medical research* **43**, 298-304
170. Sawasdee, N., Junking, M., Ngaojanlar, P., Sukomon, N., Ungsupravate, D., Limjindaporn, T., Akkarapatumwong, V., Noisakran, S., and Yenchitsomanus, P. T. (2010) Human kidney anion exchanger 1 interacts with adaptor-related protein complex 1 mu1A (AP-1 mu1A). *Biochemical and biophysical research communications*
171. Wagner, C. A., Finberg, K. E., Breton, S., Marshansky, V., Brown, D., and Geibel, J. P. (2004) Renal vacuolar H+-ATPase. *Physiological reviews* **84**, 1263-1314
172. Paunescu, T. G., Russo, L. M., Da Silva, N., Kovacikova, J., Mohebbi, N., Van Hoek, A. N., McKee, M., Wagner, C. A., Breton, S., and Brown, D. (2007) Compensatory membrane expression of the V-ATPase B2 subunit isoform in renal medullary intercalated cells of B1-deficient mice. *American journal of physiology. Renal physiology* **293**, F1915-1926
173. Vainsel, M., Fondu, P., Cadranel, S., Rocmans, C., and Gepts, W. (1972) Osteopetrosis associated with proximal and distal tubular acidosis. *Acta paediatrica Scandinavica* **61**, 429-434
174. Whyte, M. P., Murphy, W. A., Fallon, M. D., Sly, W. S., Teitelbaum, S. L., McAlister, W. H., and Avioli, L. V. (1980) Osteopetrosis, renal tubular acidosis

and basal ganglia calcification in three sisters. *The American journal of medicine* **69**, 64-74

175. Cancino, J., Torrealba, C., Soza, A., Yuseff, M. I., Gravotta, D., Henklein, P., Rodriguez-Boulan, E., and Gonzalez, A. (2007) Antibody to AP1B adaptor blocks biosynthetic and recycling routes of basolateral proteins at recycling endosomes. *Molecular biology of the cell* **18**, 4872-4884
176. Matlin, K. S., and Simons, K. (1984) Sorting of an apical plasma membrane glycoprotein occurs before it reaches the cell surface in cultured epithelial cells. *J Cell Biol* **99**, 2131-2139
177. Bartles, J. R., Feracci, H. M., Stieger, B., and Hubbard, A. L. (1987) Biogenesis of the rat hepatocyte plasma membrane in vivo: comparison of the pathways taken by apical and basolateral proteins using subcellular fractionation. *J Cell Biol* **105**, 1241-1251
178. Le Bivic, A., Quaroni, A., Nichols, B., and Rodriguez-Boulan, E. (1990) Biogenetic pathways of plasma membrane proteins in Caco-2, a human intestinal epithelial cell line. *J Cell Biol* **111**, 1351-1361
179. Scheiffele, P., Peranen, J., and Simons, K. (1995) N-glycans as apical sorting signals in epithelial cells. *Nature* **378**, 96-98
180. Yeaman, C., Le Gall, A. H., Baldwin, A. N., Monlauzeur, L., Le Bivic, A., and Rodriguez-Boulan, E. (1997) The O-glycosylated stalk domain is required for apical sorting of neurotrophin receptors in polarized MDCK cells. *The Journal of cell biology* **139**, 929-940
181. Lisanti, M. P., Sargiacomo, M., Graeve, L., Saltiel, A. R., and Rodriguez-Boulan, E. (1988) Polarized apical distribution of glycosyl-phosphatidylinositol-anchored proteins in a renal epithelial cell line. *Proceedings of the National Academy of Sciences of the United States of America* **85**, 9557-9561
182. Rodriguez-Boulan, E., and Gonzalez, A. (1999) Glycans in post-Golgi apical targeting: sorting signals or structural props? *Trends in cell biology* **9**, 291-294
183. Caplan, M. J., Anderson, H. C., Palade, G. E., and Jamieson, J. D. (1988) Sorting of newly synthesized Na^+/K^+-ATPase in polarized epithelial cells. *Prog Clin Biol Res* **268B**, 51-58
184. Deora, A. A., Gravotta, D., Kreitzer, G., Hu, J., Bok, D., and Rodriguez-Boulan, E. (2004) The basolateral targeting signal of CD147 (EMMPRIN) consists of a single leucine and is not recognized by retinal pigment epithelium. *Molecular biology of the cell* **15**, 4148-4165
185. Gonzalez, A., and Rodriguez-Boulan, E. (2009) Clathrin and AP1B: key roles in basolateral trafficking through trans-endosomal routes. *FEBS letters* **583**, 3784-3795
186. Gephart, J. D., Singh, B., Higginbotham, J. N., Franklin, J. L., Gonzalez, A., Folsch, H., and Coffey, R. J. (2011) Identification of a novel mono-leucine basolateral sorting motif within the cytoplasmic domain of amphiregulin. *Traffic* **12**, 1793-1804
187. Trombetta, E. S. (2003) The contribution of N-glycans and their processing in the endoplasmic reticulum to glycoprotein biosynthesis. *Glycobiology* **13**, 77R-91R

188. Spiro, R. G. (2002) Protein glycosylation: nature, distribution, enzymatic formation, and disease implications of glycopeptide bonds. *Glycobiology* **12**, 43R-56R
189. Nakatsu, F., and Ohno, H. (2003) Adaptor protein complexes as the key regulators of protein sorting in the post-Golgi network. *Cell structure and function* **28**, 419-429
190. Hirst, J., Irving, C., and Borner, G. H. (2013) Adaptor protein complexes AP-4 and AP-5: new players in endosomal trafficking and progressive spastic paraplegia. *Traffic* **14**, 153-164
191. Lam, S. K., Tse, Y. C., Robinson, D. G., and Jiang, L. (2007) Tracking down the elusive early endosome. *Trends in plant science* **12**, 497-505
192. Lam, S. K., Cai, Y., Tse, Y. C., Wang, J., Law, A. H., Pimpl, P., Chan, H. Y., Xia, J., and Jiang, L. (2009) BFA-induced compartments from the Golgi apparatus and trans-Golgi network/early endosome are distinct in plant cells. *The Plant journal : for cell and molecular biology* **60**, 865-881
193. Doherty, G. J., and McMahon, H. T. (2009) Mechanisms of endocytosis. *Annu Rev Biochem* **78**, 857-902
194. Konopka, C. A., Schleede, J. B., Skop, A. R., and Bednarek, S. Y. (2006) Dynamin and cytokinesis. *Traffic* **7**, 239-247
195. Konopka, C. A., Backues, S. K., and Bednarek, S. Y. (2008) Dynamics of Arabidopsis dynamin-related protein 1C and a clathrin light chain at the plasma membrane. *The Plant cell* **20**, 1363-1380
196. Takei, K., and Haucke, V. (2001) Clathrin-mediated endocytosis: membrane factors pull the trigger. *Trends in cell biology* **11**, 385-391
197. Rodriguez-Boulan, E., and Macara, I. G. (2014) Organization and execution of the epithelial polarity programme. *Nature reviews. Molecular cell biology* **15**, 225-242
198. Bonifacino, J. S. (2014) Adaptor proteins involved in polarized sorting. *The Journal of cell biology* **204**, 7-17
199. Bryant, D. M., and Mostov, K. E. (2008) From cells to organs: building polarized tissue. *Nature reviews. Molecular cell biology* **9**, 887-901
200. Robinson, M. S. (1997) Coats and vesicle budding. *Trends in cell biology* **7**, 99-102
201. Boehm, M., and Bonifacino, J. S. (2001) Adaptins: the final recount. *Molecular biology of the cell* **12**, 2907-2920
202. Hirst, J., Barlow, L. D., Francisco, G. C., Sahlender, D. A., Seaman, M. N., Dacks, J. B., and Robinson, M. S. (2011) The fifth adaptor protein complex. *PLoS biology* **9**, e1001170
203. Collins, B. M., McCoy, A. J., Kent, H. M., Evans, P. R., and Owen, D. J. (2002) Molecular architecture and functional model of the endocytic AP2 complex. *Cell* **109**, 523-535
204. Dell'Angelica, E. C., Klumperman, J., Stoorvogel, W., and Bonifacino, J. S. (1998) Association of the AP-3 adaptor complex with clathrin. *Science* **280**, 431-434
205. Kirchhausen, T. (2002) Clathrin adaptors really adapt. *Cell* **109**, 413-416

206. Gravotta, D., Carvajal-Gonzalez, J. M., Mattera, R., Deborde, S., Banfelder, J. R., Bonifacino, J. S., and Rodriguez-Boulan, E. (2012) The clathrin adaptor AP-1A mediates basolateral polarity. *Developmental cell* **22**, 811-823
207. Ren, X., Farias, G. G., Canagarajah, B. J., Bonifacino, J. S., and Hurley, J. H. (2013) Structural basis for recruitment and activation of the AP-1 clathrin adaptor complex by Arf1. *Cell* **152**, 755-767
208. Wang, Y. J., Wang, J., Sun, H. Q., Martinez, M., Sun, Y. X., Macia, E., Kirchhausen, T., Albanesi, J. P., Roth, M. G., and Yin, H. L. (2003) Phosphatidylinositol 4 phosphate regulates targeting of clathrin adaptor AP-1 complexes to the Golgi. *Cell* **114**, 299-310
209. Fields, I. C., King, S. M., Shteyn, E., Kang, R. S., and Folsch, H. (2010) Phosphatidylinositol 3,4,5-trisphosphate localization in recycling endosomes is necessary for AP-1B-dependent sorting in polarized epithelial cells. *Molecular biology of the cell* **21**, 95-105
210. Shteyn, E., Pigati, L., and Folsch, H. (2011) Arf6 regulates AP-1B-dependent sorting in polarized epithelial cells. *The Journal of cell biology* **194**, 873-887
211. Mattera, R., Boehm, M., Chaudhuri, R., Prabhu, Y., and Bonifacino, J. S. (2011) Conservation and diversification of dileucine signal recognition by adaptor protein (AP) complex variants. *The Journal of biological chemistry* **286**, 2022-2030
212. Bonifacino, J. S., and Traub, L. M. (2003) Signals for Sorting of Transmembrane Proteins to Endosomes and Lysosomes. *Annual review of biochemistry*
213. Bonifacino, J. S., and Dell'Angelica, E. C. (1999) Molecular bases for the recognition of tyrosine-based sorting signals. *The Journal of cell biology* **145**, 923-926
214. Fields, I. C., King, S. M., Shteyn, E., Kang, R. S., and Folsch, H. Phosphatidylinositol 3,4,5-trisphosphate localization in recycling endosomes is necessary for AP-1B-dependent sorting in polarized epithelial cells. *Mol Biol Cell* **21**, 95-105
215. Almomani, E. Y., King, J. C., Netsawang, J., Yenchitsomanus, P. T., Malasit, P., Limjindaporn, T., Alexander, R. T., and Cordat, E. (2012) Adaptor protein 1 complexes regulate intracellular trafficking of the kidney anion exchanger 1 in epithelial cells. *American journal of physiology. Cell physiology* **303**, C554-566
216. Gravotta, D., Deora, A., Perret, E., Oyanadel, C., Soza, A., Schreiner, R., Gonzalez, A., and Rodriguez-Boulan, E. (2007) AP1B sorts basolateral proteins in recycling and biosynthetic routes of MDCK cells. *Proceedings of the National Academy of Sciences of the United States of America* **104**, 1564-1569
217. Schreiner, R., Frindt, G., Diaz, F., Carvajal-Gonzalez, J. M., Perez Bay, A. E., Palmer, L. G., Marshansky, V., Brown, D., Philp, N. J., and Rodriguez-Boulan, E. (2010) The absence of a clathrin adapter confers unique polarity essential to proximal tubule function. *Kidney Int* **78**, 382-388
218. Diaz, F., Gravotta, D., Deora, A., Schreiner, R., Schoggins, J., Falck-Pedersen, E., and Rodriguez-Boulan, E. (2009) Clathrin adaptor AP1B controls adenovirus infectivity of epithelial cells. *Proceedings of the National Academy of Sciences of the United States of America* **106**, 11143-11148

219. Folsch, H., Pypaert, M., Schu, P., and Mellman, I. (2001) Distribution and function of AP-1 clathrin adaptor complexes in polarized epithelial cells. *J Cell Biol* **152**, 595-606
220. Shim, J., Sternberg, P. W., and Lee, J. (2000) Distinct and redundant functions of mu1 medium chains of the AP-1 clathrin-associated protein complex in the nematode Caenorhabditis elegans. *Molecular biology of the cell* **11**, 2743-2756
221. Shafaq-Zadah, M., Brocard, L., Solari, F., and Michaux, G. (2012) AP-1 is required for the maintenance of apico-basal polarity in the C. elegans intestine. *Development* **139**, 2061-2070
222. O'Connor-Giles, K. M., and Skeath, J. B. (2003) Numb inhibits membrane localization of Sanpodo, a four-pass transmembrane protein, to promote asymmetric divisions in Drosophila. *Developmental cell* **5**, 231-243
223. Benhra, N., Lallet, S., Cotton, M., Le Bras, S., Dussert, A., and Le Borgne, R. (2011) AP-1 controls the trafficking of Notch and Sanpodo toward E-cadherin junctions in sensory organ precursors. *Curr Biol* **21**, 87-95
224. Zizioli, D., Forlanelli, E., Guarienti, M., Nicoli, S., Fanzani, A., Bresciani, R., Borsani, G., Preti, A., Cotelli, F., and Schu, P. (2010) Characterization of the AP-1 mu1A and mu1B adaptins in zebrafish (Danio rerio). *Developmental dynamics : an official publication of the American Association of Anatomists* **239**, 2404-2412
225. Gariano, G., Guarienti, M., Bresciani, R., Borsani, G., Carola, G., Monti, E., Giuliani, R., Rezzani, R., Bonomini, F., Preti, A., Schu, P., and Zizioli, D. (2014) Analysis of three mu1-AP1 subunits during zebrafish development. *Developmental dynamics : an official publication of the American Association of Anatomists* **243**, 299-314
226. Baltes, J., Larsen, J. V., Radhakrishnan, K., Geumann, C., Kratzke, M., Petersen, C. M., and Schu, P. (2014) sigma1B adaptin regulates adipogenesis by mediating the sorting of sortilin in adipose tissue. *Journal of cell science* **127**, 3477-3487
227. Zizioli, D., Meyer, C., Guhde, G., Saftig, P., von Figura, K., and Schu, P. (1999) Early embryonic death of mice deficient in gamma-adaptin. *The Journal of biological chemistry* **274**, 5385-5390
228. Meyer, C., Zizioli, D., Lausmann, S., Eskelinen, E. L., Hamann, J., Saftig, P., von Figura, K., and Schu, P. (2000) mu1A-adaptin-deficient mice: lethality, loss of AP-1 binding and rerouting of mannose 6-phosphate receptors. *The EMBO journal* **19**, 2193-2203
229. Hase, K., Nakatsu, F., Ohmae, M., Sugihara, K., Shioda, N., Takahashi, D., Obata, Y., Furusawa, Y., Fujimura, Y., Yamashita, T., Fukuda, S., Okamoto, H., Asano, M., Yonemura, S., and Ohno, H. (2013) AP-1B-mediated protein sorting regulates polarity and proliferation of intestinal epithelial cells in mice. *Gastroenterology* **145**, 625-635
230. Folsch, H. (2005) The building blocks for basolateral vesicles in polarized epithelial cells. *Trends in cell biology* **15**, 222-228
231. Takahashi, D., Hase, K., Kimura, S., Nakatsu, F., Ohmae, M., Mandai, Y., Sato, T., Date, Y., Ebisawa, M., Kato, T., Obata, Y., Fukuda, S., Kawamura, Y. I., Dohi, T., Katsuno, T., Yokosuka, O., Waguri, S., and Ohno, H. (2011) The epithelia-specific membrane trafficking factor AP-1B controls gut immune homeostasis in mice. *Gastroenterology* **141**, 621-632

232. Owen, D. J., Collins, B. M., and Evans, P. R. (2004) Adaptors for clathrin coats: structure and function. *Annu Rev Cell Dev Biol* **20**, 153-191
233. Traub, L. M. (2005) Common principles in clathrin-mediated sorting at the Golgi and the plasma membrane. *Biochim Biophys Acta* **1744**, 415-437
234. Gaidarov, I., and Keen, J. H. (1999) Phosphoinositide-AP-2 interactions required for targeting to plasma membrane clathrin-coated pits. *The Journal of cell biology* **146**, 755-764
235. Keyel, P. A., Thieman, J. R., Roth, R., Erkan, E., Everett, E. T., Watkins, S. C., Heuser, J. E., and Traub, L. M. (2008) The AP-2 adaptor beta2 appendage scaffolds alternate cargo endocytosis. *Molecular biology of the cell* **19**, 5309-5326
236. Kelly, B. T., McCoy, A. J., Spate, K., Miller, S. E., Evans, P. R., Honing, S., and Owen, D. J. (2008) A structural explanation for the binding of endocytic dileucine motifs by the AP2 complex. *Nature* **456**, 976-979
237. Ohno, H., Stewart, J., Fournier, M. C., Bosshart, H., Rhee, I., Miyatake, S., Saito, T., Gallusser, A., Kirchhausen, T., and Bonifacino, J. S. (1995) Interaction of tyrosine-based sorting signals with clathrin-associated proteins. *Science* **269**, 1872-1875
238. Ohno, H. (2006) Physiological roles of clathrin adaptor AP complexes: lessons from mutant animals. *J Biochem* **139**, 943-948
239. Mitsunari, T., Nakatsu, F., Shioda, N., Love, P. E., Grinberg, A., Bonifacino, J. S., and Ohno, H. (2005) Clathrin adaptor AP-2 is essential for early embryonal development. *Mol Cell Biol* **25**, 9318-9323
240. Ohno, H. (2006) Clathrin-associated adaptor protein complexes. *J Cell Sci* **119**, 3719-3721
241. Blumstein, J., Faundez, V., Nakatsu, F., Saito, T., Ohno, H., and Kelly, R. B. (2001) The neuronal form of adaptor protein-3 is required for synaptic vesicle formation from endosomes. *The Journal of neuroscience : the official journal of the Society for Neuroscience* **21**, 8034-8042
242. Matsuda, S., Miura, E., Matsuda, K., Kakegawa, W., Kohda, K., Watanabe, M., and Yuzaki, M. (2008) Accumulation of AMPA receptors in autophagosomes in neuronal axons lacking adaptor protein AP-4. *Neuron* **57**, 730-745
243. White, J. K., Gerdin, A. K., Karp, N. A., Ryder, E., Buljan, M., Bussell, J. N., Salisbury, J., Clare, S., Ingham, N. J., Podrini, C., Houghton, R., Estabel, J., Bottomley, J. R., Melvin, D. G., Sunter, D., Adams, N. C., Sanger Institute Mouse Genetics, P., Tannahill, D., Logan, D. W., Macarthur, D. G., Flint, J., Mahajan, V. B., Tsang, S. H., Smyth, I., Watt, F. M., Skarnes, W. C., Dougan, G., Adams, D. J., Ramirez-Solis, R., Bradley, A., and Steel, K. P. (2013) Genome-wide generation and systematic phenotyping of knockout mice reveals new roles for many genes. *Cell* **154**, 452-464
244. Nakatsu, F., Hase, K., and Ohno, H. (2014) The Role of the Clathrin Adaptor AP-1: Polarized Sorting and Beyond. *Membranes* **4**, 747-763
245. Junking, M., Sawasdee, N., Duangtum, N., Cheunsuchon, B., Limjindaporn, T., and Yenchitsomanus, P. T. (2014) Role of adaptor proteins and clathrin in the trafficking of human kidney anion exchanger 1 (kAE1) to the cell surface. *Traffic* **15**, 788-802

246. Cordat, E., Li, J., and Reithmeier, R. A. (2003) Carboxyl-terminal truncations of human anion exchanger impair its trafficking to the plasma membrane. *Traffic* **4**, 642-651
247. Cordat, E. (2006) Unraveling trafficking of the kidney anion exchanger 1 in polarized MDCK epithelial cells. *Biochemistry and cell biology = Biochimie et biologie cellulaire* **84**, 949-959
248. Los, G. V., Encell, L. P., McDougall, M. G., Hartzell, D. D., Karassina, N., Zimprich, C., Wood, M. G., Learish, R., Ohana, R. F., Urh, M., Simpson, D., Mendez, J., Zimmerman, K., Otto, P., Vidugiris, G., Zhu, J., Darzins, A., Klaubert, D. H., Bulleit, R. F., and Wood, K. V. (2008) HaloTag: a novel protein labeling technology for cell imaging and protein analysis. *ACS chemical biology* **3**, 373-382
249. Los, G. V., and Wood, K. (2007) The HaloTag: a novel technology for cell imaging and protein analysis. *Methods Mol Biol* **356**, 195-208
250. Pimplikar, S. W., and Reithmeier, R. A. (1986) Affinity chromatography of Band 3, the anion transport protein of erythrocyte membranes. *The Journal of biological chemistry* **261**, 9770-9778
251. Beckmann, R., Smythe, J. S., Anstee, D. J., and Tanner, M. J. (1998) Functional cell surface expression of band 3, the human red blood cell anion exchange protein (AE1), in K562 erythroleukemia cells: band 3 enhances the cell surface reactivity of Rh antigens. *Blood* **92**, 4428-4438
252. Huybrechts, S. J., Van Veldhoven, P. P., Brees, C., Mannaerts, G. P., Los, G. V., and Fransen, M. (2009) Peroxisome dynamics in cultured mammalian cells. *Traffic* **10**, 1722-1733
253. Straszewski-Chavez, S. L., Visintin, I. P., Karassina, N., Los, G., Liston, P., Halaban, R., Fadiel, A., and Mor, G. (2007) XAF1 mediates tumor necrosis factor-alpha-induced apoptosis and X-linked inhibitor of apoptosis cleavage by acting through the mitochondrial pathway. *The Journal of biological chemistry* **282**, 13059-13072
254. Svendsen, S., Zimprich, C., McDougall, M. G., Klaubert, D. H., and Los, G. V. (2008) Spatial separation and bidirectional trafficking of proteins using a multi-functional reporter. *BMC cell biology* **9**, 17
255. Beckmann, R., Toye, A. M., Smythe, J. S., Anstee, D. J., and Tanner, M. J. (2002) An N-terminal GFP tag does not alter the functional expression to the plasma membrane of red cell and kidney anion exchanger (AE1) in mammalian cells. *Mol Membr Biol* **19**, 187-200
256. Ang, A. L., Taguchi, T., Francis, S., Folsch, H., Murrells, L. J., Pypaert, M., Warren, G., and Mellman, I. (2004) Recycling endosomes can serve as intermediates during transport from the Golgi to the plasma membrane of MDCK cells. *J Cell Biol* **167**, 531-543
257. Fields, I. C., Shteyn, E., Pypaert, M., Proux-Gillardeaux, V., Kang, R. S., Galli, T., and Folsch, H. (2007) v-SNARE cellubrevin is required for basolateral sorting of AP-1B-dependent cargo in polarized epithelial cells. *The Journal of cell biology* **177**, 477-488
258. Hirst, J., and Robinson, M. S. (1998) Clathrin and adaptors. *Biochim Biophys Acta* **1404**, 173-193.

259. Glickman, J. N., Conibear, E., and Pearse, B. M. (1989) Specificity of binding of clathrin adaptors to signals on the mannose-6-phosphate/insulin-like growth factor II receptor. *The EMBO journal* **8**, 1041-1047
260. Christensen, B. M., Kim, Y. H., Kwon, T. H., and Nielsen, S. (2006) Lithium treatment induces a marked proliferation of primarily principal cells in rat kidney inner medullary collecting duct. *American journal of physiology. Renal physiology* **291**, F39-48
261. Farr, G. A., Hull, M., Mellman, I., and Caplan, M. J. (2009) Membrane proteins follow multiple pathways to the basolateral cell surface in polarized epithelial cells. *The Journal of cell biology* **186**, 269-282
262. Simmen, T., Honing, S., Icking, A., Tikkanen, R., and Hunziker, W. (2002) AP-4 binds basolateral signals and participates in basolateral sorting in epithelial MDCK cells. *Nat Cell Biol* **4**, 154-159
263. Folsch, H., Pypaert, M., Maday, S., Pelletier, L., and Mellman, I. (2003) The AP-1A and AP-1B clathrin adaptor complexes define biochemically and functionally distinct membrane domains. *The Journal of cell biology* **163**, 351-362
264. Owen, D. J., and Evans, P. R. (1998) A structural explanation for the recognition of tyrosine-based endocytotic signals. *Science* **282**, 1327-1332
265. Carvajal-Gonzalez, J. M., Gravotta, D., Mattera, R., Diaz, F., Perez Bay, A., Roman, A. C., Schreiner, R. P., Thuenauer, R., Bonifacino, J. S., and Rodriguez-Boulan, E. (2012) Basolateral sorting of the coxsackie and adenovirus receptor through interaction of a canonical YXX{Phi} motif with the clathrin adaptors AP-1A and AP-1B. *Proc Natl Acad Sci U S A* **109**, 3820-3825
266. Eskelinen, E. L., Meyer, C., Ohno, H., von Figura, K., and Schu, P. (2002) The polarized epithelia-specific mu 1B-adaptin complements mu 1A-deficiency in fibroblasts. *EMBO reports* **3**, 471-477
267. Wu, F., Saleem, M. A., Kampik, N. B., Satchwell, T. J., Williamson, R. C., Blattner, S. M., Ni, L., Toth, T., White, G., Young, M. T., Parker, M. D., Alper, S. L., Wagner, C. A., and Toye, A. M. (2010) Anion exchanger 1 interacts with nephrin in podocytes. *J Am Soc Nephrol* **21**, 1456-1467
268. Karet, F. E., Gainza, F. J., Gyory, A. Z., Unwin, R. J., Wrong, O., Tanner, M. J., Nayir, A., Alpay, H., Santos, F., Hulton, S. A., Bakkaloglu, A., Ozen, S., Cunningham, M. J., di Pietro, A., Walker, W. G., and Lifton, R. P. (1998) Mutations in the chloride-bicarbonate exchanger gene AE1 cause autosomal dominant but not autosomal recessive distal renal tubular acidosis. *Proceedings of the National Academy of Sciences of the United States of America* **95**, 6337-6342
269. Alper, S. L. (2010) Familial renal tubular acidosis. *Journal of nephrology* **23 Suppl 16**, S57-76
270. Fry, A. C., Su, Y., Yiu, V., Cuthbert, A. W., Trachtman, H., and Frankl, F. E. (2012) Mutation Conferring Apical-Targeting Motif on AE1 Exchanger Causes Autosomal Dominant Distal RTA. *J Am Soc Nephrol*
271. Vince, J. W., Carlsson, U., and Reithmeier, R. A. (2000) Localization of the Cl^- /HCO_3^- anion exchanger binding site to the amino- terminal region of carbonic anhydrase II. *Biochemistry* **39**, 13344-13349.

272. Vince, J. W., and Reithmeier, R. A. (2000) Identification of the carbonic anhydrase II binding site in the Cl^-/HCO_3^- anion exchanger AE1. *Biochemistry* **39**, 5527-5533
273. Su, Y., Al-Lamki, R. S., Blake-Palmer, K. G., Best, A., Golder, Z. J., Zhou, A., and Karet Frankl, F. E. (2014) Physical and Functional Links between Anion Exchanger-1 and Sodium Pump. *J Am Soc Nephrol*
274. Robinson, M. S. (2004) Adaptable adaptors for coated vesicles. *Trends in cell biology* **14**, 167-174
275. Ohno, H., Fournier, M. C., Poy, G., and Bonifacino, J. S. (1996) Structural determinants of interaction of tyrosine-based sorting signals with the adaptor medium chains. *The Journal of biological chemistry* **271**, 29009-29015
276. Gan, Y., McGraw, T. E., and Rodriguez-Boulan, E. (2002) The epithelial-specific adaptor AP1B mediates post-endocytic recycling to the basolateral membrane. *Nat Cell Biol* **4**, 605-609
277. Schauble, N., Lang, S., Jung, M., Cappel, S., Schorr, S., Ulucan, O., Linxweiler, J., Dudek, J., Blum, R., Helms, V., Paton, A. W., Paton, J. C., Cavalie, A., and Zimmermann, R. (2012) BiP-mediated closing of the Sec61 channel limits $Ca2^+$ leakage from the ER. *EMBO J* **31**, 3282-3296
278. Sevier, C. S., Weisz, O. A., Davis, M., and Machamer, C. E. (2000) Efficient export of the vesicular stomatitis virus G protein from the endoplasmic reticulum requires a signal in the cytoplasmic tail that includes both tyrosine-based and di-acidic motifs. *Molecular biology of the cell* **11**, 13-22
279. Sundqvist, A., Zieba, A., Vasilaki, E., Herrera Hidalgo, C., Soderberg, O., Koinuma, D., Miyazono, K., Heldin, C. H., Landegren, U., Ten Dijke, P., and van Dam, H. (2013) Specific interactions between Smad proteins and AP-1 components determine TGFbeta-induced breast cancer cell invasion. *Oncogene* **32**, 3606-3615
280. Soderberg, O., Gullberg, M., Jarvius, M., Ridderstrale, K., Leuchowius, K. J., Jarvius, J., Wester, K., Hydbring, P., Bahram, F., Larsson, L. G., and Landegren, U. (2006) Direct observation of individual endogenous protein complexes in situ by proximity ligation. *Nature methods* **3**, 995-1000
281. Patterson, S. T., and Reithmeier, R. A. (2010) Cell surface rescue of kidney anion exchanger 1 mutants by disruption of chaperone interactions. *J Biol Chem* **285**, 33423-33434
282. Ang, S. L., and Rossant, J. (1994) HNF-3 beta is essential for node and notochord formation in mouse development. *Cell* **78**, 561-574
283. Duffield, A., Folsch, H., Mellman, I., and Caplan, M. J. (2004) Sorting of H,K-ATPase beta-subunit in MDCK and LLC-PK cells is independent of mu 1B adaptin expression. *Traffic* **5**, 449-461
284. Conner, S. D., and Schmid, S. L. (2003) Regulated portals of entry into the cell. *Nature* **422**, 37-44
285. Macia, E., Ehrlich, M., Massol, R., Boucrot, E., Brunner, C., and Kirchhausen, T. (2006) Dynasore, a cell-permeable inhibitor of dynamin. *Developmental cell* **10**, 839-850
286. Mayor, S., and Pagano, R. E. (2007) Pathways of clathrin-independent endocytosis. *Nature reviews. Molecular cell biology* **8**, 603-612

287. Sandvig, K., Torgersen, M. L., Raa, H. A., and van Deurs, B. (2008) Clathrin-independent endocytosis: from nonexisting to an extreme degree of complexity. *Histochemistry and cell biology* **129**, 267-276
288. Guo, X., Mattera, R., Ren, X., Chen, Y., Retamal, C., Gonzalez, A., and Bonifacino, J. S. (2013) The adaptor protein-1 mu1B subunit expands the repertoire of basolateral sorting signal recognition in epithelial cells. *Developmental cell* **27**, 353-366
289. Carvajal-Gonzalez, J. M., Gravotta, D., Mattera, R., Diaz, F., Perez Bay, A., Roman, A. C., Schreiner, R. P., Thuenauer, R., Bonifacino, J. S., and Rodriguez-Boulan, E. (2012) Basolateral sorting of the coxsackie and adenovirus receptor through interaction of a canonical YXXPhi motif with the clathrin adaptors AP-1A and AP-1B. *Proceedings of the National Academy of Sciences of the United States of America* **109**, 3820-3825
290. Rapoport, I., Chen, Y. C., Cupers, P., Shoelson, S. E., and Kirchhausen, T. (1998) Dileucine-based sorting signals bind to the beta chain of AP-1 at a site distinct and regulated differently from the tyrosine-based motif-binding site. *The EMBO journal* **17**, 2148-2155
291. Damke, H., Baba, T., Warnock, D. E., and Schmid, S. L. (1994) Induction of mutant dynamin specifically blocks endocytic coated vesicle formation. *The Journal of cell biology* **127**, 915-934
292. Wang, C. C., Sato, K., Otsuka, Y., Otsu, W., and Inaba, M. (2012) Clathrin-mediated endocytosis of mammalian erythroid AE1 anion exchanger facilitated by a YXXPhi or a noncanonical YXXXPhi motif in the N-terminal stretch. *The Journal of veterinary medical science / the Japanese Society of Veterinary Science* **74**, 17-25
293. Devonald, M. A., and Karet, F. E. (2004) Renal epithelial traffic jams and one-way streets. *J Am Soc Nephrol* **15**, 1370-1381
294. Chu, C. Y., King, J., Berrini, M., Rumley, A. C., Apaja, P. M., Lukacs, G. L., Alexander, R. T., and Cordat, E. (2014) Degradation Mechanism of a Golgi-Retained Distal Renal Tubular Acidosis Mutant of the Kidney Anion Exchanger 1 in Renal Cells. *Am J Physiol Cell Physiol*
295. Gaush, C. R., Hard, W. L., and Smith, T. F. (1966) Characterization of an established line of canine kidney cells (MDCK). *Proc Soc Exp Biol Med* **122**, 931-935
296. Chu, C. Y., King, J., Berrini, M., Rumley, A. C., Apaja, P. M., Lukacs, G. L., Alexander, R. T., and Cordat, E. (2014) Degradation mechanism of a Golgi-retained distal renal tubular acidosis mutant of the kidney anion exchanger 1 in renal cells. *American journal of physiology. Cell physiology* **307**, C296-307
297. Chu, C. Y., King, J. C., Berrini, M., Alexander, R. T., and Cordat, E. (2013) Functional rescue of a kidney anion exchanger 1 trafficking mutant in renal epithelial cells. *PloS one* **8**, e57062
298. Mendes, F., Wakefield, J., Bachhuber, T., Barroso, M., Bebok, Z., Penque, D., Kunzelmann, K., and Amaral, M. D. (2005) Establishment and characterization of a novel polarized MDCK epithelial cellular model for CFTR studies. *Cellular physiology and biochemistry : international journal of experimental cellular physiology, biochemistry, and pharmacology* **16**, 281-290

299. Borovac, J., Barker, R. S., Rievaj, J., Rasmussen, A., Pan, W., Wevrick, R., and Alexander, R. T. (2012) Claudin-4 forms a paracellular barrier, revealing the interdependence of claudin expression in the loose epithelial cell culture model opossum kidney cells. *American journal of physiology. Cell physiology* **303**, C1278-1291
300. Kizer, N. L., Lewis, B., and Stanton, B. A. (1995) Electrogenic sodium absorption and chloride secretion by an inner medullary collecting duct cell line (mIMCD-K2). *Am J Physiol* **268**, F347-355
301. Orlowski, J., and Grinstein, S. (2004) Diversity of the mammalian sodium/proton exchanger SLC9 gene family. *Pflugers Arch* **447**, 549-565
302. Hull, R. N., Cherry, W. R., and Weaver, G. W. (1976) The origin and characteristics of a pig kidney cell strain, LLC-PK. *In vitro* **12**, 670-677
303. Rabito, C. A. (1986) Occluding junctions in a renal cell line (LLC-PK1) with characteristics of proximal tubular cells. *Am J Physiol* **250**, F734-743